Synthesis of Thiourea and Urea Organocatalysts by Opioids

By Bo Liu (B.Sc.)

Supervisors: Dr. Kieran Nolan

Prof. Nicholas Gathergood

(Tallinn University of Technology, Estonia)

For the award of Master's Degree by Research in Organic Chemistry

School of Chemical Sciences

Dublin City University

July 2017

Declaration

I hereby certify that this material, which I now submit for assessment on the programme of study leading to the award of a Master's degree by research is entirely my own work, that I have exercised reasonable care to ensure that the work is original, and does not to the best of my knowledge breach any law of copyright, and has not been taken from the work of others save and to the extent that such work has been cited and acknowledged within the text of my work.

Signed: _____

Bo Liu

(Candidate) ID No.: 12211565

Date: _____

Table of Contents

List of Abbreviations

*: stereogenic center

A

Å: Angstrom

[α]: specific rotation

Ac: acetyl

aq.: aqueous

Ar: aryl

atm: atmosphere

B

BINAP: 2,2'-bis(diphenylphosphino)-1,1'-binaphthyl

BINOL: 1,1'-bi-2-naphthol

BINSA: 1,1'-binaphthyl-2,2'-disulfonic acid

Boc: *tert*-butoxycarbonyl

C

ºC: degrees Celsius

cm^{-1}: wavenumber (s)

COD: 1,5-cyclooctadiene

COSY: correlation spectroscopy

δ: chemical shift in parts per million

D

DABCO: 1,4-diazabicyclo[2.2.2]octane

DBU: 1,8-diazabicyclo[5.4.0]undec-7-ene

DCM: dichloromethane

DCE: 1,2-dichloroethane

de: diastereomeric excess

DEPT: distortionless enhancement by polarization transfer

DHQ: dihydroquinine

DHQD: dihydroquinidine

DIOP: 2,3-*O*-isopropylidene-2,3-dihydroxy-1,4-bis(diphenylphosphino)butane

DiPAMP: ethane-1,2-diylbis[(2-methoxyphenyl)phenylphosphane]

DMF: dimethylformamide

DMSO: dimethyl sulfoxide

DPEN: 1,2-diphenylethane-1,2-diamine

dr: diastereomeric ratio

E

ee: enantiomeric excess

endo: endothermic

eq.: equivalent

er: enantiomeric ratio

ESI: electrospray ionization

Et: ethyl

et al.: and others

exo.: exothermic

Exp.: experiment

F

FGI: Functional Group Interconversion

Fig.: Figure

G

g: gram (s)

H

h: hour (s)

HMQC: heteronuclear multiple quantum correlation

HOMO: highest occupied molecular orbital

HPLC: high-performance liquid chromatography

Hz: Hertz

I

IR: infrared

J

J: coupling constant (in NMR spectrometry)

K

kg: kilogram (s)

L

LC-MS: liquid chromatography-mass spectrometry

L-DOPA: L-3,4-dihydroxyphenylalanine

Lit.: literature

LUMO: lowest unoccupied molecular orbital

M

M^+: parent molecular ion

Me: methyl

MeOH: methanol

min: minute (s)

mL: milliliter

mol: mole (s)

mmol: millimole

m.p.: melting point

MS: mass spectrometry

Ms: methanesulfonyl

m/z: mass to charge ratio

N

NMR: nuclear magnetic resonance

O

OTs: tosylate (*p*-toluenesulfonate)

P

Ph: phenyl

PhSH: thiophenol

PMP: 4-methoxyphenyl

ppm: parts per million

^{i}Pr: isopropyl

PPh_3: triphenylphosphine

R

RI: relatively intensity

rt: room temperature

S

S_N2: bimolecular nucleophilic substitution

S_N2': bimolecular nucleophilic substitution with allylic rearrangement

SOMO: singly occupied molecular orbital

T

TADDOL: α,α,α',α'-tetraaryl-1,3-dioxolane-4,5-dimethanol

TBD: 1,5,7-triazabicyclo[4.4.0]dec-5-ene

TBS: *tert*-butyldimethylsilyl

TEA: triethylamine

TEMP.: temperature

THF: tetrahydrofuran

TIPS: triisopropylsilyl

TIPBs: triisopropylbenzenesulfonyl

TLC: thin layer chromatography

TMG: 1,1,3,3-tetramethylguanidine

TMSCN: trimethylsilyl cyanide

TsCl: 4-toluenesulfonyl chloride

V

VANOL: 3,3'-diphenyl-2,2'-bi-1-naphthalol

VAPOL: 2,2'-diphenyl-(4-biphenanthrol)

X

XRD: X-ray powder diffraction

List of Figures

List of Schemes

List of Tables

List of Appendix Figures and Tables

Acknowledgements

The work in this thesis was carried out from September 2012 to June 2015 in the School of Chemical Sciences, Dublin City University, under the supervision of Prof. Nick Gathergood and Dr. Kieran Nolan.

First of all, I would like to thank Dr. Peter Kenny for giving me an opportunity to carry out my master's research at Dublin City University and I also acknowledge Prof. Nick Gathergood for introducing me to the fascinating field of synthesis of opioid derivatives.

I also am deeply thankful to Alan Coughlan for his constant help, critical advice and training which helped me greatly in understanding the subject and ultimately enabling me to tackle challenging problems. I am also grateful to all the members of the Gathergood group, especially Dong, Hannah, Andrew and Adam.

Special thanks go to all the staff in the School of Chemical Sciences, particularly to Damien (HPLC), John (NMR), Ambrose (stores) and Vinny (IR). This thesis would not have been possible without their support.

Synthesis of Thiourea and Urea Organocatalysts by Opioids

By Bo Liu

Abstract

Organocatalysis is one of the fastest growing fields of research in organic chemistry. The many advantages of organocatalysts include their low costs, low toxicity, the ready availability of natural resources and in many cases, low reactivity with moisture and oxygen. These traits can be preferable to some classes of metal-based catalysts although a case-by-case comparison is required. When benefits over metal-based catalysts are realized, organocatalysts can make a contribution to green chemistry. One major advantage is that metal residues, which are difficult to remove from products when using metal-based catalysts, are avoided by an organocatalytic step which is of significance to the synthesis of pharmaceutical products, where metal content is strictly controlled.

Effective chiral organocatalysts can be derived from natural molecules from the chiral pool, which are a primary source of enantiomerically pure stereoisomers. Proline and the cinchona alkaloids are two key examples of organocatalyst precursors which have been widely studied. This work expands the scope of natural alkaloid precursors to include opiates.

Opiates, such as morphine and codeine, are abundant alkaloids readily available from the opium poppy and industrial plants and means by which to extract these compounds are well established. This is due to their ubiquitous use as analgesic drugs to relieve pain. The aim of this project was to prepare novel thiourea and urea organocatalysts from a series of opioid derivatives and study their performance in model asymmetric synthetic reactions suited to thiourea catalysts. The selected reaction was a Michael addition reaction between diethyl malonate and *trans*-β-nitrostyrene. One urea and one thiourea organocatalyst were prepared, both of the C_2-symmetric group, and characterized by NMR, IR, melting point, optical rotation, MS and the compound structures were unambiguously assigned based on single crystal XRD results. The thiourea derivative catalyst gave high yields for the Michael addition reaction however, enantioinduction was poor, with less than 10% *ee* observed.

Chapter 1 Literature Review

1.1 Chiral compounds

The majority of new drugs are chiral; it is expected that approximately 95% of pharmaceutical drugs will be chiral compounds by 2020.[1] The reason why chiral compounds are so important to the pharmaceutical industry, is mainly due to the multitude of chiral target sites in the body, where a chiral drug can interact with high-binding affinity compared to an achiral compound. Although this is not true in all cases, it is often a starting point for drug design and development. Demand for enantiopure chiral compounds is expected to continue to rise, primarily for the pharmaceutical industry, but also in other sectors including: flavour and aroma chemicals (such as hair spray additives), clothing, specialty materials and agrochemicals.[2] One such example where enantiomers have different biological activities was observed with mecoprop-P and dichlorprop. The (*S*)-enantiomers were preferentially degraded in most species of broadleaf weeds compared to the (*R*)-enantiomers which showed more resistance to degradation (Fig. 1.1).[3] This is but one of many diverse examples of the importance of chirality within the design of novel molecules.

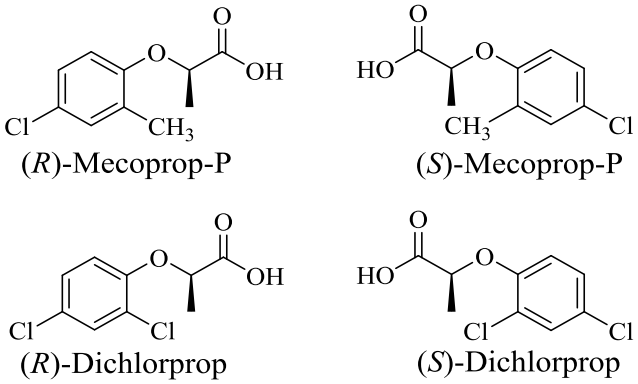

Fig. 1.1 Chemical structure of mecoprop-P and dichlorprop enantiomers.[3]

1.2 Primary sources of chiral compounds

The synthesis of enantiomerically pure compounds is an important area of chemistry. In 1980, Prof. Seebach introduced the term "synthesis of enantiomerically pure compounds" to include all the processes for obtaining chiral enantiopure compounds.[4] The three main approaches for the synthesis of enantiomerically pure chiral

compounds are; 1) resolution of racemates, 2) asymmetric synthesis by catalytic or stoichiometric processes and 3) the chiral pool approach.

1.2.1 Resolution of racemates

Resolution techniques were the first methods for resolving racemic mixtures and this method is still popular for process-scale operations in the industry today. Resolution techniques can be subdivided into three methods:

1. Crystallization: The oldest method of separating enantiomers from their racemates. A pair of diastereomeric salts exhibits different physical and chemical properties such as solubility, melting points, boiling points, adsorptions and phase distribution characteristics. Consequently, diastereomers can be separated. Several methods may be applied to convert a racemic mixture to a mixture of diastereomers, including salt formation with an enantiomerically pure acid or base, or use of a chiral auxiliary which can be removed after resolution. Another technique is to manually separate two kinds of crystals of tartaric acid isomers from supersaturated solution sodium ammonium tartrate, where differences in morphology can be observed under a microscope, which was historically performed by Louis Pasteur in 1849.[5,6] The resolution of binaphthol by cholesterol esterase is another example utilising combined kinetic resolution (see the following section) with selective crystallization. The racemic binaphthol is first converted into a diester, then kinetic resolution using a cholesterol esterase results in selective hydrolysis to yield the (*S*)-BINOL product which precipitates. The remaining diester in the mother liquid undergoes basic hydrolysis to give (*R*)-BINOL (Scheme 1.1).[7,8]

2. Chromatography: Widely used in development laboratories and separation of enantiomers can be achieved by employing a chiral column. However, the disadvantage of this method is the high cost of the columns used.

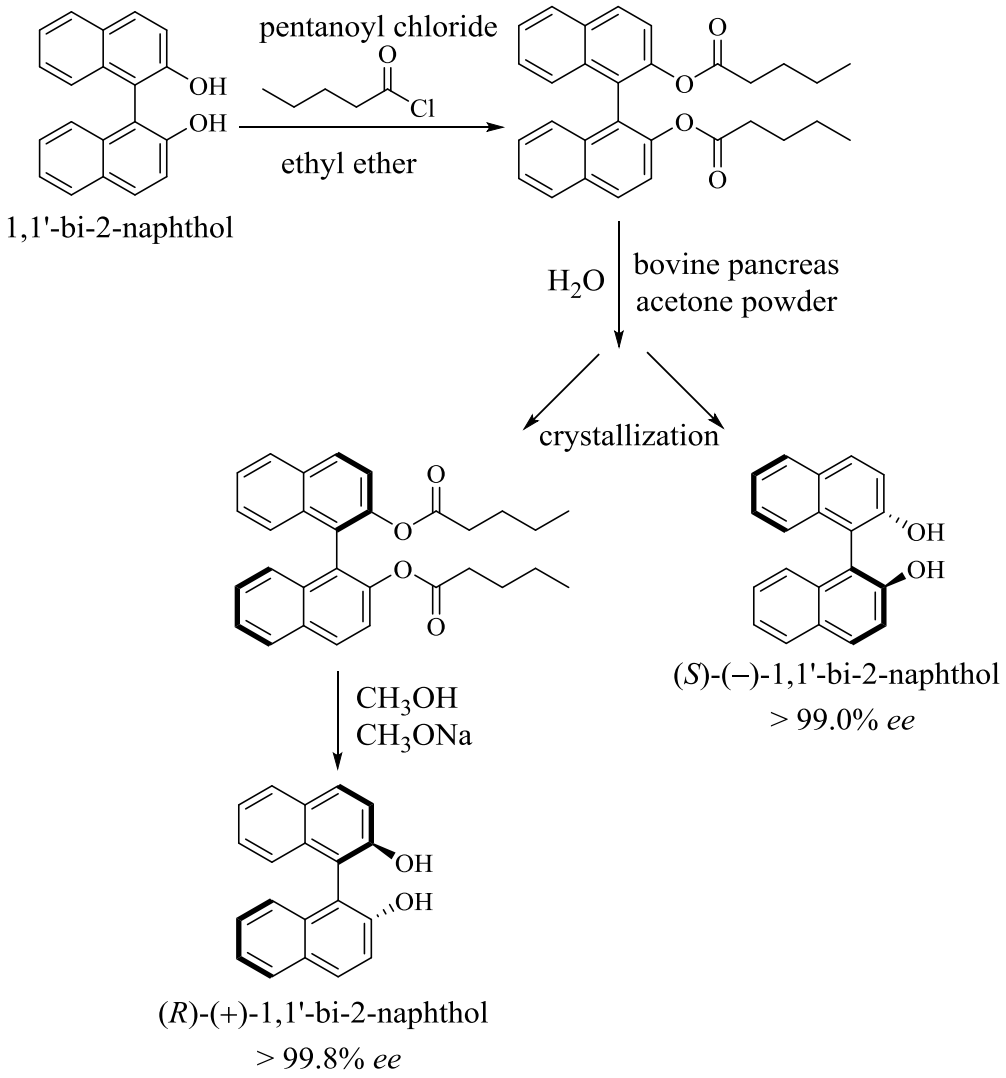

Scheme 1.1 Resolution of 1,1'-bi-2-naphthol by crystallization and kinetic resolution.[7,8]

3. Kinetic resolution: with a chiral reagent, one of the enantiomers of a racemic mixture is transformed into the corresponding product faster than the other, due to their different consumption rates in a chemical reaction. However, the maximum theoretical yield of 50% is the critical drawback of the method. The dynamic kinetic resolution, which is an important extension of kinetic resolution, can convert the achiral reactant with 100% completion, because both enantiomers are connected in a chemical equilibrium. In this way, the faster-reacting enantiomer is replenished during the reaction with the expense of the slower-reacting enantiomer.[9] One of the more classic applications of the dynamic kinetic resolution is Noyori asymmetric hydrogenation.[10]

1.2.2 Asymmetric synthesis

Asymmetric synthesis is a process in which a compound with a defined stereogenic center is selectively formed.[11] The techniques used can be divided into three approaches: the substrate-controlled approach, the use of chiral auxiliaries and directed catalytic methods.

The substrate-controlled approach is a reaction where the formation of a new stereogenic center is controlled by another chiral center already present in the substrate. The limitation of the substrate-controlled approach is that enantiopure starting materials are limited and may not suit a selected target molecule synthesis.

The chiral auxiliary approach is similar to the substrate-controlled approach, in which chirality is induced into an achiral molecule by using an appended chiral entity, usually through a new covalent bond to the achiral starting material. The auxiliary is subsequently removed at the end of reaction as an additional step.

The catalyst approach is a catalytic transformation promoted by a chiral catalyst generally used with low catalyst loadings, therefore enhancing the economic value of the process. The approach of using chiral catalysts capable of making chiral products from various substrates is the most significant advance in asymmetric synthesis. The catalyst can be a chiral Lewis acid or base, a chiral organocatalyst, a chiral organometallic complex or a biocatalyst. A simplified overview of typical asymmetric synthetic methods is shown in Fig. 1.2.

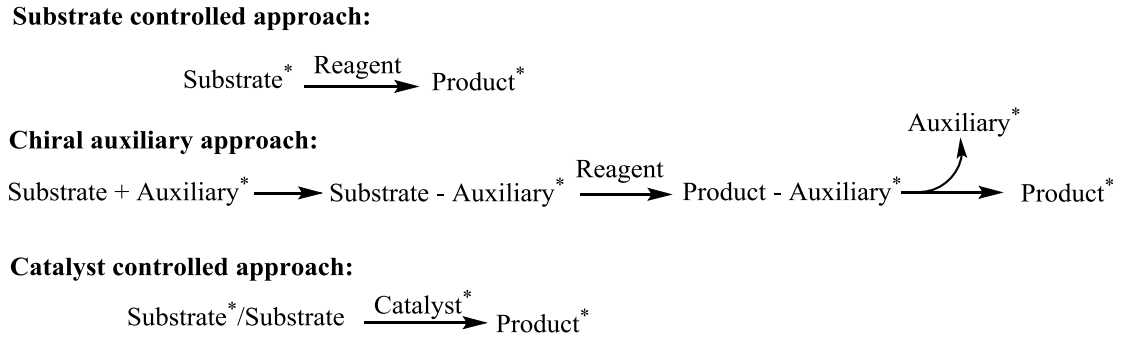

Fig. 1.2 Three approaches of asymmetric synthesis (chirality denoted by * symbol).

1.2.3 Chiral pool approach

The chiral pool is a versatile tool which allows naturally occurring chiral molecules to be synthetically transformed into the desired target molecules.[12] Natural sources have provided a variety of chiral pool materials in high enantiomeric purity and frequently at low costs, such as natural amino acids, hydroxyl acids, terpenes, carbohydrates and alkaloids (Fig. 1.3). They have been widely used as chiral building blocks in the organic synthesis of natural products; additionally, some bioactive compounds have been used in various industrial applications.

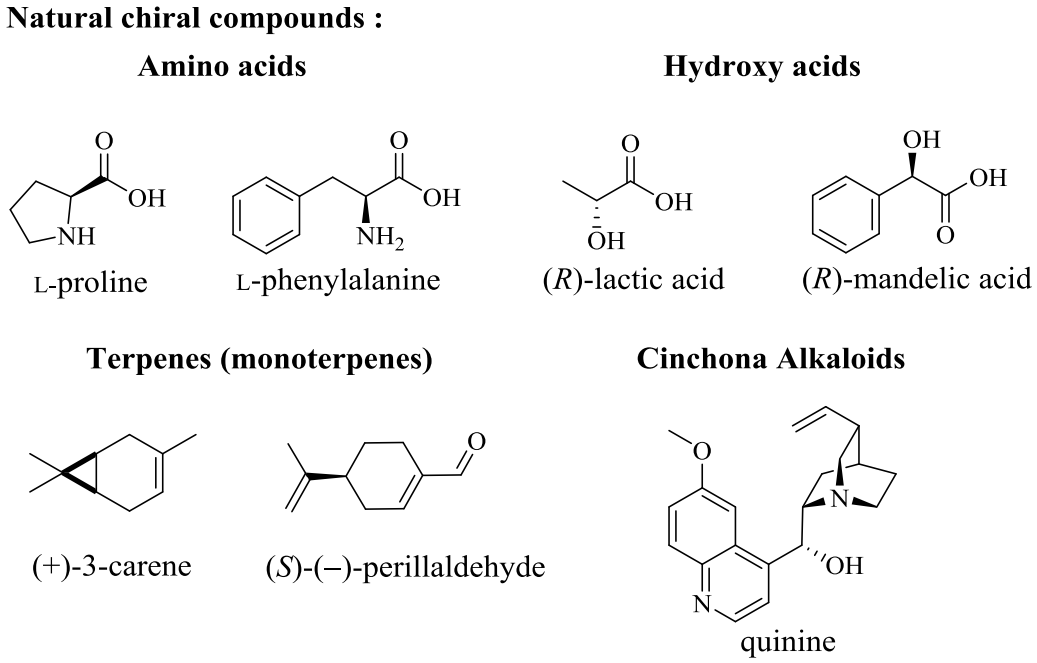

Fig. 1.3 Examples of natural chiral compounds.

Amino acids are the basic organic compounds, which are essential for all life processes. Chiral amino acids are not only extensively used by pharma industries, because of their ready availability in enantiomerically enriched forms, they can also be used as starting building blocks for transformations into other compounds, such as heterocycles, due to the diversity of functional groups present.[13] For instance, Samanta *et al.* reported the synthesis of amino acid derived chiral aziridines from α-amino acids following a four-step synthetic procedure.[13,14] Additionally, Rao *et al.* developed a versatile and efficient method for the synthesis of (2*S*)-2-(hydroxymethyl)-*N*-Boc-2,3-dihydro-4-pyridone from L-(−)-phenylalanine from L-phenylalanine (Scheme 1.2).[13,15]

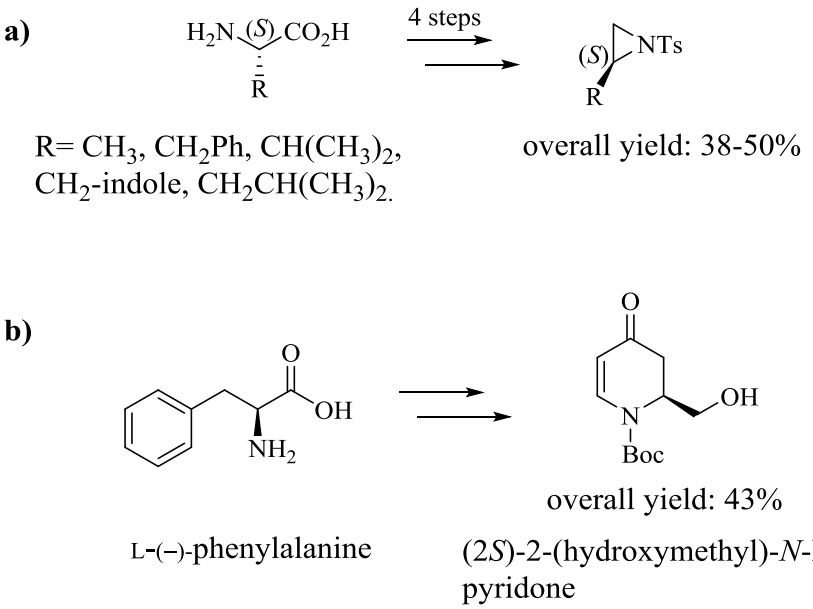

Scheme 1.2 Synthesis of heterocyclic building blocks using amino acids. a) Synthesis of chiral aziridines. b) Synthesis of (2*S*)-2-(hydroxymethyl)-*N*-Boc-2,3-dihydro-4 -pyridone from L-(−)-phenylalanine.[13-15]

Furthermore, synthesis of a wide range of natural and non-natural products using α-amino acids as the chiral pool in a substrate-controlled manner have also been reported. Srihari *et al.* achieved the stereoselective total synthesis of a securinega alkaloid (−)-allonorsecurinine. The stereocenter in the lactone moiety of the final product was readily prepared from the chiral inducer L-proline (Scheme 1.3).[16,17]

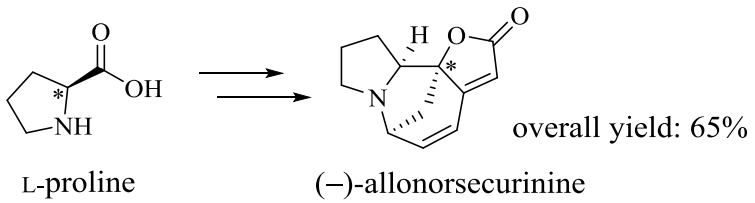

Scheme 1.3 Total synthesis of (−)-allonorsecurinine by a chiral inducer L-proline.[16,17]

Terpenes are a large and diverse class of organic compounds obtained from plants. Pharmaceutical, food, agricultural and chemical industries have exploited many important terpenes for their potential and effectiveness as medicines, flavor enhancers, pesticides, and fine chemicals, respectively. Important terpenes include carvone (flavor), menthol and camphor (flavor, repellent, nonprescription drug), *etc*.[18] Natural optically active monoterpenes have also been applied as catalysts or building blocks

and considered as good chiral starting materials or substrates for the synthesis of targeted and natural compounds such as the pharmacological import β-amino acid derivatives. For example, Szakonyl *et al.* reported the total synthesis of carane-based β- and γ-amino acid derivatives from the monoterpene perillaldehyde. They synthesised β- and γ-amino acid derivatives *via* a conjugate addition reaction using two intermediates (A and B in Scheme 1.4), respectively, both prepared from (−)-(4*S*)-perillaldehyde.[19]

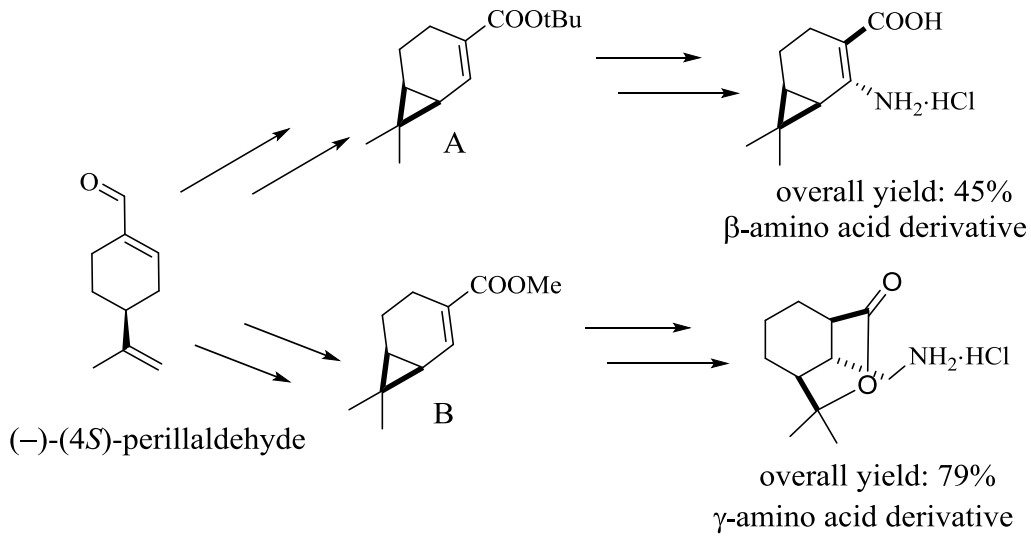

Scheme 1.4 Total synthesis of β- and γ-amino acid derivatives by (−)-(4*S*)-perillaldehyde.[19]

Likewise, the cinchona alkaloid quinine is another example. It is isolated from the bark of the cinchona tree, has demonstrated its applicability as a chiral scaffold in asymmetric synthetic catalyst design, as well as being commercialised as a potent antimalarial agent.[20]

The limitation of the chiral pool approach is that only a few compounds are available in optically pure forms from nature on a large scale. It is usually the case that chiral pool building blocks are incorporated into chiral ligands which then enable the transfer of chirality from a natural source to the desired target molecules.[21]

1.3 Other sources of chiral compounds

In the last few decades, green chemistry has been recognized as a subject and methodology for achieving sustainable development and has also been able to promote innovative technologies that eliminate or reduce the use and generation of hazardous substances. Since the twelve principles of green chemistry were developed by Paul Anastas and John Warner,[22] catalysis has been one of the fundamental pillars of green chemistry and also been regarded as the heart of modern synthetic chemistry, because almost commercial chemical reactions involve at least one catalytic steps. Furthermore, with being driven by factors such as growing consumption of petroleum products, environmental regulations, technology developments, the global catalyst market has grown steadily over the past seven year's decades and is expected to reach US $34.3 billion by 2024, according to a new report from the Grand View research, Inc.[23] In comparison with historical approaches, such as chiral pool synthesis and chiral reagents, the design and application of new catalysts can pursue the "ideal" synthetic process to produce useful compounds in 100% yield with 100% selectivity in an economical, energy-saving, environmentally benign and sustainable way.[23,24] Catalysts are generally divided into three main types: homogeneous catalysts, heterogeneous catalysts, and biocatalysts. Transition metal catalysts, organocatalysts, and organometallic catalysts have become an important role in the field of homogeneous catalysis as being well studied, particularly for fine chemicals and pharmaceuticals due to being more active and selective compared to heterogeneous catalysts.[25]

1.3.1 Transition-metal catalysts

Chiral ligands are enantiopure organic compounds that chelate with a metal center to form asymmetric catalysts. Thus, the transfer of chirality from the catalyst to the product of a reaction can be brought about by chiral ligands surrounding the metal core. A general representation of a chiral metal-based catalyst is shown in Fig. 1.4.

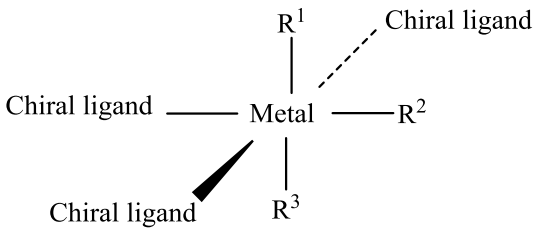

Fig. 1.4 General representation of chiral metal-based catalyst.

The design and synthesis of new chiral ligands (including phosphine based examples) are crucial for the development of transition-metal-catalyzed asymmetric catalysis. Most of the commonly utilized transition metals include palladium, ruthenium and rhodium complexes, bearing chiral ligands to provide a chiral environment for asymmetric induction. For instance, rhodium (I) complexes containing chiral phosphine ligands are used extensively as asymmetric hydrogenation catalysts. The first was the discovery by Wilkinson *et al.* of the properties of the rhodium complex $RhCl(PPh_3)_3$ as a hydrogenation catalyst for unhindered olefins.[26] Based on the structure of the rhodium catalyst, Knowles *et al.* replaced the achiral triphenylphosphine ligands in the rhodium complex with the chiral phosphine ligand methylpropylphenylphosphine (69% *ee* of (−)-methylpropyl phenyl phosphine). This created the first asymmetric hydrogenation catalyst (**1**) and was then applied to an asymmetric hydrogenation reaction to give hydratropic acid in 15% *ee* (Scheme 1.5).[27]

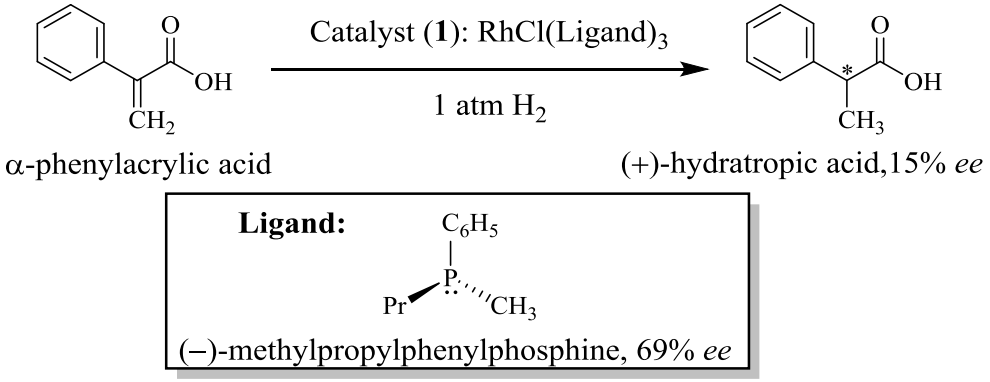

Scheme 1.5 Hydrogenation of α-phenylacrylic acid by Knowles's catalyst (**1**): a rhodium catalyst containing (−)-methylpropylphenylphosphine (69% *ee*) to give (+)-hydratropic acid in 15% *ee*.[27]

The Knowles group also used a rhodium complex catalyst (**2**) containing phosphine, with the DiPAMP ligand increasing enantioselectivity to 95% in the hydrogenation of dehydroamino acids.[28] The methodology was used on a commercial scale for the synthesis of L-DOPA (3,4-dihydroxy-L-phenylalanine), a drug used for the treatment of Parkinson's disease (Scheme 1.6).[29]

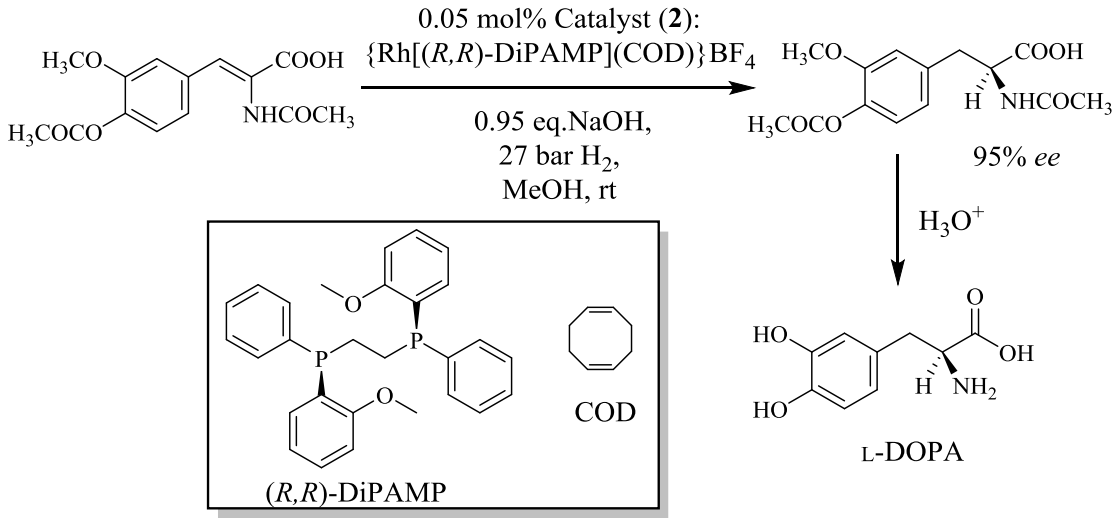

Scheme 1.6 Synthesis of L-DOPA using DiPAMP catalyst (**2**).[28]

Kagan and Dang bridged two monodentate phosphines to form the first chiral bidentate phosphine ligand, which is the first example of a C_2-symmetric phosphine ligand. Up to 72% *ee* was reported in the hydrogenation of unsaturated acids with the use of the rhodium complex containing the ligand DIOP (Scheme 1.7).[30]

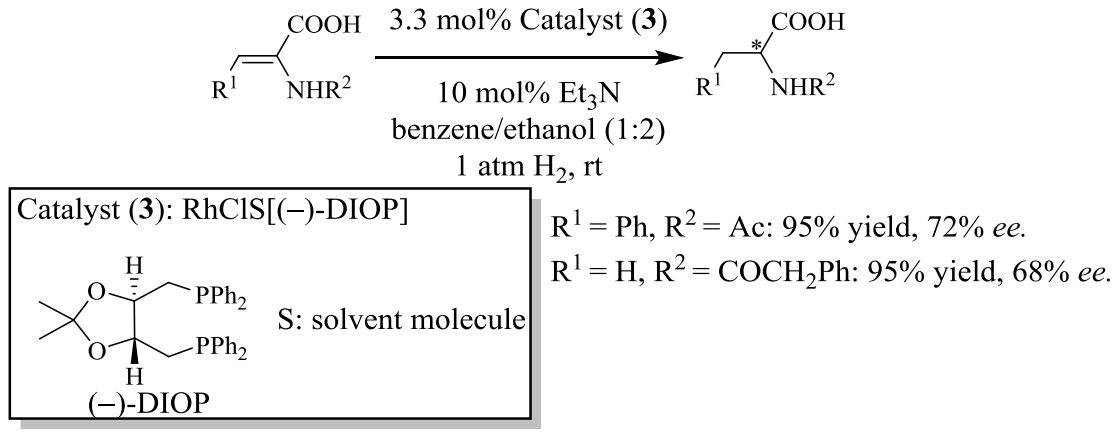

Scheme 1.7 Asymmetric hydrogenation of unsaturated acids by the catalyst (**3**).[30]

This work on metal-based catalysts significantly expanded the scope of asymmetric hydrogenation. Noyori *et al.* made the first breakthrough in using BINAP-Ru(II) dicarboxylate complexes.[31] These chiral Ru complexes serve as catalyst precursors for the highly enantioselective hydrogenation of carbon-carbon double bonds, the asymmetric hydrogenation of which had been difficult to achieve by rhodium catalysts

reported until then. An example is the hydrogenation of ketones by $RuCl_2$ (BINAP) catalyst (**4**) to give high enantioselectivity for the β-hydroxy ester product, shown in Scheme 1.8.

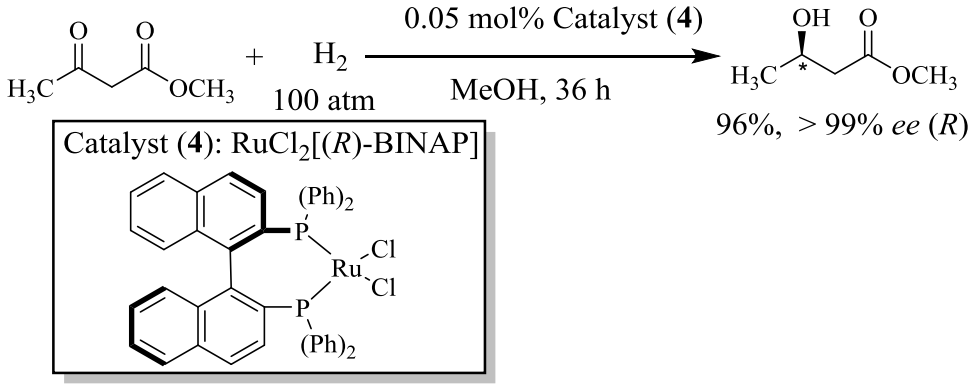

Scheme 1.8 Asymmetric hydrogenation of β-keto ester by $RuCl_2$[(*R*)-BINAP].[31]

With the development and application of a number of transition-metal catalysts, most industrial development projects aimed at scaling up transition-metal-catalyzed-reaction for increasing the turnover numbers.[32] However, the use of such catalysts has shown some disadvantages:

- Metal catalysts may not be stable to oxygen or moisture.
- Product inhibition can become a problem due to binding of the product to the catalyst.[33]
- Catalyst disposal can be problematic, especially if a high toxicity metal is present.
- The high cost in many cases makes catalyst recycling essential, which is not always possible due to degradation.

1.3.2 Organocatalysis

Naturally occurring enzymes have been considered powerful biocatalysts for organic transformations, providing products with high yield and enantioselectivity under mild conditions because of their wide substrate tolerance.[34] The use of analogous small organic molecules as catalysts has attracted a large amount of research groups' interest over the last 15 years. Complementing biocatalysis and transition metal catalysis, asymmetric organocatalysis, defined as the use of small organic molecules as catalysts for asymmetric reactions, recognised as an independent synthetic tool for the synthesis

of chiral organic molecules. Advantages over transition-metal catalysts include:[24]

- High tolerance to air and moisture, thus specialist equipment such as vacuum lines are not necessary.
- Easy to handle even on a large scale and a potential for lower toxicity due to the absence of metals which is attractive for the synthesis of pharmaceutical products.
- Inexpensive, with many materials being readily available from natural products compared to transition metals, such as L-proline and other natural amino acids.
- Easy to scale-up and easy screening.
- Some organocatalysts are bio-derived and biodegradable.

Therefore, the use of organocatalysts can be considered a convenient synthetic philosophy, and a complementary synthetic toolkit alongside transition metal catalysts. Transition metal catalysts are a valuable class of compounds due to the wide scope of possible reactions, very high activity and large knowledge base available. Both areas will complement each other for years to come.

1.3.3 Classification of organocatalysis

Organocatalysts are synthesised from organic compounds generally originating from biological sources. They donate or remove electrons or protons as their activation mode.[35] Hence, according to Benjamin List, organocatalysis can be broadly classified as: Lewis base catalysis, Lewis acid catalysis, Brønsted base and Brønsted acid catalysis;[35,36] while organocatalysis can also be sub-classified into covalent and non-covalent catalysis, according to the interaction between the substrate and the catalyst.[37] The working principles of that organocatalysis will be described accordingly.

1.3.3.1 Lewis base catalysis

Lewis base catalysis reactions start with a nucleophilic addition of the Lewis base (**B:**) to the substrate **S,** which leads to a donation of a pair of electrons from the Lewis base (**B:**) to form a covalent bond with the substrate **S** and the formation of the adduct $\mathbf{B^{+}\text{-}S^{-}}$. This adduct undergoes a reaction to give the intermediate species $\mathbf{B^{+}\text{-}P^{-}}$**,** from which the product **P** is released. The catalyst (**B:**) then re-enters the catalytic cycle (Fig. 1.5).

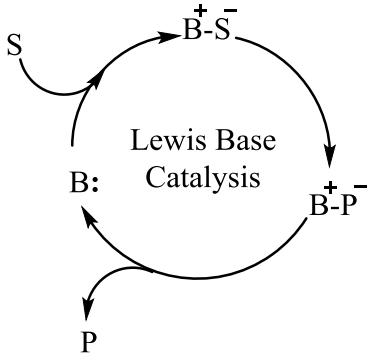

Fig. 1.5 Simplified catalytic mechanisms of Lewis base catalysis[36] (**S** = Substrate, **B:** = Lewis base catalyst, **P** = Product).

These catalysts are nitrogen, carbon, oxygen, phosphorus and sulfur based Lewis bases such as amines, carbenes, formamides, phosphoramides, phosphanes, and sulfides. Among these catalysts, the nitrogen-based and phosphorus-based compounds are the most studied, partly due to their ready availability from the chiral pool.[38] For instance, nitrogen-based Lewis organocatalysts convert the substrates into either activated nucleophiles or electrophiles *via* diverse mechanisms with reactive intermediates,[39] such as iminium ions, enamines,[40] acyl ammonium ions,[41] and 1-, 2-, 3- ammonium enolates,[42] *etc*. Typical examples of such catalytic processes include enamine catalysis, reported by List *et al.*, which classically involve an intermolecular aldol reaction of isobutyraldehyde with acetone (20 vol.%) by the amino acid L-proline (**5**), *via* formation of an enamine intermediate.[36,43] MacMillan *et al.* reported iminium catalysis in a Diels-Alder reaction of α,β-unsaturated aldehydes with dienes by imidazolidinone (**6**), *via* an iminium ion which is generated from the reaction of an amine catalyst with a carbonyl substrate (Scheme 1.9).[36,44]

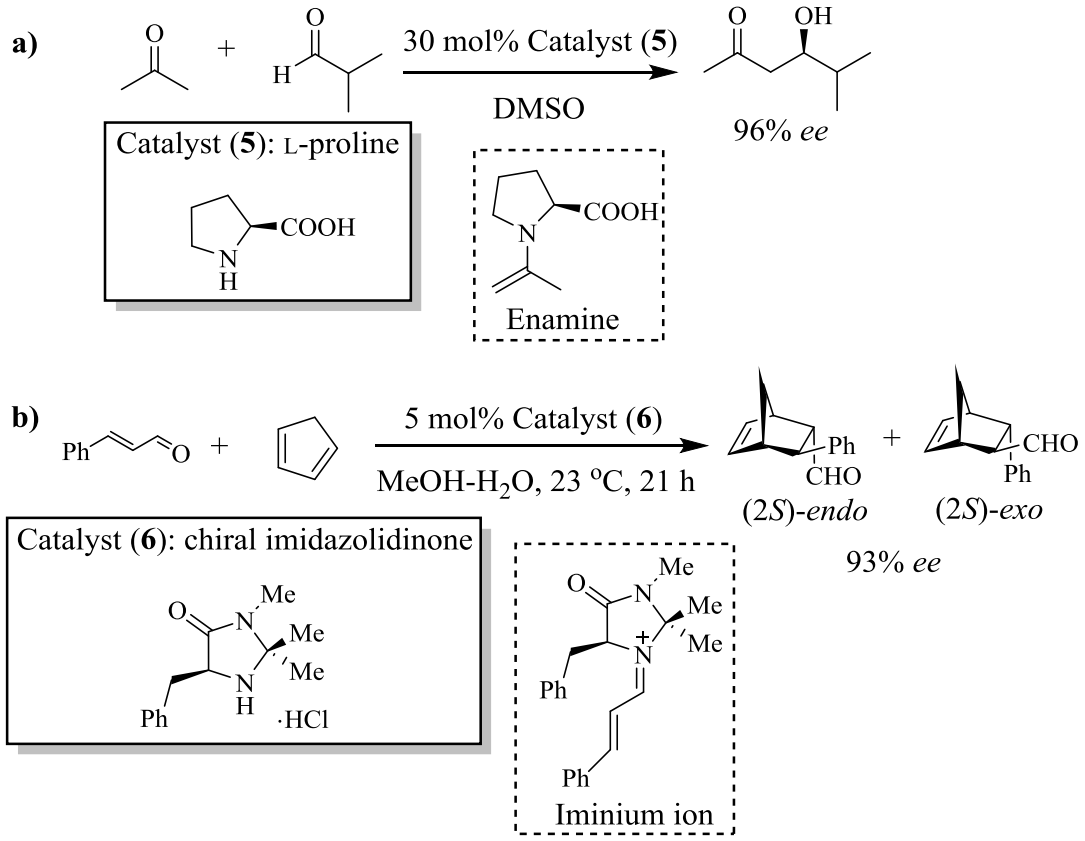

Scheme 1.9 a) Intermolecular aldol reaction catalyzed by L-proline *via* enamine intermediate;[43] b) Chiral imidazolidinone catalyzed Diels-Alder reaction of cinnamaldehyde with cyclopenta-1,3-diene *via* iminium ion catalysis.[44]

Both these examples of Lewis base catalysis utilise the amine catalysts as nucleophiles, where a nucleophilic attack by the catalyst on a substrate it activates a reaction with either intermediate nucleophilic enamines or intermediate electrophilic iminium ions.[45,46] After the initial recognition of activation of carbonyl compounds *via* enamine and iminium ion intermediates by chiral amines, several new modes of chemical activation in aminocatalysis have been discovered. Today's aminocatalytic transformations of carbonyl compounds *via* iminium ion and enamine intermediates by chiral amines has been categorised in three distinct activation modes: LUMO-lowering, HOMO-raising, and SOMO-activations, according to functionalization of the α, β, γ and ε positions of carbonyl compounds.[47,48] As shown in Scheme 1.10, these three activations have in common the formation of an iminium ion by reversible condensation of the chiral amine. The LUMO-lowering activation is the basic principle of iminium ion catalysis. This activation is based on the formation of an electrophilic iminium ion species by LUMO-lowering at the β-carbon of an α,β-unsaturated carbonyl compound, making it capable of β-functionalization with a nucleophilic

attack.[49] In contrast, the HOMO-raising activation involves the formation of the enamine and dienamine that increases the MOMO energy, delivering α-functionalization[50] and γ-functionalization[51] by a range of electrophiles, respectively. Moreover, trienamine catalysis was established by Chen *et al.* recently and provided an extension of the HOMO-raising activation strategy for amine catalysis. The key feature of the strategy is the simultaneous activation of both the γ- and ε-positions by raising of the HOMO of the trienamine intermediates and selective reactivity at the ε-carbon position in the Diels-Alder and tandem reaction.[52,53] SOMO-activation relies on the formation of an electrophilic 3π-electron radical cation, provided by single-electron oxidation of the enamine intermediate.[54]

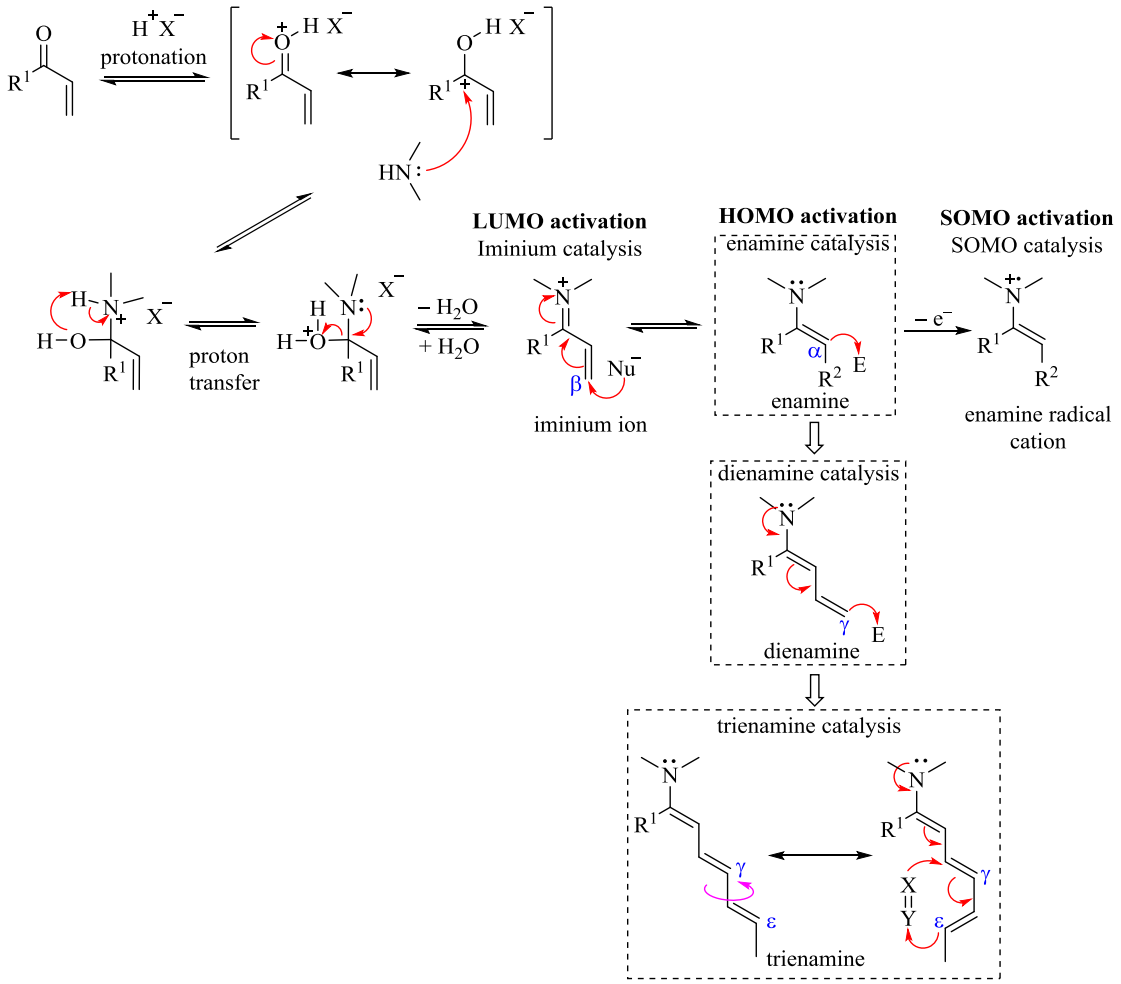

Scheme 1.10 Aminocatalytic activation modes (E: electrophile; Nu: nucleophile; X = Y: dienophile).

Recently, Kappler *et al.* used a formamide derivative catalyst (**7**) as a Lewis base catalyst for chlorination of alcohols with an inherently safe sole reagent benzoyl

chloride.[55] Using this novel method, chiral substrates can be converted in excellent yields and stereoselectivities, and the reactions can even be performed under solvent-free conditions. Additionally, the primarily formed chlorides in the reaction mixture can be further transformed into a range of amines, azides, ethers, sulfides and nitriles in a one-pot synthetic route, avoiding isolation of the intermediate alkyl chlorides-formed. Synthesis of the drug *S*-Fendiline with 95% stereoselectivity is an example. Hence, the authors claimed that this method would meet one of the major demands of the chemical industry and the principles of sustainable chemistry.

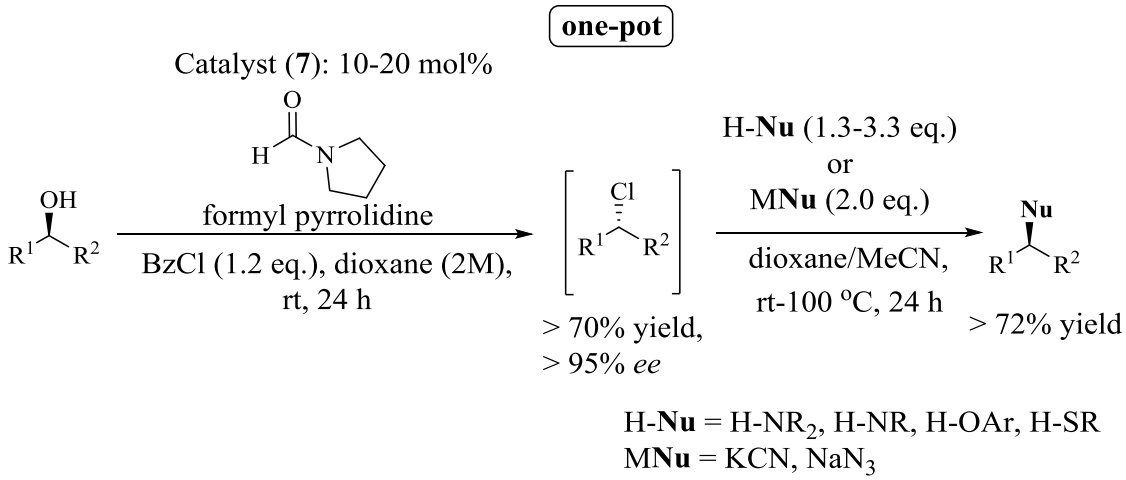

Scheme 1.11 One-pot chlorination by formyl pyrrolidine and subsequent trapping with nucleophiles.[55]

1.3.3.2 Lewis acid catalysis

A Lewis acid (**A**) is an atom or a molecule that can accept a pair of electrons and form an ionic interaction or a hydrogen-bond. It activates the nucleophilic substrate (**S:**) to give the adduct $\mathbf{A}^{-}$-$\mathbf{S}^{+}$. This adduct is converted into an intermediate species $\mathbf{A}^{-}$-$\mathbf{P}^{+}$ and is then followed by elimination of the product **P**. The catalyst **A** is free to re-enter the next catalytic reaction in the same manner (Fig. 1.6).

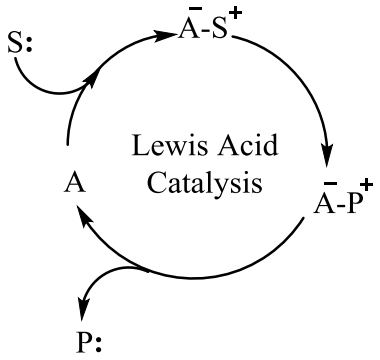

Fig. 1.6 Simplified catalytic mechanism of Lewis acid catalysis[36] (**S** = Substrate, **A** = Lewis acid catalyst, **P** = Product).

A key subset of Lewis acidic organocatalysts is phase transfer catalysts. This type of catalyst is designed to be soluble in both the organic and aqueous phase so that the catalyst can bind to a reactant from one phase, as an ion pair, and shuttle it into the phase which contains the other reactant. Phase-transfer catalysis has been recognised as a versatile methodology for organic synthesis in both academia and industry, as it features simple experimental operations, mild reaction conditions, use of and environmental benign reagents and solvents, and the possibility to conduct large-scale reactions.[56] Therefore, phase-transfer catalysis is often considered as a useful tool to develop greener and more sustainable processes with comparison to alternative synthetic methodology.[57]

Cinchona alkaloids have a long history in medicine and have also been proven to be a popular for organocatalysts, due to their unique structure, commercial availability and low cost.[58] The first successful use of cinchona alkaloids for chiral phase-transfer catalysis was conducted by the Merck group in 1984 for asymmetric methylation of a phenylindanone derivative with excellent enantioselectivity. Later on, these types of catalysts were successfully utilized for synthesis of α-amino acids by O'Donnell *et al.*. Consecutively, new cinchona alkaloid-derived catalysts bearing an *N*-anthracenylmethyl group were developed by the research groups of Lygo and Corey, which led to the establishment of the cinchona alkaloids family for asymmetric phase-transfer catalysis.[56] With functionalization of the C9- and C6'-hydroxyl group, and/or quaternization of the bridgehead tertiary amine, diverse generations of cinchona quaternary ammonium salts, including from simple monomers to polymeric form, have been well developed in recent years, and remarkable selectivities from various

asymmetric syntheses were observed.[58,59] For instance, Yasuda *et al.* synthesised the first example of a cinchona alkaloid-based phase-transfer catalyst (**8**), which isquaternized at both the quinuclidine nitrogen (*N*) and the quinoline nitrogen (*N'*).[60] They reported that the novel *N*,*N*'-disubstituted cinchona alkaloid-derived phase transfer catalyst afforded significant remarkable reactivity and enantioselectivity in the intermolecular spirocyclization reaction under mild conditions (**a** in Scheme 1.12); More recently, new dimeric cinchona alkaloid-derived quaternary ammonium salts (phase-transfer catalysts) were designed and synthesised by Svia *et al.*. They used the commercially available starting material *p*-tolualdehyde to prepare the new of type of chiral phase-transfer catalyst (**9**) with high yield, and applied them to the asymmetric Henry reaction to convert aldehydes to nitromethane with very good yields and excellent enantiomeric excess at room temperature observed (**b** in Scheme 1.12).[61]

Cinchona alkaloid-derived quaternary ammonium salts

Pioneering work:

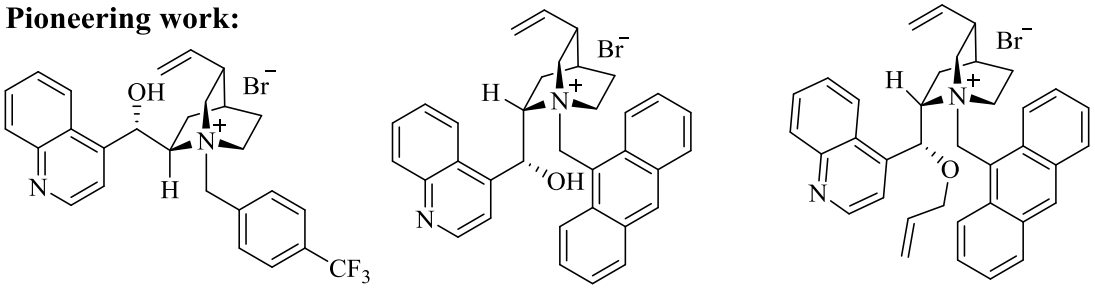

Recent work:

a)

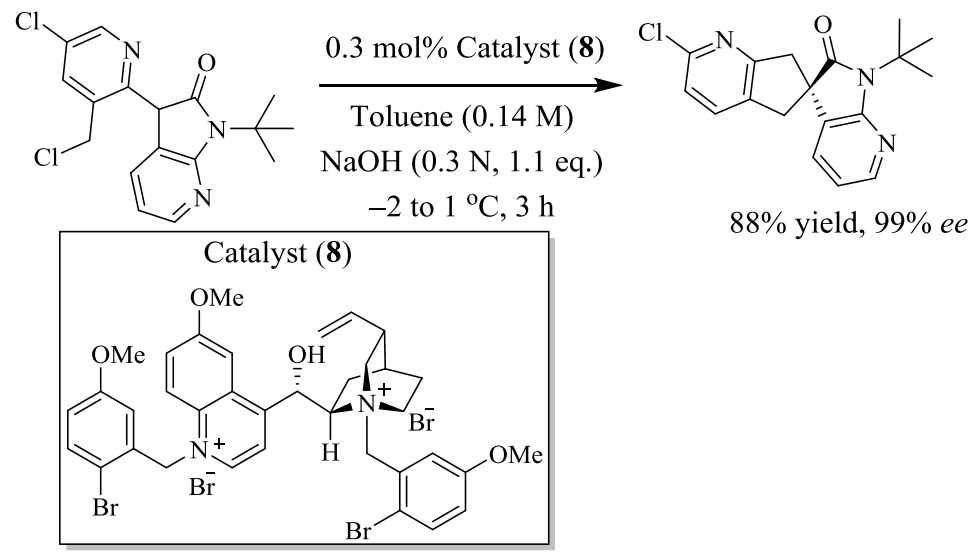

b)

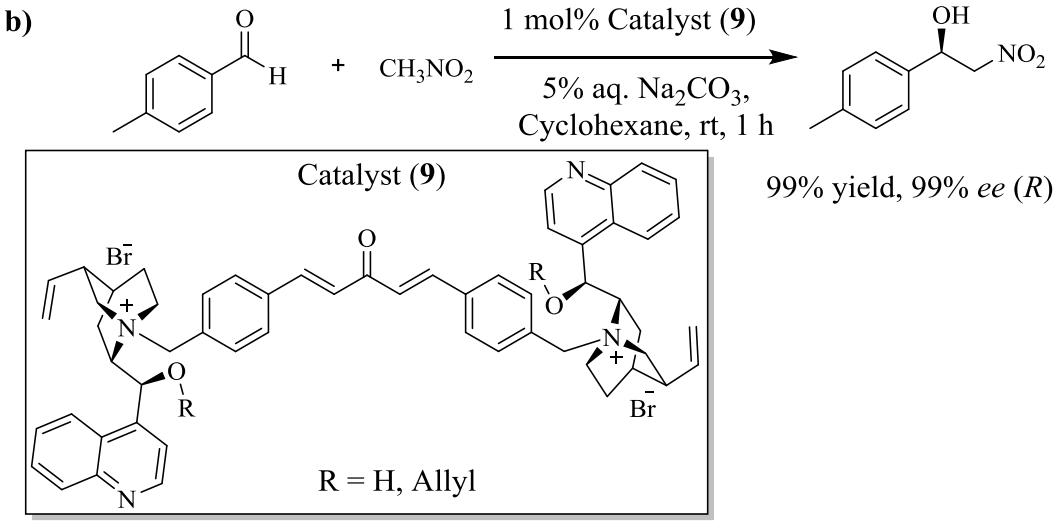

Scheme 1.12 Pioneering work of cinchona alkaloid-derived phase-transfer catalysts and examples of recently developed novel cinchona alkaloid-derived quaternary ammonium salts by a) Yasuda *et al.*[60] and b) Svia *et al.*[61], respectively.

As mentioned previously, phosphine compounds are most frequently used as chiral

ligands to develop transition-metal catalysts for asymmetric reactions. A variety of privileged chiral phosphine ligands has been synthesised which are commercially available. Therefore, considering the abundant structural and stereochemical diversity of commercially available chiral phosphine compounds, and also the limited scope of asymmetric phase-transfer catalysis to quaternary ammonium salts, the creation of a new domain in phase-transfer catalysis by exploiting the effective quaternary phosphonium salts has become a hot topic, especially in the last few years.[62] Regarding the fact that quaternary ammonium salts derived from cinchona alkaloids have excellent catalytic performance in various types of reactions, the design of a new family of phosphonium phase-transfer catalysts using the chiral pool building block amino acids has been recently reported. For instance, Lu *et al.* reported a bifunctional amino acid-derived chiral phosphine catalyst (**10**) for catalysing the asymmetric Michael addition of oxindole to methyl vinyl ketone in high yield and enantioselectivity (**a** in Scheme 1.13). They proposed the key of the catalytic system is the *in situ* formation of the zwitterion (**10'**) by the reaction of the phosphine catalyst (**10**) to the electrophilic methyl vinyl ketone; which serves as an efficient ion-pairing activation mode.[63] Progressively, based on the method for reactions using an *in situ*-generated phosphonium betaine catalyst (**10'**) designed by Lu,[63] Zhao *et al.* developed a new bifunctional thiourea-phosphine catalyst (**11**). A highly enantioselective Mannich-type reaction with dimethyl 2-fluoromalonate and benzaldehyde-derived *N*-Boc imine was achieved by the *in situ*-generated zwitterion (**11**'), from the combination of the catalyst (**11**) and an acrylate (**b** in Scheme 1.13).[64] Meanwhile, this group also developed dipeptide-derived multifunctional phosphonium bromide (**12**) and they found it was an effective catalyst for the asymmetric cyclization *via* tandem Michael addition/intramolecular S_N2 reaction with the conjugate ketone and malonate (**c** in Scheme 1.13).[65] In both cases, the thiourea moiety of the catalyst was necessary to achieve high levels of enantioselectivity in the asymmetric reactions.[66]

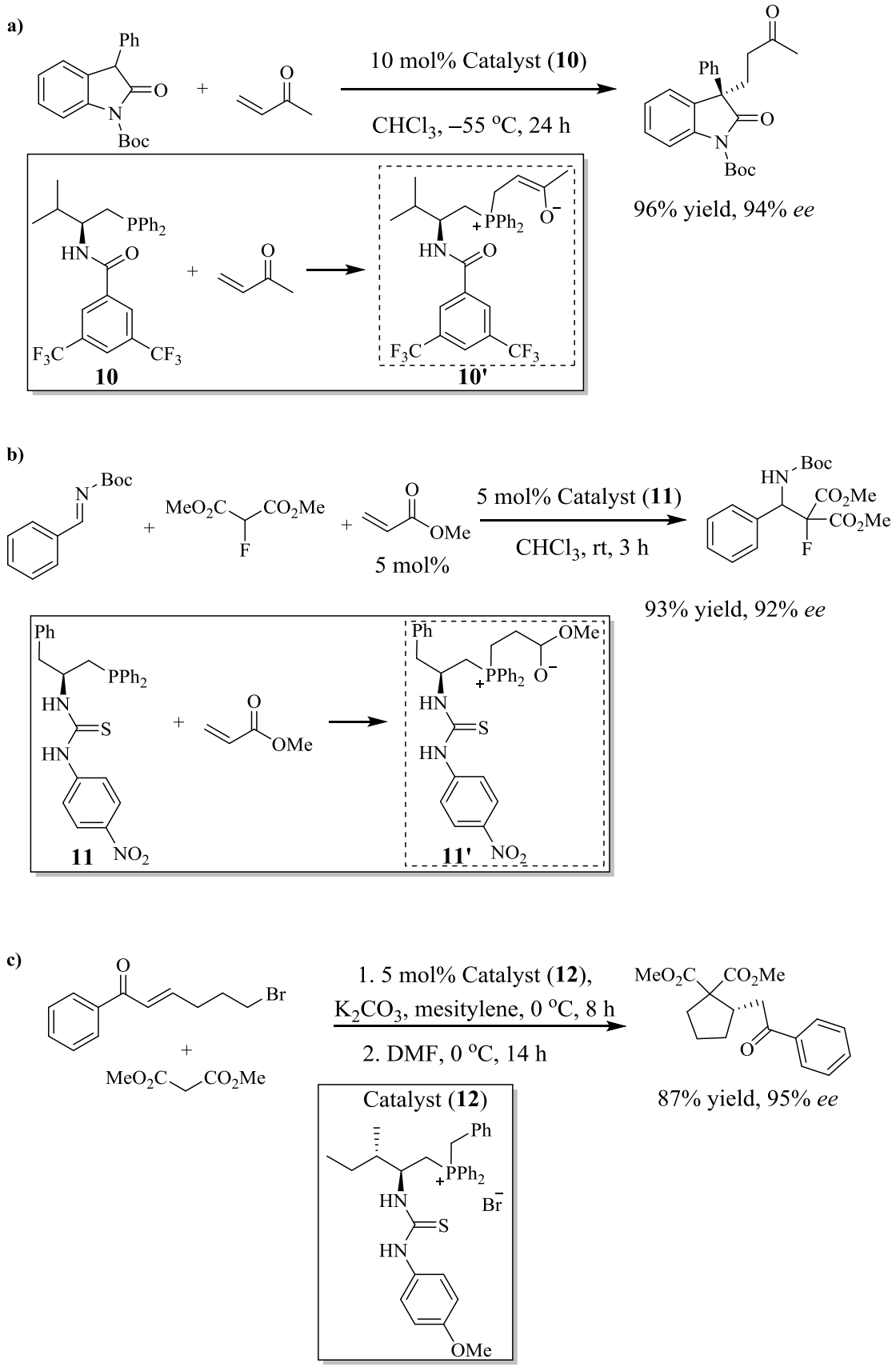

Scheme 1.13 Examples of bifunctional amino acid-derived quaternary phosphonium salts by Lu *et al.* (a)[63] and Zhao *et al.* (b)[64] and (c)[65].

1.3.3.3 Brønsted base catalysis

A Brønsted base (**B:**) can be defined as a molecular entity that can accept a proton from an acid or the corresponding chemical species. Brønsted base catalysis is initiated by a Brønsted base (**B:**) *via* a partial (or sometimes full) deprotonation of the substrate **S-H** to form the intermediates $\mathbf{B^{+}H\text{-}S^{-}}$ and then $\mathbf{B^{+}H\text{-}P^{-}}$. Elimination of the product **P-H** enables the catalyst (**B:**) to re-enter the catalytic cycle (Fig. 1.7).

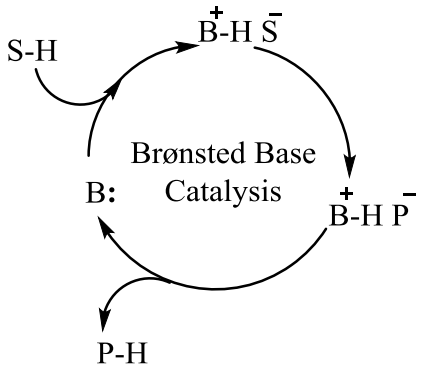

Fig. 1.7 Simplified catalytic mechanisms of Brønsted base catalysis (**B:** = Brønsted base catalyst, **S** = Substrate, **P** = Product, **H** = hydrogen).

Since organic Brønsted bases were recognised as efficient promoters for the formation of carbon-carbon and carbon-heteroatom bonds in organic synthesis,[67] chiral organic Brønsted base catalysis has advanced significantly with the development of both natural and designed catalysts capable of catalytically controlling reaction stereoselectivity.[68] Several nitrogen-containing functionalities have been used for the design of chiral Brønsted bases catalysts, such as tertiary amines, amidines (DBU), and guanidines (TBD) are the most prominent, due to their strongest Brønsted basicity.[67] Among them, the catalytic performance of some guanidines are much better than the other bases, according to the report from Schuchardt *et al.*.[69] In the Brønsted base mechanism, the guanidine accepts a proton from the substrate and catalyzes the reaction as the guanidinium cation. Then the guanidinium cation can either activate the electrophile *via* hydrogen-bonding interactions in a monofunctional mode, or both the electrophile and nucleophile simultaneously in a bifunctional manner (Fig. 1.8).[70]

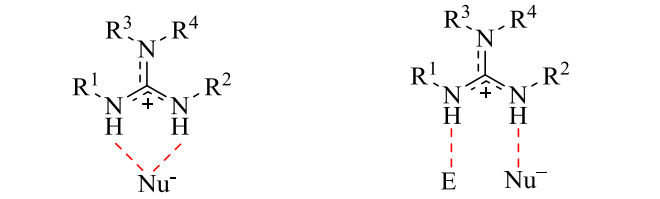

Fig. 1.8 Plausible mono- and bifunctional activation modes of guanidine scaffolds in Brønsted base catalysis (E = electrophile and Nu^- = nucleophile).[70]

With such a unique hydrogen-bonding mode, many chiral guanidine derivatives have been reported in the literature and have been used in various asymmetric reactions.[71] More recently, Ahmad *et al.* reported a novel chiral guanidine derived catalyst (**13**). The new catalyst was evaluated in the Pictet-Spengler reaction of tryptamine to *p*-nitrobenzaldehyde, in which the cyclized product was obtained in good yields with up to 64% *ee* using the additives malonic acid with $BF_3{\cdot}Et_2O$ (Scheme 1.14).[72]

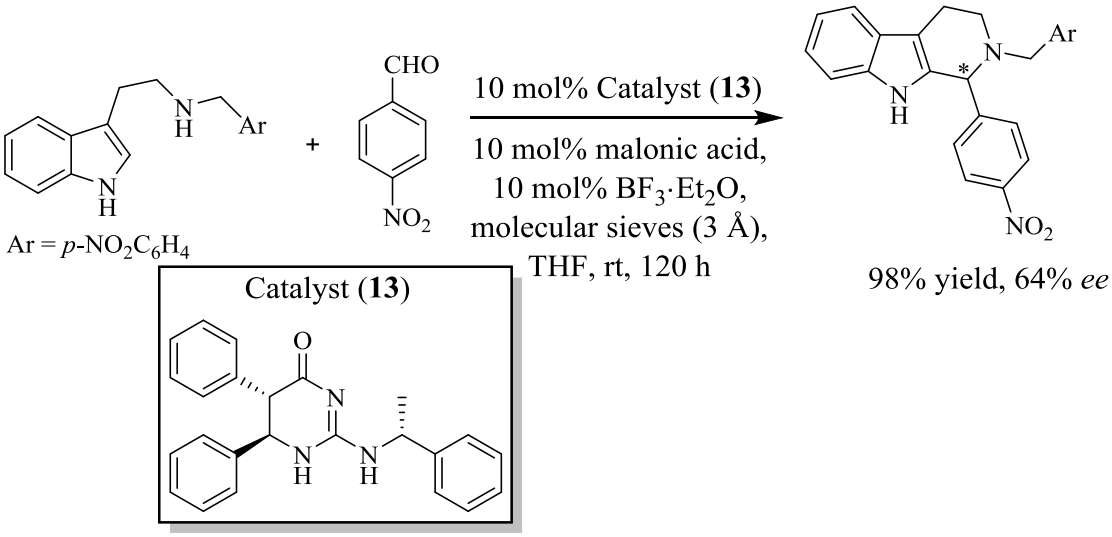

Scheme 1.14 Catalysis of Pictet-Spengler reaction by the novel chiral guanidine derivative (**13**).[72]

Cinchona alkaloids have not only been applied in phase-transfer catalysis, their derivatives can also serve as an active center for Brønsted base catalysis. Cinchona alkaloids are natural templates for Brønsted bases. Their quinuclidine tertiary amine can act as a base to deprotonate a substrate with relatively acidic protons, for example, malonates or thiols, forming a contact ion-pair complex by the reaction with the resulting anion and protonated catalyst. This interaction provides a chiral environment

around the anion and permits enantioselective reactions with electrophiles.[73] In addition, the presence of the C9-hydroxyl group (hydrogen-bond donor site) and tertiary amine (hydrogen-bond acceptor site) enables most cinchona alkaloid derivatives to be employed in asymmetric reactions as bifunctional Brønsted bases catalysts (Fig. 1.9).

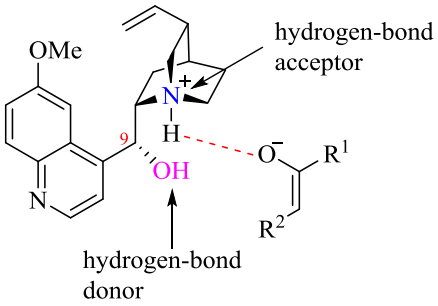

Fig. 1.9 Cinchona alkaloids as catalysts for reactions *via* chiral contact ion pairs.[73]

Palomo *et al.* designed novel cinchona-derived bifunctional squaramide catalyst (**14**) for the direct asymmetric α-functionalization of 2-cyanomethylpyridine *N*-oxide with enone in 100% conversion and up to 92% *ee* (Scheme 1.15), also an improvement on the result from the previous report by Fagnou *et al.* (59% conversion, 10% *ee*).[74] Palomo considered that the *N*-oxide group of the substrate plays a strategic role as a removable activating and stereodirecting element in the conjunction reaction with the new Brønsted base bearing a bulky silyl group.[75]

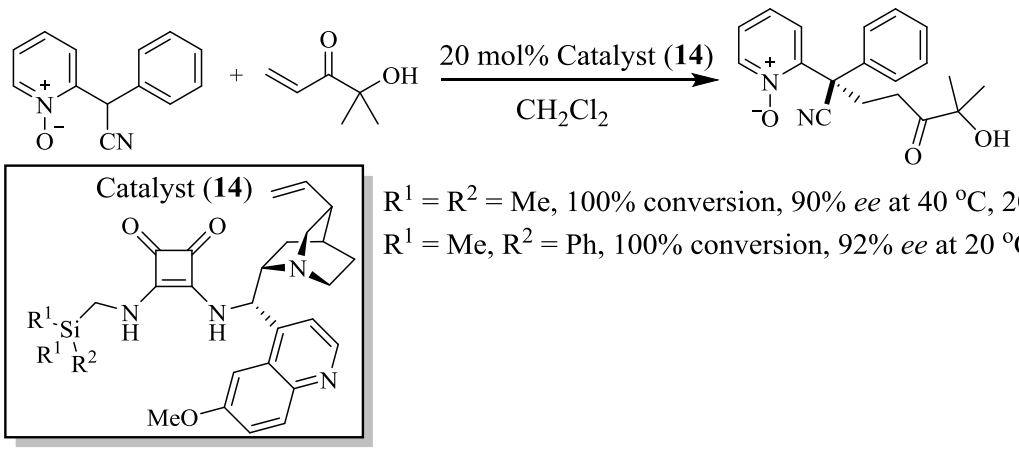

Scheme 1.15 Conjugate addition of 2-cyanomethylpyridine by the novel cinchona-derived bifunctional squaramide catalyst (**14**).[75]

On the other hand, using 2,3-bis(dicyclohexylamino) cyclopropenimine (**15**) as an organo-superbase, Jørgensen *et al.* investigated a novel asymmetric cycloaddition reaction of 2-acyl cycloheptatriene with an azomethine ylide which proceeds as a [3+2] cycloaddition, affording the 1,3-dipolar cycloaddition product in high yield and excellent enantioselectivity (up to 99% *ee*). They proposed that the chiral cyclopropenimine Brønsted base catalyst (**15**) deprotonated the α-proton of the azomethine ylide and forms hydrogen-bonds with the carbonyl moiety of 2-acyl cycloheptatriene. This coordination contributes the stereochemical outcome of the reaction (Scheme 1.16).[76]

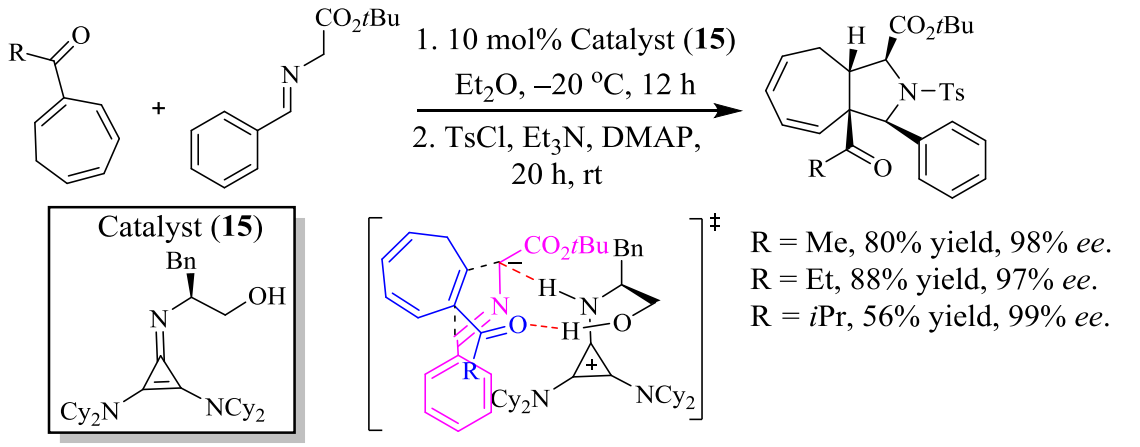

Scheme 1.16 Catalysis of cycloaddition of 2-acyl cycloheptatriene with azomethine ylide by the chiral cyclopropenimine Brønsted base (**15**) and a plausible interaction of the catalyst with azomethine ylide and 2-acyl cycloheptatriene.[76]

1.3.3.4 Brønsted acid catalysis

In contrast to Lewis acid catalysis, Brønsted acid catalysis has become a new type of organocatalysis for a range of enantioselective carbon-carbon formation reactions.[77] Brønsted acids (**A**-**H**) are defined as molecular compounds that are able to lose or donate a proton and initiate a catalytic cycle *via* activation through (partial) protonation of a substrate (**S:**). In general, catalysis by chiral Brønsted acids can be understood by two variations in the mechanism; (1) specific (strong) Brønsted acid catalysis and (2) general Brønsted acid catalysis. Specific Brønsted acid catalysis is where catalysts are strong enough to protonate the substrate fully prior to the subsequent transformation (**a** in Fig. 1.10), such as BINOL derivatives (*i.e.* chiral phosphoric acids). The general Brønsted acid catalysis route is where the catalysts can only partially protonate the transition state of the reaction *via* hydrogen-bonding

interactions (**b** in Fig. 1.10), so it is a characteristic of weak acids, with such catalysts including thioureas/ureas and TADDOL derivatives. As well as being neutral compounds, these catalysts activate carbonyl compounds by hydrogen-bonding, so they are also called hydrogen-bonding catalysts.[78] It is difficult to make a clear distinction between specific Brønsted acid catalysts and general Brønsted acid catalysts, because a catalyst that acts as a specific acid in one transformation may act as a general acid in another.[79] Nonetheless, the relative pK_a value of the Brønsted acid usually indicates the nature of the catalyst.[77]

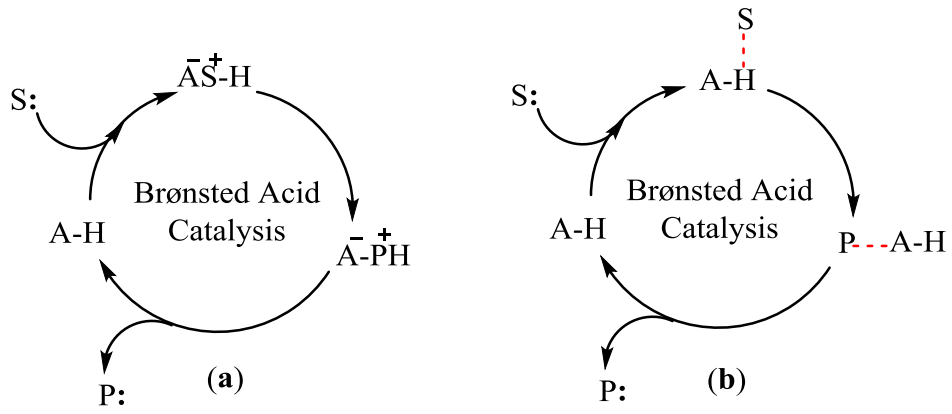

Fig. 1.10 Simplified catalytic mechanisms of Brønsted acid catalysis with a Brønsted acid acting as (a) a proton donor ("specific Brønsted acid") or (b) a hydrogen-bonding donor ("general Brønsted acid"). (**A-H** = Brønsted acid catalyst, **S** = Substrate, **P** = Product, **H** = hydrogen).

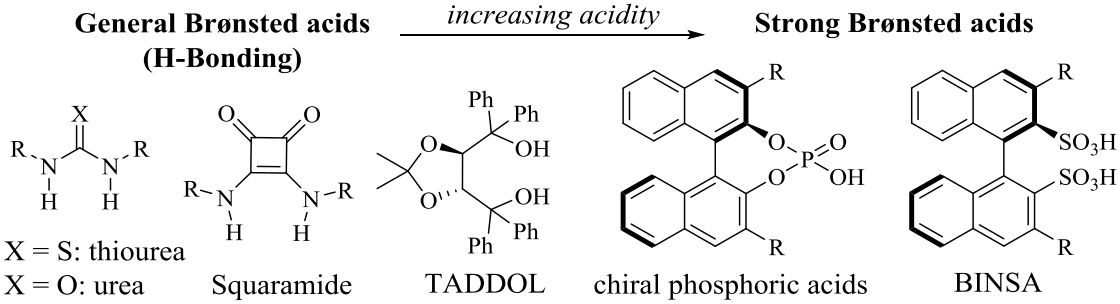

Fig. 1.11 Types of chiral Brønsted acids.[78]

1.3.3.5 Specific (strong) Brønsted acid catalysis

The potential for using relatively strong chiral organic Brønsted acids as catalysts has been largely ignored over the last few decades. Since BINOL and its derivatives were

utilised as important chiral scaffolds in designing organocatalysts,[80] BINOL-derived Brønsted acids have been well developed recently, such as chiral BINSA derivatives, axially chiral dicarboxylic acids. As the first chiral strong chiral Brønsted acid, BINOL-derived chiral phosphoric acids have been used as efficient catalysts for asymmetric reactions, and as useful building blocks for the synthesis of a novel class of organocatalysts.[77]

The pioneering work in the field was conducted by Akiyama *et al.*[81] and Terada *et al.*[82]. They reported relatively strong chiral cyclic phosphoric acid diesters as catalysts (**16** and **17**), which are prepared from a 3,3'-disubstituted BINOL scaffold and are efficient and highly enantioselective catalysts for the Mannich reactions of aldimines (**a** and **b** in Scheme 1.17). Based on Akiyama's work, Terada found that functionalization of the 3,3'-position with bulky substituents can have a dramatic effect on both the yields and enantiomeric excess of the products. Thus, most chiral phosphoric acid-derived catalysts used contain some substitutions at the 3,3'-position and have been found in many asymmetric reactions.[83] More recently, Terada *et al.* reported the first successful enantioselective Mannich reaction of enamide and thiazolone by chiral phosphoric acid containing a 9-anthryl group (**18**) at the 3.3'-positions, which proceeds with high diastereo- and enantioselectivity (**c** in Scheme 1.17).[84]

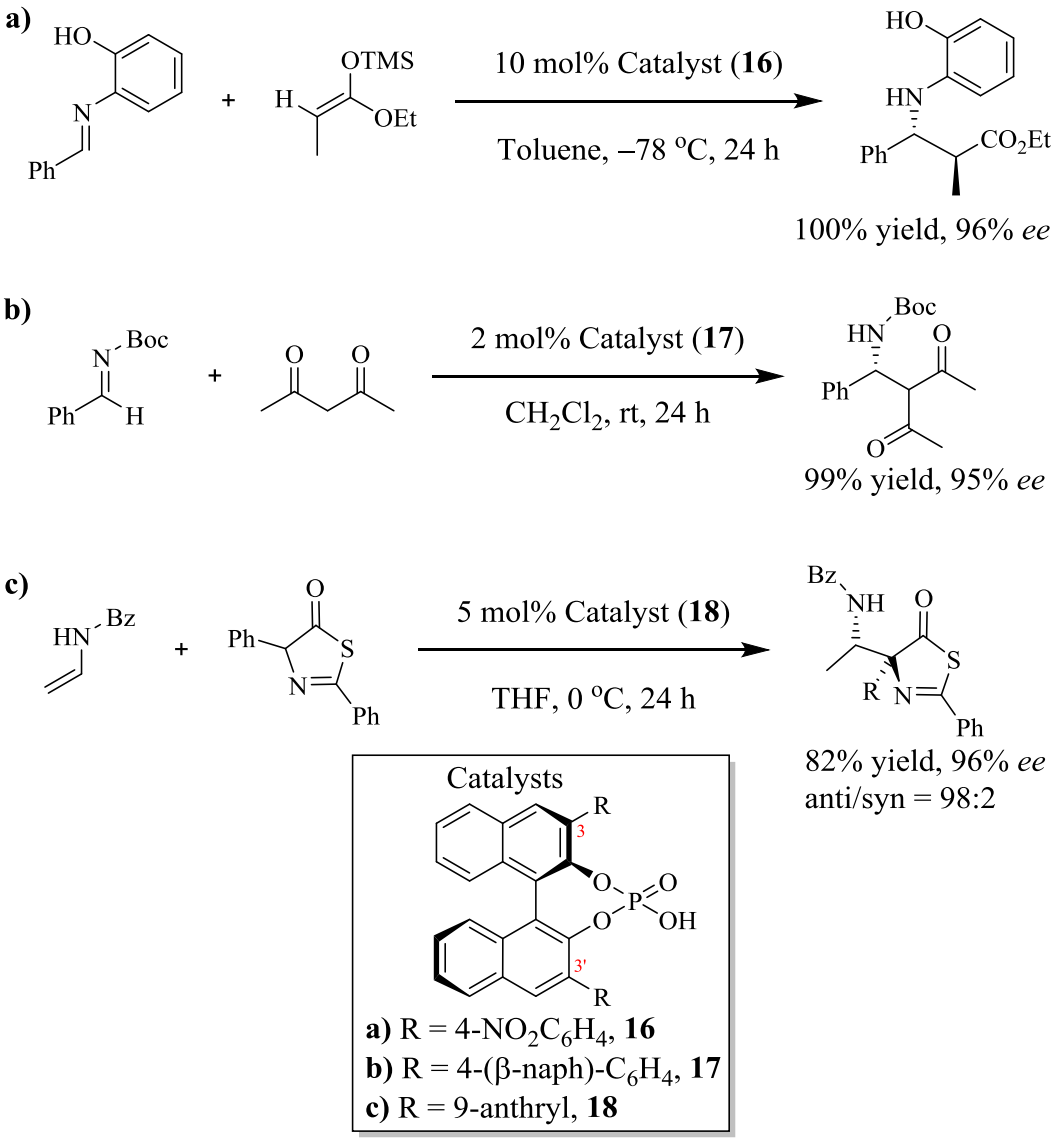

Scheme 1.17 Chiral phosphoric acids reported by Akiyama *et al.*[81] and Terada *et al.*.[82,84]

However, due to the relatively low acidity of chiral phosphoric acids (pK_a = 13.3 in MeCN),[83] their function has been limited to more basic nitrogen-based electrophiles such as imines or aziridines.[85] In order to activate the reaction of aldehydes and ketones by chiral phosphoric acids, Yamamoto *et al.* introduced the *N*-trifluoromethanesulfonyl group into the chiral phosphoric acid to synthesise a new chiral BINOL-derived, *N*-triflyl phosphoramide (**19**) and utilized the stronger Brønsted acid to obtain cyclohexene derivatives with high enantioselectivities from the Diels-Alder reaction of α,β-unsaturated ketones with electron-rich dienes (Scheme 1.18).[86]

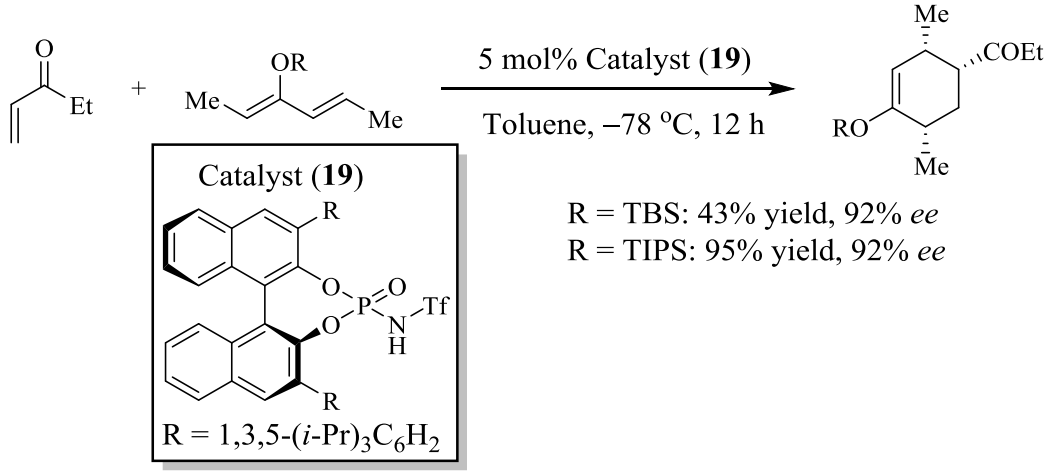

Scheme 1.18 Chiral *N*-triflyl phosphoramide catalyzed Diels-Alder reaction.

N-phosphoramide catalyst (pK_a = 6.4 in MeCN),[83] are more acidic than the phosphoric acids and their derivatives have been used for the reaction in which the substrates are difficult to activate. However, the structural variety of *N*-phosphoramide is less prevalent of this type of catalyst as well as their limited use in many reactions, and most use bulky substituents to achieve high selectivity.[83] Still, more novel *N*-phosphoramide-derived catalysts have been reported recently. For example, List *et al.* synthesised a novel Brønsted acid catalyst imino-imidodiphosphate (**20**), which was derived from the *N*-triflyl phosphoramide (**19**) by Staudinger coupling. The new highly acidic catalyst was successfully utilised for the asymmetric Prins cyclization of aliphatic and aromatic aldehydes, affording the product in high yield with excellent enantiomeric ratio of 95.5:4.5 in high yield (Scheme 1.19).[87]

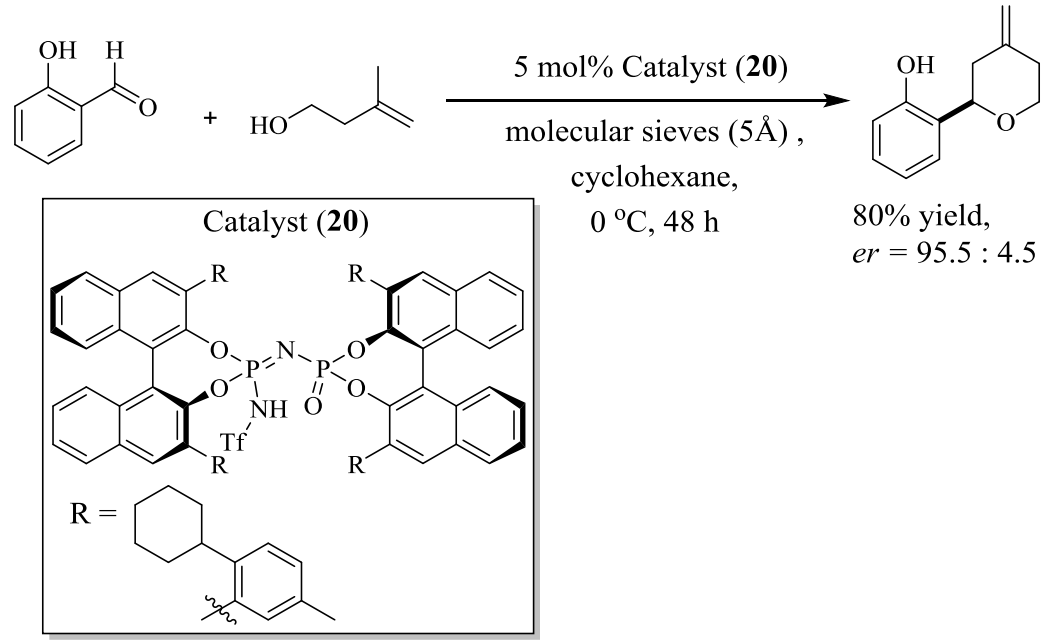

Scheme 1.19 Asymmetric Prins cyclization of aliphatic and aromatic aldehydes by the imino-imidodiphosphate (**20**).[87]

Catalysts prepared from the VANOL/VAPOL ligands have also been found to catalyse asymmetric aziridination of imines efficiently giving high yields and excellent enantioselectivities.[88] Wulff *et al.* employed a similar synthetic method as used to make chiral phosphoric acid, which involved converting a chiral BINOL framework to a chiral phosphoric acid by treatment with $POCl_3$, followed by hydrolysis.[89] The group created new derivatives of VAPOL and VANOL using the biaryl diol ligands VAPOL and VANOL.[90] Using the chiral VAPOL phosphoric acid catalyst (**21**), Liang *et al.* obtained high enantioselectivities and good yields for the addition of imides to imines.[91] However, desymmetrization of *meso*-aziridines by Shawn *et al.* gave relatively low yields and enantioselectivities using the BINOL chiral phosphoric acid catalyst (**22**) (Scheme 1.20).[92]

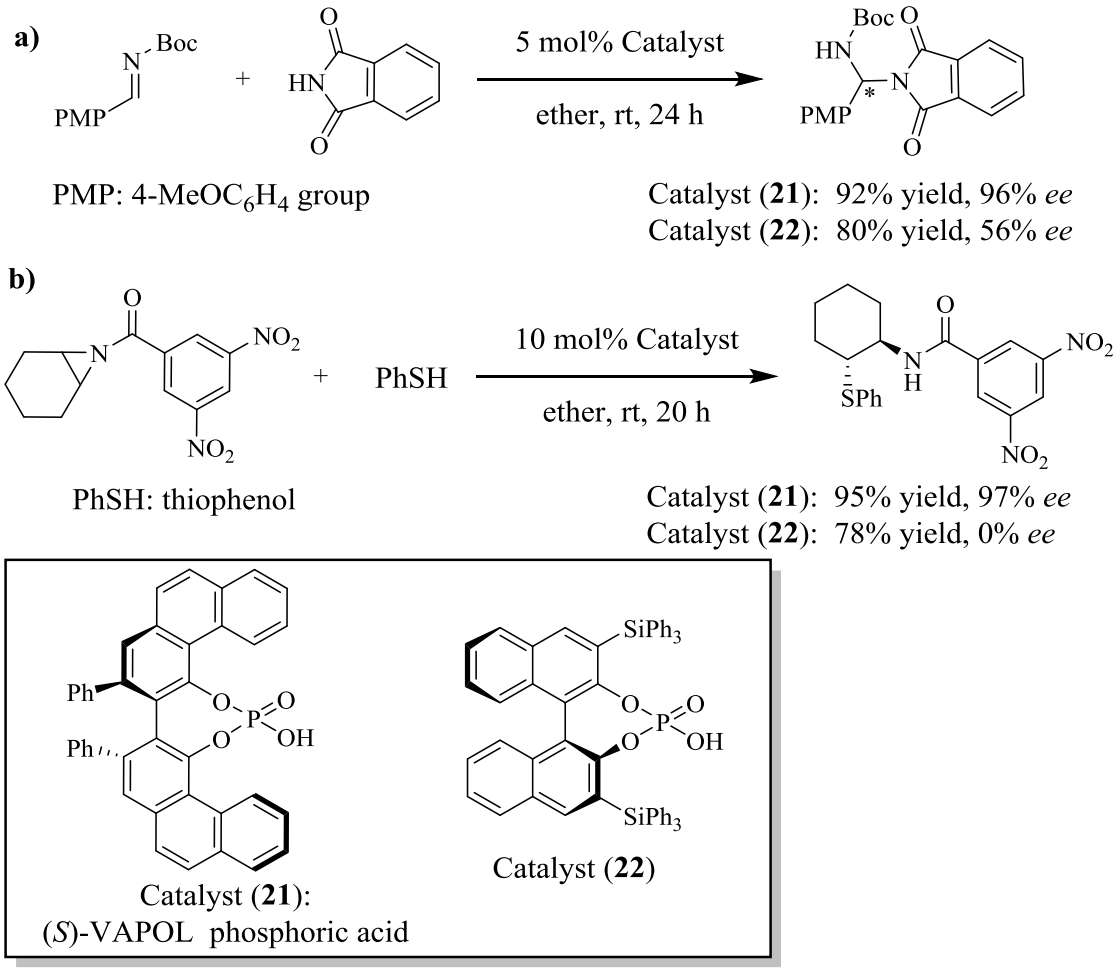

Scheme 1.20 a) Comparison of enantioselectivity between BINOL phosphoric acid and VAPOL phosphoric acid for the addition of substituted phthalimides to *N*-Boc imines.[91] b) Comparison of enantioselectivities between BINOL phosphoric acid and VAPOL phosphoric acid for desymmetrization of *meso*-aziridines.[92]

1.3.3.6 General Brønsted acid catalysis

The general Brønsted acid catalytic process is related to enzymatic catalysis where hydrogen-bonding within a transition state occurs. The majority of hydrogen-bonding catalysts are based on the (thio)urea motif and increasing use of thio(urea)-based catalysts in synthetic reactions has been found in the last decade, most part due to their hydrogen-bonding interactions with negatively charged atoms of the substrates in the transition states.[93]

Use of hydrogen-bonding catalysts began with the promotion of racemic organic reactions. Using X-ray crystallography, Hine showed that donation of hydrogen-bonding by 1,8-biphenylenediol (**23**)[94] to the oxygen atom of Lewis basic substrates, which could effectively active a substrate for a nucleophilic attack in

aminolysis reaction of phenyl glycidyl ether. The subsequent discovery by Etter *et al.* shows that an *N*,*N'*-diarylureas (**24**) co-crystallize with a variety of Lewis basic functional groups, such as nitroaromatics, ethers, ketones and sulfoxides, *via* hydrogen-bonding interactions.[95,96] The donation of two hydrogen-bonds by a single urea molecule to the Lewis base was implicated. A similar dual-hydration model was proposed by computational studies conducted by Jørgensen *et al.* to explain the accelerating effect of water on the Diels-Alder reactions and Claisen rearrangement.[97] These studies provided the basis for the development of (thio)urea-based organocatalysts. Curran *et al.* reported that the outcome of allylation reactions and Claisen rearrangements can be affected by the presence of urea and thiourea, including Etter-type diarylurea (**24A**).[98,99] Based on some of the key features of the thiourea scaffold, such as good solubility in a variety of solvents and the lower electronegativity of sulfur, Schreiner *et al.* carried out an investigation of thiourea derivatives as catalysts for the Diels-Alder reaction of cyclopentadiene and α,β-unsaturated carbonyl compounds in a similar approach used for Lewis acid catalysis. They proposed that the introduction of electron-withdrawing CF_3 group substituents in the *meta*-position of the aryl ring (**24B**) would enhance the catalytic ability by generating a more rigid conformation due to H-bonding between the sulfur atom and the *ortho*-protons by computational modelling.[100]

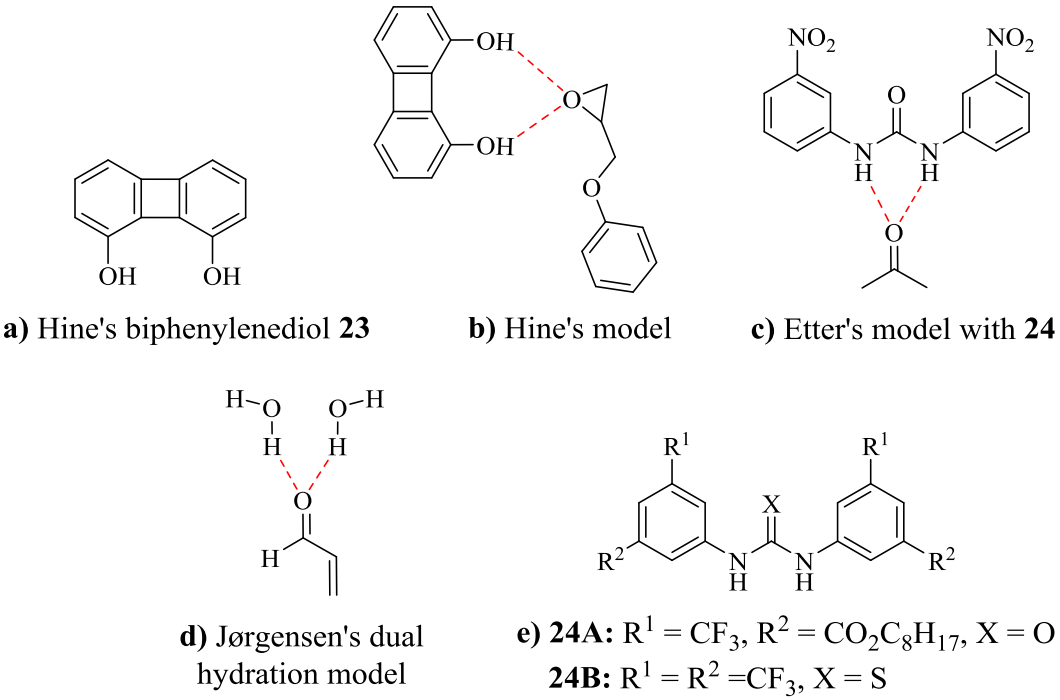

Fig. 1.12 a) Hine's biphenylenediol catalyst (**23**); b) rationale for the catalysis of the in aminolysis reaction by **23** through double hydrogen-bond donation; c) a representation of the binding between Etter's urea catalyst (**24**) and acetone; d) Jørgensen's dual hydration model for explanation of rate enhancement for Diels-Alder reactions and Claisen rearrangement in the presence of water; e) Curran's and Schreiner's (thio)urea catalysts **(24A** and **24B**, respectively).

Based on the structure of bifunctional Schiff base-thiourea (**25** in Fig. 1.13) by Jacobsen[101] and tertiary amine-based thiourea (**26** in Fig. 1.13) by Takemoto,[102] the development of bifunctional amine-based (thio)urea derivatives have created new impulses to the field of organocatalysis. This type of catalysts possesses a thiourea or a urea moiety (hydrogen-donor site) and a basic group such as primary, secondary amine, which not only can activate both nucleophilic and electrophilic reactions simultaneously, but also can control the approach of the substrates stereoselectivity (**b** in Fig. 1.13).[103] More recently, over 30 new primary amine-thiourea catalysts have been developed since 2006 and have emerged as new catalysts for a wide range of enantioselective transformations.[104]

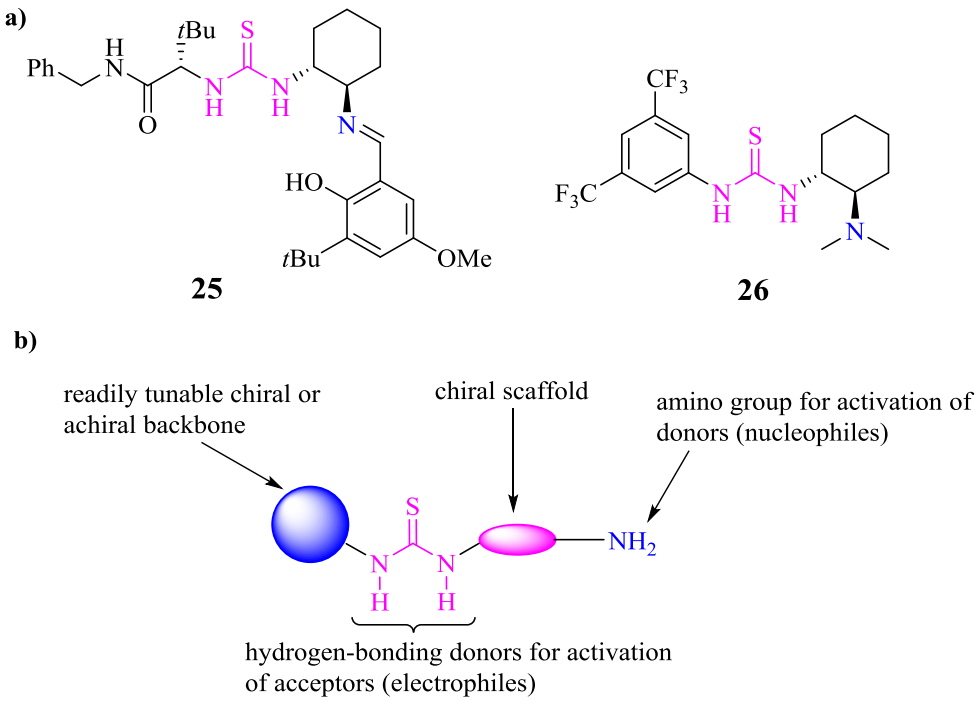

Fig. 1.13 a) Pioneering bifunctional amine-thiourea organocatalysts and b) their general structures.

Jacobsen *et al.* reported a new primary amino-thiourea catalyst (**27**) which enables the formal aza-Diels-Alder reaction of enones and cyclic imines for the enantiostereoselective synthesis of chiral indolo- and benzoquinolizidine compounds (Scheme 1.21).[105] The hydrogen-bond donor and primary amine are essential functional components of the catalyst for simultaneous activation of both the enone and imine reaction components.

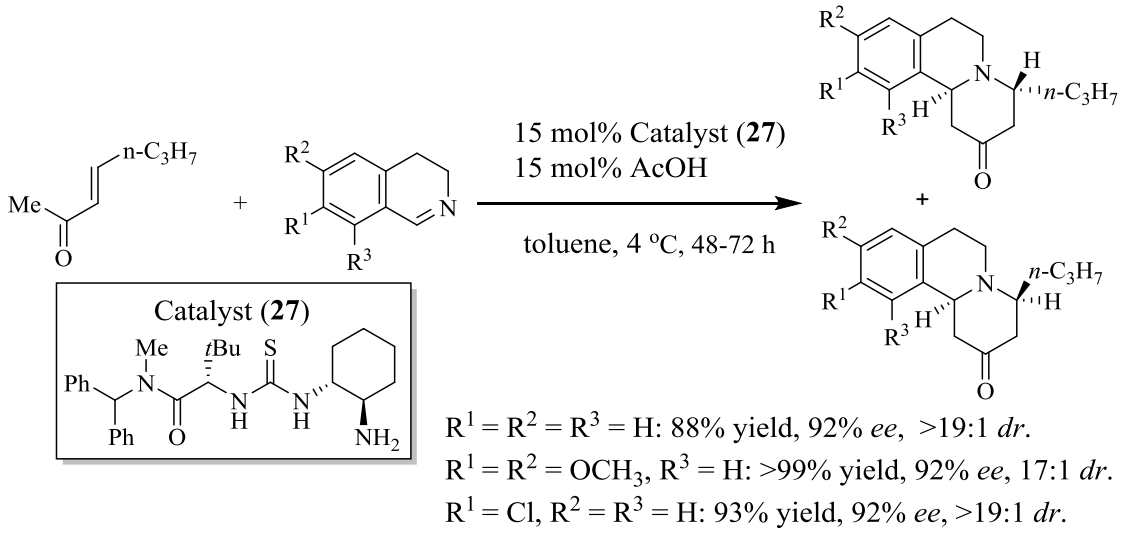

Scheme 1.21 Catalysis of aza-Diels-Alder reaction of enone and 3,4-dihydroisoquinolines by Jacobsen's catalyst.[105]

Recently Wang *et al.* presented the first asymmetric formal thio [3+3] cycloaddition for the construction of optically active thiopyrano-indole annulated heterocyclic compounds in high yields with up to 96% *ee*, using a novel bifunctional tertiary amine-thiourea catalyst (**28**) derived from 1,2-diphenylethane-1,2-diamine (DPEN) (Scheme 1.22).[106] According to density functional theory calculations, the authors confirmed that the high reactivity between indoline-2-thione (keto-*S*) and 2-benzylidenemalononitrile as simultaneous activation of both reactants, leading to form a stable multiple hydrogen-bond complex with the bifunctional thiourea catalyst. Thus, carbon-carbon bond formation step occurs in a highly chiral environment.

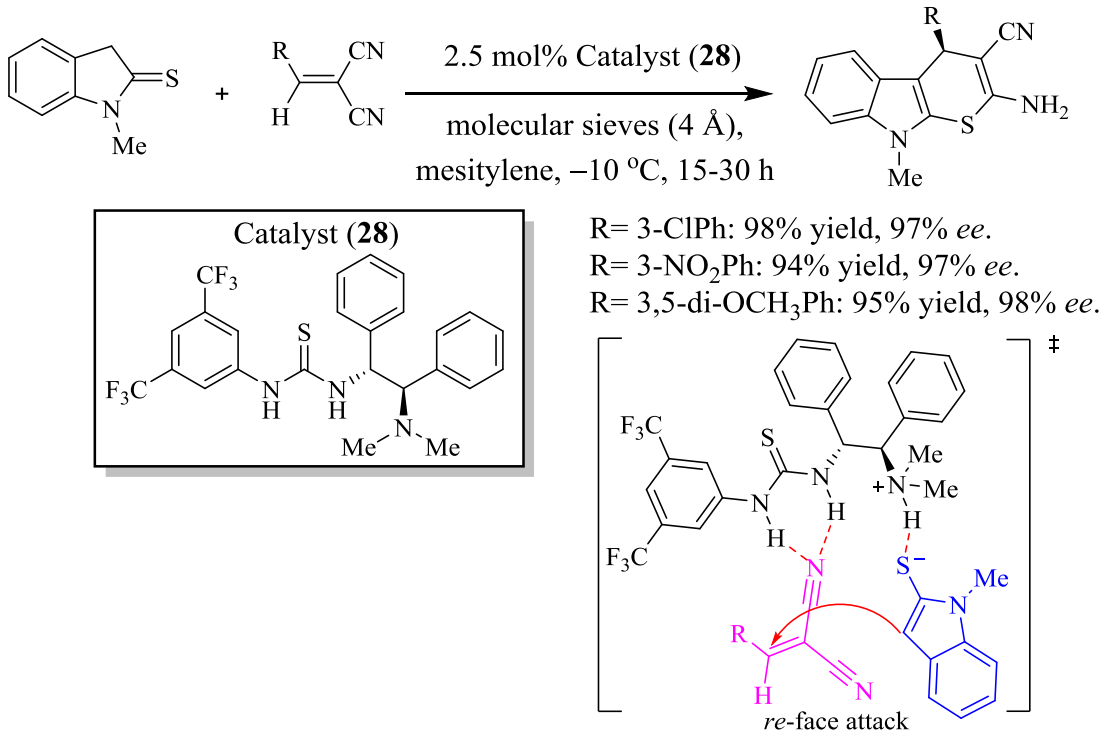

Scheme 1.22 Enantioselective formal thio [3+3] cycloaddition by the DPEN-derived bifunctional tertiary amine-thiourea catalyst (**28**) and the proposed transition-state model.[106]

Regarding various organocatalysts based on the (thio)urea core are broadly utilised in the field of hydrogen-bond donor catalysis,[107] bifunctional squaramide derivatives have emerged as an effective alternative to the urea and thiourea catalyst since they were reported by Rawal *et al.* for a highly enantioselective Michael addition of 1,3-dicarbonyl compounds to nitroolefins.[108] Several studies investigated the squaramide structural difference to the analogous thioureas and ureas. The two NH groups in thiourea, urea and squaramide can act effectively as two hydrogen-bond

donor sites. However, the presence of two carbonyl oxygen atoms in squaramide provides other two-fold hydrogen-bond acceptor sites, whereas there is only one in urea. Thus, the aromaticity of squaramide is enhanced in the presence of both hydrogen-bond accepting anions and hydrogen-bond donating cations (**a** in Fig. 1.14).[109] Therefore, squaramide could be considered as a better binding unit and anion hosts than thiourea and urea.[110,111] Moreover, compared to the counterpart thiourea, the distance between the two NH groups of squaramide (*ca.* 2.72 Å) is about 0.6 Å longer than that of a thiourea (*ca.* 2.13 Å);[108] Both (thio)urea and squaramide have the possibility of delocalizing the nitrogen lone pair, thereby restricting the rotation of C-N bond. However, only in squaramide can further delocalization occur through the cyclobutenedione system (**b** in Fig. 1.14).[112] Thus, the pK_a value of a squaramide[113] is lower compared to their thiourea and urea analogous[114] (**c** in Fig. 1.14), which leads to stronger hydrogen-bonding and increased catalytic activity.[113]

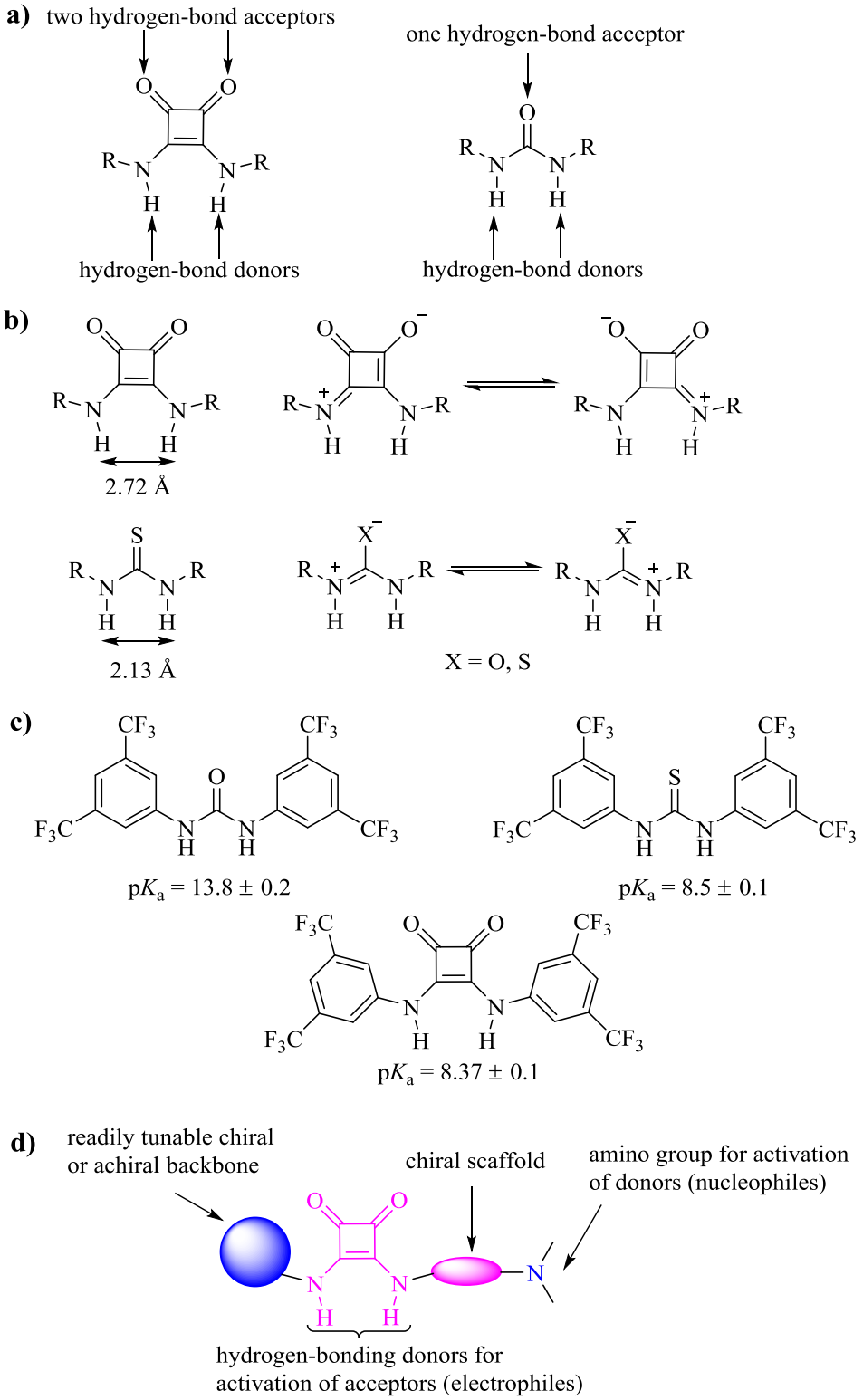

Fig. 1.14 a) and b) Structural difference between the squaramide and the (thio)urea; c) Comparison of pK_a values of (thio)urea and squaramide derivatives in DMSO; d) General structure of squaramide organocatalyst.

Regarding a variety of bifunctional thiourea catalysts incorporating amino functionalities, a squaramide catalyst also contains a chiral scaffold bearing a basic

group (**d** in Fig. 1.14) and most of the squaramide catalysts have been developed with a secondary amine or a tertiary amine as the basic site and been successfully employed in many transformations as bifunctional organocatalysts.[112] For instance, bifunctional pyrrolidine-squaramide catalysts have been mostly reported recently as they were specifically designed for addressing remote reactivity through hydrogen-bond-direct dienamine-mediated catalysis.[115] Jørgensen *et al.* developed the first hydrogen-bond-direct dienamine-mediated [2+2] cycloaddition of α,β-unsaturated aldehydes with nitroolefins using the secondary amine-squaramide catalyst (**29**) derived from 2-aminomethylpyrrolidine.[116] The formation of dienamine between the secondary amine of the catalyst and α,β-unsaturated aldehyde, and simultaneous activation of the nitroolefin through hydrogen-bonding, towards the cyclobutane product bearing a quaternary stereocenter in high yield and excellent enantioselectivity (Scheme 1.23).[116] Moreover, according to the theoretical mechanistic calculation, Jørgensen found that the reaction occurs in a stepwise manner. The first step involves a carbon-carbon bond formation between the γ-carbon of the dienamine and the β-carbon of the nitroolefin (intermediate **A**), followed by the second carbon-carbon formation between the β-carbon of iminium ion and the carbon of the nitro group (intermediate **B**) to form a catalyst-bound cyclobutane intermediate (intermediate **C**).

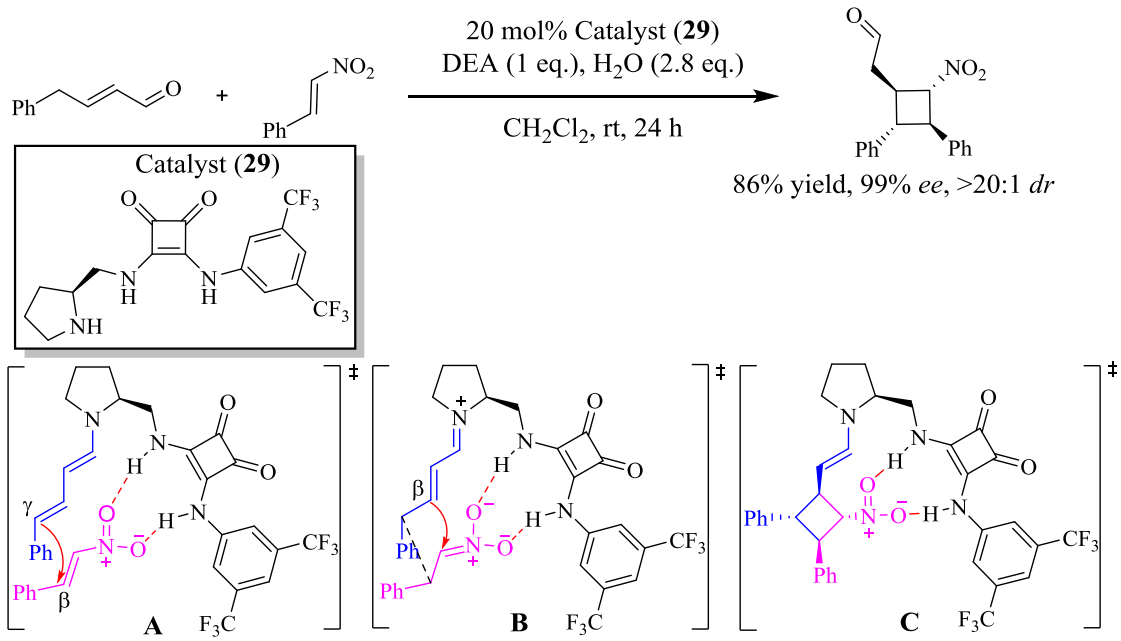

Scheme 1.23 Enantioselective [2+2] cycloaddition reaction of α,β-unsaturated aldehyde with nitroolefin catalyzed by the pyrrolidine-squaramide catalyst (**29**).[116]

Later on, using the same catalyst, Vicario *et al.* established a highly diastereo- and

enantioselective formal [5+2] cycloaddition of oxidopyrylium ylide and enal. The mechanistic study shows that a dienamine intermediate is formed after condensation of the enal with the catalyst (**29**), which raises the HOMO energy of the dipolarophile. Thus, creating an exclusive β,γ-reactivity provided direct access to the product contain an 8-oxabicyclo[3.2.1]octane moiety in high yield with excellent diastereo- and enantioselectivity (Scheme 1.24).[117]

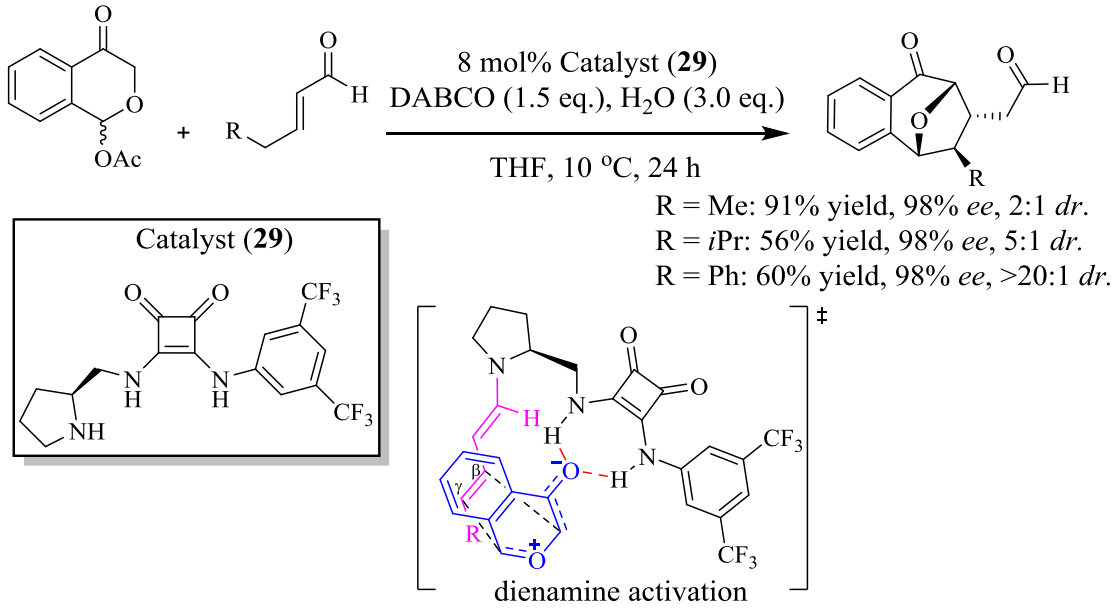

Scheme 1.24 Enantioselective [5+2] cycloaddition between oxidopyrylium ylides and enals *via* dienamine activation catalyzed by the pyrrolidine-squaramide catalyst (**29**).[117]

More recently, Li *et al.* reported a highly enantioselective asymmetric addition reaction of thioglycolates and *N*-Boc aldimine was promoted by a tertiary amine-squaramide catalyst (**30**) to furnish *N*,*S*-acetal derivatives in high yield and excellent enantioselectivity (Scheme 1.25).[118] According to the absolution configuration of product, the author proposed the *N*-Boc aldimine is activated and orientated by the hydrogen-bonds of the squaramide catalyst, simultaneously the tertiary amine of the catalyst provide suitable basicity to enhance the nucleophilicity of the thioglycolate.

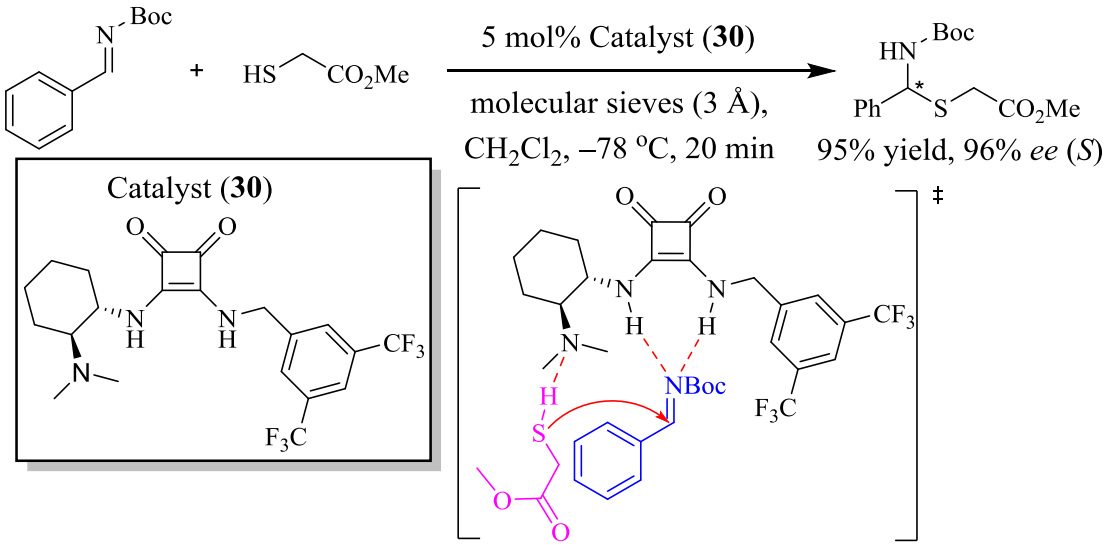

Scheme 1.25 Asymmetric addition reaction of *N*-Boc aldimine and thioglycolate catalyzed by the bifunctional tertiary-amine squaramide catalyst (**30**).[118]

1.4 Bifunctional chiral phosphoric acids

1.4.1 Catalysis by acids

Brønsted acids have been widely utilised as catalysts for numerous organic transformations. Although acting as catalysts, Brønsted acids still have some disadvantages in carbon-carbon bond formation reactions, such as high catalyst loading and undesired side reactions.[119] Development of novel Brønsted acid catalysts has been continuously studied due to their broad synthetic applicability. The majority of the early research was to develop highly active Brønsted acids, known as superacids, which can generate unstable and highly reactive protonated intermediates.[119]

As mentioned earlier it is expected that interactions with Brønsted acids, such as hydrogen-bonding, are suppressed between the conjugate base ($\mathbf{A}^-$) and the protonated substrate intermediate ($\mathbf{S}^+\mathbf{H}$) (Fig. 1.15).

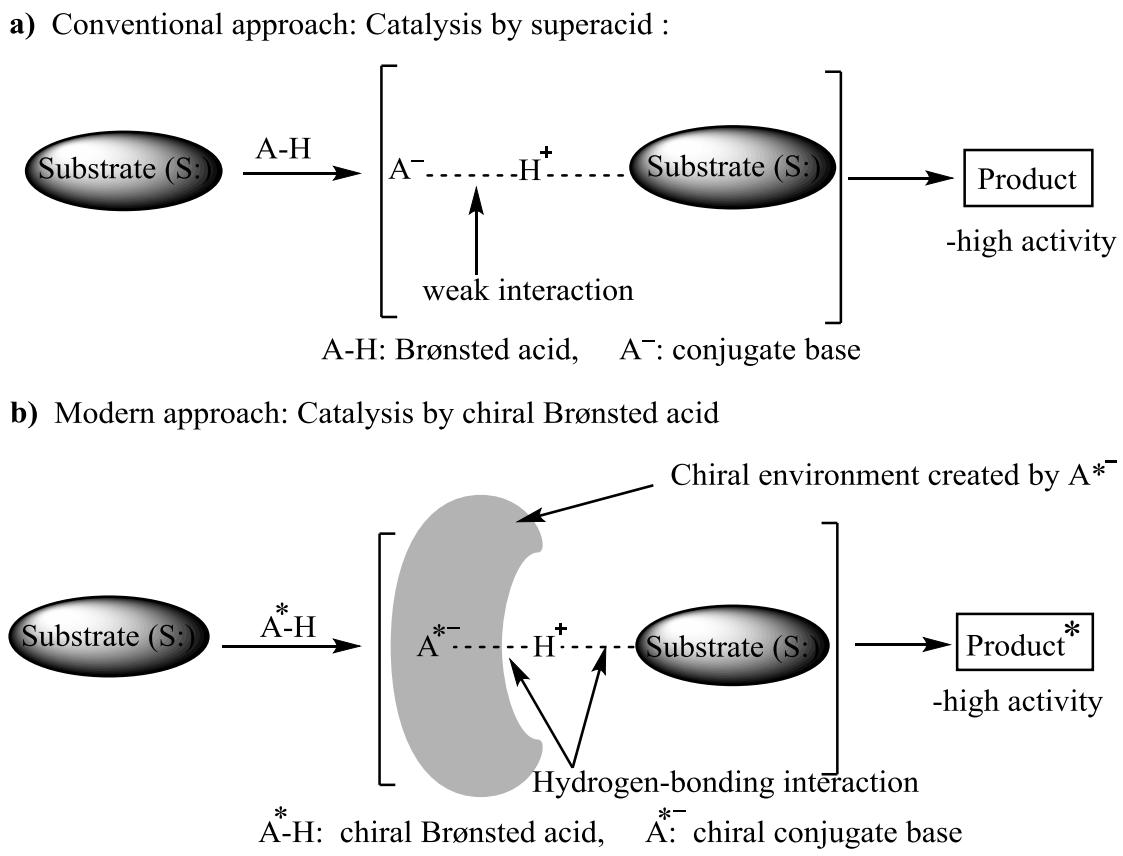

Fig. 1.15 Brønsted acid and chiral Brønsted acid catalysis in organic transformations.[120]

Previously it was considered that Brønsted acids would only activate a substrate (**S**:) by protonation. Therefore, the conjugate base (**A**$^-$) would be expected to only influence catalytic activity, rather than taking part in the selective formation of products. After focusing on studies of chiral Brønsted acid catalysis, in which enantiomeric products are obtained using a catalytic amount of a chiral organic molecule bearing an acidic functionality,[121] the hydrogen-bonding between the conjugate base (**A***$^-$) and the protonated substrate intermediate (**S**$^+$**H**) was determined to be the key to enantioselective catalysis.[120] Therefore, the organic transformations proceed under a chiral environment created by the chiral conjugated base (**A***$^-$), which remains in the vicinity of the substrate through a hydrogen-bonding interaction.[120] In other words, when the Brønsted acid has donated its proton to the substrate (**S:**), the conjugate base (**A***$^-$) remains to create the chiral environment for the subsequent bond-forming step (Fig. 1.15).

Since the first example of chiral Brønsted acid catalysis was reported by Jacobsen *et al.* in the enantioselective Strecker reaction catalyzed by peptide-based thiourea

derivatives as hydrogen-bond-donor catalysts,[101,122] enantioselective catalysis by chiral Brønsted acids has become of great interest. With development of chiral Brønsted acid catalysis, the binaphthol-derived chiral phosphoric acid class of molecules was discovered and has emerged as an attractive and applicable class of enantioselective organocatalysis for numerous organic transformations.

1.4.2 Structural features of chiral phosphoric acids

Many reactions using BINOL-derived phosphoric acids have been mention previously. Several features of this type of catalyst are essential for efficient asymmetric transformations:[120]

- Phosphoric acids are expected to capture electrophilic components through hydrogen-bonding interactions without the formation of loose ion-pairs due to their relatively strong but appropriate acidity, for example, the pK_a of $(EtO)_2P(O)OH$ is 1.39.
- Besides the acidic proton on the Brønsted acidic site, the phosphoryl oxygen on the Brønsted basic site can act as a hydrogen-bonding acceptor, so that it would convey acid/base dual function even for monofunctional phosphoric acid catalysts.
- When a ring structure is introduced to the phosphoric acid, an acidic functionality is still available. The ring system prevents the free rotation at the α-position of the phosphorus center.
- A substituent group (STG) can be introduced into the ring system to provide a chiral environment for enantioselective transformations (Fig. 1.16).

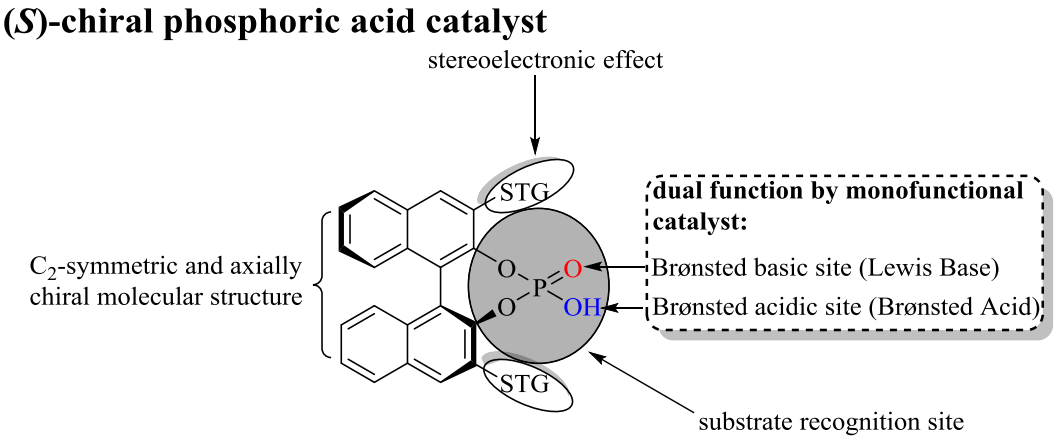

Fig. 1.16 Description of structure of (*S*)-chiral phosphoric acid catalyst.[120]

As mentioned above, it is anticipated that an efficient substrate recognition site could be constructed around the activation site of the phosphoric acid catalysts, namely the acidic proton, as a result of the acid/base dual function and the stereoelectronic influence of the substituents (STG). Binaphthol (BINOL) is well known as an axially chiral molecule having C_2-symmetry, and derivatives have been extensively utilised as chiral ligands for metal-catalyzed reactions.[123] Thus, BINOL derivatives were selected as chiral sources to assemble the catalyst with the advantage that both enantiomers are commercially available and numerous protocols for introducing substituents at 3,3'-position of the binaphthyl scaffold are known.

1.4.3 Catalysis of Mannich reaction by a chiral phosphoric acid

The enantioselective Mannich reaction is one of carbon-carbon bond formation reactions for the synthesis of chiral compounds containing nitrogen, such as optically active β-amino carbonyl compounds, which are a versatile resource for preparation of biologically active natural products and drug candidates.[124] L-Proline and peptides were discovered to have the excellent catalytic ability for Mannich type reactions.[125] The mechanism of the Mannich reaction begins with the formation of an iminium ion, which is generated from the reaction between an amine and formaldehyde. A carbonyl-containing compound, such as a ketone, can tautomerize to the enol form and then attack the iminium ion to give the product. Scheme 1.26 shows the proposed mechanism of the Mannich reaction catalyzed by acid.

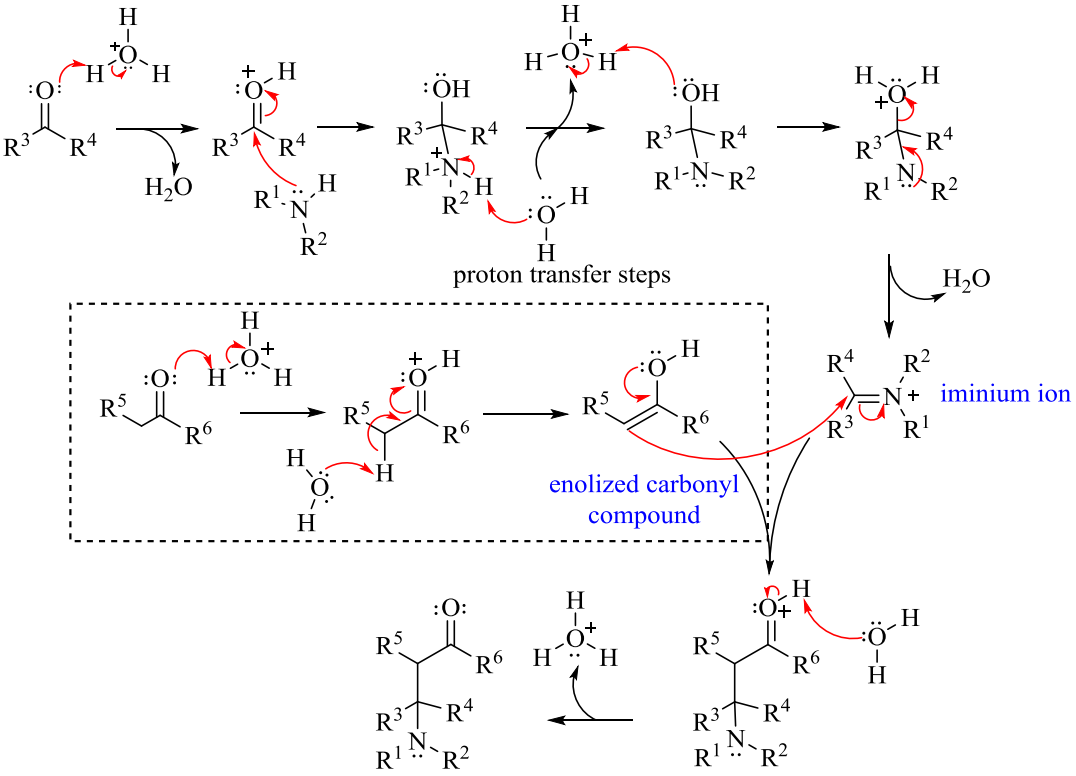

Scheme 1.26 Proposed mechanism of Mannich reaction catalyzed by acid.[126]

The exact mechanism of a chiral phosphoric acid catalyzed-Mannich reaction is not a straightforward procedure, because there are a large number of possible interactions that may take place between the catalyst and the substrates used in the reactions. Since BINOL derived phosphoric acids were developed by Akiyama *et al.* and Terada *et al.*, they disclosed the stereochemical outcome of Mannich reaction using different reaction modes.[83]

Akiyama *et al.* developed a chiral cyclic phosphoric acid diester catalyst (**16)** starting from (*R*)-BINOL and applied this catalyst to the Mannich reaction of ketene silyl acetal with aldimine to form β-amino esters (Scheme 1.27). Good *syn* diastereoselectivity and high enantioselectivity (up to 96% *ee*) were observed and they found that the introduction of 4-nitrophenyl groups on the 3,3'-position exhibited two enhancements: improvement of enantioselectivity and acceleration of the reaction rate. It was proposed that the reaction proceeded *via* an iminium salt generated from the aldimine and that the 3,3'-diaryl groups shielded the phosphate group, resulting in asymmetric induction. Akiyama also explained the reaction mechanism using density functional theory calculations. According to the results of the calculations, he disclosed

that the reaction occurs by a double hydrogen-bonding activation (dual activation mode), in which the acidic proton on the Brønsted acidic site of the catalyst activates the imine by protonation, and an additional hydrogen-bonding interaction between the phenol proton of the imine and the Lewis basic site of the catalyst. Thus, the resulting in the formation of the intermediate complex (**A**) between the catalyst and the imine, which provides a rigid and stronger chiral environment around the substrate.[83,127]

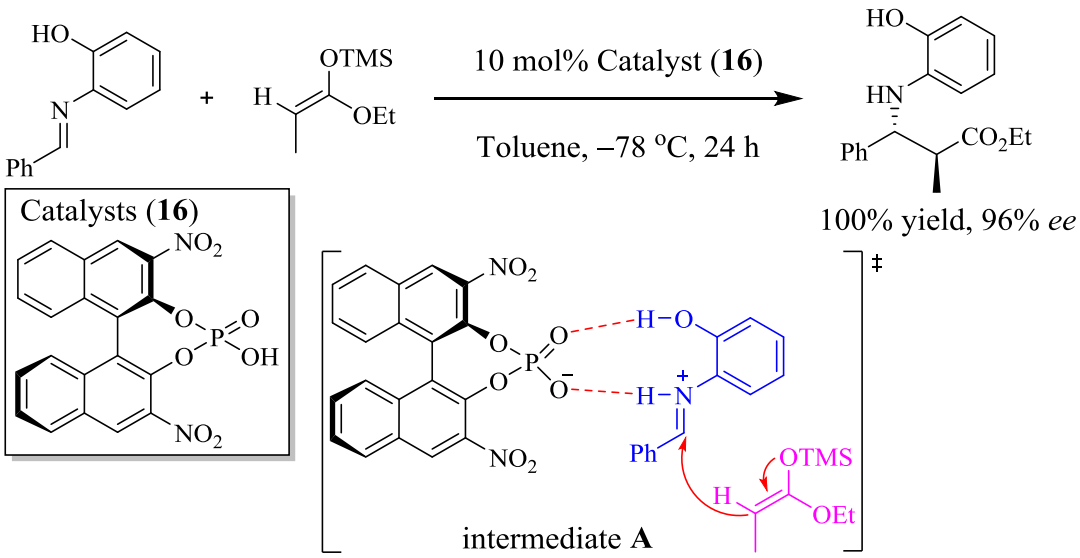

Scheme 1.27 Mannich reaction of ketene silyl acetal with aldimine catalyzed by **16** *via* a dual activation mode.[83,127]

In parallel, Terada *et al.* reported that the highly enantioselective direct Mannich reaction of *N*-Boc imine and acetyl acetone catalyzed by the chiral phosphoric acid catalyst (**17)** (Scheme 1.28). They considered that the reaction proceeds through bifunctional activation, which leads to generate two possible intermediates between the catalyst and reactant through hydrogen-bonding. One is from between the enol proton of the acetyl acetone tautomer and the phosphoryl oxygen of Brønsted basic site of the catalyst, the other is formed by the interaction of OH group on the Brønsted acidic site of the catalyst with the nitrogen atom of *N*-Boc imine having two possible orientations.[121] Subsequently, *N*-Boc imine is activated by the catalyst through the acidic proton, meanwhile, the phosphoryl oxygen interacts with the OH group of the enol, resulting in the formation of two possible intermediate **B** and **B**', respectively. Due to the close contacts of the Boc group of the imine with biphenyl substituents of the catalyst to prevent the free rotation around the hydrogen-bond, intermediate **B** is more likely to give the excepted configuration of product.[83,128]

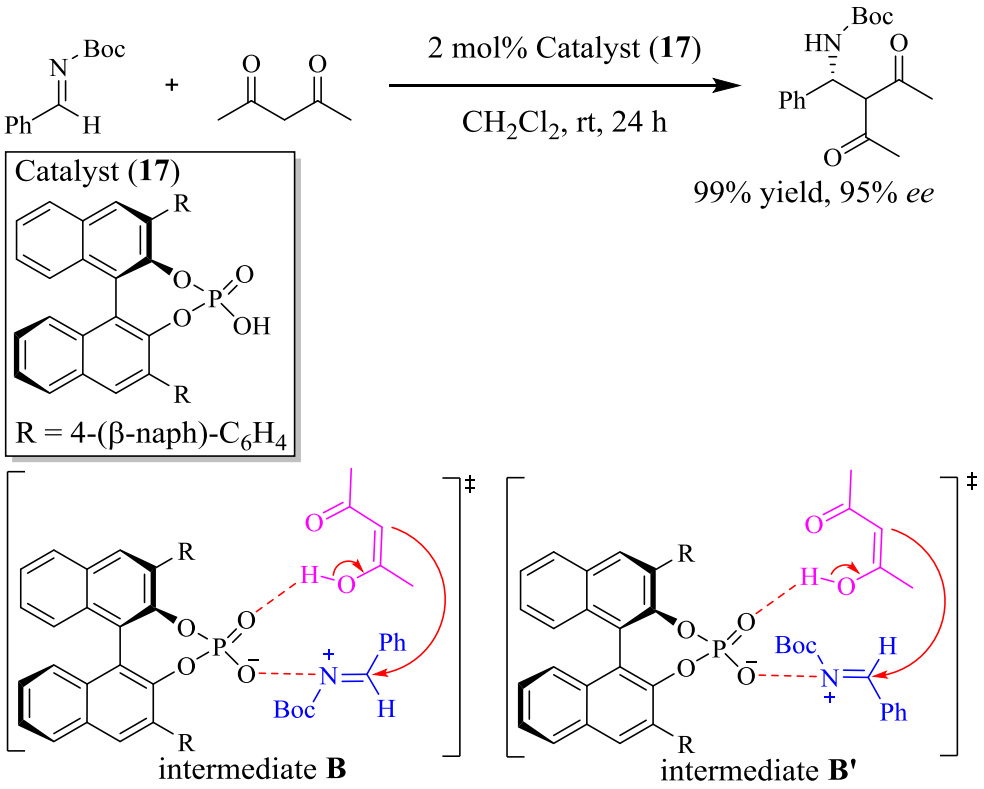

Scheme 1.28 Mannich reaction of *N*-Boc imine and acetyl acetone catalyzed by **17** *via* a bifunctional activation mode.[83,121]

In addition to the dual and bifuntional activation modes, the mono activation by single contact for the Mannich reaction has been also reported. For instance, Rueping *et al.* developed the first enantioselective domino Mannich–ketalization reaction of 2-hydroxyphenyl imines with cyclic enol ethers. In the presence of *N*-triflylphosphoramide derivative (**31**), formation of an intermediate **C** by mono activation of the imine leads to stereoselective addition of the enol ether followed by cyclization of the hydroxyl group, resulting in 4-aminobenzopyran product in good yields with excellent enantioselectivities.[83,129]

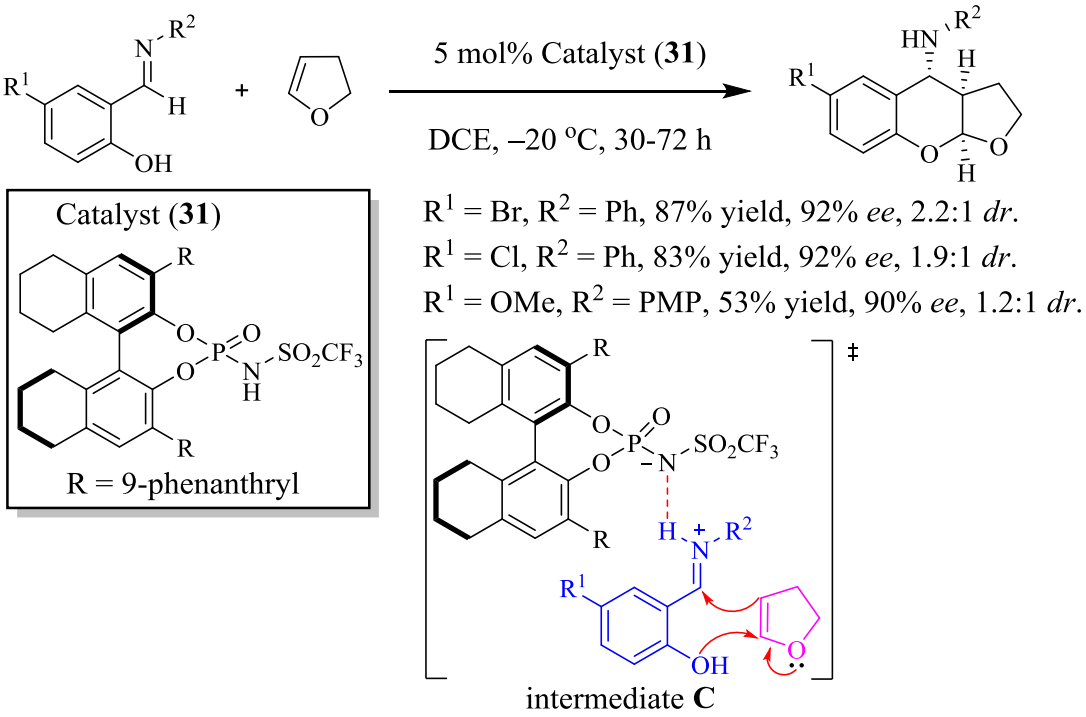

Scheme 1.29 Enantioselective domino Mannich–ketalization of 2-hydroxyphenyl imines with cyclic enol ethers catalyzed by **31** *via* a mono activation mode.[83,129]

1.5 Cinchona alkaloid-based thiourea and urea derivatives

1.5.1 The cinchona alkaloids

Alkaloids are a group of naturally occurring chemical substances and most originate from plants. Most alkaloids contain carbon, basic nitrogen substituents, and oxygen. They are usually used as drugs with pronounced effects on the nervous systems of humans and animals, for example, caffeine, cocaine and morphine.[130]

Cinchona alkaloids are natural products found in the bark of several species of cinchona trees. In the early 17th century, extracts from powdered bark of the cinchona species, such as quinine, were used for the treatment of malaria until it was replaced by synthetic analogues, for example, chloroquine and primaquine.[131] Having over 300 years of medicinal roles in human society, approximately 700 metric tons of cinchona alkaloids are extracted from cinchona bark annually, nearly half of which is used in the food and beverages industry as a bitter additive. The rest of the remaining quinine and quinidine is still used as an important antimalarial drug scaffold, muscle relaxant, and a cardiac depressant.[132]

Cinchona alkaloids contain five chiral centers (N1, C3, C4, C8 and C9), two basic molecular units, two rigid ring moieties (an aromatic quinoline ring and aliphatic quinuclidine ring as a tertiary amine), and a methylenic alcohol group linking the two. The studies on structural features of cinchona alkaloids have been summarized recently (Fig. 1.12):

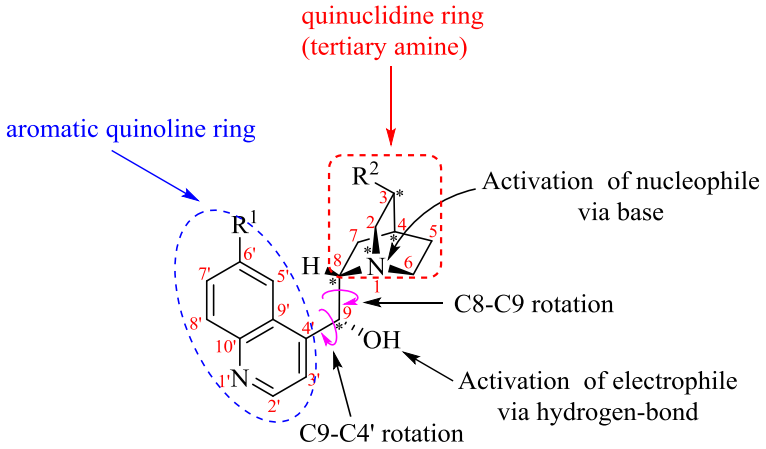

Fig. 1.17 Structure of cinchona alkaloids.

1. The relative position adopted by the bulky ring systems of quinoline and quinuclidine possibly generates a rigid chiral pocket around the substrate, which enforces enantioselective induction during organic reactions.[133]
2. Free rotation around the linker atoms C8-C9, which create a dynamic environment, provides many conformations with different stabilities and abilities to impart enantioselectivity in a given catalytic process.[134]
3. The quinoline aromatic ring contains a potential secondary binding site and acts as a site for adsorption onto solid surfaces in heterogeneous catalysis. This flat aromatic ring could enable the formation of donor-acceptor complexes with electron-deficient molecules due to the electron-donating abilities.[133]
4. The C9-stereogenic center makes diastereomers available, which provide access to both enantiomers of a product with almost identical selectivity. The free hydroxyl group on the C9 plays an important role for high catalytic reactivity and selectivity.[135]

Over the past 30 years, the cinchona alkaloids have been studied mainly for being efficient chiral reagents, chiral auxiliaries and privileged catalysts. Various cinchona

alkaloids and their derivatives have been synthesised and utilised as catalysts in many asymmetric reactions to give a variety of enantiopure products.[136] For instance, the application of cinchona alkaloid derivatives in phase-transfer catalyst and Brønsted base catalysis has been mentioned early.

1.5.2 Cinchona alkaloid-based thiourea, urea and squaramide derivatives

The developing concept of bifunctional catalysts using the natural cinchona alkaloids has resulted in the design and synthesis of the novel cinchona derivatives for asymmetric reactions. Urea- and thiourea-substituted cinchona alkaloid derivatives represent a large and dominant platform for the hydrogen-bonding promoted asymmetric catalysis, and recently followed by incredible growth in the form of squaramides.[137] Since Takemoto reported the high enantioselective Michael addition of dimethyl malonate to nitroolefins using the first bifunctional amine-thiourea (**26** in Fig. 1.13), the significant progress of design and application of new bifunctional cinchona alkaloid based-thioureas/ureas have been made by the groups of Chen, Soós, Connon and Dixon, respectively (Scheme 1.30).[138] Following the structure of Takemoto's thiourea (**26**), they designed the first cinchona derived thiourea catalysts by modification of C9-hydroxyl group of the cinchona alkaloid starting materials for promoting different asymmetric conjugate and Michael additions. Soós *et al.* reported a highly enantioselective Michael addition of nitromethane to chalone using catalyst (**32**). Using the same catalyst, Connon *et al.* found high enantioselectivities and yields in the Michael addition of malonate into nitroalkenes. Dixon *et al.* reported high selectivities in the same reaction with comparable results, employing the catalyst (**33**) which shows high activity but moderate enantioselectivity in the Michael addition of thiophenol to α,β-unsaturated imide reported by Chen *et al.*.[138] Based on their pioneering work, C9 epimeric cinchona alkaloid catalysts show more effective (higher activity and selectivity) than analogues from natural stereochemistry cinchona alkaloids.

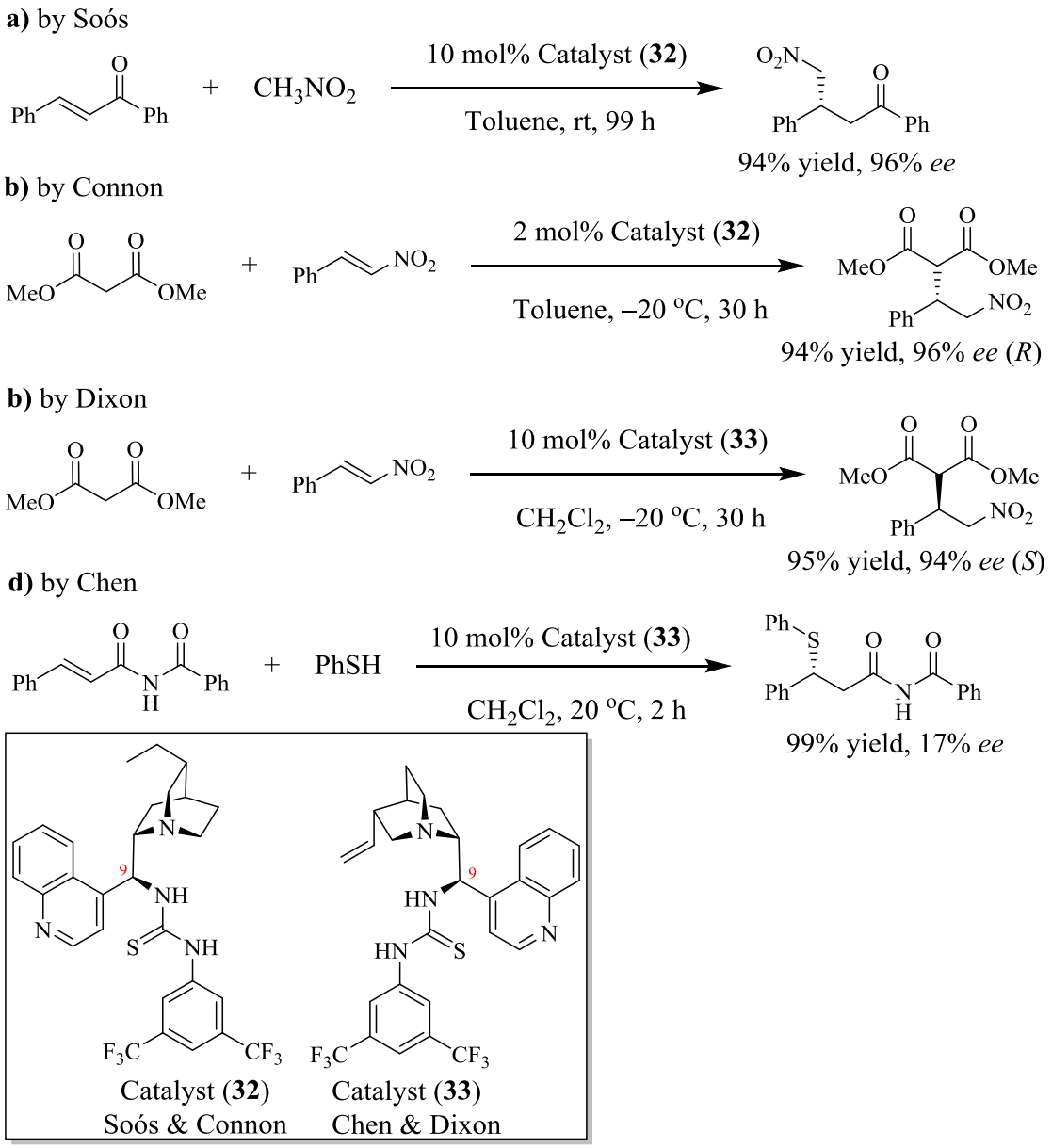

Scheme 1.30 The pioneering work of cinchona derived thiourea catalysts in conjugate addition reactions.[138]

Due to the similar functional groups which cinchona derived thiourea derivative (**32**) and Takemoto's thiourea (**26**) share, the catalytic activities of both thioureas are very similar. As shown in Fig. 1.18, the thiourea moieties in **32** and **26** provide double hydrogen-bonding interactions to coordinate and activate electrophile (hydrogen-bonding acceptor), while the tertiary amines in both compounds activate nucleophile by deprotonation.

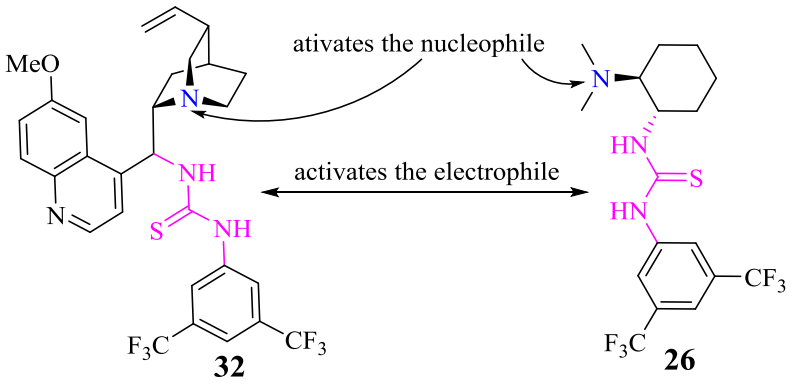

Fig. 1.18 Comparison of cinchona alkaloid-based thiourea (**32**) and Takemoto's thiourea (**26**).

Based on these early examples of bifunctional cinchona derived thiourea catalysts, there has been a great advance in designing novel thioureas and ureas for synthetically useful organic transformations. Han *et al.* developed the first enantioselective nitro-Mannich reaction of 5*H*-oxazol-4-ones with various alkyl and aryl sulfonamides using cinchonine-derived urea (**34**). They found the different substituted groups on the aromatic rings of imines did not affect the reaction rate and enantioselectivity, but the substituents at the nitrogen atom of imines affected the diastereoselectivity. Hence, the *N*-TIPBs-alkylimines generated the product β-alkyl-substituted α-hydroxy-β-amino acids in the good yields with excellent diastereo- and enantioselectivities. Base on the successful initial work, the authors also scaled up the reaction to the gram scale without compromising the enantioselectivity (Scheme 1.31).[139]

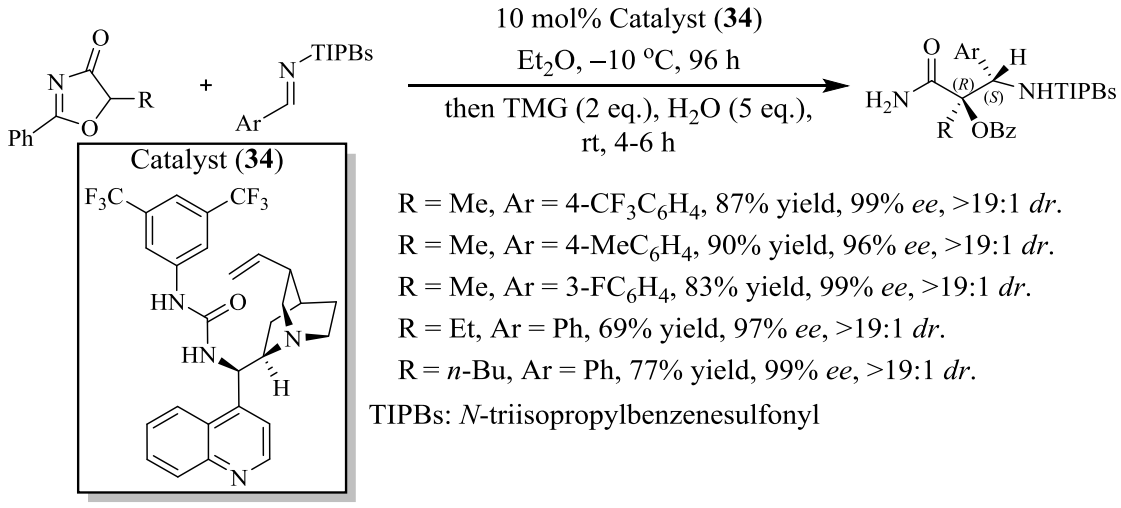

Scheme 1.31 Asymmetric Mannich reaction of 5*H*-oxazol-4-ones with *N*-TIPBs-arylimines catalyzed by the cinchonine-derived urea (**34**).[139]

Demir *et al.* have recently reported an asymmetric aldol reaction of α-azido ketones to ethyl pyruvate catalyzed by a cinchona-based bifunctional urea (**35**). With established the optimum reaction condition, the reaction led to furnish ethyl 4-aryl-3-azido-2-hydroxy-2-methyl-4-oxobutanoates with high enantioselectivity and diastereoselectivity ratio, but in moderate yields (Scheme 1.32).[140]

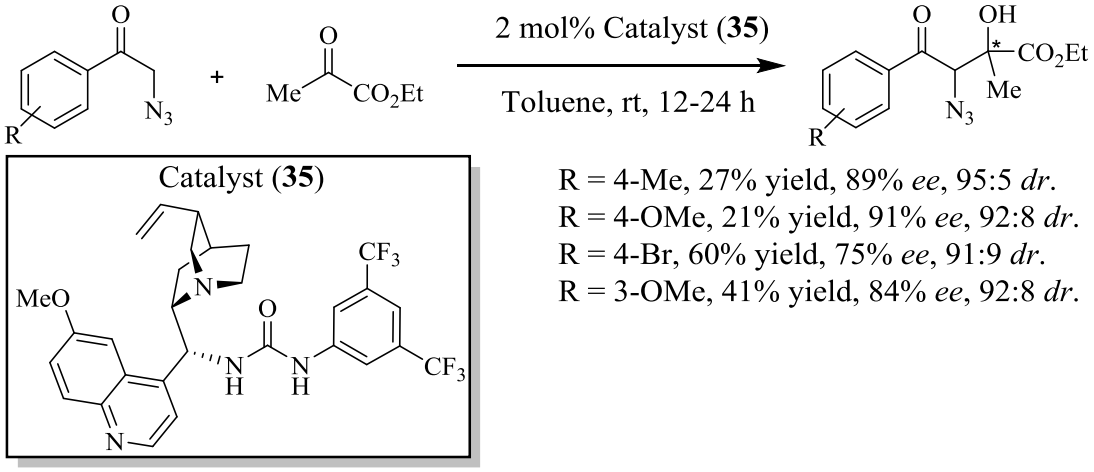

Scheme 1.32 Asymmetric aldol reaction of α-azido ketones to ethyl pyruvate catalyzed by the cinchona-based bifunctional urea (**35**).[140]

Lu *et al.* developed the first asymmetric aldol reaction of isocyanoesters with β,γ-unsaturated α-ketoesters using C6'-thiourea cinchona alkaloid derivative (**36**).

After acidic hydrolysis, the reaction afforded the chiral β-hydroxy-α-amino acid esters were obtained in good yields and excellent enantioselectivities (up to 92% *ee*).[141]

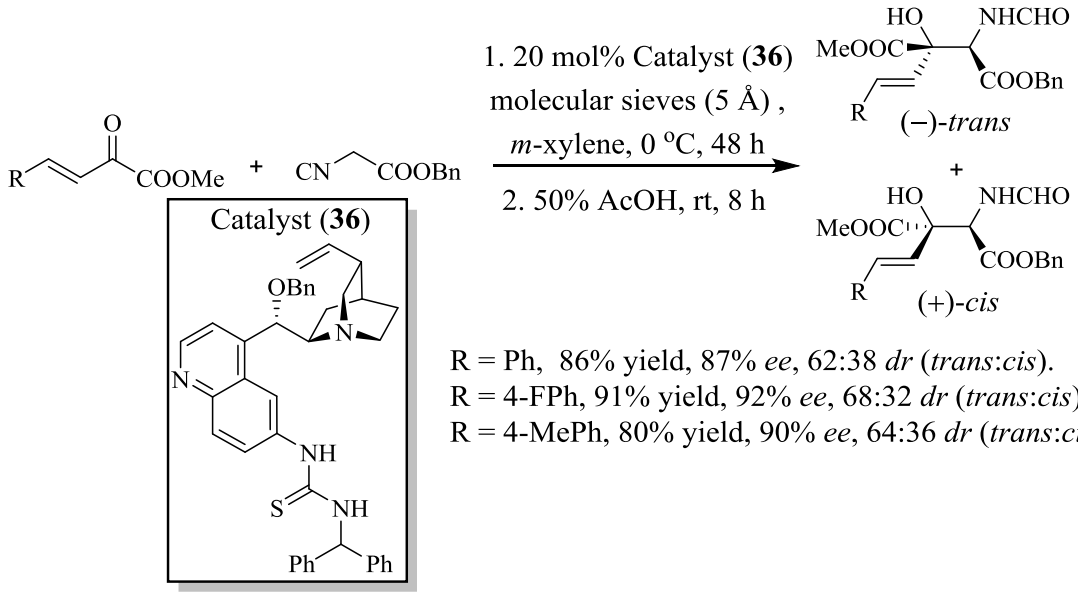

R = Ph, 86% yield, 87% *ee*, 62:38 *dr* (*trans*:*cis*).
R = 4-FPh, 91% yield, 92% *ee*, 68:32 *dr* (*trans*:*cis*).
R = 4-MePh, 80% yield, 90% *ee*, 64:36 *dr* (*trans*:*cis*).

Scheme 1.33 Asymmetric aldol reaction of isocyanoesters with β,γ-unsaturated α-ketoesters catalyzed by the C6'-thiourea cinchona derivative (**36**).[141]

He *et al.* reported that application of a novel C9-thiourea cinchona derivative (**37**) as the most efficient catalyst in the enantioselective oxaziridination of aldimines. With using *meta*-chloroperoxybenzoicacid (*m*-CPBA) as the oxidant, the reaction afforded several optically active oxzairdines in good yields with moderate to excellent enantioselectivities (up to 99% *ee*). Based on the experimental results, they found that the greater steric substrates generate a higher yields and *ee* values, such as isopropyl or tertiary butyl, and the electron-donating groups of substrates enhance the enantioselectivities (Scheme 1.34).[142]

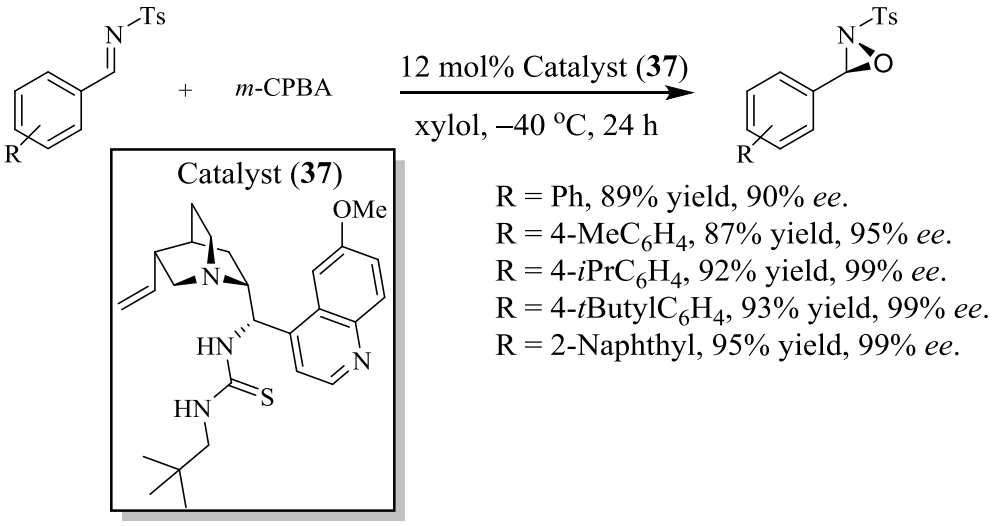

Scheme 1.34 Asymmetric oxaziridination of aldimines catalyzed by the C9-thiourea cinchona derivative (**37**).[142]

On the other hand, since Rawal *et al.* designed the first cinchona-derived squaramide as an efficient catalyst for the asymmetric Michael addition reaction,[108] the squaramide bifunctional catalysts have attracted some attention in recent years. A series of chiral cinchona derived-squaramides have been developed and employed them successfully in various asymmetric reactions. As mentioned previously, due to the unique structural features, cinchona-derived squaramides have shown some advantages. For instance, Connon *et al.* presented that the quinine-derived squaramide catalyst (**38**) shows better catalytic performance than the corresponding thiourea catalyst (**39**) in the asymmetric coupling reaction of homophthalic anhydride with benzaldehyde (Scheme 1.35).[143]

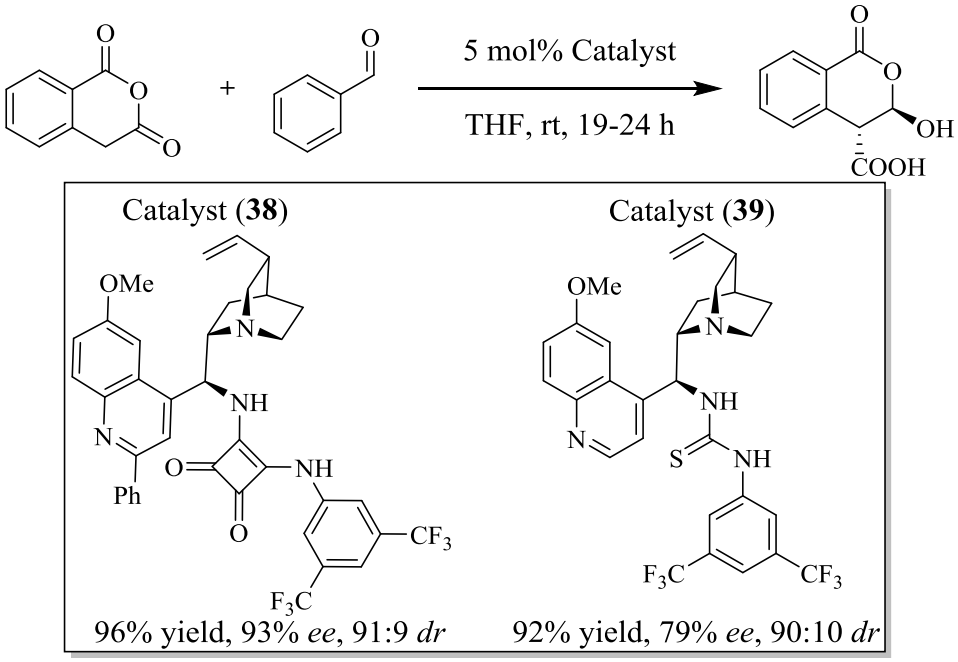

Scheme 1.35 Comparison of the catalytic efficiency of the catalyst (**38**) and (**39**) in the addition of homophthalic anhydride to benzaldehyde.[143]

More recently, Zhao *et al.* developed an asymmetric cascade Friedel-Crafts alkylation reaction of 1-naphthol with 3-trifluoroethylidene oxindole using a quinine-derived squaramide catalyst (**40**), to afford the corresponding α-aryl-β-trifluoromethyl dihydrocoumarin derivative in high yields with excellent enantioselectivities (up to 98% *ee*). They also found when using the other squaramide (**41**) as a catalyst for the reaction, a lower enantioselectivity was not observed (74% *ee*), although the reaction proceeded efficiently to furnish the desired product in good yield (90%).[144]

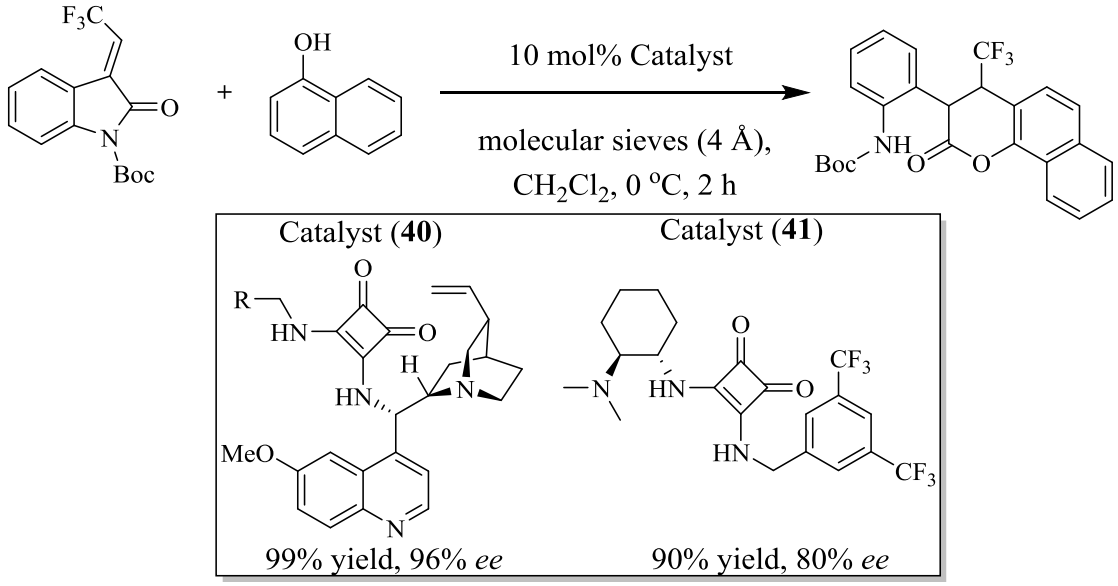

Scheme 1.36 Comparison of the catalytic efficiency of the catalyst (**40**) and (**41**) in the asymmetric Friedel-Crafts alkylation of 1-naphthol with 3-ylidene oxindole.[144]

1.5.3 Catalysis of asymmetric Michael addition reactions by cinchona-derived urea and thiourea derivatives

The Michael addition reaction is an addition reaction of a carbanion or another carbon nucleophile (reaction donor), such as dimethyl malonate, to an α,β-unsaturated carbonyl compound or electrophile (reaction acceptor) to form the corresponding addition product using a base catalyst. Michael addition reactions begin with deprotonation of the reaction donor with the base to form an enolate. This enolate then attacks the reaction acceptor to form the product with the formation of a new carbon-carbon bond. Scheme 1.37 shows the mechanism of the Michael addition reaction.

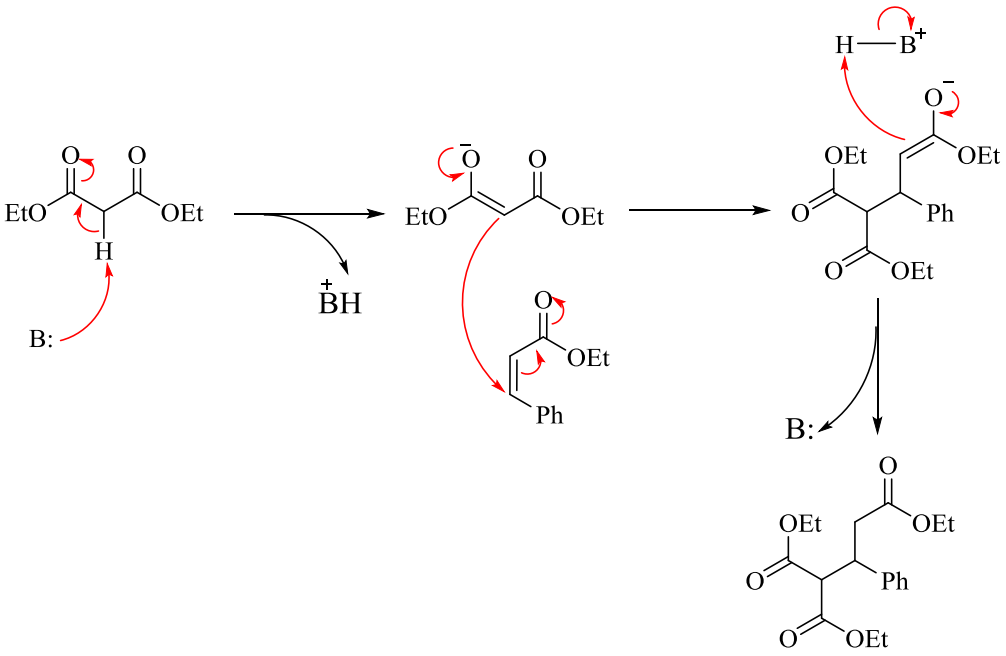

Scheme 1.37 Proposed mechanism of the Michael addition reaction.[145]

The first asymmetric conjugate addition of 1,3-dicabonaly to nitroenynes was reported by Li *et al.*. They used The 1,4-addition product were obtained in good yields with *ee* values up to 93% using cinchona alkaloid-based thiourea (**42**). The authors claimed that the reaction method worked well with both aryl- and alkyl-substituted nitroenyne substrates, thus it provided a catalytic and transition-metal-free entry to the precursors of pharmaceutical important chiral β-alkynyl acid derivatives.[146]

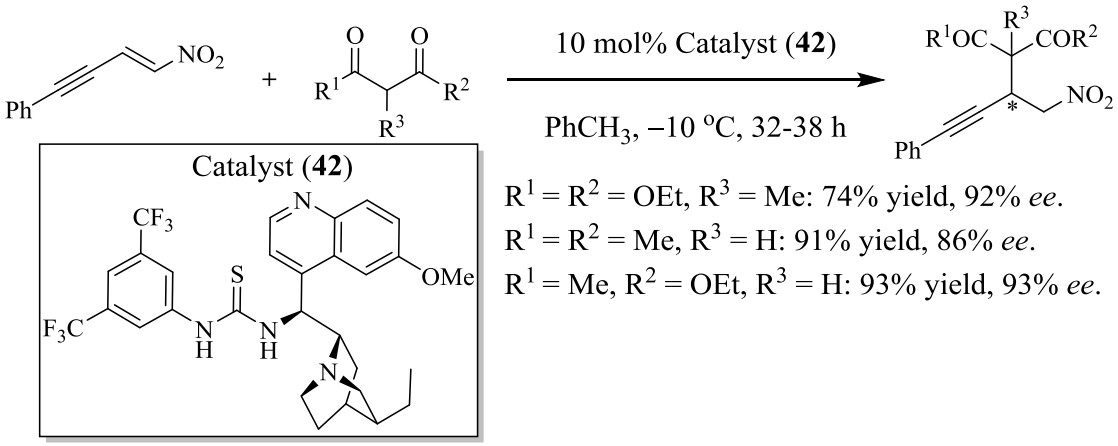

Scheme 1.38 Enantioselective Michael reactions of nitroenynes with malonates catalyzed the cinchona-derived thiourea (**42**).[146]

Matsubara *et al.* developed a novel enantioselective synthesis of 2-substituted chromans through an intermolecular oxy-Michael addition of phenol derivatives bearing (*E*)-α,β unsaturated ketones, using the quinidine-derived urea (**43**), the corresponding thiourea (**44**), and the quinine-derived urea (**45**) and as catalysts, respectively. High yields and good enantioselectivities were achieved using these three catalysts. The urea (**43**) appeared to be more efficient than the thiourea (**44**), while the urea catalyst (**45**) also revealed to be more efficient catalyst for affording the opposite enantiomer of product with good enantioselectivities.[147]

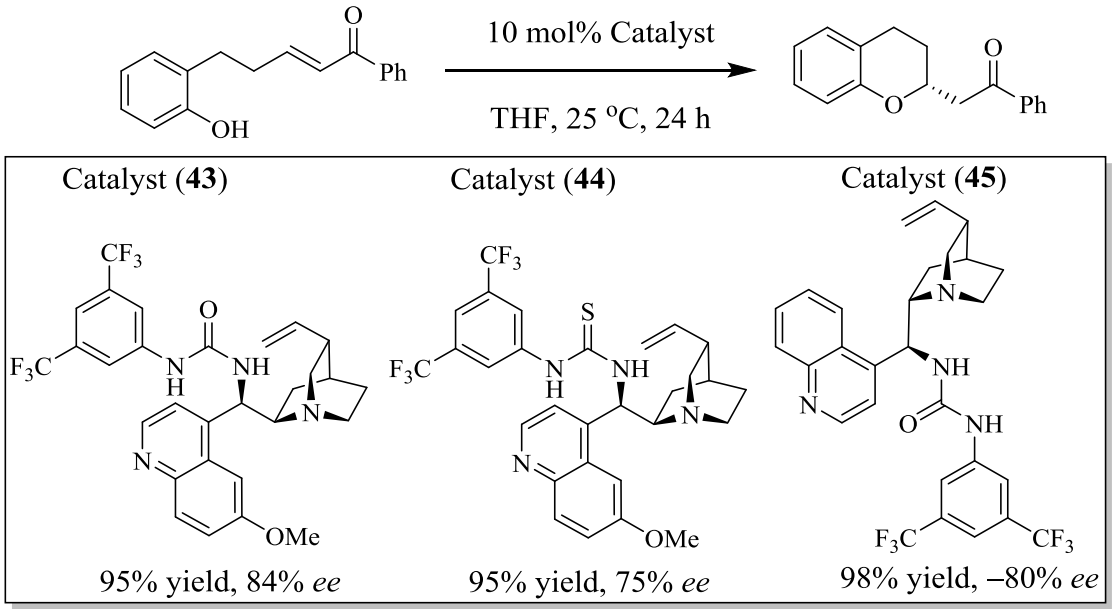

Scheme 1.39 Application of the cinchona alkaloid-based ureas (**43** and **45**) and the thiourea (**44**) in oxy-Michael addition of phenol derivatives.[147]

1.6 Opium alkaloid-based organocatalysts

1.6.1 The morphine alkaloids

The opiates are isolated from the sap of the poppy plant. The opium alkaloids which occur naturally in the largest amounts are morphine, codeine, noscapine, thebaine and papaverine.[148] Fig. 1.15 shows some examples of natural morphine alkaloids and the synthetic derivative naltrexone. Morphine has been widely used as a powerful analgesic since it was isolated in its pure form in 1803.[149] The commercial manufacturing of codeine is performed (from morphine) due to the high abundance of morphine in nature from poppy extracts, coupled with the low annual demand for this painkiller. Medically important derivatives of thebaine can also be synthesised from

codeine *via* codeine methyl ether.[150] These opiates have been investigated as drugs with analgesic or pain-relieving effects.

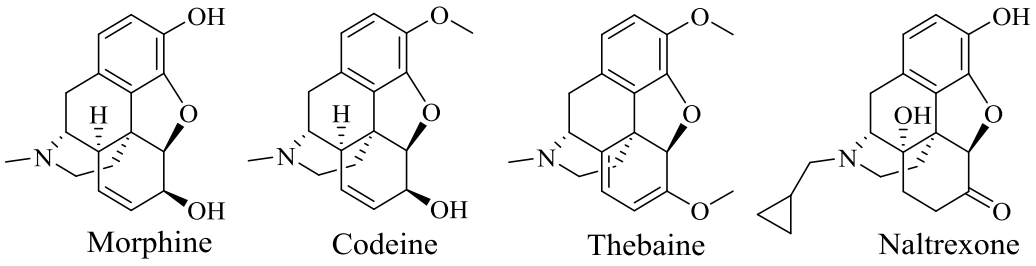

Fig. 1.19 Examples of morphine alkaloids.

1.6.2 The structure of morphine alkaloids

As natural compounds with unique chiral structures, opiate alkaloids, in particular morphine and codeine, possess a wide range of structural features. Thus, an examination of the structural features common to the phenanthrene opiate subfamily is important for further modification and study of their chemical and pharmacological profiles. For example, morphine has a rigid pentacyclic structure consisting of a benzene ring (A), two partially unsaturated cyclohexane rings (B and C), a piperidine ring (D) and a tetrahydrofuran ring (E).[151] The morphine molecule adopts a three-dimensional "T" shape with rings A, B and E forming a near perfect vertical plane and rings C and D forming a more distorted horizontal plane.[152] There are two hydroxyl functional groups located at C3 (pK_a= 9.9) and C6 (allylic OH) respectively; an ether linkage between C4 and C5 and unsaturation between C7 and C8; a basic tertiary amine function at position C17; five chiral centers: C5(*R*), C6(*S*), C9(*R*), C13(*S*) and C14(*R*) in the unique chiral scaffold exhibit a high degree of stereochemical diversity[151] and it is hypothesized that the possibility for enantioselective catalysis exists. Fig. 1.20 shows the three-dimensional structure and structural features of morphine.

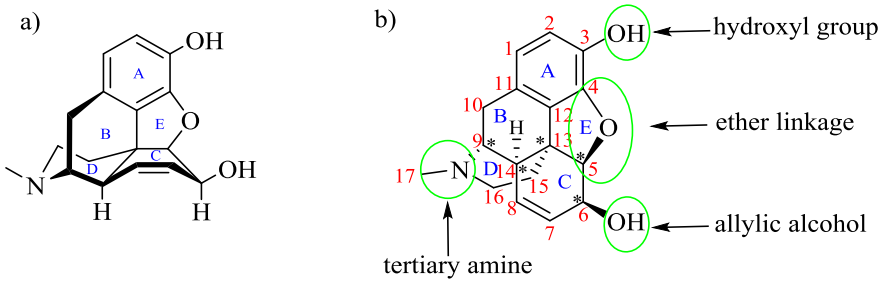

Fig. 1.20 The three-dimensional structure (a) and structural features (b) of morphine.

Although both quinine (pK_a = 4.29) and codeine (pK_a = 8.15)[153] have different pK_a values, these two weak bases share some common structural features: an aromatic ring, a double bond, a secondary alcohol, tertiary nitrogen and aromatic methyl ether (Fig. 1.21). With a prolific history and successful application in organocatalysis of the cinchona alkaloids, the investigation of morphine alkaloids and their derivatives as a novel class of organocatalysts is the main purpose of this research work.

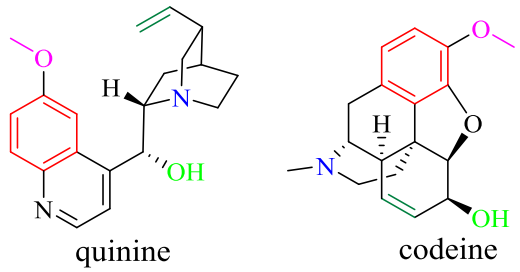

Fig. 1.21 Common features in quinine and codeine.

1.6.3 Catalysis of reactions by morphine alkaloids

High enantioselectivity has been successfully achieved by using chiral alkaloids such as quinine and quinidine. Morphine-derived alkaloids have rarely been investigated as chiral ligands in asymmetric reactions. The first asymmetric reaction carried out using such related alkaloids was published by Wells *et al.*.[154] They investigated the use of codeine, dihydrocodeine and oxycodone to modify a platinum surface in the asymmetric hydrogenation of methyl pyruvate and butane-2,3-dione, but very low enantioselectivities were obtained.

Dabiri *et al.* demonstrated the asymmetric addition reaction of diethylzinc to benzaldehyde with a catalytic amount of 14-hydroxyl substituted 6-ketomorphinans.[155] They optimised the conditions by lowering the temperature and increasing the catalyst loading to give high yield and good enantioselectivities: At the lower temperature of −30 ºC, the alcohol product, with 80% *ee* (*S*) and 89% *ee* (*S*) were obtained by using 20 mol% of **46** and 20 mol% of **48**, respectively. The alcohol product with only 53% *ee* (*R*) was isolated when using 10 mol% of **47**. When the temperature was increased to 10 ºC, **46** and **48** still afforded better enantioselectivities than **47**, using 10 mol% of catalyst loading (Scheme 1.40). Based on the results they obtained, Dabiri *et al.* recommended morphine alkaloids certainly deserved further study in asymmetric catalysis applications.

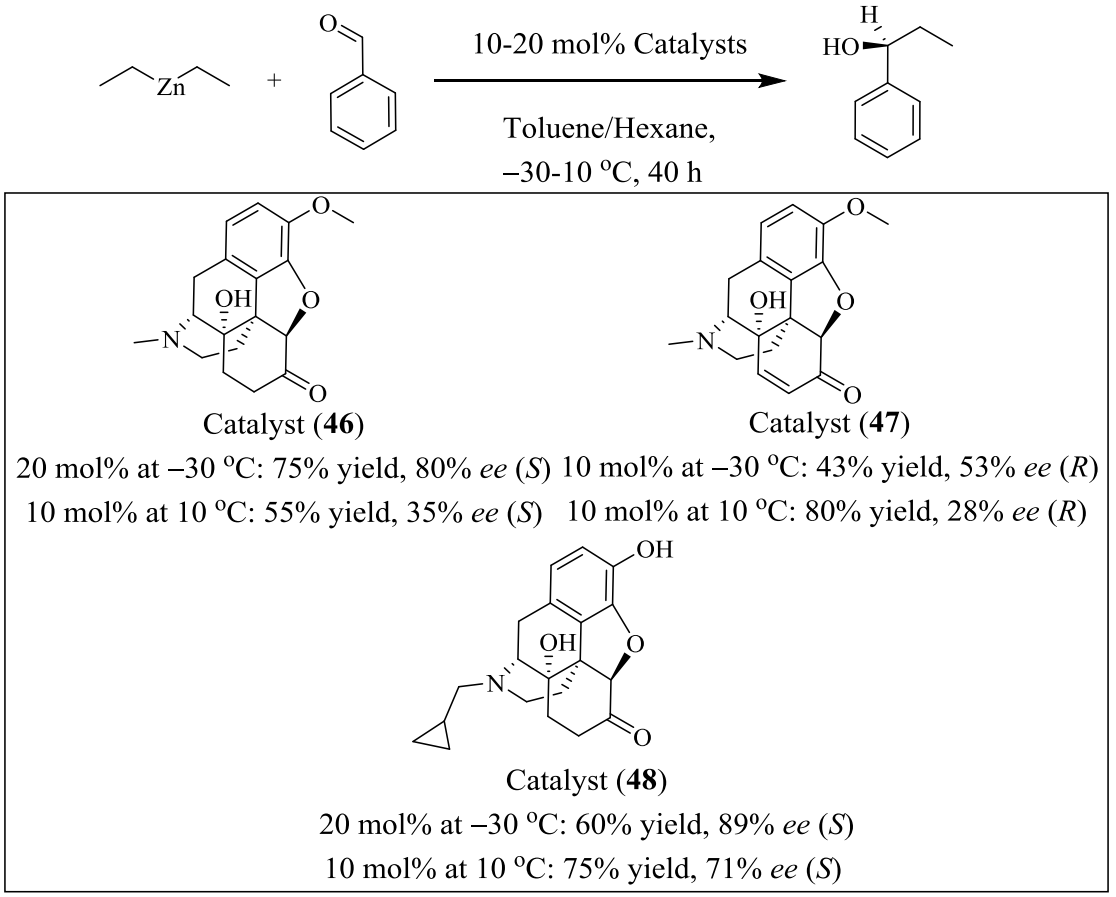

Scheme 1.40 Enantioselective addition reaction of diethylzinc to benzaldehyde catalyzed by opioid derivatives.[155]

1.7 Conclusion

Enantioselective organocatalysis has emerged as a powerful and efficient synthetic tool being a complementary mode of catalysis in the field of asymmetric synthesis, due to having the potential for saving in cost, time and energy, conducting easy experimental procedure with a less chemical waste output. With respect to industrial applications, especially in medicinal industries, the requirement of catalysts is considerate extremely important for the construction of new candidate drugs, such as its generality, convenience and robustness. Organocatalysts meet all these standards and have already been used in search of pure enantiomeric drugs for leading to 100% yield and 100% *ee*.[156]

Among the available methods for synthesis of enantiopure chiral compounds, asymmetric catalysis has been demonstrated to be an important alternative to access chiral molecules as one molecule of the chiral catalyst can transfer its chiral information to many new chiral molecules. Therefore, since the successful demonstration of L-proline in many asymmetric syntheses, the design and synthesis of the structural versatility of chiral organocatalysts have appeared as a viable strategy for preparation of enantiomeric compounds or building blocks.[157] The most notable advance is certainly the development and application of a range of chiral molecules for the synthesis of new catalysts. Undertaking organic transformations in an environmentally benign manner is increasingly important. Therefore, the catalytic properties of optically active small organic molecules have attracted a great deal of attention.[158]

On the other hand, due to the ability of the simultaneous donation of two hydrogen-bonds for electrophile activation and transition-state organization, both ureas thioureas and even squaramides have been employed in asymmetric reactions. Thus, the design and application of bifunctional chiral (thio)ureas have been continuously developed with the discovery of several structural factors that influence the behaviour of new catalysts in asymmetric reactions. In general, a bifunctional catalyst incorporates an electron-poor aryl group (3,5-CF_3 disubstituted) on one of the attached substitutes, which leads to decrease the pK_a for increasing the hydrogen-bond donating. Furthermore, to ensure the asymmetric character of the catalysis, the skeleton of the ligand must be chiral,[159] such as the cinchona alkaloid scaffold in their (thio)urea

derivatives, which has been discussed in the chapter. The combination of (thio)urea moiety with amines, for example, tertiary amines, has also been utilized for design of bifunctional catalysts with the capability of simultaneously activating both the electrophile and the nucleophile. This allows not only to improve catalytic activity, but more importantly to contribute a greater degree of stereocontrol.[159] Researchers have also discovered that various types of chiral, highly pre-organized and available scaffolds in natural products that can be easily combined into the (thio)urea architectures for the fine-tuning of the catalyst system. For example, application of the novel class of thiourea catalysts bearing a bulky, rigid and chiral terpene skeleton in many asymmetric reactions has been reviewed more recently.[159]

Opiates and their semi-synthetic derivatives have long been investigated as potent analgesic compounds for medicinal purposes. However, the development of a class of chiral bifunctional (thio)urea derivatives that are based on the morphine alkaloids has remained uncovered in many literatures, due to its novelty. Thus, gaining inspiration from those successful example of cinchona-derived thioureas and ureas, and also from the presence of the common structural features between cinchona and morphine alkaloids, alongside utilization of the literature data to develop novel alkaloid structures, one can propose that the use of sustainable chiral building blocks or chiral ligands, such as codeine as a starting material, could allow for the future development of novel families of morphine alkaloid-based organocatalysts.

1.8 References

(1) Ghanem, A.; Ahmed, M.; Ishii, H.; Ikegami, T. Immobilized β-Cyclodextrin-Based Silica vs Polymer Monoliths for Chiral Nano Liquid Chromatographic Separation of Racemates. *Talanta* **2015**, *132*, 301–314.

(2) Kodama, S.; Saito, Y.; Chinaka, S.; Yamamoto, A.; Hayakawa, K. Chiral Capillary Electrophoresis of Agrochemicals in Real Samples. *J. Health Sci.* **2006**, *52* (5), 489–494.

(3) Liu, W.; Tang, M. Enantioselective Activity and Toxicity of Chiral Herbicides. In *Herbicides - Mechanisms and Mode of Action*; InTech, **2011**; pp 63–80.

(4) Seebach, D. Organic Synthesis—Where Now? *Angew. Chem., Int. Ed.* **1990**, *29* (11), 1320–1367.

(5) Kostyanovsky, R. G. Louis Pasteur Did It for Us Especially. *Mendeleev Commun.* **2003**, *13* (3), 85–90.

(6) Tobe, Y. The Reexamination of Pasteur's Experiment in Japan. *Mendeleev Commun.* **2003**, *13* (3), 93–94.

(7) Kazlauskas, R. J. (S)-(−)- and (R)-(+)-1,1'-Bi-2-Naphthol. *Org. Synth.* **2003**, *70*, 60.

(8) Cai, D.; Hughes, D. L.; Verhoeven, T. R.; Reider, P. J. Resolution of 1,1′-Bi-2-Naphthol. *Org. Synth.* **2003**, *76*, 1.

(9) Lorenz, H.; Seidel-Morgenstern, A. Processes to Separate Enantiomers. *Angew. Chem., Int. Ed.* **2014**, *53* (5), 1218–1250.

(10) Kitamura, M.; Ohkuma, T.; Tokunaga, M.; Noyori, R. Dynamic Kinetic Resolution in BINAP-Ruthenium (II) Catalyzed Hydrogenation of 2-Substituted 3-Oxo Carboxylic Esters. *Tetrahedron: Asymmetry* **1990**, *1* (1), 1–4.

(11) Moss, G. P. Basic Terminology of Stereochemistry (IUPAC Recommendations 1996). *Pure Appl. Chem.* **1996**, *68* (12), 2193–2222.

(12) Rouf, A.; Taneja, S. C. Ab Initio Electronic Circular Dichroism of Fullerenes, Single-Walled Carbon Nanotubes, and Ligand-Protected Metal Nanoparticles. *Chirality* **2014**, *26* (2), 63–78.

(13) Singh, P.; Samanta, K.; Das, S. K.; Panda, G. Amino Acid Chirons: A Tool for Asymmetric Synthesis of Heterocycles. *Org. Biomol. Chem.* **2014**, *12* (33), 6297–6339.

(14) Samanta, K.; Panda, G. Regioselective Ring-Opening of Amino Acid-Derived Chiral Aziridines: An Easy Access to *cis*-2,5-Disubstituted Chiral Piperazines. *Chem. Asian J.* **2011**, *6* (1), 189–197.

(15) Kumar, A. S.; Haritha, B.; Rao, B. V. A Versatile and Efficient Synthesis of (2S)-2-(Hydroxymethyl)-*N*-Boc-2,3-Dihydro-4-Pyridone. *Tetrahedron Lett.* **2003**, *44* (22), 4261–4263.

(16) Reddy, A. S.; Srihari, P. A Facile Approach to the Synthesis of Securinega Alkaloids: Stereoselective Total Synthesis of (−)-Allonorsecurinine. *Tetrahedron Lett.* **2012**, *53* (44), 5926–5928.

(17) Paek, S. M.; Jeong, M.; Jo, J.; Heo, Y. M.; Han, Y. T.; Yun, H. Recent Advances in Substrate-Controlled Asymmetric Induction Derived from Chiral Pool α-Amino Acids for Natural Product Synthesis. *Molecules* **2016**, *21* (7), 951.

(18) Schwab, W.; Fuchs, C.; Huang, F. C. Transformation of Terpenes into Fine Chemicals. *Eur. J. Lipid Sci. Technol.* **2013**, *115* (1), 3–8.

(19) Szakonyi, Z.; Csőr, Á.; Haukka, M.; Fueloep, F. Stereoselective Synthesis of Carane-Based Chiral β- and γ-Amino Acid Derivatives *via* Conjugate Addition. *Tetrahedron* **2015**, *71* (29), 4846–4852.

(20) Yeboah, E. M.; Yeboah, S. O.; Singh, G. S. Recent Applications of Cinchona Alkaloids and Their Derivatives as Catalysts in Metal-Free Asymmetric Synthesis. *Tetrahedron* **2011**, *67* (10), 1725–1762.

(21) Kotha, S. Opportunities in Asymmetric Synthesis: An Industrial Prospect. *Tetrahedron* **1994**, *50* (12), 3639–3662.

(22) Anastas, P.; Eghbali, N. Green Chemistry: Principles and Practice. *Chem. Soc. Rev.* **2010**, *39* (1), 301–312.

(23) Zhou, Q. L. Transition-Metal Catalysis and Organocatalysis: Where Can Progress Be Expected? *Angew. Chem., Int. Ed.* **2016**, *55* (18), 5352–5353.

(24) Shaikh, I. R. Organocatalysis: Key Trends in Green Synthetic Chemistry, Challenges, Scope towards Heterogenization, and Importance from Research and Industrial Point of View. *J. Catal.* **2014**, *2014*, 1–35.

(25) Farnetti, E.; Di Monte, R.; Kašpar, J. Homogeneous and Heterogeneous Catalysis. In *Inorganic and Bio-Inorganic Chemistry*; Bertini, I., Ed.; EOLSS, **2009**; Vol. II, p 54.

(26) Osborn, J. A.; Jardine, F. H.; Young, J. F.; Wilkinson, G. The Preparation and Properties of Tris (Triphenylphosphine) Halogenorhodium (I) and Some Reactions Thereof Including Catalytic Homogeneous Hydrogenation of Olefins and Acetylenes and Their Derivatives. *J. Chem. Soc. A* **1966**, 1711–1732.

(27) Knowles, W. S.; Sabacky, M. J. Catalytic Asymmetric Hydrogenation Employing a Soluble, Optically Active, Rhodium Complex. *Chem. Commun.* **1968**, No. 22, 1445–1446.

(28) Knowles, W. S. Asymmetric Hydrogenations (Nobel Lecture). *Angew. Chem., Int. Ed.* **2002**, *41* (12), 1998–2007.

(29) Yun, O. Profile of William S. Knowles. *Proc. Natl. Acad. Sci. U. S. A.* **2005**, *102*

(47), 16913–16915.

(30) Dang, T. P.; Kagan, H. B. The Asymmetric Synthesis of Hydratropic Acid and Amino-Acids by Homogeneous Catalytic Hydrogenation. *Chem. Commun.* **1971**, *7* (10), 481.

(31) Noyori, R.; Ohkuma, T.; Kitamura, M.; Takaya, H.; Sayo, N.; Kumobayashi, H.; Akutagawa, S. Asymmetric Hydrogenation of β-Keto Carboxylic Esters: A Practical, Purely Chemical Access to β-Hydroxy Exters in High Enantiomeric Purity. *J. Am. Chem. Soc.* **1987**, *109*, 5856–5858.

(32) Beller, M.; Blaser, H. U. *Organometallics as Catalysts in the Fine Chemical Industry*; Beller, M., Blaser, H. U., Eds.; Springer, **2012**; Vol. 42.

(33) Heller, D.; De Vries, A. H.; De Vries, J. G. Catalyst Inhibition and Deactivation in Homogeneous Hydrogenation. In *The Handbook of Homogeneous Hydrogenation*; **2007**; pp 1483–1516.

(34) Davis, B. G. Enzyme Catalysis: Sweet Flexibility. *Nat. Chem.* **2010**, *2* (2), 85–86.

(35) List, B. Organocatalysis. *Beilstein J. Org. Chem.* **2012**, *8*, 1358–1359.

(36) Seayad, J.; List, B. Asymmetric Organocatalysis. *Org. Biomol. Chem.* **2005**, *3* (5), 719–724.

(37) Marcos, V.; Alemán, J. Old Tricks, New Dogs: Organocatalytic Dienamine Activation Of α,β-Unsaturated Aldehydes. *Chem. Soc. Rev.* **2016**, *45* (24), 6812–6832.

(38) Methot, J. L.; Roush, W. R. Nucleophilic Phosphine Organocatalysis. *Adv. Synth. Catal.* **2004**, *346* (9–10), 1035–1050.

(39) Reisinger, C. *Epoxidations and Hydroperoxidations of α,β-Unsaturated Ketones:*

An Approach through Asymmetric Organocatalysis.; Springer Science & Business Media, **2012**.

(40) Pellissier, H. Recent Developments in Organocatalytic Dynamic Kinetic Resolution. *Tetrahedron* **2016**, *72* (23), 3133–3150.

(41) Robinson, E. R.; Fallan, C.; Simal, C.; Slawin, A. M.; Smith, A. D. Anhydrides as α,β-Unsaturated Acyl Ammonium Precursors: Isothiourea-Promoted Catalytic Asymmetric Annulation Processes. *Chem. Sci.* **2013**, *4* (5), 2193–2200.

(42) Van, K. N.; Morrill, L. C.; Smith, A. D.; Romo, D. Catalytic Generation of Ammonium Enolates and Related Tertiary Amine-Derived Intermediates: Applications, Mechanism, and Stereochemical Models (n → π*). In *Lewis Base Catalysis in Organic Synthesis*; Vedejs, E., Denmark, S. E., Eds.; John Wiley & Sons, **2016**; pp 527–653.

(43) List, B. Proline-Catalyzed Asymmetric Reactions. *Tetrahedron* **2002**, *58* (28), 5573–5590.

(44) Ahrendt, K. A.; Borths, C. J.; MacMillan, D. W. New Strategies for Organic Catalysis: The First Highly Enantioselective Organocatalytic Diels-Alder Reaction. *J. Am. Chem. Soc.* **2000**, *122* (17), 4243–4244.

(45) Sulzer-Mossé, S.; Alexakis, A. Chiral Amines as Organocatalysts for Asymmetric Conjugate Addition to Nitroolefins and Vinyl Sulfones *via* Enamine Activation. *Chem. Commun.* **2007**, No. 30, 3123–3135.

(46) Xu, L. W.; Luo, J.; Lu, Y. Asymmetric Catalysis with Chiral Primary Amine-Based Organocatalysts. *Chem. Commun.* **2009**, *14*, 1807–1821.

(47) Arceo, E.; Melchiorre, P. Extending the Aminocatalytic HOMO-Raising Activation Strategy: Where Is the Limit? *Angew. Chem., Int. Ed.* **2012**, *51* (22), 5290–5292.

(48) Reboredo, S.; Parra, A.; Alemán, J. Trienamines: Their Key Role in Extended Organocatalysis for Diels-Alder Reactions. *Asymmetric Catal.* **2013**, *1* (1), 24–31.

(49) Lelais, G.; MacMillan, D. W. Modern Strategies in Organic Catalysis: The Advent and Development of Iminium Activation. *Aldrichimica Acta* **2006**, *39* (3), 79–87.

(50) Mukherjee, S.; Yang, J. W.; Hoffmann, S.; List, B. Asymmetric Enamine Catalysis. *Chem. Rev.* **2007**, *107* (12), 5471–5569.

(51) Bertelsen, S.; Marigo, M.; Brandes, S.; Diner, P.; Jørgensen, K. A. Dienamine Catalysis: Organocatalytic Asymmetric γ-Amination Of α,β-Unsaturated Aldehydes. *J. Am. Chem. Soc.* **2006**, *128* (39), 12973–12980.

(52) Jia, Z. J.; Jiang, H.; Li, J. L.; Gschwend, B.; Li, Q. Z.; Yin, X.; Grouleff, J.; Chen, Y. C.; Jørgensen, K. A. Trienamines in Asymmetric Organocatalysis: Diels−Alder and Tandem Reactions. *J. Am. Chem. Soc.* **2011**, *133* (13), 5053–5061.

(53) Kumar, I.; Ramaraju, P.; Mir, N. A. Asymmetric Trienamine Catalysis: New Opportunities in Amine Catalysis. *Org. Biomol. Chem.* **2013**, *11* (5), 709–716.

(54) Beel, R.; Kobialka, S.; Schmidt, M. L.; Engeser, M. Direct Experimental Evidence for an Enamine Radical Cation in SOMO Catalysis. *Chem. Commun.* **2011**, *47* (11), 3293–3295.

(55) Huy, P. H.; Motsch, S.; Kappler, S. M. Formamides as Lewis Base Catalysts in S_N Reactions—Efficient Transformation of Alcohols into Chlorides, Amines, and Ethers. *Angew. Chem., Int. Ed.* **2016**, *55* (34), 10145–10149.

(56) Tan, J.; Yasuda, N. Contemporary Asymmetric Phase Transfer Catalysis: Large-Scale Industrial Applications. *Org. Process Res. Dev.* **2015**, *19* (11), 1731–1746.

(57) Albanese, D. C.; Foschi, F.; Penso, M. Sustainable Oxidations under Phase-Transfer Catalysis Conditions. *Org. Process Res. Dev.* **2016**, *20* (2), 129–139.

(58) Jew, S. S.; Park, H. G. Cinchona-Based Phase-Transfer Catalysts for Asymmetric Synthesis. *Chem. Commun.* **2009**, No. 46, 7090–7103.

(59) Boratyński, P. J. Dimeric Cinchona Alkaloids. *Mol. Diversity* **2015**, *19* (2), 385–422.

(60) Xiang, B.; Belyk, K. M.; Reamer, R. A.; Yasuda, N. Discovery and Application of Doubly Quaternized Cinchona-Alkaloid-Based Phase-Transfer Catalysts. *Angew. Chem., Int. Ed.* **2014**, *53* (32), 8375–8378.

(61) Vijaya, P. K.; Murugesan, S.; Siva, A. Highly Enantioselective Asymmetric Henry Reaction Catalyzed by Novel Chiral Phase Transfer Catalysts Derived from Cinchona Alkaloids. *Org. Biomol. Chem.* **2016**, *14* (42), 10101–10109.

(62) Enders, D.; Nguyen, T. V. Chiral Quaternary Phosphonium Salts: A New Class of Organocatalysts. *Org. Biomol. Chem.* **2012**, *10* (28), 5327–5331.

(63) Zhong, F.; Dou, X.; Han, X.; Yao, W.; Zhu, Q.; Meng, Y.; Lu, Y. Chiral Phosphine Catalyzed Asymmetric Michael Addition of Oxindoles. *Angew. Chem., Int. Ed.* **2013**, *52* (3), 943–947.

(64) Wang, H. Y.; Zhang, K.; Zheng, C. W.; Chai, Z.; Cao, D. D.; Zhang, J. X.; Zhao, G. Asymmetric Dual-Reagent Catalysis: Mannich-Type Reactions Catalyzed by Ion Pair. *Angew. Chem., Int. Ed.* **2015**, *54* (6), 1775–1779.

(65) Cao, D.; Zhang, J.; Wang, H.; Zhao, G. Dipeptide-Derived Multifunctional Quaternary Phosphonium Salt Catalyzed Asymmetric Cyclizations *via* a Tandem Michael Addition/S_N2 Sequence. *Chem. Eur. J.* **2015**, *21* (28), 9998–10002.

(66) Liu, S.; Kumatabara, Y.; Shirakawa, S. Chiral Quaternary Phosphonium Salts as

Phase-Transfer Catalysts for Environmentally Benign Asymmetric Transformations. *Green Chem.* **2016**, *18* (2), 331–341.

(67) Palomo, C.; Oiarbide, M.; López, R. Asymmetric Organocatalysis by Chiral Brønsted Bases: Implications and Applications. *Chem. Soc. Rev.* **2009**, *38* (2), 632–653.

(68) Ting, A.; Goss, J. M.; McDougal, N. T.; Schaus, S. E. Brønsted Base Catalysts. In *Asymmetric Organocatalysis*; List, B., Ed.; Springer Berlin Heidelberg, **2010**; Vol. 291, pp 145–200.

(69) Schuchardt, U.; Sercheli, R.; Vargas, R. M. Transesterification of Vegetable Oils: A Review. *J. Braz. Chem. Soc.* **1998**, *9* (1), 199–210.

(70) Cho, B.; Wong, M. W. Unconventional Bifunctional Lewis-Brønsted Acid Activation Mode in Bicyclic Guanidine-Catalyzed Conjugate Addition Reactions. *Molecules* **2015**, *20* (8), 15108–15121.

(71) Selig, P. Guanidine Organocatalysis. *Synthesis* **2013**, *45* (6), 703–718.

(72) Ahmad, S.; Shukla, L.; Szawkało, J.; Roszkowski, P.; Maurin, J. K.; Czarnocki, Z. Synthesis of Novel Chiral Guanidine Catalyst and Its Application in the Asymmetric Pictet-Spengler Reaction. *Catal. Commun.* **2017**, *89*, 44–47.

(73) Ricci, A. Asymmetric Organocatalysis at the Service of Medicinal Chemistry. *ISRN Org. Chem.* **2014**, *2014*, 29.

(74) Schipper, D. J.; Campeau, L. C.; Fagnou, K. Catalyst and Base Controlled Site-Selective sp^2 and sp^3 Direct Arylation of Azine *N*-Oxides. *Tetrahedron* **2009**, *65* (16), 3155–3164.

(75) Izquierdo, J.; Landa, A.; Bastida, I.; López, R.; Oiarbide, M.; Palomo, C. Base-Catalyzed Asymmetric α-Functionalization of 2-(Cyanomethyl)azaarene *N*-Oxides Leading to Quaternary Stereocenters. *J. Am. Chem. Soc.* **2016**, *138*

(10), 3282–3285.

(76) Lauridsen, V. H.; Ibsen, L.; Blom, J.; Jørgensen, K. A. Asymmetric Brønsted Base Catalyzed and Directed [3+2] Cycloaddition of 2-Acyl Cycloheptatrienes with Azomethine Ylides. *Chem. Eur. J.* **2016**, *22* (10), 3259–3263.

(77) Akiyama, T.; Mori, K. Stronger Brønsted Acids: Recent Progress. *Chem. Rev.* **2015**, *115* (17), 9277–9306.

(78) Petersen, K. S. Chiral Brønsted Acid Catalyzed Kinetic Resolutions. *Asian J. Org. Chem.* **2016**, *5* (3), 308–320.

(79) Akiyama, T.; Itoh, J.; Fuchibe, K. Recent Progress in Chiral Brønsted Acid Catalysis. *Adv. Synth. Catal.* **2006**, *348* (9), 999–1010.

(80) Ma, Q.; Ma, M.; Tian, H.; Ye, X.; Xiao, H.; Chen, L. H.; Lei, X. A Novel Amine Receptor Based on the Binol Scaffold Functions as a Highly Effective Chiral Shift Reagent for Carboxylic Acids. *Org. Lett.* **2012**, *14* (23), 5813–5815.

(81) Akiyama, T.; Itoh, J.; Yokota, K.; Fuchibe, K. Enantioselective Mannich-Type Reaction Catalyzed by a Chiral Brønsted Acid. *Angew. Chem., Int. Ed.* **2004**, *43* (12), 1566–1568.

(82) Uraguchi, D.; Terada, M. Chiral Brønsted Acid-Catalyzed Direct Mannich Reactions *via* Electrophilic Activation. *J. Am. Chem. Soc.* **2004**, *126* (17), 5356–5357.

(83) Parmar, D.; Sugiono, E.; Raja, S.; Rueping, M. Complete Field Guide to Asymmetric BINOL-Phosphate Derived Brønsted Acid and Metal Catalysis: History and Classification by Mode of Activation; Brønsted Acidity, Hydrogen Bonding, Ion Pairing, and Metal Phosphates. *Chem. Rev.* **2014**, *114* (8), 9047–9153.

(84) Kikuchi, J.; Momiyama, N.; Terada, M. Chiral Phosphoric Acid Catalyzed

Diastereo- and Enantioselective Mannich-Type Reaction between Enamides and Thiazolones. *Org. Lett.* **2016**, *18* (11), 2521–2523.

(85) Cheon, C. H.; Yamamoto, H. A Brønsted Acid Catalyst for the Enantioselective Protonation Reaction. *J. Am. Chem. Soc.* **2008**, *130* (29), 9246–9247.

(86) Nakashima, D.; Yamamoto, H. Design of Chiral *N*-Triflyl Phosphoramide as a Strong Chiral Brønsted Acid and Its Application to Asymmetric Diels−Alder Reaction. *J. Am. Chem. Soc.* **2006**, *128* (30), 9626–9627.

(87) Liu, L.; Kaib, P. S.; Tap, A.; List, B. A General Catalytic Asymmetric Prins Cyclization. *J. Am. Chem. Soc.* **2016**, *138* (34), 10822–10825.

(88) Zhang, Y.; Lu, Z.; Wulff, W. D. Catalytic Asymmetric Aziridination with Catalysts Derived from VAPOL and VANOL. *Synlett* **2009**, No. 17, 2715–2739.

(89) Desai, A. A.; Huang, L.; Wulff, W. D.; Rowland, G. B.; Antilla, J. C. Gram-Scale Preparation of VAPOL Hydrogenphosphate: A Structurally Distinct Chiral Brønsted Acid. *Synthesis* **2010**, No. 12, 2106–2109.

(90) Desai, A. A.; Wulff, W. D. New Derivatives of VAPOL and VANOL: Structurally Distinct Vaulted Chiral Ligands and Brønsted Acid Catalysts. *Synthesis* **2010**, No. 21, 3670–3680.

(91) Liang, Y.; Rowland, E. B.; Owland, G. B.; Perman, J. A.; Antilla, J. C. VAPOL Phosphoric Acid Catalysis: The Highly Enantioselective Addition of Imides to Imines. *Chem. Commun.* **2007**, No. 43, 4477–4479.

(92) Larson, S. E.; Baso, J. C.; Li, G.; Antilla, J. C. Chiral Phosphoric Acid-Catalyzed Desymmetrization of *meso*-Aziridines with Functionalized Mercaptans. *Org. Lett.* **2009**, *11* (22), 5186–5189.

(93) Klare, H.; Neudörfl, J. M.; Goldfuss, B. New Hydrogen-Bonding Organocatalysts: Chiral Cyclophosphazanes and Phosphorus Amides as

Catalysts for Asymmetric Michael Additions. *Beilstein J. Org. Chem.* **2014**, *10*, 224–236.

(94) Hine, J.; Ahn, K.; Gallucci, J. C.; Linden, S. M. 1,8-Biphenylenediol Forms Two Strong Hydrogen-Bonds to the Same Oxygen Atom. *J. Am. Chem. Soc.* **1984**, *106* (25), 7980–7981.

(95) Etter, M. C. Encoding and Decoding Hydrogen-Bond Patterns of Organic Compounds. *Acc. Chem. Res.* **1990**, *23* (4), 120–126.

(96) Etter, M. C.; Urbanczyk-Lipkowska, Z.; Zia-Ebrahimi, M.; Panunto, T. W. Hydrogen Bond-Directed Cocrystallization and Molecular Recognition Properties of Diarylureas. *J. Am. Chem. Soc.* **1990**, *112* (23), 8415–8426.

(97) Severance, D. L.; Jorgensen, W. L. Effects of Hydration on the Claisen Rearrangement of Allyl Vinyl Ether from Computer Simulations. *J. Am. Chem. Soc.* **1992**, *114* (27), 10966–10968.

(98) Curran, D. P.; Kuo, L. H. Altering the Stereochemistry of Allylation Reactions of Cyclic α-Sulfinyl Radicals with Diarylureas. *J. Org. Chem.* **1994**, *59* (12), 3259–3261.

(99) Curran, D. P.; Kuo, L. H. Acceleration of a Dipolar Claisen Rearrangement by Hydrogen-Bonding to a Soluble Diaryl Urea. *Tetrahedron Lett.* **1995**, *36* (37), 6647–6650.

(100) Schreiner, P. R.; Wittkopp, A. Hydrogen-Bonding Additives Act like Lewis Acid Catalysts. *Org. Lett.* **2002**, *4* (2), 217–220.

(101) Sigman, M. S.; Jacobsen, E. N. Schiff Base Catalysts for the Asymmetric Strecker Reaction Identified and Optimized from Parallel Synthetic Libraries. *J. Am. Chem. Soc.* **1998**, *120* (19), 4901–4902.

(102) Okino, T.; Hoashi, Y.; Takemoto, Y. Enantioselective Michael Reaction of

Malonates to Nitroolefins Catalyzed by Bifunctional Organocatalysts. *J. Am. Chem. Soc.* **2003**, *125* (42), 12672–12673.

(103) Held, F. E.; Tsogoeva, S. B. Asymmetric Cycloaddition Reactions Catalyzed by Bifunctional Thiourea and Squaramide Organocatalysts: Recent Advances. *Catal. Sci. Technol.* **2016**, *6* (3), 645–667.

(104) Serdyuk, O. V.; Heckel, C. M.; Tsogoeva, S. B. Bifunctional Primary Amine-Thioureas in Asymmetric Organocatalysis. *Org. Biomol. Chem.* **2013**, *11* (41), 7051–7071.

(105) Lalonde, M. P.; McGowan, M. A.; Rajapaksa, N. S.; Jacobsen, E. N. Enantioselective Formal Aza-Diels-Alder Reactions of Enones with Cyclic Imines Catalyzed by Primary Aminothioureas. *J. Am. Chem. Soc.* **2013**, *135* (5), 1891–1894.

(106) Chen, X.; Qi, Z. H.; Zhang, S. Y.; Kong, L. P.; Wang, Y.; Wang, X. W. Enantioselective Construction of Functionalized Thiopyrano-Indole Annulated Heterocycles *via* a Formal Thio [3+3] Cyclization. *Org. Lett.* **2015**, *17* (1), 42–45.

(107) Zhang, X.; Zhang, Z.; Boissonnault, J.; Cohen, S. M. Design and Synthesis of Squaramide-Based MOFs as Efficient MOF-Supported Hydrogen-Bonding Organocatalysts. *Chem. Commun.* **2016**, *52* (52), 8585–8588.

(108) Malerich, J. P.; Hagihara, K.; Rawal, V. H. Chiral Squaramide Derivatives Are Excellent Hydrogen-Bond Donor Catalysts. *J. Am. Chem. Soc.* **2008**, *130* (44), 14416–14417.

(109) Quiñonero, D.; Prohens, R.; Garau, C.; Frontera, A.; Ballester, P.; Costa, A.; Deyà, P. M. A Theoretical Study of Aromaticity in Squaramide Complexes with Anions. *Chem. Phys. Lett.* **2002**, *351* (1), 115–120.

(110) Gaeta, C.; Talotta, C.; Della Sala, P.; Margarucci, L.; Casapullo, A.; Neri, P.

Anion-Induced Dimerization in *p*-Squaramidocalix[4]arene Derivatives. *J. Org. Chem.* **2014**, *79* (8), 3704–3708.

(111) Wu, X.; Busschaert, N.; Wells, N. J.; Jiang, Y. B.; Gale, P. A. Dynamic Covalent Transport of Amino Acids across Lipid Bilayers. *J. Am. Chem. Soc.* **2015**, *137* (4), 1476–1484.

(112) Chauhan, P.; Mahajan, S.; Kaya, U.; Hack, D.; Enders, D. Bifunctional Amine-Squaramides: Powerful Hydrogen-Bonding Organocatalysts for Asymmetric Domino/Cascade Reactions. *Adv. Synth. Catal.* **2015**, *357* (2–3), 253–281.

(113) Žabka, M.; Šebesta, R. Experimental and Theoretical Studies in Hydrogen-Bonding Organocatalysis. *Molecules* **2015**, *20* (9), 15500–15524.

(114) Jakab, G.; Tancon, C.; Zhang, Z.; Lippert, K. M.; Schreiner, P. R. (Thio)urea Organocatalyst Equilibrium Acidities in DMSO. *Org. Lett.* **2012**, *14* (7), 1724–1727.

(115) Roca-López, D.; Uria, U.; Reyes, E.; Carrillo, L.; Jørgensen, K. A.; Vicario, J. L.; Merino, P. Mechanistic Insights into the Mode of Action of Bifunctional Pyrrolidine-Squaramide-Derived Organocatalysts. *Chem. Eur. J.* **2016**, *22* (3), 884–889.

(116) Albrecht, Ł.; Dickmeiss, G.; Acosta, F. C.; Rodríguez-Escrich, C.; Davis, R. L.; Jørgensen, K. A. Asymmetric Organocatalytic Formal [2+2] Cycloadditions *via* Bifunctional Hydrogen-Bond Directing Dienamine Catalysis. *J. Am. Chem. Soc.* **2012**, *134* (5), 2543–2546.

(117) Orue, A.; Uria, U.; Reyes, E.; Carrillo, L.; Vicario, J. L. Catalytic Enantioselective [5+2] Cycloaddition between Oxidopyrylium Ylides and Enals under Dienamine Activation. *Angew. Chem.* **2015**, *127* (10), 3086–3089.

(118) Feng, B. X.; Wang, B.; Li, X. Asymmetric Additions of Thioglycolates and

N-Boc Aldimines Catalyzed by a Bifunctional Tertiary-Amine Squaramide. *Org. Biomol. Chem.* **2016**, *14* (39), 9206–9209.

(119) Cheon, C. H.; Yamamoto, H. Super Brønsted Acid Catalysis. *Chem. Commun.* **2011**, *47* (11), 3043–3056.

(120) Terada, M. Binaphthol-Derived Phosphoric Acid as a Versatile Catalyst for Enantioselective Carbon-Carbon Bond Forming Reactions. *Chem. Commun.* **2008**, No. 35, 4097–4112.

(121) Terada, M. Chiral Phosphoric Acids as Versatile Catalysts for Enantioselective Transformations. *Synthesis* **2010**, No. 12, 1929–1982.

(122) Vachal, P.; Jacobsen, E. N. Structure-Based Analysis and Optimization of a Highly Enantioselective Catalyst for the Strecker Reaction. *J. Am. Chem. Soc.* **2002**, *124* (34), 10012–10014.

(123) Chen, Y. H.; Cheng, D. J.; Zhang, J.; Wang, Y.; Liu, X. Y.; Tan, B. Atroposelective Synthesis of Axially Chiral Biaryldiols *via* Organocatalytic Arylation of 2-Naphthols. *J. Am. Chem. Soc.* **2015**, *137* (48), 15062–15065.

(124) Cai, X. H.; Xie, B. Recent Advances on Organocatalysed Asymmetric Mannich Reactions. *ARKIVOC* **2013**, *2013* (1), 264–293.

(125) Yang, J. W.; Chandler, C.; Stadler, M.; Kampen, D.; List, B. Proline-Catalysed Mannich Reactions of Acetaldehyde. *Nature* **2008**, *452* (7186), 453–455.

(126) Mannich, C.; Krösche, W. Ueber Ein Kondensationsprodukt Aus Formaldehyd, Ammoniak Und Antipyrin. *Arch. Pharm.* **1912**, *250* (1), 647–667.

(127) Yamanaka, M.; Itoh, J.; Fuchibe, K.; Akiyama, T. Chiral Brønsted Acid Catalyzed Enantioselective Mannich-Type Reaction. *J. Am. Chem. Soc.* **2007**, *129* (21), 6756–6764.

(128) Gridnev, I. D.; Kouchi, M.; Sorimachi, K.; Terada, M. On the Mechanism of Stereoselection in Direct Mannich Reaction Catalyzed by BINOL-Derived Phosphoric Acids. *Tetrahedron Lett.* **2007**, *48* (3), 497–500.

(129) Rueping, M.; Lin, M. Y. Catalytic Asymmetric Mannich-Ketalization Reaction: Highly Enantioselective Synthesis of Aminobenzopyrans. *Chem. Eur. J.* **2010**, *16* (14), 4169–4172.

(130) Wink, M. Modes of Action of Herbal Medicines and Plant Secondary Metabolites. *Medicines* **2015**, *2* (3), 251–286.

(131) Cragg, G. M.; Newman, D. J. Natural Products: A Continuing Source of Novel Drug Leads. *Biochim. Biophys. Acta, Gen. Subj.* **2013**, *1830* (6), 3670–3695.

(132) Flannery, E. L.; Chatterjee, A. K.; Winzeler, E. A. Antimalarial Drug Discovery-Approaches and Progress towards New Medicines. *Nat. Rev. Microbiol.* **2013**, *11* (12), 849–862.

(133) Mink, L.; Ma, Z.; Olsen, R. A.; James, J. N.; Sholl, D. S.; Mueller, L. J.; Zaera, F. The Physico-Chemical Properties of Cinchona Alkaloids Responsible for Their Unique Performance in Chiral Catalysis. *Top. Catal.* **2008**, *48* (1), 120–127.

(134) Dijkstra, G. D.; Kellogg, R. M.; Wynberg, H.; Svendsen, J. S.; Marko, I.; Sharpless, K. B. Conformational Study of Cinchona Alkaloids. A Combined NMR, Molecular Mechanics and X-Ray Approach. *J. Am. Chem. Soc.* **1989**, *111* (21), 8069–8076.

(135) Marcelli, T.; Hiemstra, H. Cinchona Alkaloids in Asymmetric Organocatalysis. *Synthesis* **2010**, No. 8, 1229–1279.

(136) Yu, B.; Xing, H.; Yu, D. Q.; Liu, H. M. Catalytic Asymmetric Synthesis of Biologically Important 3-Hydroxyoxindoles: An Update. *Beilstein J. Org. Chem.* **2016**, *12*, 1000–1039.

(137) Singh, G. S.; Yeboah, E. Recent Applications of Cinchona Alkaloid-Based Catalysts in Asymmetric Addition Reactions. *Rep. Org. Chem.* **2016**, *6*, 47–75.

(138) Connon, S. J. Asymmetric Catalysis with Bifunctional Cinchona Alkaloid-Based Urea and Thiourea Organocatalysts. *Chem. Commun.* **2008**, No. 22, 2499–2510.

(139) Han, Z.; Yang, W.; Tan, C. H.; Jiang, Z. Organocatalytic Asymmetric Mannich Reactions of 5*H*-Oxazol-4-ones: Highly Enantio-and Diastereoselective Synthesis of Chiral α-Alkylisoserine Derivatives. *Adv. Synth. Catal.* **2013**, *355* (8), 1505–1511.

(140) Okumuş, S.; Tanyeli, C.; Demir, A. S. Asymmetric Aldol Addition of α-Azido Ketones to Ethyl Pyruvate Mediated by a Cinchona-Based Bifunctional Urea Catalyst. *Tetrahedron Lett.* **2014**, *55* (31), 4302–4305.

(141) Lin, N.; Deng, Y. Q.; Zhang, Z. W.; Wang, Q.; Lu, G. Asymmetric Synthesis of Chiral β-Hydroxy-α-Amino Acid Derivatives by Organocatalytic Aldol Reactions of Isocyanoesters with β,γ-Unsaturated α-Ketoesters. *Tetrahedron: Asymmetry* **2014**, *25* (8), 650–657.

(142) Ji, N.; Yuan, J.; Xue, S.; Zhang, J.; He, W. Novel Chiral Thiourea Organocatalysts for the Catalytic Asymmetric Oxaziridination. *Tetrahedron* **2016**, *72* (4), 512–517.

(143) Cornaggia, C.; Manoni, F.; Torrente, E.; Tallon, S.; Connon, S. J. A Catalytic Asymmetric Reaction Involving Enolizable Anhydrides. *Org. Lett.* **2012**, *14* (7), 1850–1853.

(144) Zhao, Y. L.; Lou, Q. X.; Wang, L. S.; Hu, W. H.; Zhao, J. L. Organocatalytic Friedel-Crafts Alkylation/Lactonization Reaction of Naphthols with 3-Trifluoroethylidene Oxindoles: The Asymmetric Synthesis of Dihydrocoumarins. *Angew. Chem., Int. Ed.* **2017**, *56* (1), 338–342.

(145) Michael, A. Ueber Die Addition von Natriumacetessig- Und

Natriummalonsäureäthern Zu Den Aethern Ungesättigter Säuren. *J. für Prakt. Chemie* **1887**, *35* (1), 349–356.

(146) Li, X. J.; Peng, F. Z.; Li, X.; Wu, W. T.; Sun, Z. W.; Li, Y. M.; Shao, Z. H. Enantioselective and Regioselective Organocatalytic Conjugate Addition of Malonates to Nitroenynes. *Chem. Asian J.* **2011**, *6* (1), 220–225.

(147) Miyaji, R.; Asano, K.; Matsubara, S. Asymmetric Chroman Synthesis *via* an Intramolecular Oxy-Michael Addition by Bifunctional Organocatalysts. *Org. Biomol. Chem.* **2014**, *12* (1), 119–122.

(148) Hosseini, B.; Shahriari-Ahmadi, F.; Hashemi, H.; Marashi, M. H.; Mohseniazar, M.; Farokhzad, A.; Sabokbari, M. Transient Expression of *cor* Gene in Papaver Somniferum. *BioImpacts* **2011**, *1* (4), 229–236.

(149) Rosenblum, A.; Marsch, L. A.; Joseph, H.; Portenoy, R. K. Opioids and the Treatment of Chronic Pain: Controversies, Current Status, and Future Directions. *Exp. Clin. Psychopharmacol.* **2008**, *16* (5), 405–416.

(150) Barber, R. B.; Rapoport, H. Synthesis of Thebaine and Oripavine from Codeine and Morphine. *J. Med. Chem.* **1975**, *18* (11), 1074–1077.

(151) Benyhe, S.; Zádor, F.; Ötvös, F. Biochemistry of Opioid (Morphine) Receptors: Binding, Structure and Molecular Modelling. *Acta Biol.* **2015**, *59* (1), 17–37.

(152) Canfield, D. V.; Barrick, J.; Giessen, B. C. Structure of Codeine. *Acta Crystallogr., Sect. C: Cryst. Struct. Commun.* **1987**, *43* (5), 977–979.

(153) Shalaeva, M.; Kenseth, J.; Lombardo, F.; Bastin, A. Measurement of Dissociation Constants (pK_a Values) of Organic Compounds by Multiplexed Capillary Electrophoresis Using Aqueous and Cosolvent Buffers. *J. Pharm. Sci.* **2008**, *97* (7), 2581–2606.

(154) Wells, P. B.; Simons, K. E.; Slipszenko, J. A.; Griffiths, S. P.; Ewing, D. F.

Chiral Environments at Alkaloid-Modified Platinum Surfaces. *J. Mol. Catal. A: Chem.* **1999**, *146* (1–2), 159–166.

(155) Dabiri, M.; Salehi, P.; Kozehgary, G.; Heydari, S.; Heydari, A.; Esfandyari, M. Enantioselective Addition of Diethylzinc to Aromatic Aldehydes Catalyzed by 14-Hydroxylsubstituted Morphinans. *Tetrahedron: Asymmetry* **2008**, *19* (16), 1970–1972.

(156) MacMillan, D. W. The Advent and Development of Organocatalysis. *Nature* **2008**, *455*, 304–308.

(157) Tzeng, Z. H.; Chen, H. Y.; Huang, C. T.; Chen, K. Camphor Containing Organocatalysts in Asymmetric Aldol Reaction on Water. *Tetrahedron Lett.* **2008**, *49* (26), 4134–4137.

(158) Dondoni, A.; Massi, A. Asymmetric Organocatalysis: From Infancy to Adolescence. *Angew. Chem., Int. Ed.* **2008**, *47* (25), 4638–4660.

(159) Narayanaperumal, S.; Rivera, D. G.; Silva, R. C.; Paixao, M. W. Terpene-Derived Bifunctional Thioureas in Asymmetric Organocatalysis. *ChemCatChem* **2013**, *5* (10), 2756–2773.

Chapter 2

Synthesis and Structural Characterisation of Thiourea and Urea Opioid Derivatives

2.1 Synthesis of opioid derivatives

An introduction to the morphine alkaloid structure has been discussed in Chapter 1. In order to synthesise the target compounds, some of the key desired manipulations of the opiate scaffold for organocatalyst development, which includes (Scheme 2.1), are listed below:

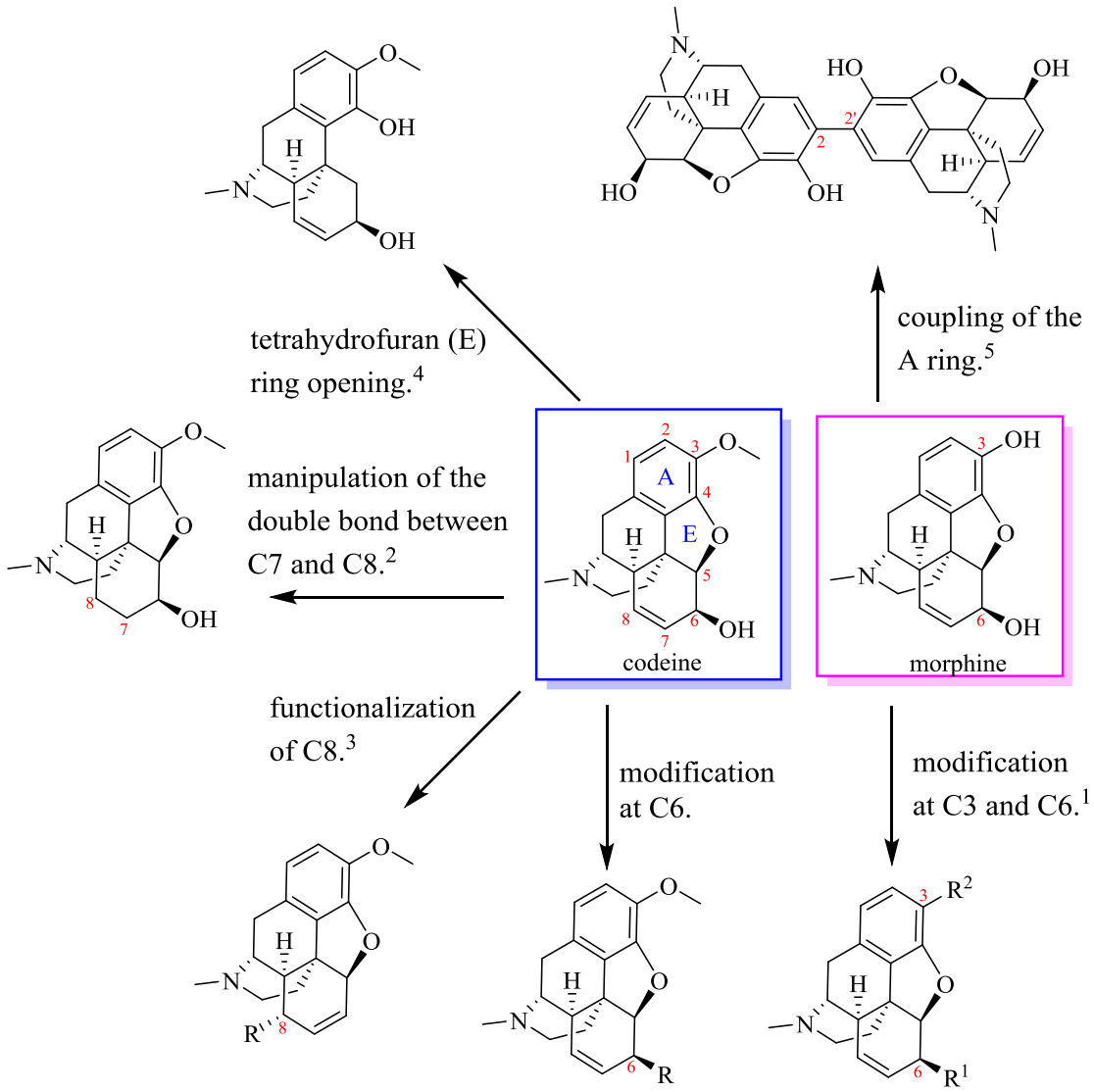

Scheme 2.1 Modification of codeine and morphine for synthesis of catalysts.

- Modification of the phenolic hydroxyl at the C3 and of the secondary C6-hydroxyl of codeine and morphine.[1]
- Manipulation of the double bond between C7 and C8.[2]
- Functionalization of the C8-position.[3]
- Opening of the tetrahydrofuran ring.[4]

- C-C bond formation using transition metal catalysis to couple at the A ring.[5]

Codeine and morphine differ by the extra C18-methyl group present in codeine. We consider this a protecting group for morphine, albeit a robust one. On the other hand, the two reactive hydroxyl groups located on the C3- and C6-position of morphine can be easily substituted.

To facilitate the synthetic process scale-up, the goal of the synthetic route was set up to meet the following criteria: 1. convergent, 2. through same intermediates for convenience, 3. safe and green, 4. commercial availability of starting material. The retrosynthetic analysis (Scheme 2.2) revealed that the skeletal framework of the target molecules can be assembled at the thiourea and urea functionalities. The *N,N'*-disubstituted thiourea (**5**) can be accomplished readily by the facile coupling of C8-substituted opioid isothiocyanate precursor (**2**) with C8-substituted opioid amino precursor (**4**).[6] The synthesis of C8-substituted opioid amino precursor (**4**) would also allow the preparation of the corresponding the *N,N'*-disubstituted urea (**6**) by reacting with C8-substituted opioid isocyanate precursor (**2'**).[7] All opioid precursors can be synthesised from the starting material codeine, which is commercially available in bulk quantities through series of substitution reactions at C6- and C8-positions. The yield and purity of two intermediates (**1**) and (**4**) were also crucial for synthesis of the target molecules.

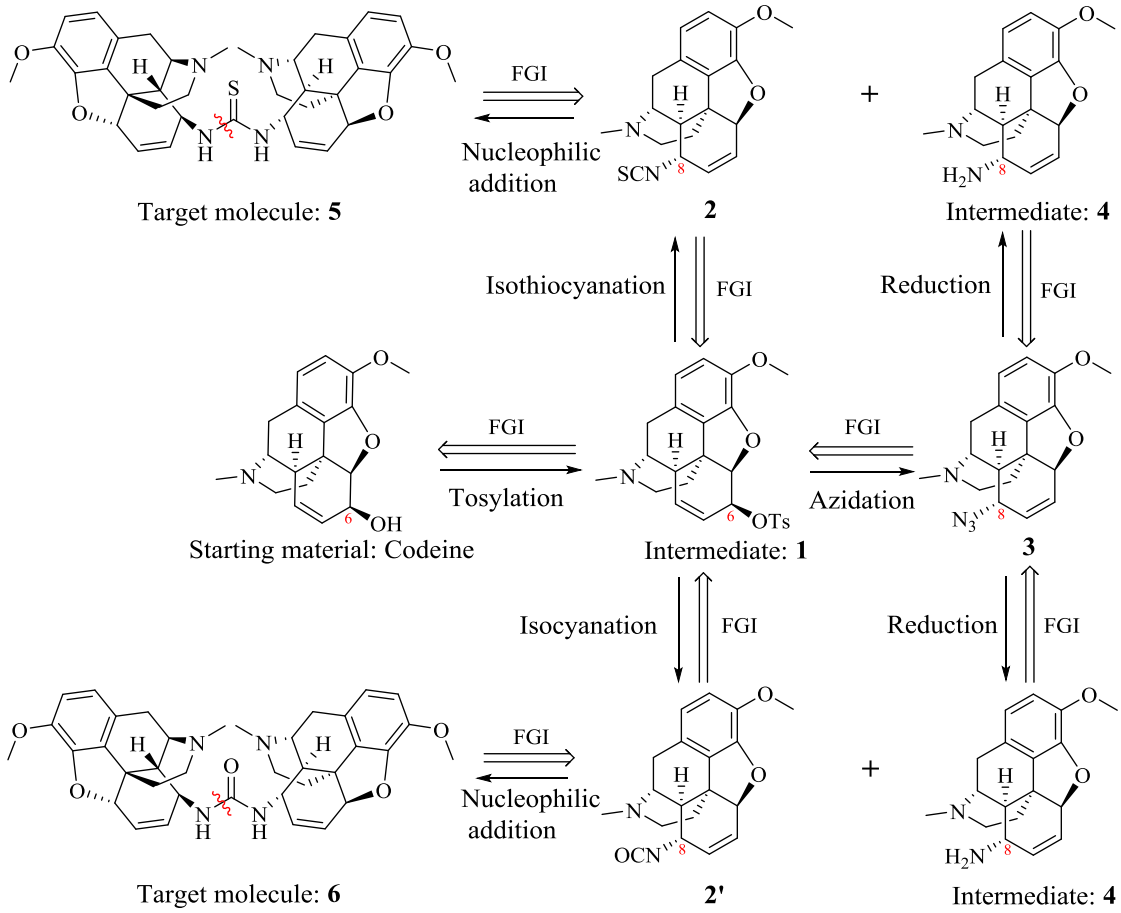

Scheme 2.2 Retrosynthetic analysis of thiourea (**5**) and urea (**6**) derivatives (FGI: Functional Group Interconversion).

2.1.1 Synthesis of 6-*O*-tosylcodeine (1)

Alcohols are poor substrates for nucleophilic substitution reactions due to being a strong base. Mesylates and tosylates are sulfonate compounds that make alcohols into good leaving groups, by turning them into organosulfonates: tosylate and mesylates. Bases such as triethylamine and pyridine can catalyse the reaction and also neutralize the by-product, HCl, preventing acid-catalyzed rearrangement reactions. In the reaction, a nucleophile such as a hydroxyl group can attack the electrophilic center of the sulfonyl chloride and substitute the chloride. The base then removes a proton from the intermediate to give the sulfonate product. The alcohol is converted into a good leaving group.[8] Thus, it would be relatively easy to synthesise other derivatives by starting with the sulfonate product. Tosylation of the codeine was carried out under low-temperature conditions and with an excess of pyridine, which allows the reaction was complete within 24 hours (Scheme 2.3). The mechanism for the formation of 6-*O*-tosylcodeine is shown in Scheme 2.4.

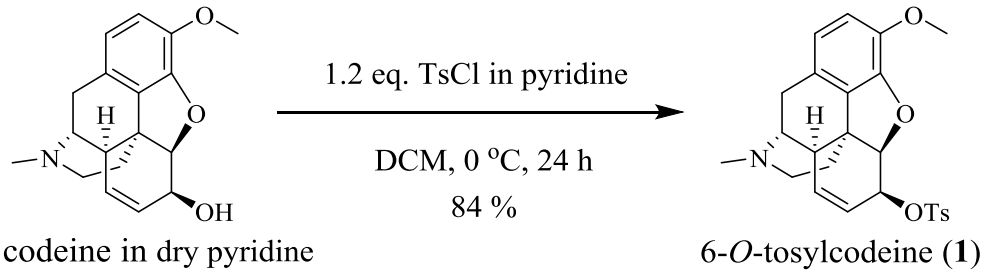

Scheme 2.3 Synthesis of 6-*O*-tosylcodeine (**1**).[9]

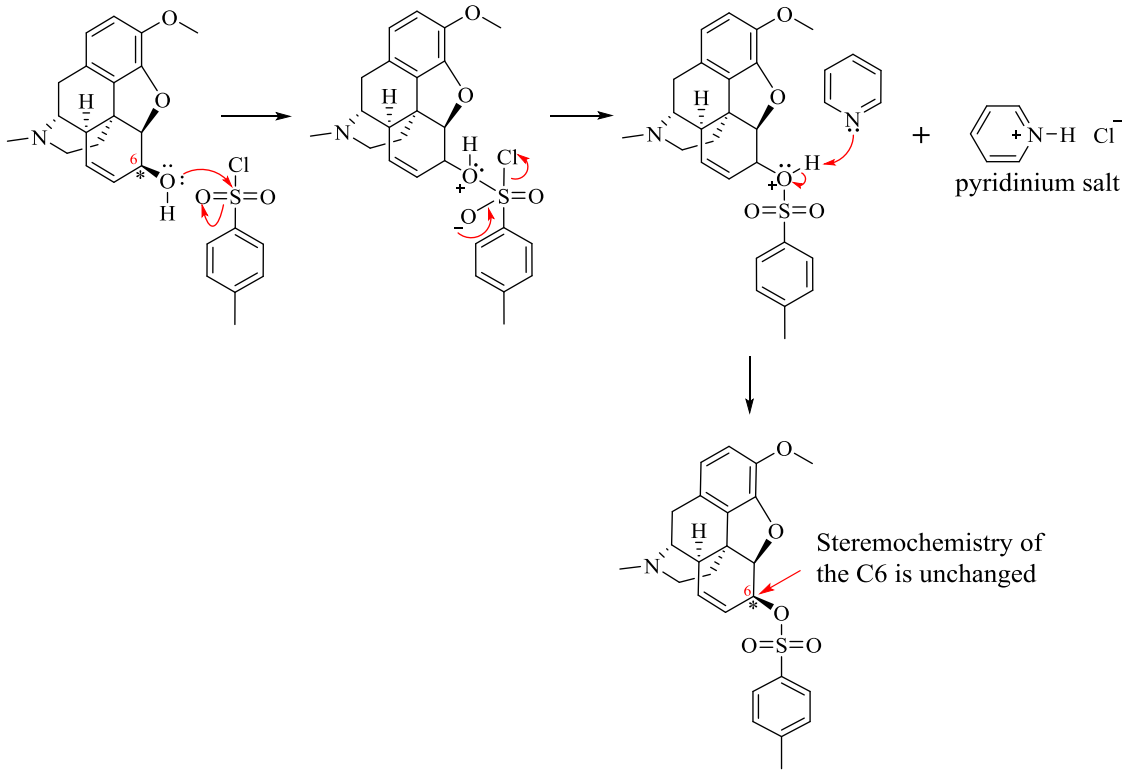

Scheme 2.4 Mechanism for the formation of 6-*O*-tosylcodeine (**1**).[10]

As shown in Scheme 2.4, the nucleophilic oxygen of hydroxyl group on the C6 attacks electrophilic sulfur from the front side, which leads to the formation of O-S bond with losing chloride. Generation of the tosylate product proceeds with retention of configuration at chiral C6 *via* S_N2 nucleophilic substitution reaction. This means the stereochemistry of the product remains the same as of the starting material codeine. This configuration of the product was confirmed by NMR analysis (see Section 2.2). The procedure of synthesis of 6-*O*-tosylcodeine (**1**) was arrived at after multiple experiments examining the temperature, time and the dry pyridine/DCM ratio. The optimized reaction conditions allowed for the purification of the compound *via*

trituration in diethyl ether. This is the first intermediate compound for the synthesis of the other opioid derivatives of this part of the project. All opioid derivatives shown in Scheme 2.5 were synthesised with optimised reagents ratio and conditions in order to obtain the maximised yield and were from the procedure were identified by ^{1}H and ^{13}C NMR spectroscopy (Appendix A).

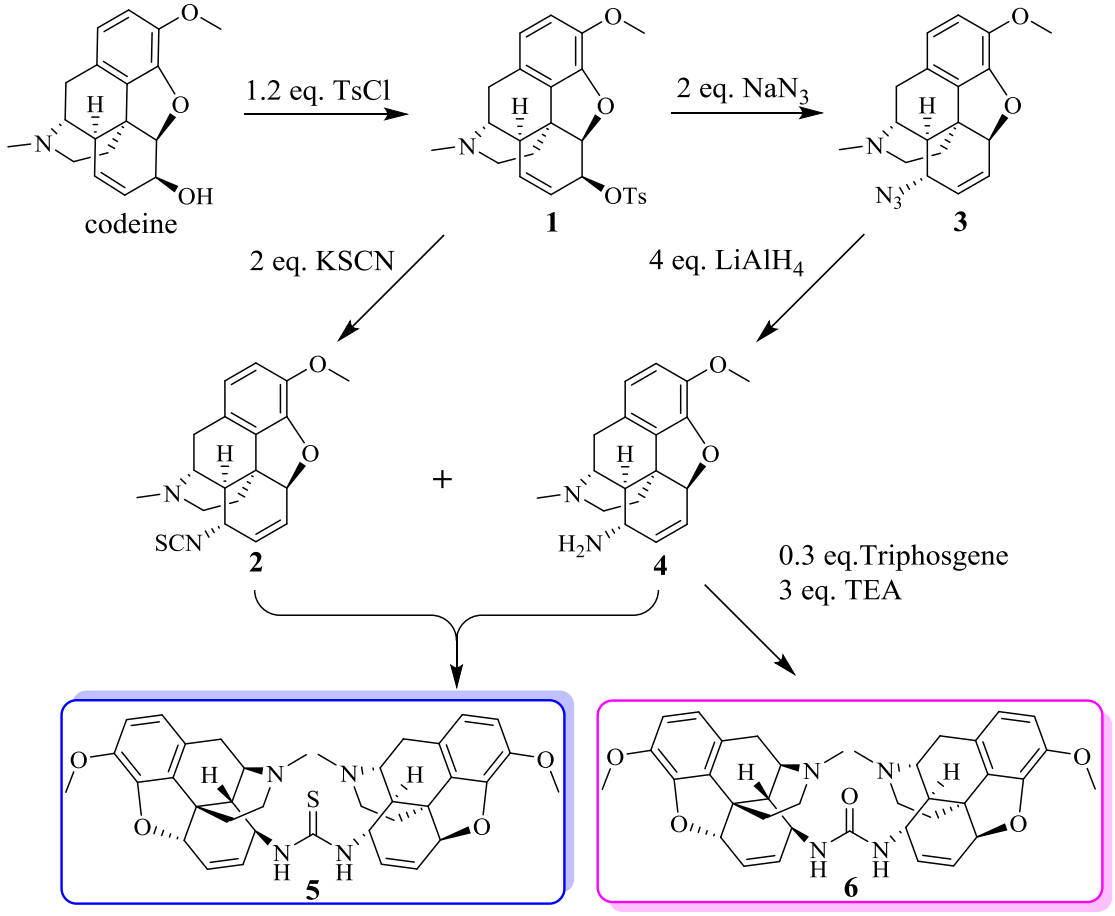

Scheme 2.5 General synthetic procedure of *N,N'*-disubstituted thiourea (**5**) and urea (**6**) derivatives.

2.1.2 Synthesis of 8-isothiocyanocodide (2) and 8-azidocodide (3)

6-*O*-tosylcodeine (**1**) was the first intermediate for both the synthesis of 8-isothiocyanocodide (**2**)[11] and 8-azidocodide (**3**) (Scheme 2.6).[12] In both reactions, substitution of the tosyl group with the isothiocyanate ion (NCS^-) or an azide anion (N_3^-) can occur *via* two different mechanisms (Scheme 2.7). The first mechanism is an S_N2' reaction where the nucleophile attacks the alkene at C8 to give the isothiocyanate or azide in the C8-position directly. The second mechanism is an S_N2 reaction where the nucleophile attacks the saturated C6, followed by a [3,3] sigmatropic

rearrangement which shifts the thiocyanate or azide group from the C6- to the C8-position.[11] Use of dry solvents led two reactions being completed within 4 hours. Purification of 8-isothiocyanocodide (**2**) was by flash chromatography after filtration, whereas 8-azidocodide (**3**) which is the important precursor to the amine (**4**), was easily obtained in high purity by extraction and crystallization with diethyl ether and acetone[12] or by flash chromatography. It is interesting that at low temperatures, it is postulated that the S_N2 reaction occurs with formation of the kinetically favoured product to form 6-substituted opiates such as in the case of 6-*O*-tosylcodeine (**1**) as the main product. At high temperature, however, the possible reaction pathway of S_N2' and subsequent allylic rearrangement of any formed 6-substituted opiates to the corresponding 8-substituted opiates can occur.[11]

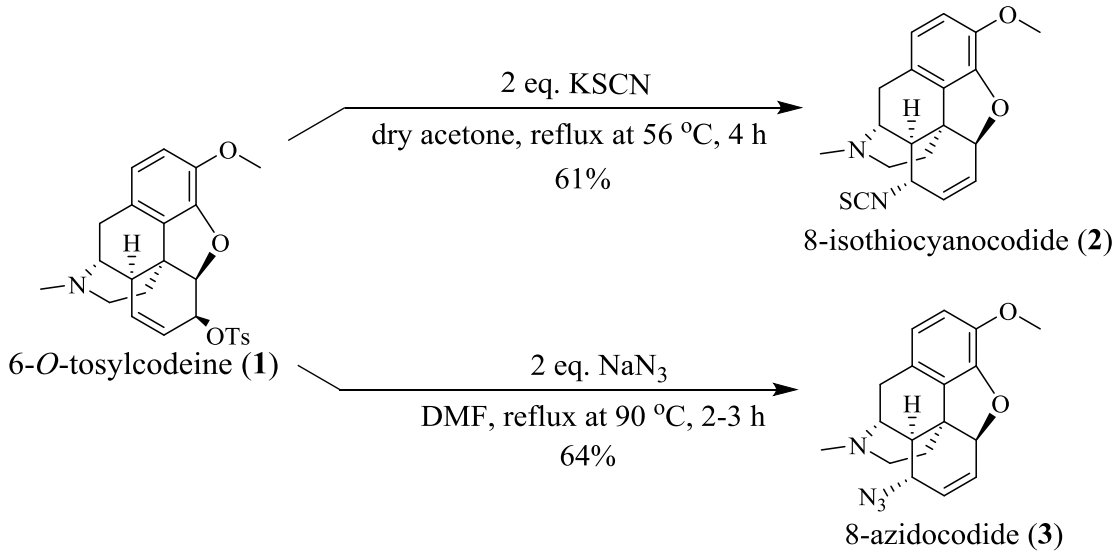

Scheme 2.6 Synthesis of 8-isothiocyanocodide (**2**)[11] and 8-azidocodide (**3**).[12]

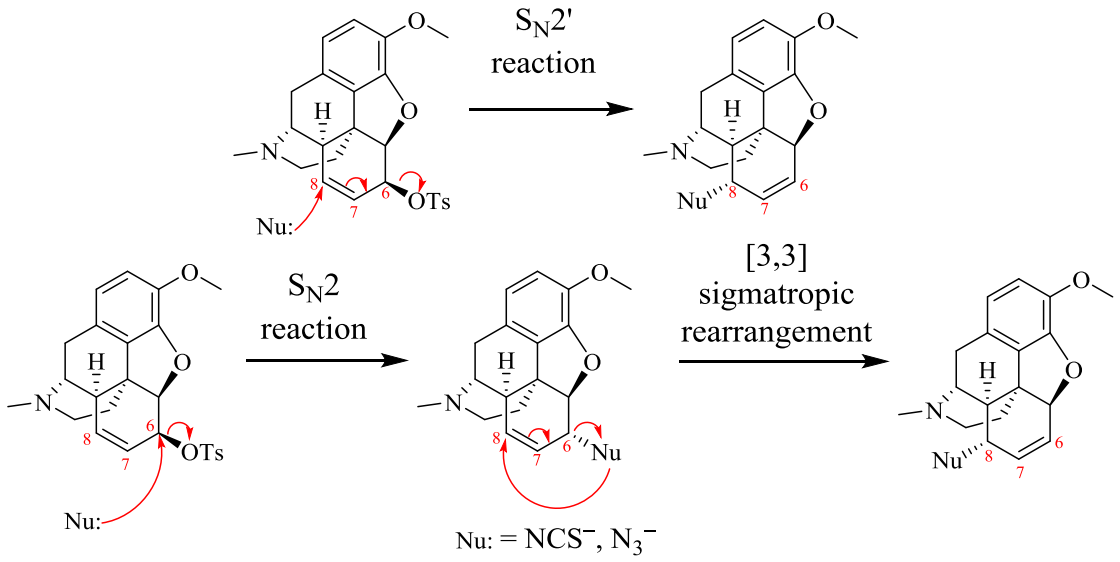

Scheme 2.7 Proposed mechanism of synthesis of 8-isothiocyanocodide (**2**) and 8-azidocodide (**3**) (S_N2' and S_N2 reactions).[11]

2.1.3 Synthesis of 8-aminocodide (4)

8-Aminocodide (**4**) is the key compound for the synthesis of both *N,N'*-disubstituted thiourea (**5**) and *N,N'*-disubstituted urea (**6**). Using 4 equivalent of 1.0 M $LiAlH_4$ in THF,[11] the reduction of 8-azidocodide was completed within 3 hours and accompanied by unreacted starting material 8-azidocodide by TLC monitoring (**3**) and no evidence of any S_N2' products were observed, but non-opioid impurities by NMR analysis (Scheme 2.8). Purification of the crude product was achieved by column chromatography. Trituration of 8-aminocodide with diethyl ether occurs slowly and the product was isolated as 0.42 g of waxy crystals in 46% yield. This result was slightly better than 20% yield from the previous work using 3 equivalent of $LiAlH_4$.[11] It should be noticed that the excess of $LiAlH_4$ would not be recommended to use for the synthesis, due to time-consuming on filtration work. The reduction of 8-azidocodide (**3**) using PPh_3 was also examined, however, we found that the crude product was difficult to purify by flash chromatography.

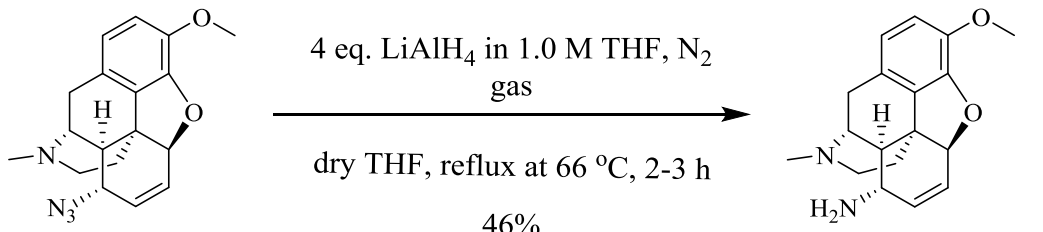

Scheme 2.8 Synthesis of 8-aminocodide (**4**).[11]

2.1.4 Synthesis of *N,N'*-disubstituted thiourea (5) and urea (6) derivatives

N,N'-disubstituted thiourea derivative (**5**) was synthesised by a nucleophilic addition of 8-aminocodide (**4**) to 8-isothiocyanocodide (**2**).[11] In the reaction, the 8-aminocodide (**4**) acts as a nucleophile to attack the electrophilic carbon of 8-isothiocyanocodide (**2**), then the N atom from the 8-isothiocyanocodide abstracts a proton from 8-aminocodide to form urea. The proposed mechanism is shown in Scheme 2.9b. The reaction was heated under reflux conditions in dry THF for 24 hours and purification of the crude product was achieved by column chromatography to give the target compound (**7**) in 44% yield and unreacted materials (**2**) and (**4**) were observed by TLC monitoring.

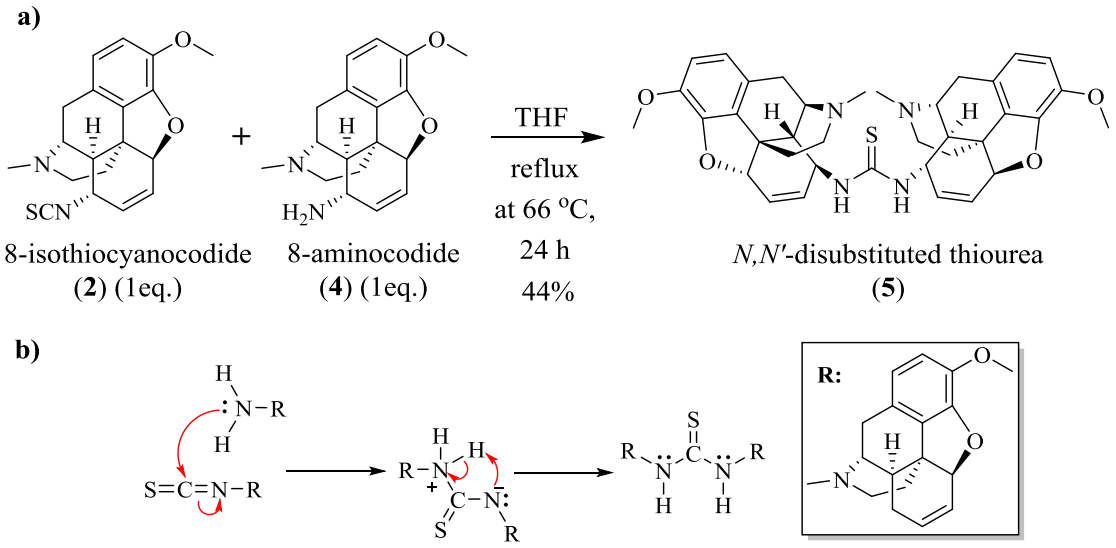

Scheme 2.9 a) Synthesis of *N,N'*-disubstituted thiourea derivative (**5**).[11] b) Proposed mechanism for the synthesis of *N,N'*-disubstituted thiourea derivatives by nucleophilic addition of a secondary amine to isothiocyanate.

Phosgenation of amines is an important reaction in the manufacturing of *N*-containing compounds such as isocyanates, carbamates and *N,N'*-disubstituted urea derivatives.[13] Therefore, the urea derivative (**6**) was synthesised by a phosgenation of 8-aminocodide (**4**) with triphosgene (Scheme 2.10). With triphosgene as a reactant for the reaction, it is considered to have three advantages:

1. A one-pot synthesis of the urea derivative with an amine, without the use of another opioid derivative, shortens the total synthesis process.

2. Compared to diphosgene and phosgene, triphosgene is safer to handle as a reagent due to its solid nature. It is also soluble in most organic solvents, which makes it easy to carry out an aqueous workup after the reaction is complete.[14,15]
3. The reaction conditions can be carried out at low temperature or even room temperature (under anhydrous conditions) unlike the conditions required for diphosgene or phosgene that require lower temperatures and potentially hazardous setups. The elevated temperatures available would speed up the rate of reaction.

Theoretically, when using 0.35 equivalents of triphosgene and an excess of triethylamine (3 eq.), the 8-isocyanocodide (**2**') (Scheme 2.10) would be expected to form as an intermediate and then reacted with the second portion of 8-aminocodide to generate the target urea compound. Therefore, the novel compound 8-isocyanocodide (**2**') could be detected with urea product by TLC, due to having a similar R_f value of 8-isothiocyanocodide (**2**). However, isolation of isocyanates was not able to reach by the method from the literature.[15,16]After monitoring the reaction by TLC after 24 and 72 hours respectively, only the desired urea product and the unreacted 8-aminocodide (**4**) were detected, rather than the expected 8-isocyanocodide (**2**'). The purification of urea derivative was achieved by chromatography to give the urea in a moderate 28% yield.

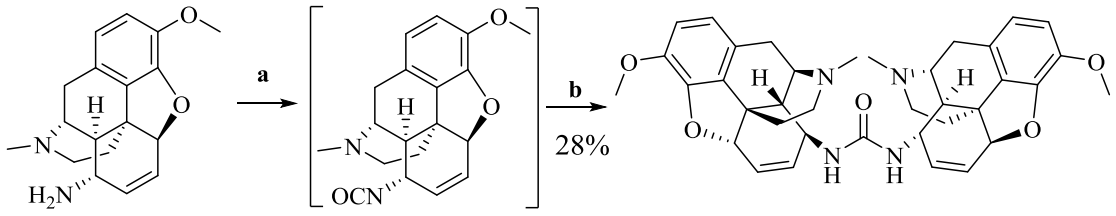

Scheme 2.10 Synthesis of *N,N'*-disubstituted urea derivative (**6**) by triphosgene: a) 3 eq. TEA, 0.3 eq. triphosgene, dry DCM, N_2 gas, 0 ºC, 1 h. b) 1 eq. 8-aminocodide (**4**), rt, 72 h.[15,16]

A second method of forming the urea using diethyl carbonate was examined. The literature procedure utilised a solvent-free process and the use of nontoxic reagents and recoverable catalysts, making it an environmentally friendly chemical procedure. The method of synthesis of a urea using volatile diethyl carbonate and

1,5,7-triazabicyclo[4.4.0]dec-5-ene (TBD) under solvent-free condition was thus examined.[17] With knowing the R_f value of the *N,N'*-disubstituted urea derivative (**6**), the formation of product was observed by TLC monitoring. However, the desired product could not be isolated from impurities by column chromatography.

The isolated yield obtained was poor for both target compounds. There are two issues need to be concerned: reaction condition and long-time purification. For both reactions, starting materials were observed by TLC, which indicates the reactions were not fully completed. Thus, it is necessary to optimise the reaction conditions such as solvents used, temperature and reagents ratio in the future work. Due to the existence of impurities in the crude mixture, the excess of silica was used in order to reach separation quality. However, overloading of silica not only extended time to isolate products from impurities, but the loss was also prominent when more silica is around, especially when compound slowly decompose or reacts with the silica surface. Therefore, calculating the amount of silica to be used is crucial for purification of compounds.

2.1.5 Attempted synthesis of chiral phosphoric acid based opioid derivative

As mentioned in chapter 1, chiral phosphoric acids can also be synthesised from VAPOL and $POCl_3$.[18] The study of the VAPOL structure led to a synthesis of a novel chiral phosphoric acid, which is based on the opiate scaffold. The structures of codeine and (*R*)-VAPOL are shown in Fig. 2.1, both contain a similar polycyclic ring structure. The structure of the VAPOL molecule is very close to the combination of two codeine molecules. Thus, it may be possible to synthesize a novel chiral phosphoric acid by the reaction of codeine and $POCl_3$.

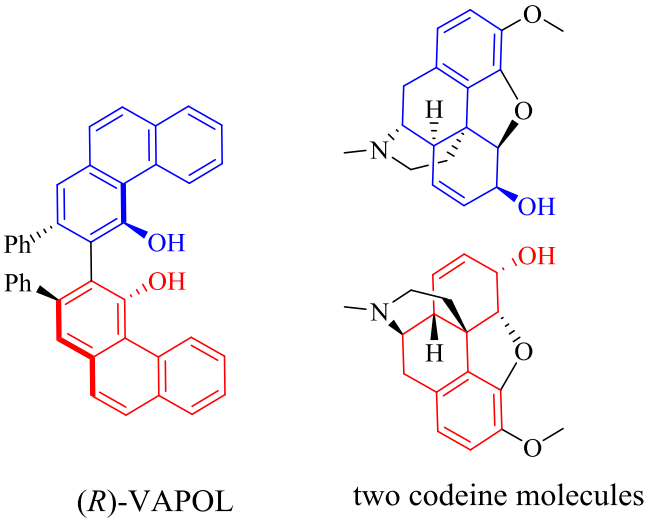

Fig. 2.1 Comparison of codeine and VAPOL structures.

By following the same synthetic procedure for preparation of the chiral phosphoric acids derived from VAPOL, but using codeine instead of VAPOL, codeine was reacted with 0.5 equivalents of $POCl_3$ and the reaction was completed within 6 hours (Scheme 2.11).[18] After workup the main product, however, was identified as α-chlorocodide (**7**), rather than a desired chiral phosphoric acid derivative. The original synthesis of α-chlorocodide (**7**) by $SOCl_2$ at low temperature[19,20] was also carried out in order to confirm the product from the reaction of $POCl_3$. With the ^1H NMR and ^{13}C spectra being identical, the alternative synthetic method of α-chlorocodide was confirmed.

According to the proposed mechanism (Scheme 2.12), the hydroxyl group on the C6-position of codeine was converted into a better leaving group by nucleophilic attack on the electrophilic phosphorus of $POCl_3$ with the generation of Cl^- at the same time. The $OPOCl_2$ group was then S_N2 attacked by Cl^- on the C6-position to leading of inversion configuration of the kinetic product α-chlorocodide (**7**), generating PO_2Cl and Cl^-. The function of $SOCl_2$ is virtually identical to the $POCl_3$ in this context. Formation of an epimer of α-chlorocodide (**5**) would possibly occur in this reaction. However, the configuration of the product from the reaction was proved by ^1H NMR analysis and further details are given in the following section.

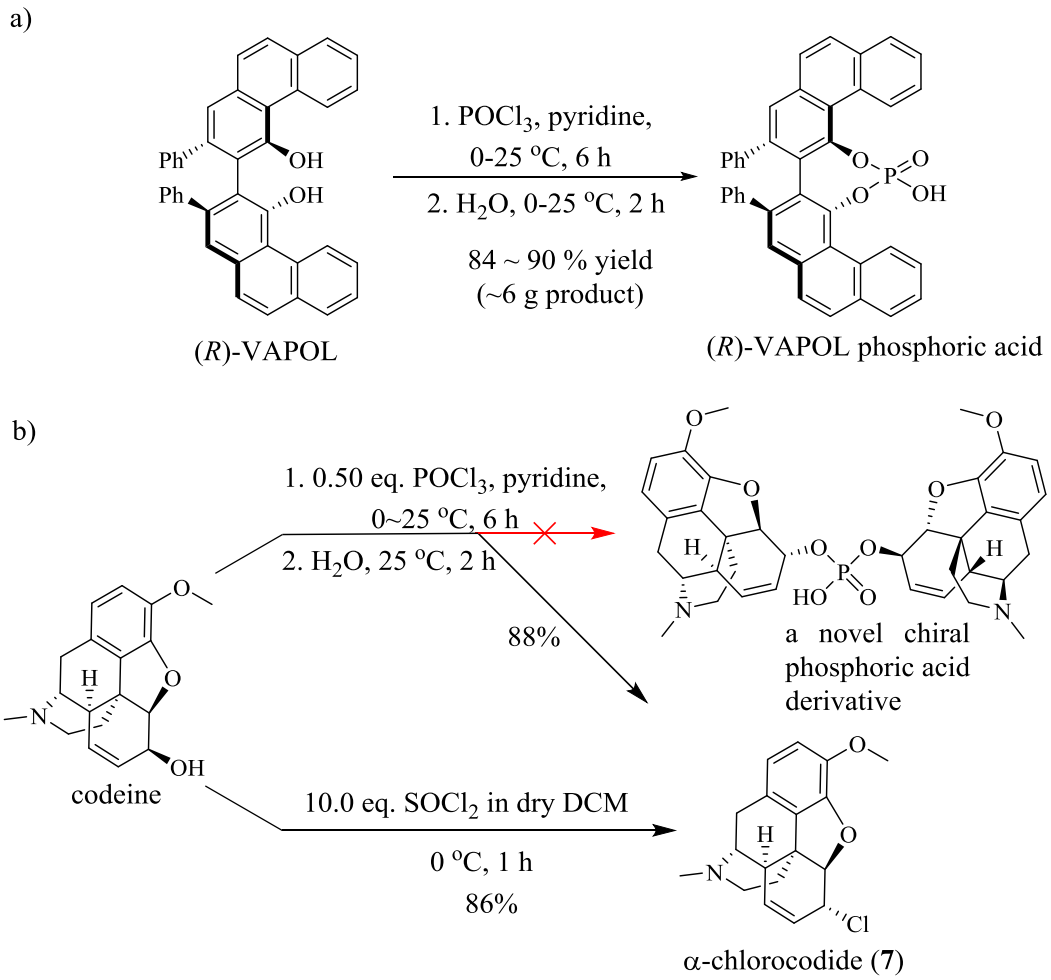

Scheme 2.11 a) Synthesis of (*R*)-VAPOL hydrogenphosphate.[18] b) Attempted synthesis of chiral phosphoric acid derivative and of α-chlorocodide (**7**).[19,20]

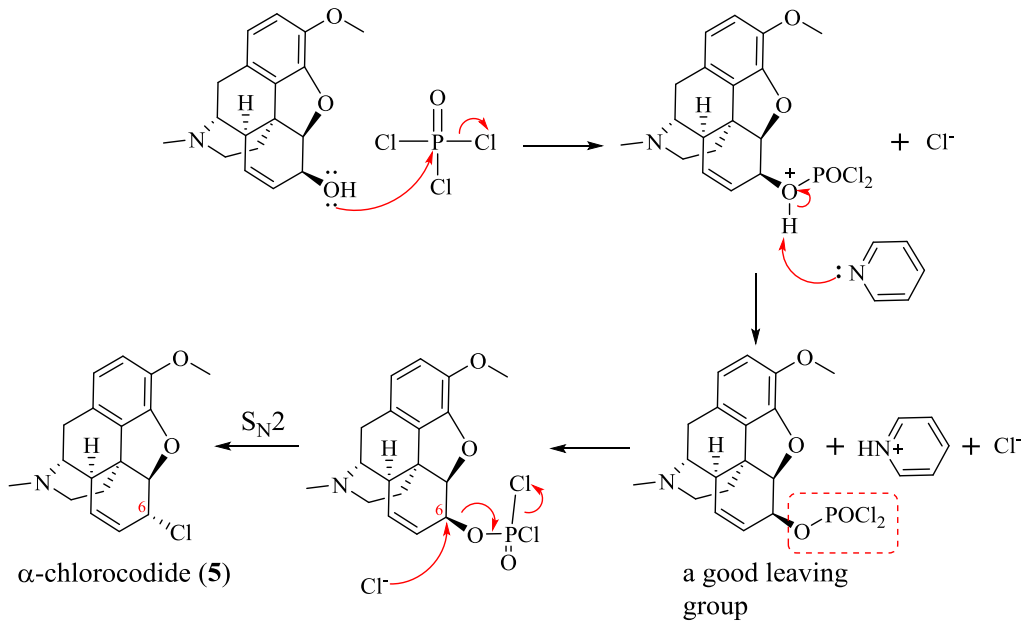

Scheme 2.12 Proposed mechanism of reaction of codeine with $POCl_3$.

2.2 Characterization of opioid precursors

2.2.1 ^{1}H NMR of opioid precursors

Previously study on the ^{1}H and ^{13}C NMR spectra of codeine were performed by Batterham *et al.*[21] and Carroll *el at.*[22], respectively. The ^{1}H and ^{13}C spectra of opioid derivatives were assigned according to their study on codeine spectra and are in agreement with previous work[11] and literature.[3,20,21]

6-*O*-tosylcodeine (**1**), 8-isothiocyanocodide (**2**), 8-azidocodide (**3**), 8-aminocodide (**4**) and α-chlorocodide (**7**) are isolated from the substitution reaction of codeine. Therefore, these compounds have common structural features of codeine (Fig. 2.2), which can be illustrated by their ^{1}H NMR spectra.

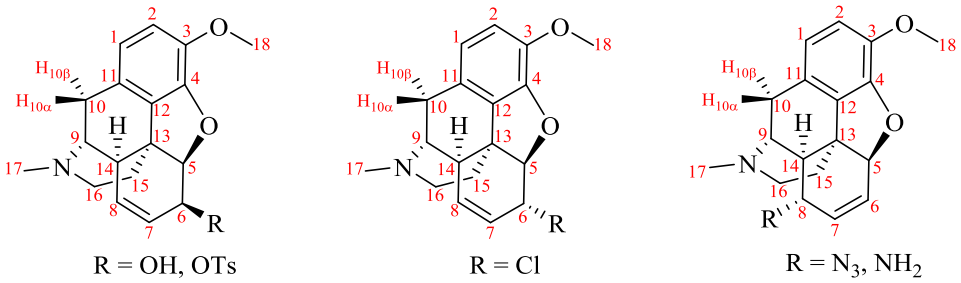

Fig. 2.2 Structures and numbering systems for opioid derivatives synthesised.

As shown in comparison ^{1}H spectra (Fig. 2.3), in codeine and its derivatives, the doublets of aromatic protons H2 and H1(J = 8.2 Hz) were shifted downfield and the ortho effect of the C3 methoxyl group caused the upfield resonance of H2. The protons of methyl group H17and H18 were easily assigned as they present singlets with the similar chemical shift. The protons H9 and diastereotopic protons (H10, H16 and H15) in codeine derivatives also have similar chemical shifts with those in codeine. The occurrence of substitution reaction at the C6-position in the C-ring, contributing to the differences of the chemical shift of H5, H6, H7, H8 and even H14, due to the flexibility of the C-ring.

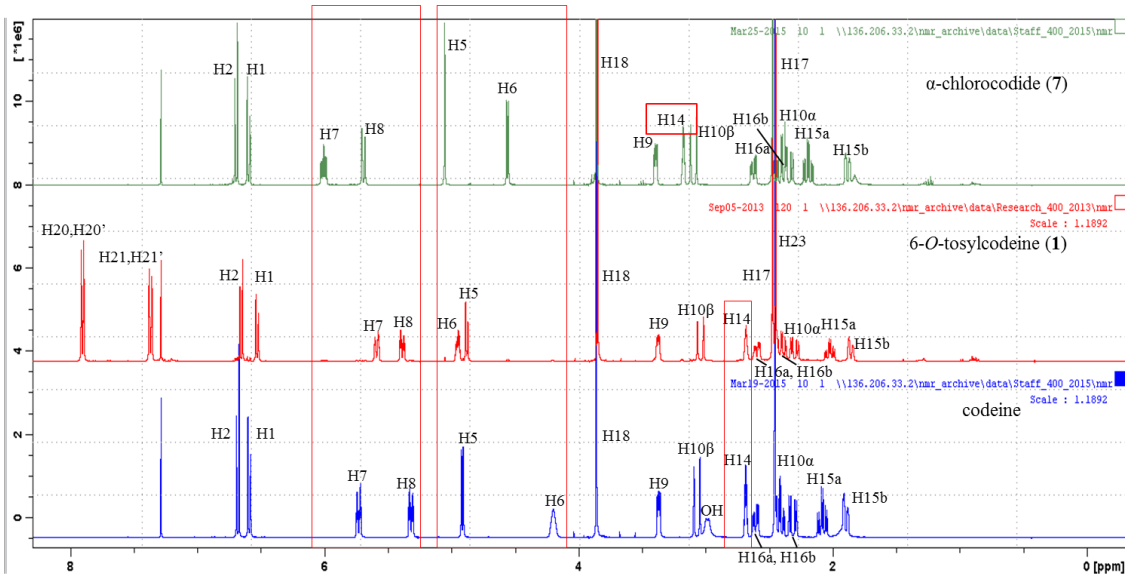

Fig. 2.3 Comparative ^{1}H spectra of codeine and its C6-substituted derivatives (400 MHz, in $CDCl_3$), difference highlighted in red.

Codeine and isocodeine are epimeric alcohols.[23] Jacobson *et al.* confirmed the configuration about C6 in the ring C of both codeine and isocodeine with comparing of their ^{1}H NMR spectra and noted the variation in the chemical shift of H14.[24] They reported that the C6-hydroxyl group in codeine is equatorially oriented and is suited far from the H14. Thus, As showed in Fig. 2.3, H14 appeared relatively shielded with its chemical shift at δ = 2.66 (Table 2.1) in the upfield region, whereas as compared with the chemical shift of H14 (δ = 3.08) in isocodeine,[24] as C6-hydroxyl group is fairly close to the H14 to form a *cis*-diaxial relationship (Fig. 2.4). In contrast, the resonance of H6 proton in the 6-*O*-tosylcodeine (**1**) shifted to the downfield due to electron withdrawing from the tosylate group, but remained the unaffected H14. It suggests that the C6 configuration of 6-*O*-tosylcodeine (**1**) and codeine are identical (Fig. 2.4). Furthermore, the absence of the hydroxyl group (δ= 2.99 ppm) and the presence of proton signals for tosylate group protons: H20, H20', H21, H21' in the aromatic region, and of methyl group H23 in the upfield region, the other proton signals remained as same as those in the codeine. This tells that the tosylation of codeine to afford 6-O-tosylcodeine (**1**) with having the identical configuration of the scaffold. Likewise, H14 in the α-chlorocodide (**7**) located at downfield region δ = 3.17 (Table 2.1) and could expect to be deshielded by C6-hydroxyl group in the *cis*-diaxial relationship, which is exactly similar to the one the isocodeine. Therefore, the chlorine in α-chlorocodide (**7**) is axially oriented in the C6-iso series of the C-ring, which is in

the isocodeine series (Fig. 2.4).[25] On the other hand, the H7 proton in the α-chlorocodide (**7**) shifted to the further downfield region, which was more deshielded than the H8 proton as expected due to its proximity to the chlorine atom. Accompanied by the chemical shift of H7, H5 correspondingly shifted to the downfield, which revealed the presence of their correlation relationship.

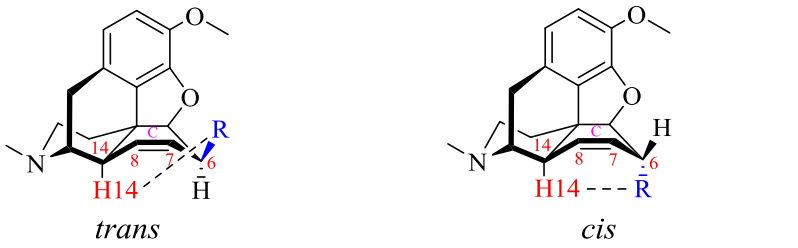

R = OH: codeine
R = OTs: 6-*O*-tosylcodeine (**1**)

R = OH: isocodeine
R = Cl: α-chlorocodide (**7**)

Fig. 2.4 Comparison of configurations of codeine and its C6-substituted derivatives.

Table 2.1 Collated common ^{1}H NMR for codeine and its substituted derivatives **1**, **2**, **3**, **4**, **7** ($CDCl_3$ used as NMR solvent, ^{1}H NMR data recorded in δ values ppm at 400 MHz).

	H1	H2	H5	H6	H7	H8	H9	H10β	H10α
Codeine	6.59	6.68	4.90	4.20	5.70	5.30	3.35	3.05	2.30
1	6.44	6.56	4.79	4.88-4.84	5.50	5.30	3.27	2.95	2.20
2	6.58	6.64	4.93-4.88	5.80-5.71	5.80-5.71	3.72	3.42	3.04	2.42-2.34
3	6.57	6.64	4.95-4.85	5.87-5.74	5.87-5.74	3.21	3.42	3.02	2.42-2.32
4	6.55	6.63	4.90	5.60	5.67	3.21	3.51	3.00	2.42-2.33
7	6.59	6.69	5.05	4.55	6.00	5.69	3.39	3.09	2.35

	H14	H15a	H15b	H16a	H16b	H17	H18	
Codeine	2.66	2.06	1.89	2.60	2.40	2.44	3.85	2.99 (OH)
1	2.58	1.92	1.77	2.49	2.30	2.38	3.76	
2	2.51-2.44	1.87	1.75	2.51-2.44	2.20	2.42-2.34	3.77	
3	2.28	1.87	1.74	2.51-2.44	2.18	2.42-2.32	3.77	

4	1.96	1.84	1.75	2.43	2.22	2.42-2.33	3.78	1.18 (NH_2)
7	3.17	2.19	1.88	2.62	2.40	2.45	3.85	

The ^{1}H NMR spectra of the C8-substituted derivatives show a considerable shift of several protons by comparing with their positions in codeine (Fig. 2.5). As shown in the ^{1}H NMR spectra of the compounds **2**, **3** and **4**, the successful substitution reaction at the C8-position was indicated by the disappearance of multiplets signals from olefinic proton H7 and H8, and formation of another multiplets which represents H6 and H7 in the downfield region. Thus, H8 resonance was upfield as expected. The electronegativity from the substituents also affect the chemical shifts of H8s in the C8 derivatives. H8 of 8-isothiocyanocodide appears relatively deshielded due to the strong electrophilic character of the isothiocyanate group, whereas the H8 of 8-aminocodide (**4**) is more shielded by the strongly electron donating group primary amine NH_2 as the presence of a broad and weak signal in the upfield region (δ = 1.18). Due to correlation with H8, change of chemical shift of H14 in all C8-substituted derivatives was also observed.

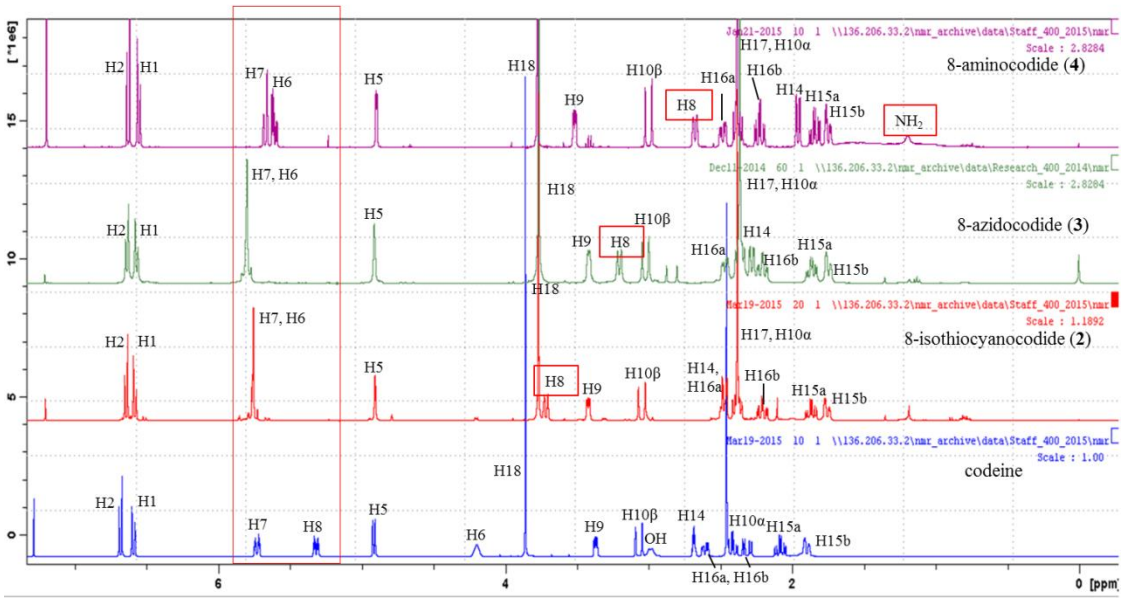

Fig. 2.5 Comparative ^{1}H spectra of codeine and its C8-substituted derivatives (400 MHz, in $CDCl_3$), difference highlighted in red.

2.2.2 ^{13}C NMR of opioid precursors

Exception of the carbon signals from substituents, there are 18 carbon signals in total, including five quaternary carbons C3, C4, C11, C12, C13 in the codeine scaffold and assignment of codeine derivatives' ^{13}C spectra was aided by reference to the published spectrum of codeine, which was report by Carroll *et al.*.[22] All chemical shift data from codeine and its derivatives were list in Table 2.2.

As shown in Fig. 2.6, the majority of the peaks for the C6-substituted derivatives can be easily assigned according to their δ values (ppm) in the ^{13}C spectrum with most similar peaks to the starting material codeine. The two aromatic carbons C1 and C2 can be easily differentiated from the olefinic C7 and C8 by the upfield shift of the latter resonances on the reduction of the double bond. C2 was even further upfield than C1 as a consequence of neighbouring C3 methoxyl substituent. Both the quaternary carbons C4 and C12 are deshielded by oxygen atom on the tetrahydrofuran E-ring, but C12 appeared more shielded than C4 to shift upfield, as it neighbours to the methylene protons of C15. The peaks of C9 and C16 were located upfield as they are close to the NCH_3 on the piperidine D-ring. The C9 resonance was further downfield than C16 as it possessed more β effect from C8 and the NCH_3 group.[22] Carroll *et al.* reported that C15 appeared in the downfield region, because it has more α- and β-substituents and fewer γ-substituents than C10. While C10 resonance was upfield with the combination γ effects from C8, C16 and the NCH_3 group.[22]

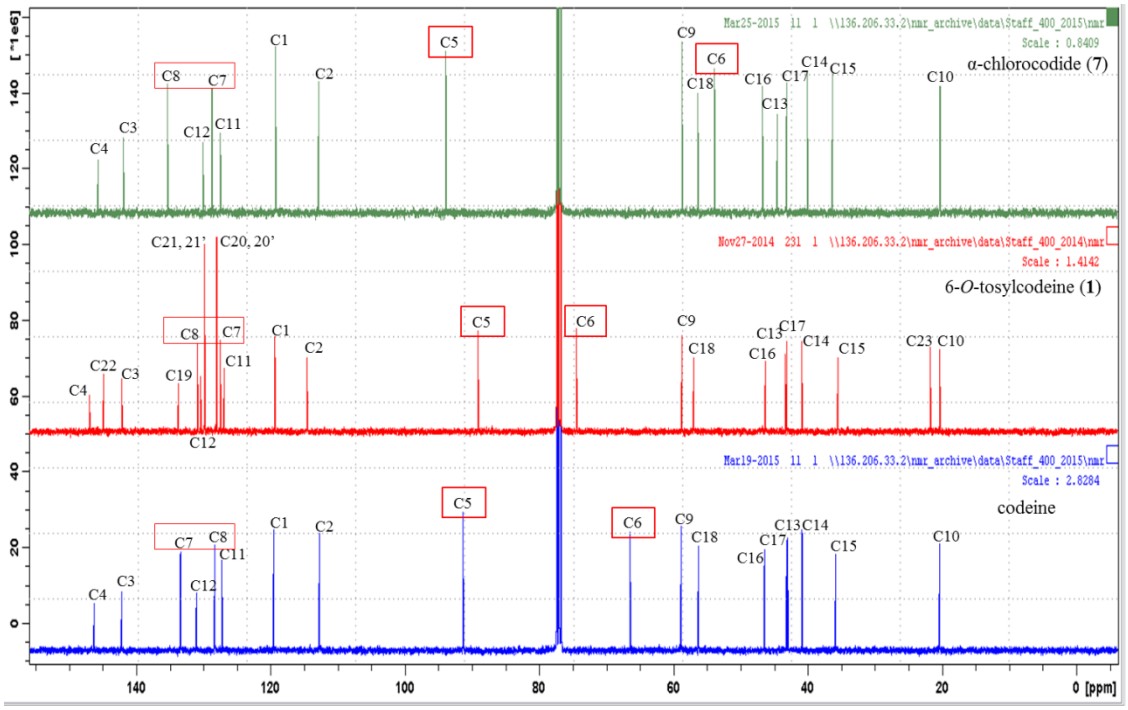

Fig. 2.6 Comparative ^{13}C spectra of codeine and its C6-substituted derivatives (100 MHz, in $CDCl_3$), difference highlighted in red.

Same as their ^{1}H spectra, the distinction between codeine and its C6-derivatives can be also observed from their ^{13}C chemical shifts of C6, C7 and C8, due to the substituent reactions of C6-allylic alcohol in the C-ring (Fig. 2.6). Compared to the ^{13}C spectrum of codeine, as bonding with the tosylate group, C6 in the 6-*O*-tosylcodeine (**1**) is deshielded by the adjacent oxygen and leads to the downfield region. Whereas, since chlorine is less electronegative than oxygen, C6 in the α-chlorocodide (**7**) appears more shielded and resonate upfield. The result reflects the ^{13}C chemical shifts can be influenced by α effect, which strongly dependent on electronegativity of the substituents. It should note that in all C6-substituted derivatives, the substitution reaction of C6-allylic alcohol also induces strong carbon shift, which caused the upfield shift of C7 and downfield shift of C8 resonances ongoing from codeine to either compared to 6-*O*-tosylcodeine (**1**) or α-chlorocodide (**7**) (Table 2.2), owing to the long range effect of the C6-substituents.[22,26] On the other hand, C6-substituents also affected the C5 resonance to the downfield region by the β effect from the chlorine in α-chlorocodide (**7**).[22] Whereas, C5 resonance in the 6-*O*-tosylcodeine (**1**) was upfield, due to neighbouring the tosylate group in the equatorially oriented configuration, which was mentioned previously. The extract aromatic signals C20,

C20', C21, C21' and the methyl signal C23 indicates the tosylate group presents in the 6-O-tosylcodeine (**1**).

Table 2.2 Collated common ^{13}C NMR for codeine and its substituted derivatives **1**, **2**, **3**, **4**, **7** ($CDCl_3$ used as NMR solvent, ^{1}H NMR data recorded in δ ppm at 100 MHz).

	C1	C2	C3	C4	C5	C6	C7	C8
Codeine	119.6	112.9	142.2	146.3	91.3	66.4	133.4	128.2
1	119.4	114.6	142.1	147.0	89.1	74.4	127.5	130.9
2	119.3	113.6	143.3	144.4	86.2	131.5/ 126.3	131.5/ 126.3	53.1
3	118.1	112.3	142.3	143.1	85.4	130.5/ 126.2	130.5/ 126.2	55.1
4	118.8	112.9	143.2	144.3	87.5	123.7	139.5	46.3
7	119.3	112.9	141.9	145.8	93.9	53.9	128.7	135.3

	C9	C10	C11	C12	C13	C14	C15	C16	C17	C18
Codeine	58.9	20.5	127.1	131.1	43.0	40.0	35.8	46.5	43.1	56.4
1	58.8	20.4	126.9	130.4	43.3	40.9	35.5	46.3	43.1	57.0
2	56.2	19.7	128.2	133.3	40.9	46.8/ 46.5	35.3	46.8/ 46.5	43.2	56.3
3	55.3	18.8	125.8	127.8	39.8	44.4	34.2	45.6	42.2	55.5
4	56.2	19.8	127.3	129.8	41.1	49.4	35.6	46.9	43.2	56.3
7	58.7	20.3	127.4	130.1	44.5	40.0	36.3	46.7	43.2	56.3

Substitution reactions at the C8-position cause the upfield C4 by *ca.* 2─3 ppm (Table 2.2). The downfield shift of C6 and the upfield shift of C8, which indicates the presence the double bond between C6 and C7. Poor resolution of peaks of C6 and C7 from 8-isothiocyanocodide (**2**) and 8-azidocodide (**3**) correspond to their multiplets were observed in the ^{1}H NMR spectrum, but not in the 8-aminocodide (**4**). Compared to the spectrum of codeine, the C5 signal appeared as upfield resonance due to the δ substituent effect at the C8-position. The downfield thiocarbonyl signal (δ = 135 ppm) in the spectrum of 8-isothiocyanocodide (**2**) proved the presence of isothiocyanate group. Furthermore, C8-substituent also caused the downfield shift of C14 with the β effect; and the upfield shifts of C9 and C13 by the γ effect. The rest of peak signals in

three C8 derivatives are nearly same as those in codeine, which implied the codeine scaffold did not alter in the reaction process.

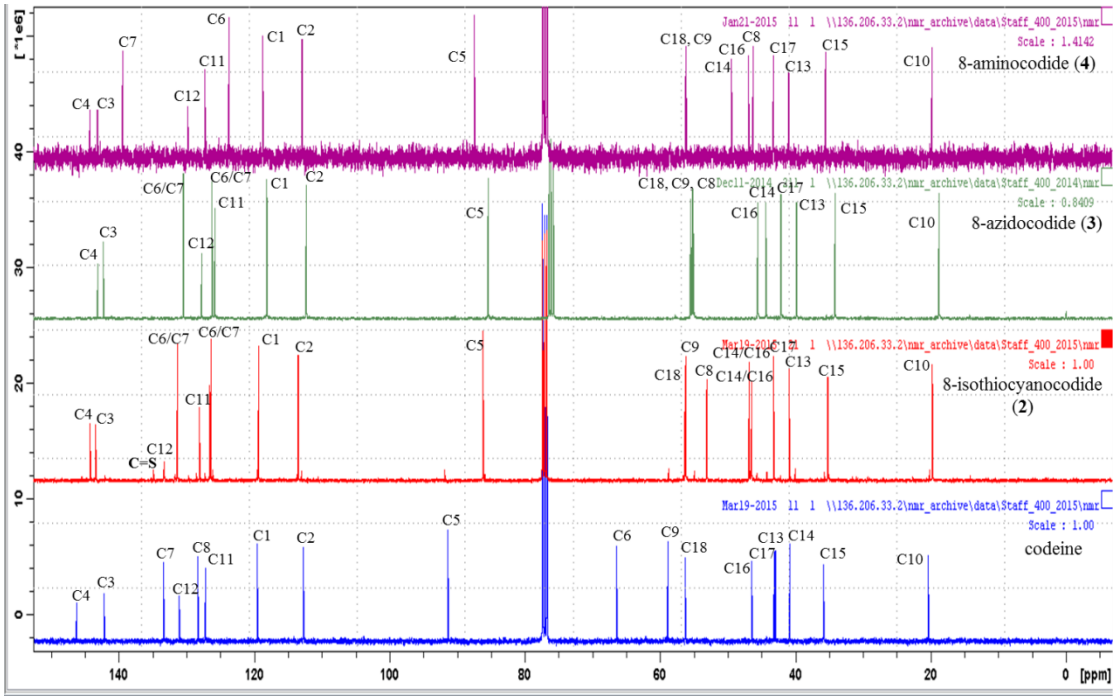

Fig. 2.7 Comparative ^{13}C spectra of codeine and its C8-substituted derivatives (100 MHz, in $CDCl_3$).

2.3 Characterization of *N,N'*-disubstituted thiourea and urea derivatives

The identification and characterization of *N,N'*-disubstituted thiourea and urea derivatives were carried out by NMR, mass spectrometry and X-ray analysis. The NMR data which includes ^{1}H, ^{13}C, DEPT-135, COSY and HMQC data were recorded at room temperature in DMSO-d_6. The mass spectrometry data of the thiourea and urea novel compounds was provided by Dr. Florence McCarthy in University College Cork and Dr. Kevin Conboy in University College Dublin, respectively. The X-ray crystallography of thiourea and urea derivatives was analyzed by Dr. Vickie McKee in Loughborough University and Dr. Brendan Twamley in Trinity College Dublin, respectively. The structure of the thiourea and urea derivatives, their molecular formulae and numbering system (based on the conventional numbering system for opiates) are shown in Fig. 2.8.

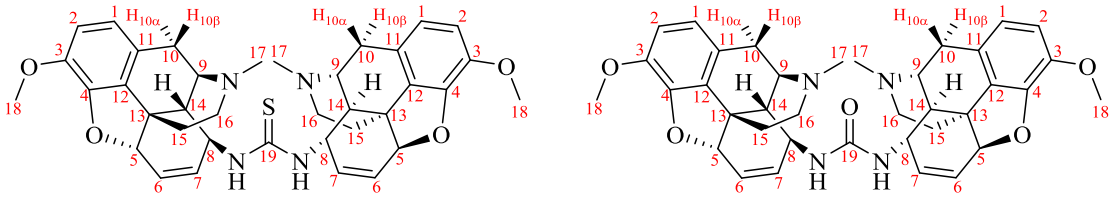

Fig. 2.8 Structures and numbering systems for the *N,N'*-disubstituted thiourea (**5**) and urea (**6**) derivatives.

2.3.1 ^{1}H NMR study of *N,N'*-disubstituted thiourea and urea derivatives

The assignment of the proton peaks is based on the multiplicity and chemical shift. As shown in Fig. 2.8, both the structures of the thiourea and urea compounds are C_2-symmetric, which makes each side of the opioid moiety on the whole molecule (thiourea/urea) equivalent by an axis of symmetry in NMR analysis. For the most part, the ^{1}H NMR spectrum of two novel compounds is similar to parent opioid derivatives, such as 8-aminocodide (**4**).

Some common features were observed from the thiourea and urea NMR due to the similar C_2-symmetric structure. From the ^{1}H spectra Fig. 2.9 and Fig. 2.10, the aromatic protons H1and H2 appear as a pair of doublets with the coupling constant of 8.2 Hz at the range of δ = 6.75 ─ 6.60 ppm, which is within the expected range of vicinal aromatic protons. H6 and H7 on the thiourea compound (**5**) appeared as a singlet, whereas the presence of a doublet of doublets was observed from the starting compound 8-aminocodide (**4**) (Fig. 2.11). It is highly unusual that the two magnetically non-equivalent signals from H6 and H7 have nearly identical resonance frequencies leading them to be close to one another, which creates two overlapping non-equivalent signals on the spectrum, *i.e.* accidental degeneracy.[27] This exception did not occur for the urea compound (**6**) as the formation of a multiplet by overlapping of H6 and H7, rather than of a singlet. A multiplet by overlapping of H6 and H7 signals was also observed from the 8-isothiocyanocodide (**2**) and 8-azidocodide (**3**) compounds (Fig. A3 and Fig. A5 in appendix A).

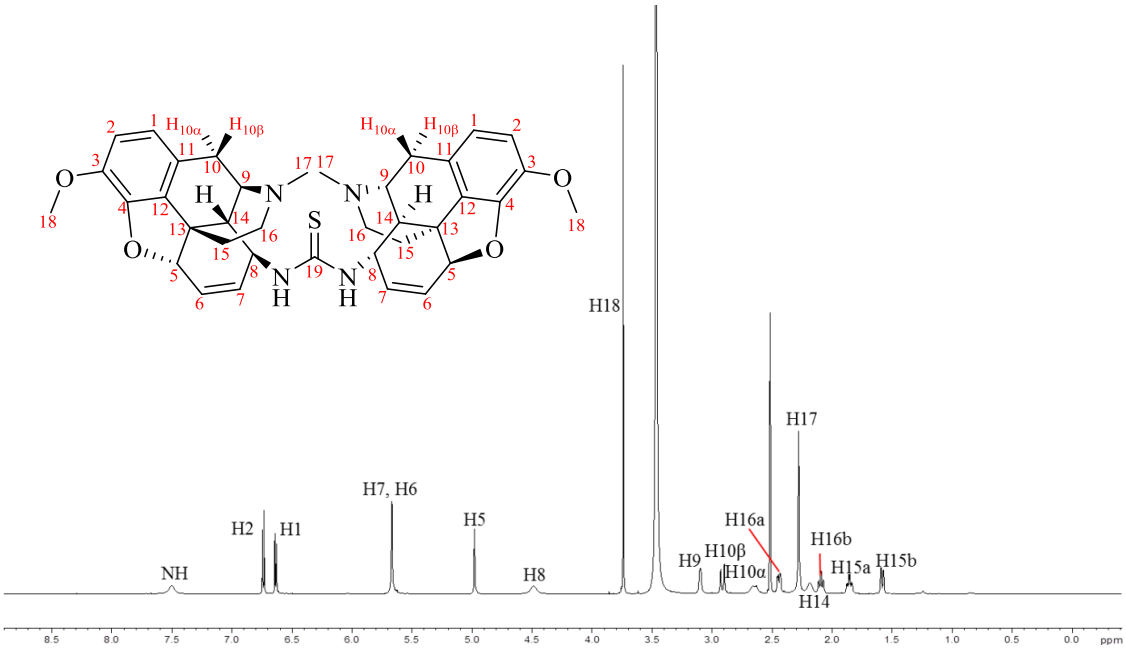

Fig. 2.9 Peak assignments of *N,N'*-disubstituted thiourea derivative (**5**) ^{1}H NMR spectrum (600 MHz) in DMSO-d_6.

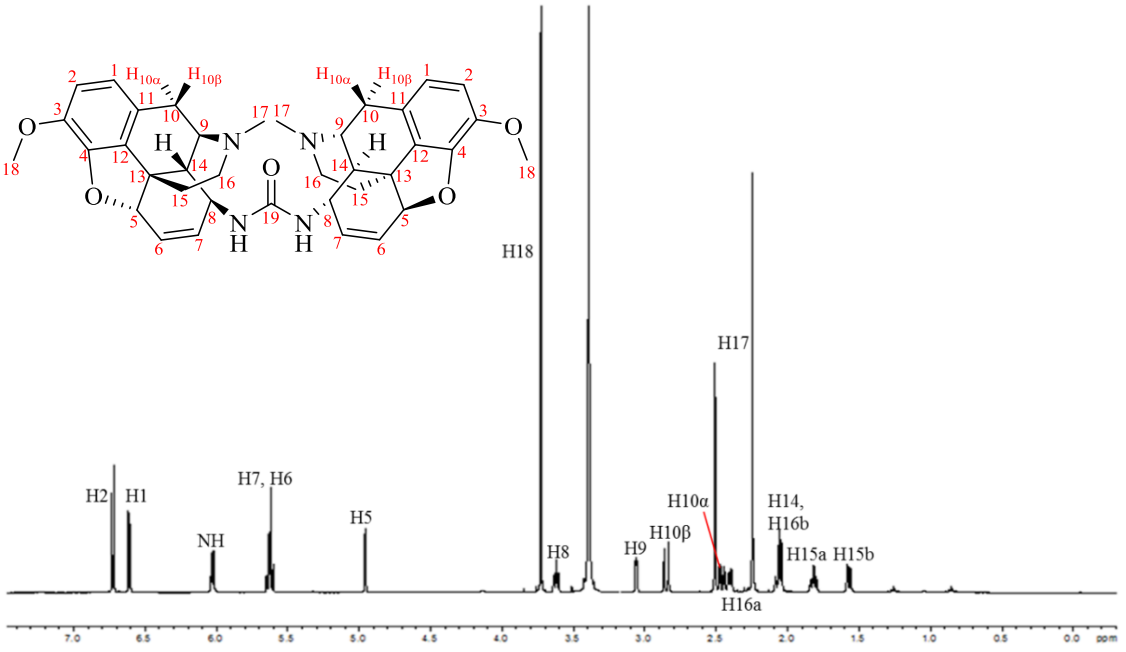

Fig. 2.10 Peak assignments of *N,N'*-disubstituted urea derivative (**6**) ^{1}H NMR spectrum (600 MHz) in DMSO-d_6.

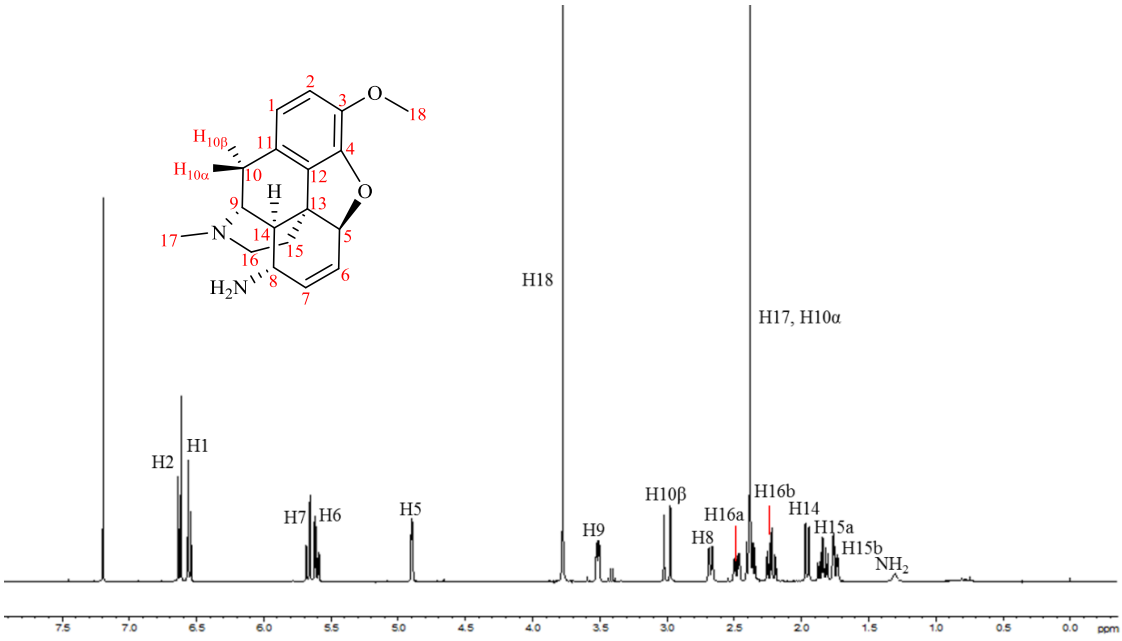

Fig. 2.11 Peak assignments of 8-aminocodide (**4**) ^{1}H NMR spectrum (400 MHz) in $CDCl_3$.

H5 on both novel compounds appears as a doublet with a small coupling constant of 1.9 Hz, which couples to H6 and H7. H8 on the thiourea compound (**5**) located at δ = 4.48 ppm as a broad singlet, while one on the urea compound (**6**) slightly shifted upfield (δ = 3.62 ppm) as an unresolved doublet of triplets. The methyl signals H18 and H17 correspond to a singlet on both novel compounds, having a similar chemical shift, located at δ = 3.74 ppm and δ = 2.28 ppm for thiourea compound (**5**) and δ = 3.73 ppm and δ = 2.25 ppm for urea compound (**6**). Locations of the H9 protons on both of the novel compounds are at δ = 3.10 ppm with the same coupling constants of 3.2 Hz and 2.7 Hz and this proton couples to H10α with the coupling constant of 3.2 Hz and to H14 with the coupling constant of 2.7 Hz. Protons attached to C10, C15 and C16 are diastereotopic due to their being in different chiral chemical environments. Two protons on the C10 have the geminal coupling ($^{2}J_{HH}$), they are not chemically equivalent: a doublet of H10β with the coupling constant 18.0 Hz does not couple to H9. According to the Karplus curve, vicinal coupling constant (^{3}J) from H10β and H9 equals 0, which means H10β is perpendicular to H9.[28] In the thiourea compound (**5**), H10α is located at δ = 2.64 ppm as a doublet of doublets with coupling to H9 (^{3}J = 5.4 Hz) and H10β (^{2}J = 12.8 Hz), while H10α in the urea compound (**6**) is located at δ = 2.46 ppm as a doublet of doublets with coupling to H9 (^{3}J = 6.1 Hz) and H10β (^{2}J = 12.5 Hz).

H16 protons on the thiourea compound (**5**) appear as a doublet of doublets and a triplet of doublets at δ = 2.43 ppm and δ = 2.09 ppm, respectively. Only a doublet of doublets for H16a was observed at δ = 2.40 from the urea compound (**6**) and the triplet of doublets for H16b overlapped with the doublet of doublets for H14 to form a multiplet.

A doublet of doublets at δ = 2.18 ppm from the thiourea compound (**5**) corresponds to H14, which couples to H9 with the coupling constant 2.5 Hz while coupling to H8 with the coupling constant 9.8 Hz. However, the corresponding proton in the urea compound could not be determined because of overlapping with H16b proton.

One of the H15 protons of both thiourea and urea compounds resonate at high field in presence of a triplet of doublets and a doublet. The chemical shifts of the triplet of doublets of the thiourea compound (**5**) and the urea compound (**6**) are at δ = 1.86 ppm and δ = 1.82 ppm, respectively, and with similar coupling constants: *J* = 7.6, 4.8 Hz for the thiourea, *J* = 7.5, 5.0 Hz for the urea. Presumably the doublet at δ = 1.60 ppm (thiourea) and δ = 1.57 ppm (urea) appear as a doublet of doublets and it could be another consequence of the poorly resolved signal.

The downfield signal of NH proton on the thiourea moiety appears as a broad singlet at δ = 7.50 ppm, while the one on the urea moiety appeared to be a sharp doublet and shift slightly upfield (at δ = 6.03 ppm). Oxygen is more electronegative than sulfur, which will cause the NH proton in the urea compound might be expected to present more downfield than one in the thiourea compound, due to deshielding from the C=O group, but the observation from their NMR spectra is actually reversed. Jirman *et al.* explained the result with comparing the Δδ (^{15}N) from acylureas and acylthioureas.[29] They found that the C=S group of thioureas is better than C=O group of the ureas in the transmission of the electron-acceptor effect of the acyl group. Furthermore, they also observed the higher electron density at both nitrogens in the benzoylurea in regard to the benzoylthiourea. According to the results, they concluded the C=S group of acylthioureas is more efficient than the C=O group of acylureas in lowering the electron density at both the nitrogen atoms.[29,30] In other words, the protons of thiourea are more acidic than those of urea, as they are hydrogen-bond donors.[31] Therefore, based on the information above, it was concluded that the chemical shift of NH proton

in the thiourea (**5**) and urea (**6**) compounds are not affected by the electronegativity of sulfur or oxygen atom, rather by the C=S and C=O as a whole.

2.3.2 ^{1}H-^{1}H COSY of *N,N'*-substituted thiourea and urea derivatives

^{1}H-^{1}H Correlation Spectroscopy (COSY) is a 2D experiment, which is a useful method to indicates which protons are coupling with each other. Two axes of the ^{1}H spectrum are plotted orthogonally and spin-spin coupling is indicated in the form of a contour plot. Correlations only appear when there is spin-spin coupling between protons. In both the COSY spectra of thiourea (**5**) and urea (**6**) (Fig. 2.12 and Fig. 2.13), a weak coupling between the NH and H8 is observed, which confirms the assignment of the proton bonded to the nitrogen of the thiourea and urea moiety. Coupling between H1 and H2 on the aromatic ring of the opiate scaffold shows strong signals; H5 couples to the singlet representing the protons H6 and H7. It is interesting to note that the coupling between H8 and H14 is observed, but not between H8 and H7. H9 couples weakly to H14, but strongly to H10α, the Geminal coupling is observed between the diastereotopic protons H10, H15 and H16 protons. In the thiourea COSY spectrum (Fig. 2.12), the vicinal coupling between H16a (δ = 2.43 ppm) couples to H15a (δ = 1.86 ppm), but not to H15b (δ = 1.60 ppm) whilst H16b (δ = 2.09 ppm) couples to both H15a (δ = 1.86 ppm) and H15b (δ = 1.60 ppm). The same can be observed in the urea COSY spectrum (Fig. 2.13), the vicinal coupling between H16a (δ = 2.40 ppm) only couples to H15a (δ = 1.82 ppm), and H16b which overlaps with H14 (δ = 2.06 ppm) couples to both H15a (δ = 1.82 ppm) and H15b (δ = 1.57 ppm). Analysis of the COSY spectra for both thiourea and urea compounds shows the peaks assignments agree with the ^{1}H NMR spectrum. The coupling data of thiourea and urea are summarized in Table 2.3 and Table 2.4 respectively with COSY spectra.

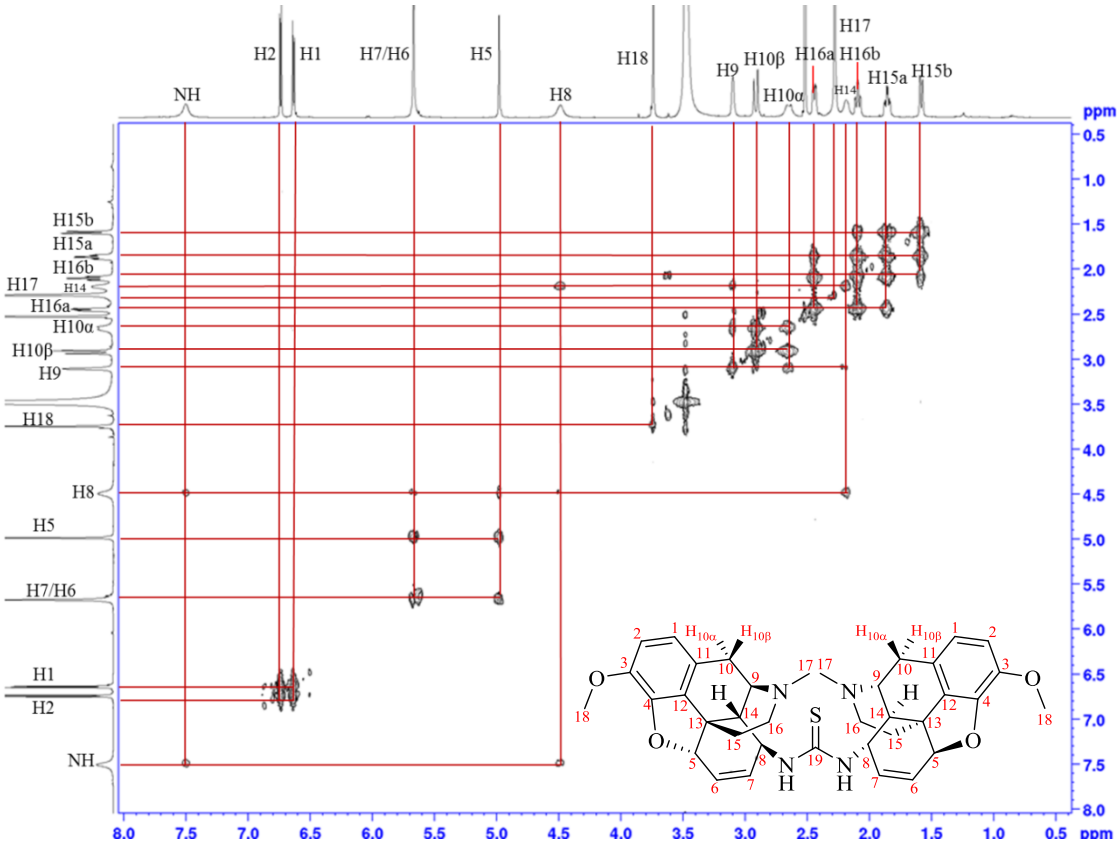

Fig. 2.12 1H-^{1}H COSY spectrum (600 MHz) in DMSO-d_6 of *N,N'*-disubstituted thiourea derivative (**5**) with coupling highlighted in red.

Table 2.3 Observed coupling in COSY spectrum of *N,N'*-disubstituted thiourea derivative (**5**) (* denotes weak coupling).

Proton	Coupling
NH	H8
H1	H2
H2	H1
H6/H7	H5
H5	H6/H7
H8	NH*, H14
H9	H10α, H14*
H10β	H10α
H10α	H9, H10β
H16a (δ = 2.43 ppm)	H16b (δ = 2.09 ppm), H15a (δ = 1.86 ppm)
H14	H8, H9*

H16b (δ = 2.09 ppm)	H16a (δ = 2.43 ppm), H15a (δ = 1.86 ppm), H15b (δ = 1.60 ppm)
H15a (δ = 1.86 ppm)	H15b (δ = 1.60 ppm), H16a (δ = 2.43 ppm), H16b (δ = 2.09 ppm)
H15b (δ = 1.60 ppm)	H16b (δ = 2.09 ppm), H15a (δ = 1.86 ppm)

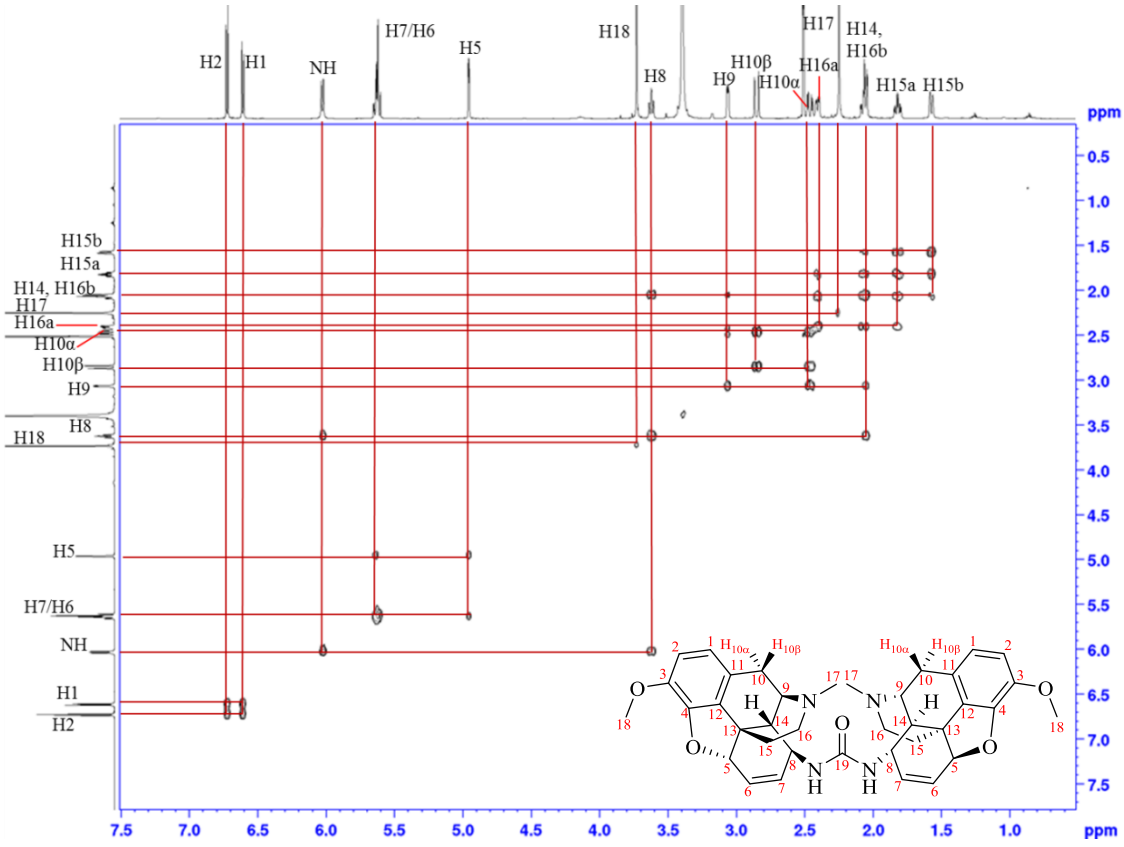

Fig. 2.13 ^{1}H-^{1}H COSY spectrum (600 MHz) of *N,N'*-disubstituted urea derivative (**6**) with coupling highlighted in red.

Table 2.4 Observed coupling in COSY spectrum of *N,N'*-disubstituted urea derivative (**6**) (* denotes weak coupling).

Proton	Coupling
H2	H1
H1	H2
NH	H8
H6/H7	H5
H5	H6/H7
H8	NH*, H14
H9	H10α, H14*

H10β	H10α
H10α	H9, H10β
H16a (δ = 2.40 ppm)	H16b (δ = 2.06 ppm), H15a (δ =1.82 ppm)
H14	H8, H9*
H16b (δ = 2.06 ppm)	H16a (δ = 2.40 ppm), H15a (δ = 1.82 ppm), H15b (δ = 1.57 ppm)
H15a (δ = 1.82 ppm)	H15b (δ = 1.57 ppm), H16a (δ = 2.40 ppm), H16b (δ = 2.06 ppm)
H15b (δ = 1.57 ppm)	H16b (δ = 2.06 ppm), H15a (δ = 1.82 ppm)

2.3.3 ^{13}C and DEPT-135 of *N,N'*-disubstituted thiourea and urea derivatives

Nuclear Magnetic Resonance (NMR) spectroscopy is not limited to the study of protons. Any elements with a nuclear spin such as ^{1}H, ^{13}C, ^{19}F will generate signals in NMR spectroscopy. Carbon-13 has a nuclear spin I = 1/2 and makes up 1.1% of all naturally occurring carbon. As a result, the sensitivity of ^{13}C NMR is lower than of ^{1}H NMR (with a relative abundance of 99.98%). The ^{13}C NMR spectrum is generally proton decoupled in routine use, which causes spin-spin coupling patterns and overlapping multiplets to be seldom observed and displays the number of non-equivalent carbon signals in a molecule within a wide chemical shift range. The distortionless Enhancement by Polarization Transfer (DEPT) is useful to determine the number of protons attached to a carbon. The signals of CH and CH_3 carbons are displayed as positive signals while the negative signal for CH_2 carbons. The signals of quaternary carbons cannot be observed from DEPT spectra. The combination of ^{13}C and DEPT-135 usually are used for the peak assignments.

In the ^{13}C spectra of thiourea and urea derivatives (Fig. 2.14 and Fig. 2.16), there are 19 carbon signals corresponding to non-equivalent carbons. C19 from both compounds fall within the expected range and disappear in the DEPT spectrum. It is interesting that the thiocarbonyl carbon signal (δ = 183.2 ppm) appears much weaker than the carbonyl carbon signal (δ = 158.4 ppm). The signals of the aromatic and vinylic carbons are in the region 145 ─ 110 ppm of the ^{13}C spectra and C6, C7, C1 and C2 are present in the DEPT. The absent signals are considered to be the quaternary carbons. C5 is identified at the range δ = 85 ─ 87 ppm which is at an analogous chemical shift

relative to the ^{13}C spectrum of codeine. Methylene group carbons C16, C15 and C10 are easy to identify as they appear as negative signals in the DEPT (Fig. 2.15 and Fig. 2.17). These assignments can be confirmed by further HMQC analysis.

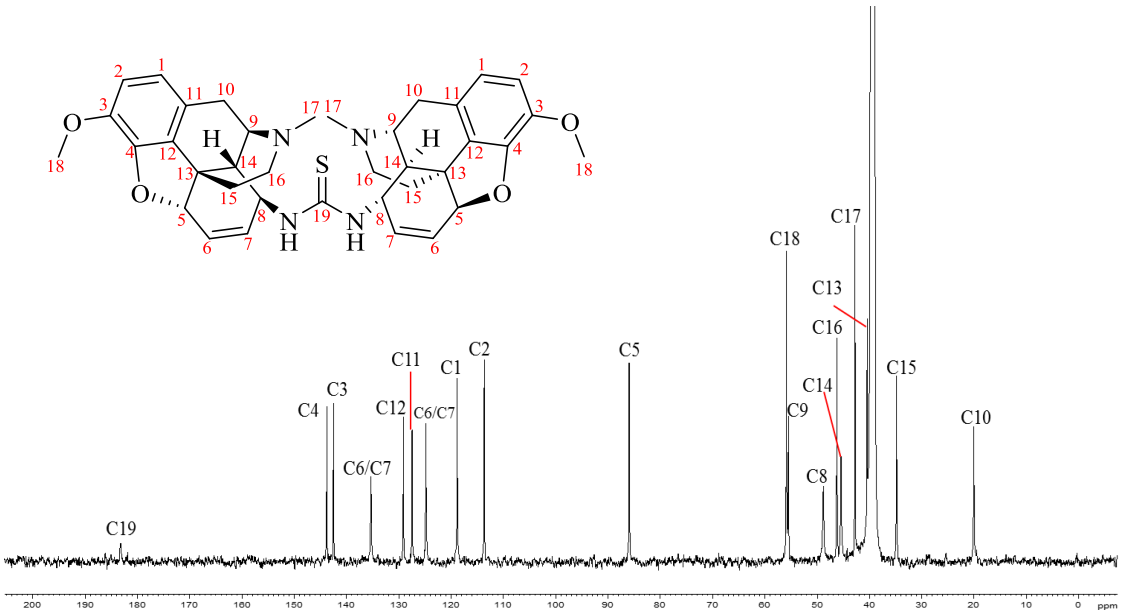

Fig. 2.14 ^{13}C spectrum of *N,N'*-disubstituted thiourea derivative (**5**) (150 MHz) in DMSO-d_6.

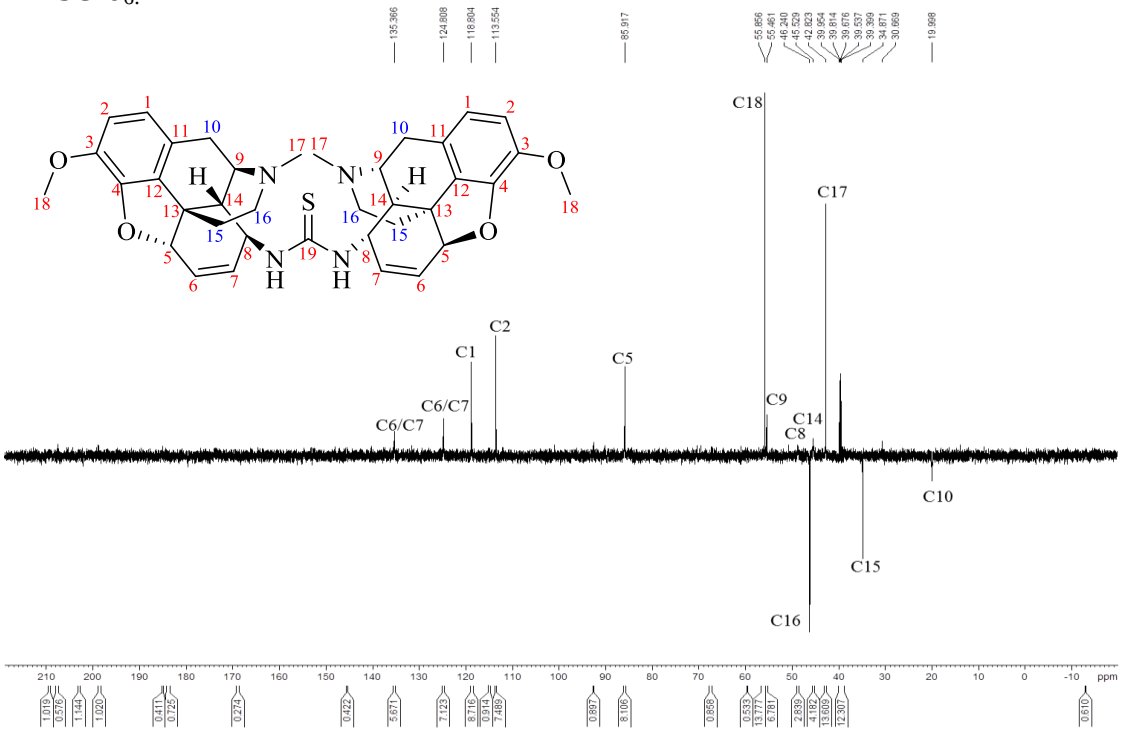

Fig. 2.15 DEPT-135 spectrum of *N,N'*-disubstituted thiourea derivative (**5**) (150 MHz) in DMSO-d_6.

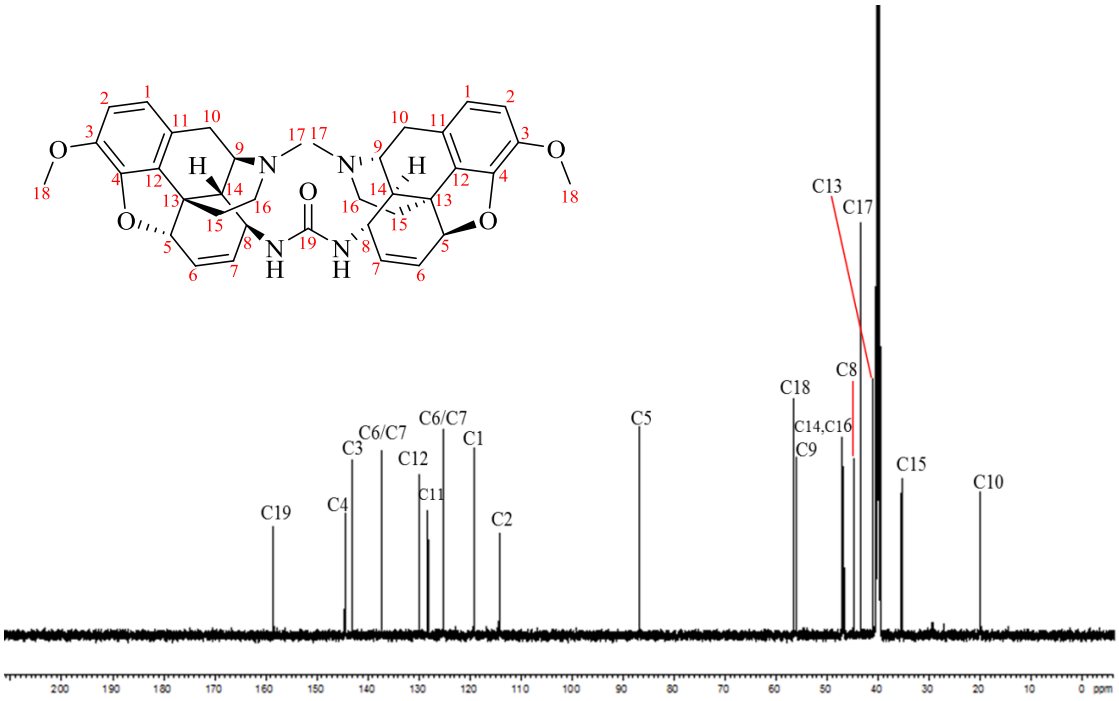

Fig. 2.16 ^{13}C spectrum of *N,N'*-disubstituted urea derivative (**6**) (150 MHz) in DMSO-d_6.

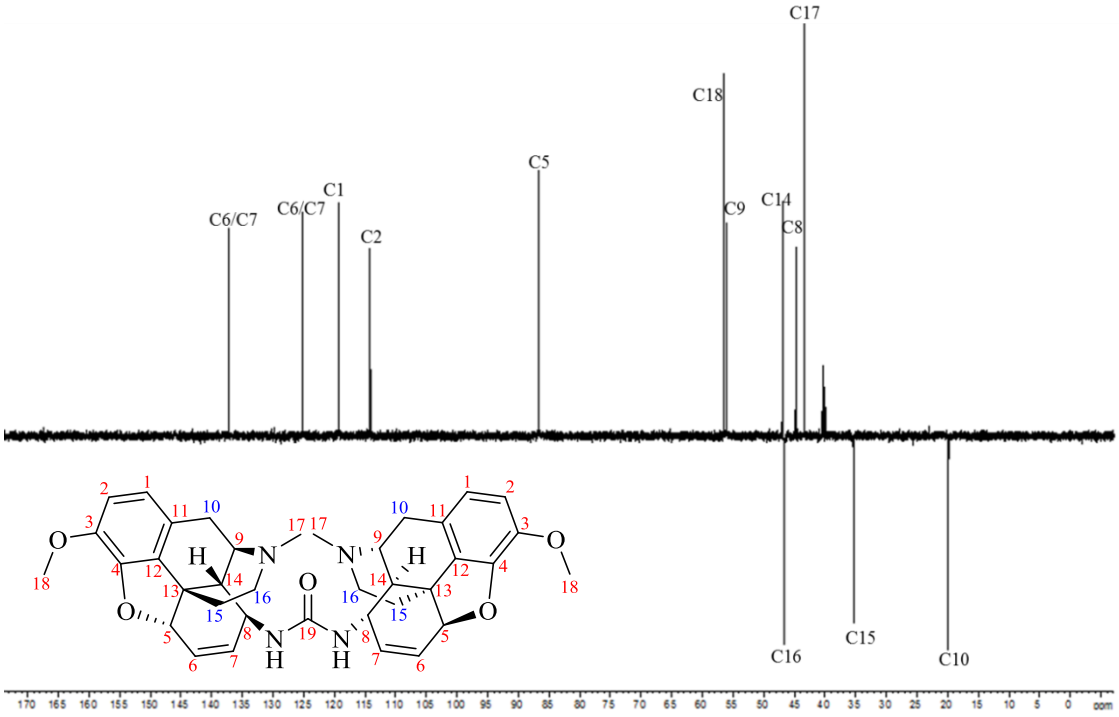

Fig. 2.17 DEPT-135 spectrum of *N,N'*-disubstituted urea derivative (**6**) (150 MHz) in DMSO-d_6.

2.3.4 HMQC of *N,N'*-disubstituted thiourea and urea derivatives

Heteronuclear Multiple Quantum Correlation (HMQC) is a two-dimensional correlation spectroscopy technique, which shows ^{13}C-^{1}H shift correlations and reveals the coupling between protons and the carbons to which they are attached. In the HQMC spectrum, a compound's ^{13}C NMR spectrum is displayed on the y-axis and its respective ^{1}H NMR spectrum is shown on the x-axis. Only directly bonded hydrogens and carbons will give cross peaks.

Fig. 2.18 and Fig. 2.19 are the HMQC spectra of the thiourea and urea derivatives, respectively, and both are almost the same due to having identical structural features. On the spectra of both novel compounds, the diastereotopic protons correlate to the carbon signal for C10, C15 and C16. Carbons C1, C2, C9, C14 C17 and C18 are also assigned by correlation with their corresponding protons. C6 and C7 of both compounds cannot be distinguished because their carbon signals in the ^{13}C NMR spectrum correspond to a singlet in the ^{1}H NMR spectrum. A summary of the HMQC correlations of thiourea and urea derivatives are shown in Table 2.5 and Table 2.6, respectively.

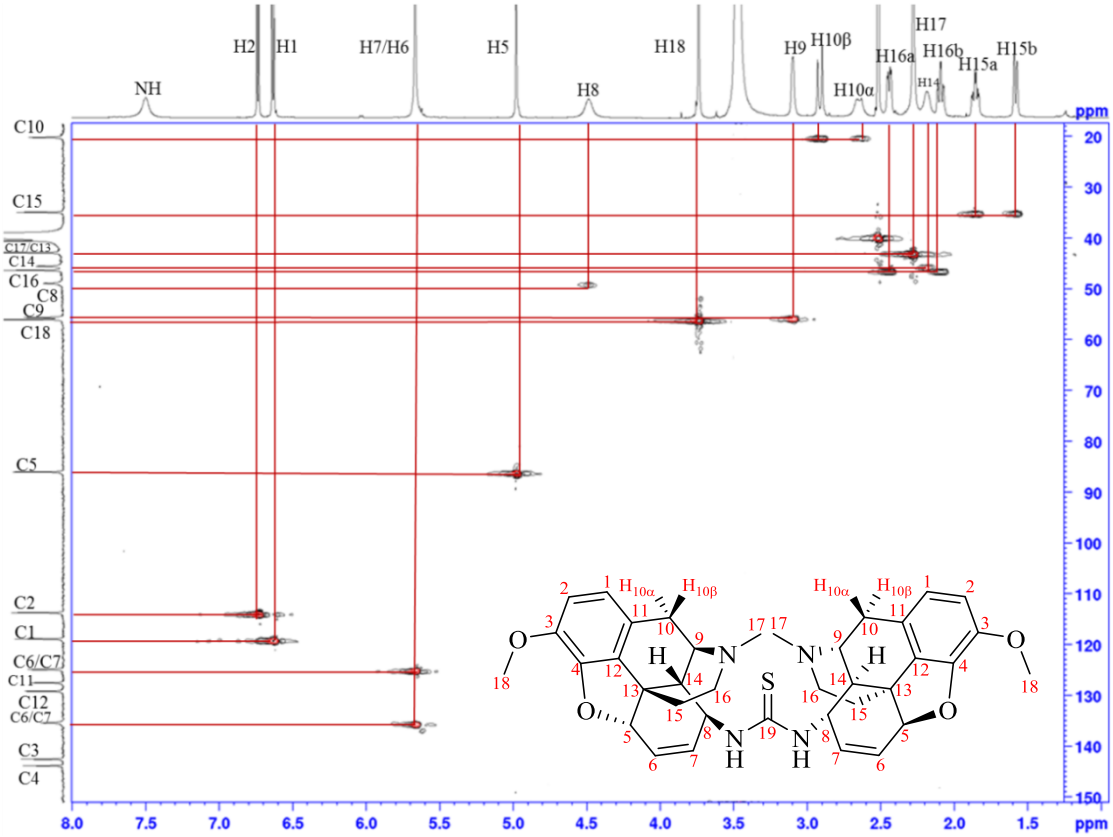

Fig. 2.18 HMQC spectrum (600 MHz) of *N,N'*-disubstituted thiourea derivative (**5**) with observed correlations.

Table 2.5 Observed coupling in HMQC spectrum of *N,N'*-disubstituted thiourea derivative (**5**).

Assigned Peak Number	Carbon δ (ppm)	Proton δ (ppm)
10	C10 (20.0)	H10β (2.91), H10α (2.64)
15	C15 (34.8)	H15a (1.86), H15b (1.60)
17	C17 (42.8)	H17 (2.28)
14	C14 (45.4)	H14 (2.18)
16	C16 (46.2)	H16a (2.43), H16b (2.09)
8	C8 (48.8)	H8 (4.48)
9	C9 (55.5)	H9 (3.10)
18	C18 (55.9)	H18 (3.74)
5	C5 (85.9)	H5 (4.98)
2	C2 (113.6)	H2 (6.74)
1	C1 (118.8)	H1 (6.63)

6/7	C6/C7 (124.8) C6/C7 (135.3)	H6/H7 (5.66)

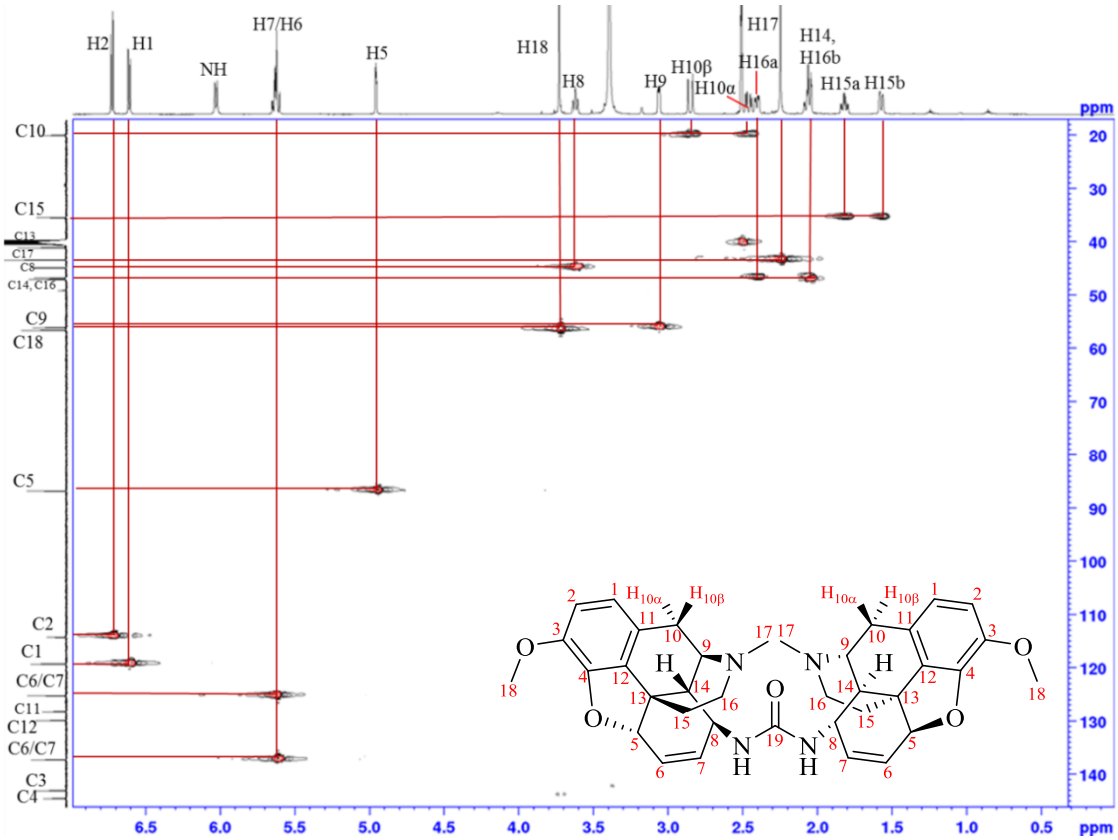

Fig. 2.19 HMQC spectrum (600 MHz) of *N,N'*-disubstituted urea derivative (**6**) with observed correlations.

Table 2.6 Observed coupling in HMQC spectrum of *N,N'*-disubstituted urea derivative (**6**).

Assigned Peak Number	Carbon δ (ppm)	Proton δ (ppm)
10	C10 (19.9)	H10β (2.85), H10α (2.46)
15	C15 (35.4)	H15a (1.82), H15b (1.57)
17	C17 (43.3)	H17 (2.25)
8	C8 (44.8)	H8 (3.62)
16	C16 (46.7)	H16a (2.40), H16b (2.06)
14	C14 (46.9)	H14 (2.06)
9	C9 (56.0)	H9 (3.06)
18	C18 (56.5)	H18 (3.73)
5	C5 (86.7)	H5 (4.96)

2	C2 (114.2)	H2 (6.72)
1	C1 (119.2)	H1 (6.61)
6/7	C6/C7 (125.2) C6/C7 (137.2)	H6/H7 (5.63)

2.3.5 IR spectroscopy of *N,N'*-disubstituted thiourea and urea derivatives

Chemical compounds exhibit different chemical properties due to the presence of different functional groups. Infrared Spectroscopy (IR) can be very sensitive towards different functional groups within a sample since different functional groups absorb different particular frequency ranges of IR radiation. Each functional group has characteristic spectral properties which are referred to as its respective "fingerprint". Therefore, IR spectroscopy is another useful method for the identification and structure analysis of a variety of chemical compounds.

Due to having a similar structure, the presence of NH in both the thiourea and urea derivatives are clearly indicated by the broad signals, which are in the region 3500 ─ 3100 cm^{-1}. The CH_3 alkane groups in both compounds appear as sharp bands in the region 3000 ─ 2800 cm^{-1}; the weak band appears at 1636 cm^{-1} and the strong band at 1502 cm^{-1} for thiourea compounds, and the weak band at 1635 cm^{-1} and the strong band at 1501 cm^{-1} for urea compounds, represent the C=C in the benzene ring. Two bands of C-N for both compounds appear in a similar region (1247 cm^{-1} for thiourea; 1275 cm^{-1} for urea). Assignment of C=S stretching is often uncertain with thiocarbonyl compounds and especially complicated in the case of thiourea. According to the correlated data on the IR spectra of thiocarbonyl derivatives from Rae and Venkataraghavan, the bands of thiocarbonyl group appear in the region 1570 ─ 1397 cm^{-1}, 1420 ─ 1260 cm^{-1} and 1140 ─ 940 cm^{-1}.[32] Thus, a strong band at 1096 cm^{-1}, which is likely to represent C=S stretching for the thiocarbonyl group on the thiourea derivative, can be observed. The carbonyl C=O group stretching band on the urea appears as a weak and broad band in the region 1700 cm^{-1}. The IR spectra of thiourea and urea derivative are shown in Fig. 2.20 and Fig. 2.21, respectively.

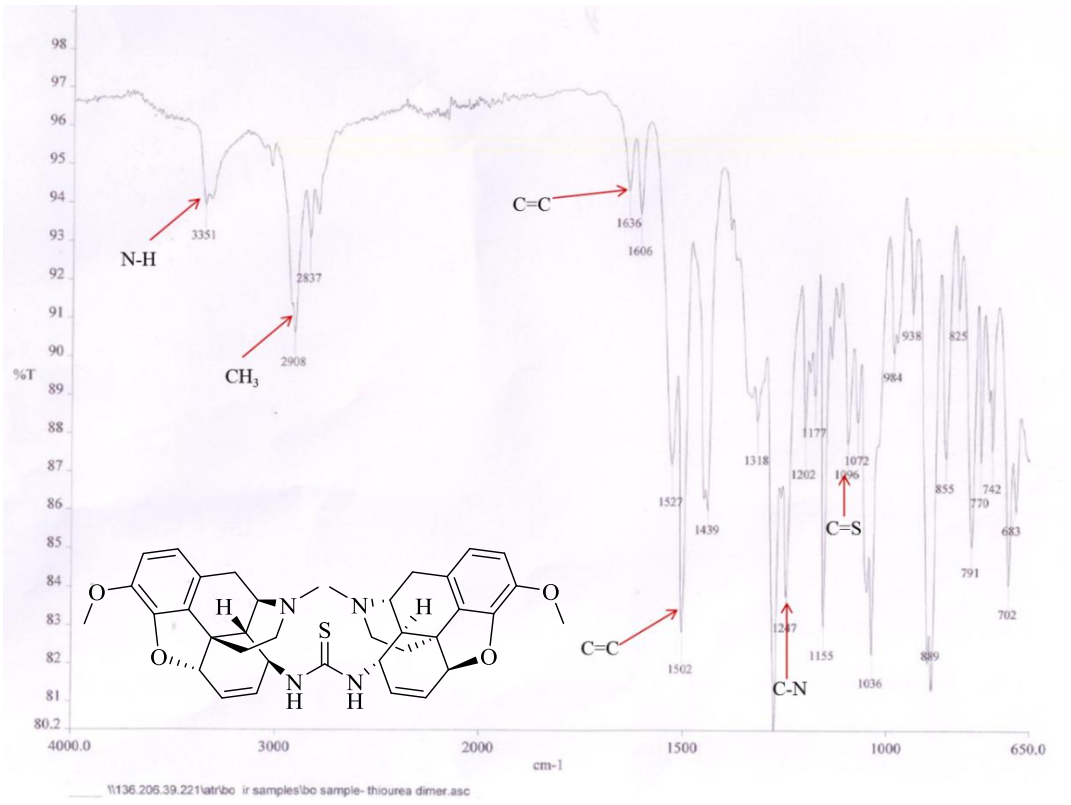

Fig. 2.20 IR spectrum of *N,N'*-disubstituted thiourea derivative (**5**).

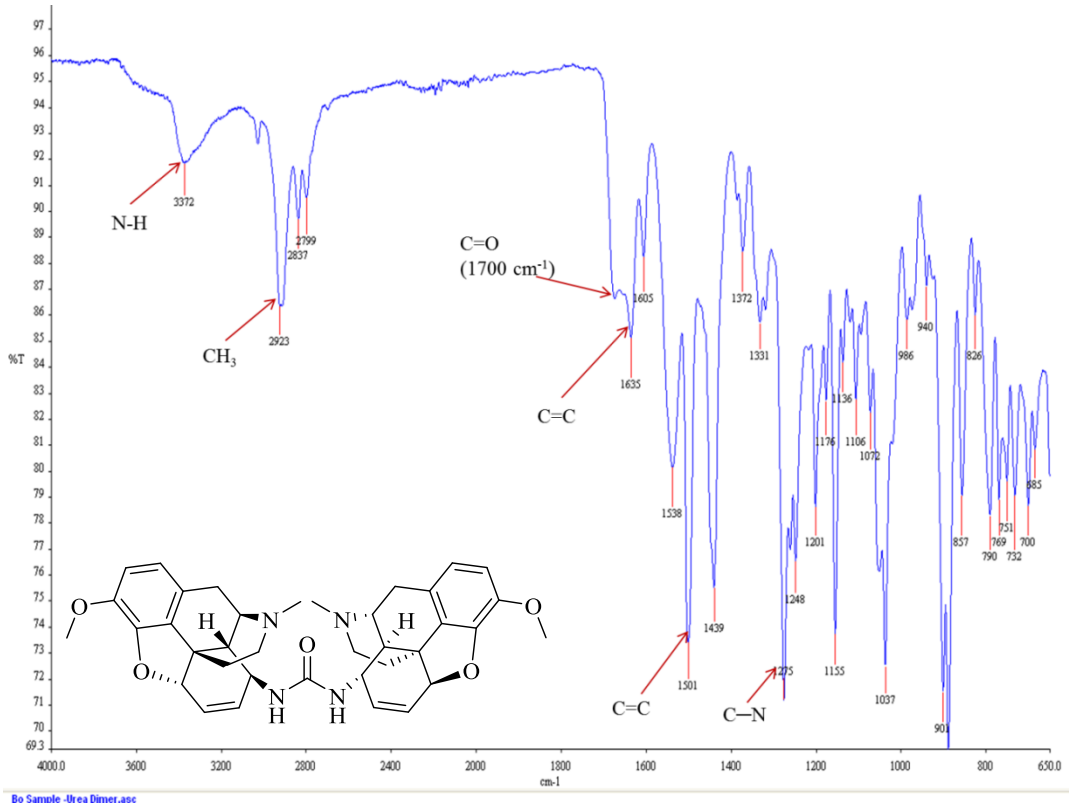

Fig. 2.21 IR spectrum of *N,N'*-disubstituted urea derivative (**6**).

2.3.6 MS of *N,N'*-disubstituted thiourea and urea derivatives

The electrospray ionisation (ESI) technique (in positive mode) was used to analyse the opiate urea and thiourea compounds. A typical mass spectrum of the *N,N'*-disubstituted thiourea (**5**) and urea (**6**) is shown in Fig. 2.22 and Fig. 2.23, respectively. An exact mass of the thiourea (**5**) was observed as m/z = 639.2977 $[M+H]^+$, which matches the expected exact mass value of 639.2900 $[M+H]^+$, while the molecular mass of the urea (**6**) was observed as m/z = 623.3202 $[M+H]^+$ which matches the exact mass value (623.3200) $[M+H]^+$.

The mass spectrum for *N,N'*-disubstituted thiourea (**5**) provided detailed information with respect to the structures of fragment ions, which is also illustrated in Fig. 2.22. The molecular ion of the starting compound 8-isothiocyanocodide (**2**) was observed at m/z = 340.6648 $[M]^+$ with relatively intensity (RI) 100%, which may be due to presence of charge localisation over the whole molecule[33] and the peak at m/z = 341.160 $[M+H]^+$ is formed directly from the molecular ion of 8-isothiocyanocodide (**2**). The protonated molecule of the other starting compound 8-aminoocodide (**4**) was also detected at m/z = 299.1739 $[M+H]^+$, but having relatively low intensity. The peak at m/z = 320.1501 represents the half mass of protonated *N,N'*-disubstituted thiourea (**5**) ion $[(M+H))/2]^+$. Likewise, the peak at m/z = 1277.5830 corresponds to a double mass of *N,N'*-disubstituted thiourea (**5**) ion $[2M]^+$. Because of using formic acid and H_2O as the mobile phase in LC-MS system, the total mass of *N,N'*-disubstituted thiourea (**5**) molecular ion and formic acid gives the value of m/z 685.3037, while m/z = 1341.5137 is the sum mass of the two *N,N'*-disubstituted thiourea (**5**) ions, formic acid and H_2O.

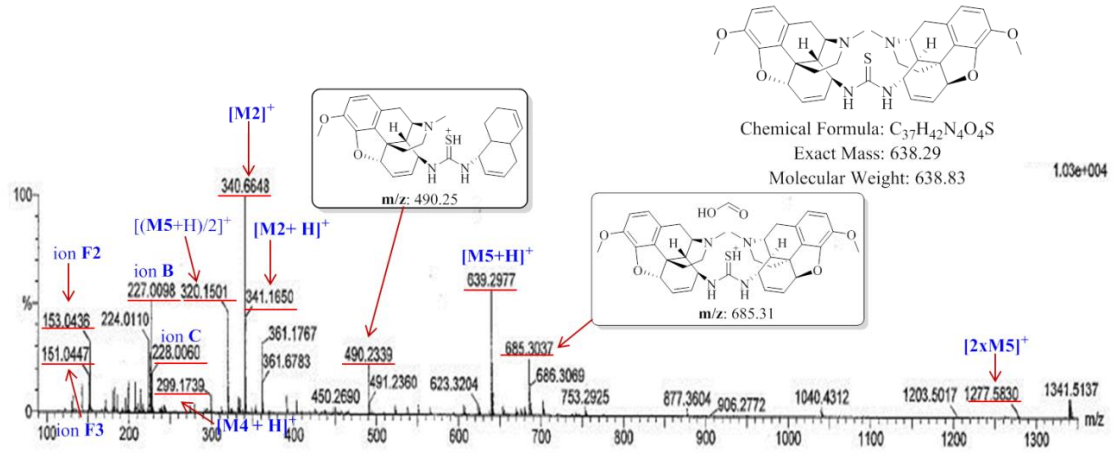

Fig. 2.22 Mass spectrum of *N,N'*-disubstituted thiourea derivative (**5**) and assignment of fragment ions. [**M5**: exact mass of the thiourea compound (**5**), **M2**: exact mass of the 8-isothiocyanocodide (**2**), **M4**: exact mass of the 8-aminocodide (**4**)]

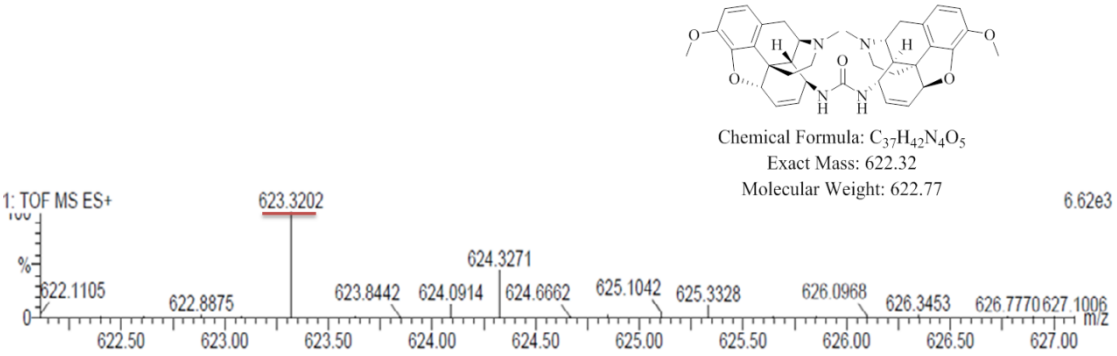

Fig. 2.23 Mass spectrum of *N,N'*-disubstituted urea derivative (**6**).

On the other hand, the fragmentation pathway of opioids alkaloids was also revealed in Scheme 2.13. The **A**-type fragment ions of 8-thiocyanocodide (**2**) (**A1**) and 8-aminocodide (**4**) (**A2**) are formed by loss of an amine group ($CH_2CHNHCH_3$) on the piperidiene D-ring, due to partial cleavage of the C13-C15 and C9-N covalent bonds.[34,35] Further expulsion of the methyl radical from methoxy group (CH_3O) on the 8-aminocodide (**4**) leads to give a product ion **C** at m/z = 228. Loss of functional groups NCS^- and NH_2 at C8-position (converting C8 to a CH_2 group) from type **A** ions of both of 8-isothiocyanocodide (**2**) (**A1**) and 8-aminocodide (**4**) (**A2**), affords the **B**-type fragment at m/z = 227, which was in good agreement with previous reports.[34,36] It is noteworthy that the product ion **D** at m/z = 225 which was proposed by Zhang *et al.*,[34] was not detected, although it can be explained by loss of 2 Hs from the **B**-type

fragment ion (m/z = 227) theoretically, instead it gives the appearance at m/z = 224. It is suggested that the presence of isotopes of ^{13}C are present in the thiourea compound.[36] Furthermore, the **E1**-type ion at m/z 197 formed by loss of epoxy ring and the methyl radical from a **D**-type fragment, was also not detected. However, with further loss of hydrogens, the **F2** and **F3** ions were given at m/z = 153 and m/z = 151, respectively.

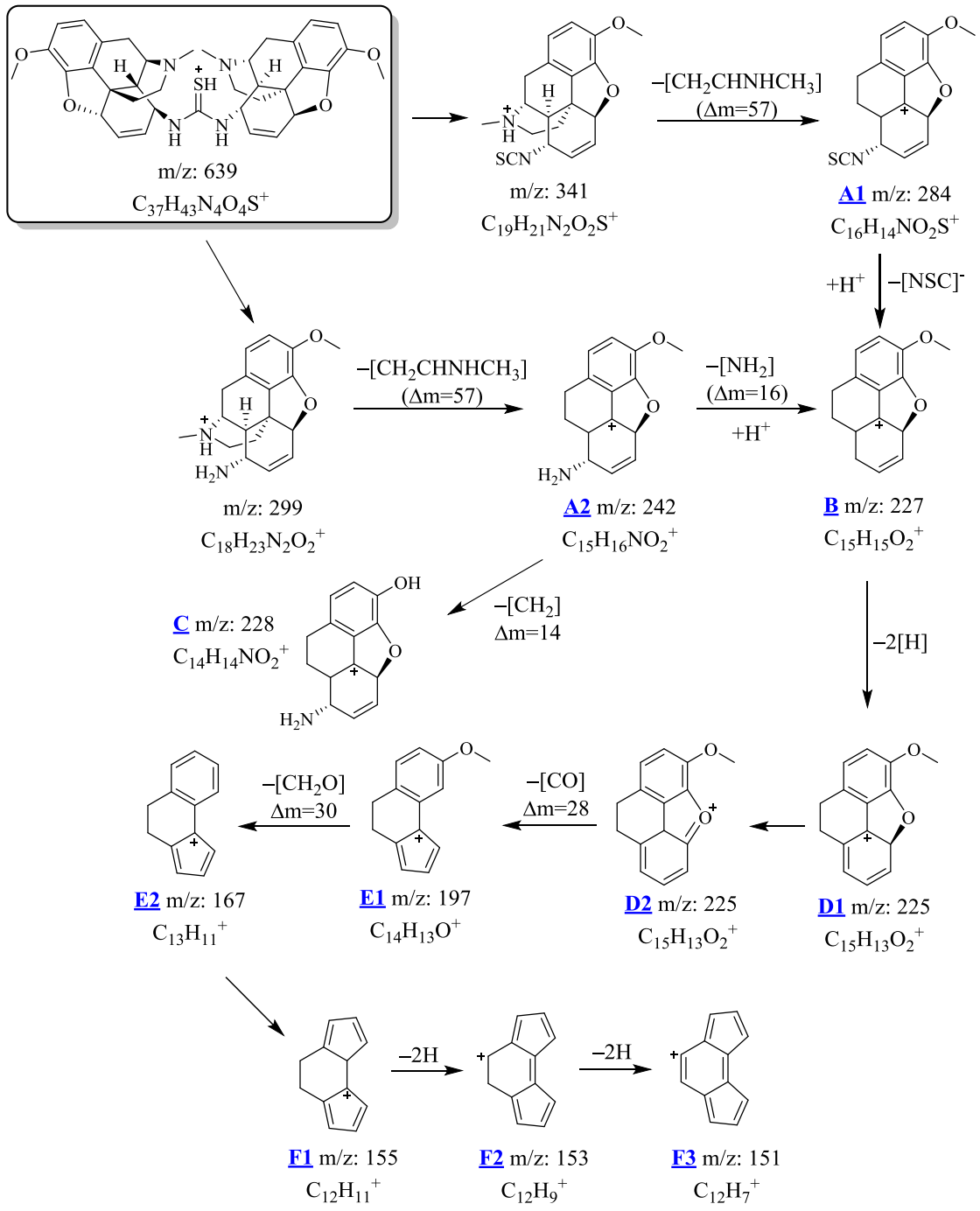

Scheme 2.13 Proposed fragmentation routes of protonated *N,N'*-disubstituted thiourea (**5**).[34-36]

2.3.7 XRD of *N,N'*-disubstituted thiourea and urea derivatives

The structure of crystals and molecules are usually identified using X-ray diffraction studies. The angle and intensities of the diffraction of X-ray beams are recorded with diffraction patterns of spots/reflections. Analysis of the diffraction pattern by Fourier mathematical methods gives information on the distribution of electron density within the unit cell. A 3D picture of the structure is built from the atomic positional coordinates and displacements parameters. Within the unit cell, bond lengths and angles measurements can be determined. The dimensions of the unit cell, intermolecular interaction and hence the crystal packing is determined.[11]

The thiourea derivative was crystallized by evaporation of an ethyl acetate/hexane solution in the orthorhombic $P2_12_12_1$ group, while the crystal of urea derivatives was grown from methanol in the orthorhombic $C222_1$ crystal system. The absolute configuration of thiourea and urea compounds were determined from the diffraction data (absolute structure parameter, -0.02(3) for thiourea and 0.06(5) for urea). The summary of the experimental details of thiourea and urea compounds are given in Appendix C.

According to the crystal structures of the two molecules in Fig. 2.24 and Fig. 2.25, it is generally thought that two rotamers *trans/trans* and *trans/cis* would form as thiourea and urea products (Fig. 2.26) due to rotation about the C-N bond.[37] However, according to the crystal structure of both molecules, existence of *trans/trans* isomers can be confirmed.

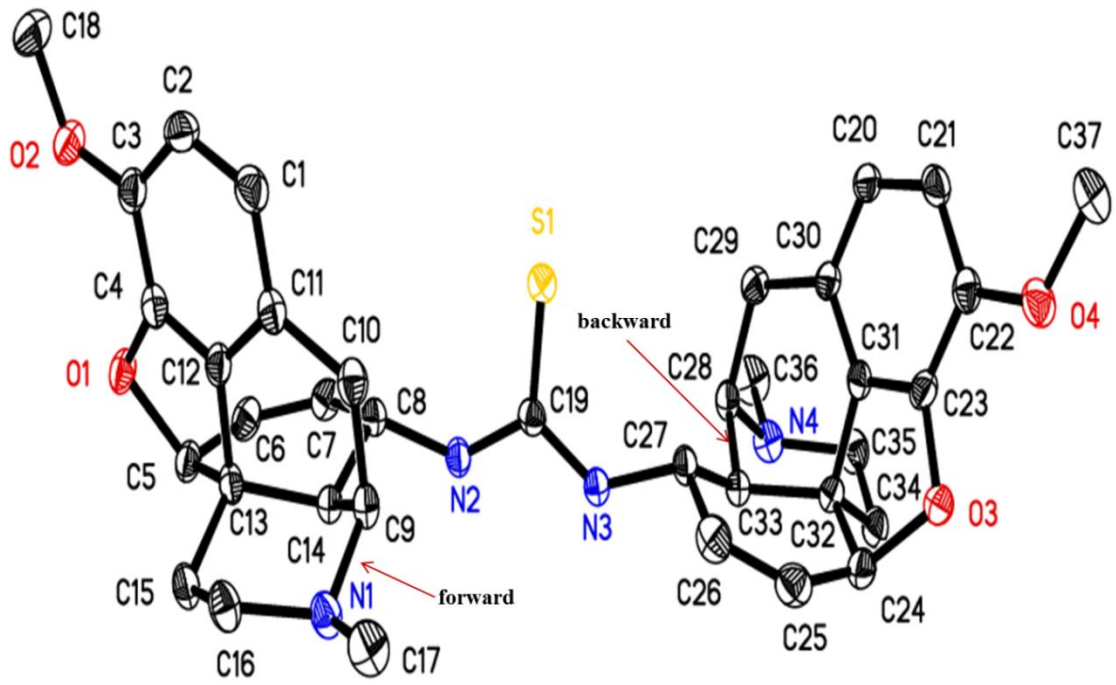

Fig. 2.24 The molecular structure of *N,N'*-disubstituted thiourea derivative (**5**) showing the atom numbering scheme. Displacement ellipsoids are drawn at the at 50% probability. Only symmetry unique atoms labelled.

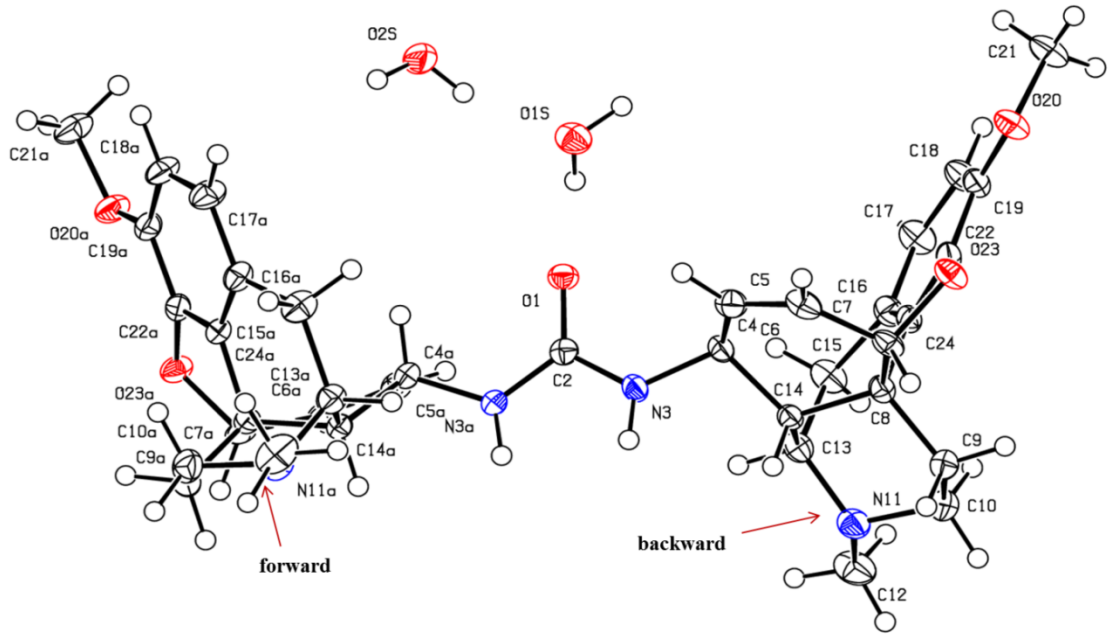

Fig. 2.25 The molecular structure of *N,N'*-disubstituted urea derivative (**6**) showing the atom numbering scheme. Displacement ellipsoids are drawn at the at 50% probability. Only symmetry unique atoms labelled.

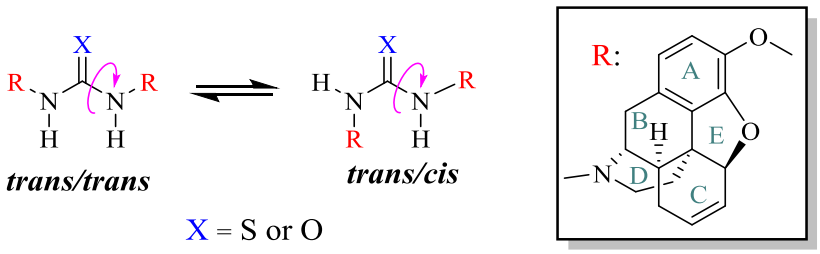

Fig. 2.26 Structure of *N,N'*-disubstituted thiourea/urea with labelled opioid rings and their rotamers.

Selected bond lengths and bonds angles are listed in Table 2.7 and Table 2.8, respectively. Both thiourea and urea molecules have an approximate (non-crystallographic) two-fold axis along the S1=C19 and O1=C2. The sulfur of the thiocarbonyl group and the oxygen atom of the carbonyl group are highlighted in yellow and red, respectively. The bond length of S1=C19 thiocarbonyl is 1.697(2) Å and O1=C2 carbonyl is 1.249(3) Å, which agrees with the observation that the S=C bond length is considerably longer than O=C bond due to dissociation energy of the O=C bond being stronger than that of S=C. Both lengths of the thiocarbonyl and carbonyl groups are within the expected range.[38] For the C-N bond, the bond length of N2-C19 (1.339(3) Å) in the thiourea compound is close to that of N3-C2 (1.346(3) Å) in the urea compound, but both compounds' C-N bond lengths are shorter than the normal one of 1.47 Å. This can be explained on a delocalization of the two lone pairs of electrons on the nitrogen atoms.[39] Both thiourea and urea compounds have the similar value of the N-C-N's bond angle. (N2-C19-N3 is 114.3(2)° in the thiourea compound, N3-C2-N3a is 114.0(2)° in the urea compound), while the bond angle of the thiourea moiety S1=C19-N2 (122.19(18)°) is nearly identical with of the urea moiety O1=C2-N3 (122.98(11)°). The angles of link section in the thiourea compound (C8-N2-C19) and in the urea compound (C4-N3-C2) are similar at the 126.28(19)° and 124.27(16)°, respectively. The distances between thiourea (urea) moiety and the C8-position of the C-ring are nearly identical, which is about 1.456(3) Å.

Each codeine structural unit in the thiourea and urea compounds are similar to previously reported opioid derivatives.[40,41] Kartha *et al.* reported that the different bond lengths for C9-N and C16-N in the D-ring of the codeine hydrobromide dihydrate.[42] However, the difference were not found in both thiourea and urea compounds, where the bond lengths for C9-N1 and C16-N1 in the thiourea are is

1.477(3) Å and 1.473(3) Å, respectively, while the urea has these bond lengths equal to 1.476(3) Å (C13-N11) and 1.472(3) Å (C10-N1), respectively. The presence of the double bonds of C6=C7 in the thiourea and C5=C6 in the urea are clearly indicated, as distance of 1.326(4) Å and 1.330(3) Å in the C-ring, respectively.

The five ring conformations of codeine scaffold in the thiourea and urea compounds can be also explained using the torsion angles data from Tables 2.9. The A-ring appears some derivation from planarity, which was expected with the feature of a benzene ring such as this. The O2 (thiourea) linked to C3 (thiourea), and O20 linked to C19 (urea) to the plane of the benzene ring with the distance of 1.366(3) Å and 1.364(2) Å, respectively. These bond lengths are same as the one in codeine (1.367(6) Å).[41] The torsion angles of −4.6(3)° (C12-C4-O1-C5) and 23.5(16)° (C13-C5-O1-C4) from the thiourea compound, and the one of −4.9(2)° (C24-C22-O23-C7) and 24.6(18)° (C8-C7-O23-C22) from the urea compound give the E-ring in an envelope conformation. The angles of ring E in both compounds are also similar: C4-O1-C5 equals to 104.57(17)° in the thiourea, while C22-O23-C7 in the urea is 105.36(13)°, respectively. The D-ring is in a chair conformation with the methyl group of the nitrogen in the equatorial position, and it joined to the B-ring through bonds, which are C13-C15 and C9-N1 in the thiourea compound, and C8-C9 and C13-N11 in the urea compound, respectively. Both sides of the D-ring facing the opposite direction: one faces forwards and the other faces backwards. C13-C5-C6=C7 of the C-ring in the thiourea and C5=C6-C7-C8 of the C-ring in the urea are relatively planar with a torsion angle of −3.8(3)° (thiourea) and −3.6(3)° (urea), and formed a more distorted horizontal plane with the D-ring. This is unlike that the boat conformation with the C6 and C14 fore and aft in the codeine molecule. Distortion of the C-ring boat confirmation could be explained by the effect of C8-position of the thiourea (urea) functionality.[43] In both the thiourea and urea molecules, the A-B-E rings are almost perpendicular to the C- and D-rings, which titles each codeine scaffold unit has the classic T-shape configuration as it was expected.

The tertiary amine and NH groups in the thiourea and urea molecules are hydrogen-bonding to water molecules. The only difference between each is that the ether oxygen (O1 and O3) from the thiourea molecule also acts as a hydrogen-bond acceptor, but hydrogen-bonds did not exist among those ether oxygen atoms in the

urea molecules. All water molecules are involved in hydrogen-bonding, with each other and with the two organic molecules. The hydrogen-bonding links the molecules to form double-layer sheets parallel to the ab plane, but there are only weak interactions linking the sheets along the c direction (Fig. 2.27 and Fig. 2.28).

Table 2.7 Selected bond lengths for *N,N'*-disubstituted thiourea (**5**) and urea (**6**) derivatives.

Bond lengths [Å]	Thiourea derivative	Bond lengths [Å]	Urea derivative
S1=C19	1.697(2)	O1=C2	1.249(3)
N2-C19	1.339(3)	N3-C2	1.346(3)
N2-C8	1.456(3)	N3-C4	1.455(2)
C9-N1	1.477 (3)	C13-N11	1.472(3)
C16-N1	1.473 (3)	C10-N11	1.472(3)
O2—C3	1.366 (3)	C19-O20	1.364(2)
C6=C7	1.326(4)	C5=C6	1.330(3)

Table 2.8 Selected bond angles for *N,N'*-disubstituted thiourea (**5**) and urea (**6**) derivatives.

Bond Angles	Thiourea derivative[°]	Bond Angles	Urea derivative[°]
N2-C19-N3	114.3(2)	N3-C2-N3a	114.0(2)
S1=C19-N2	122.19 (18)	O1=C2-N3	122.98(11)
C8-C7=C6	124.7(2)	C4-C5=C6	124.58(18)
C8-N2-C19	126.28 (19)	C4-N3-C2	124.27(16)
C4-O1-C5	104.57 (17)	C22-O23-C7	105.36(13)

Table 2.9 Selected torsion angles for *N,N'*-disubstituted thiourea (**5**) and urea (**6**) derivatives.

Torsion Angles	Thiourea derivative[°]	Torsion Angles	Urea derivative[°]
A-ring: C1=C2-C3=C4	2.9(2)	C17=C18-C19=C22	2.9(3)
A-ring: C1-C11=C12-C4	6.5(3)	C17-C16=C24-C22	5.3(3)
B-ring: C14-C9-C10-C11	31.6(2)	C14-C13-C15-C16	31.0(2)
B-ring: C12-C13-C14-C9	61.8(15)	C24-C8-C14-C13	60.1(18)

C-ring: C13-C5-C6=C7	−3.8(3)	C5=C6-C7-C8	−3.6(3)
C-ring: C14-C8-C7=C6	17.5(2)	C14-C4-C5=C6	18.5(2)
D-ring: C15-C16-N1-C9	57.5(3)	C9-C10-N11-C13	56.9(2)
D-ring: C14-C9-N1-C16	-63.1(15)	C14-C13-N11-C10	−64.54(17)
E-ring: C12-C4-O1-C5	−15.6(3)	C24-C22-O23-C7	−14.9(2)
E-ring: C13-C5-O1-C4	23.5(16)	C8-C7-O23-C22	24.6(18)

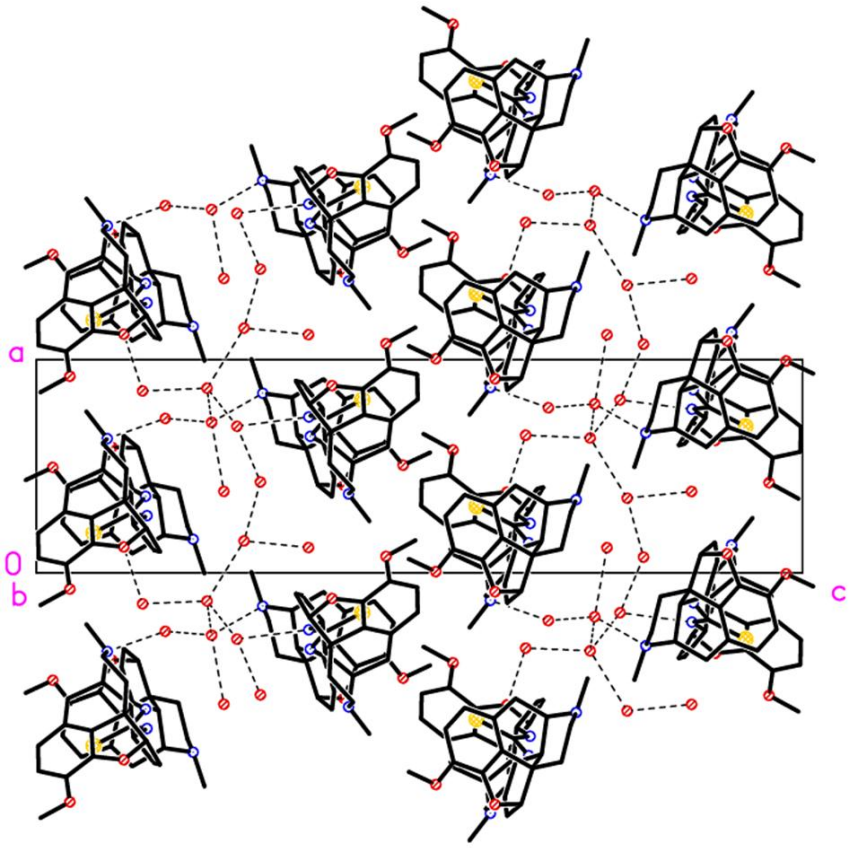

Fig. 2.27 Packing diagram of *N,N'*-disubstituted thiourea derivative (**5**) viewed along the a-axis. Hydrogen atoms omitted for clarity. Dashed lines indicate strong hydrogen-bonding (Packing diagram viewed perpendicular to the b axis).

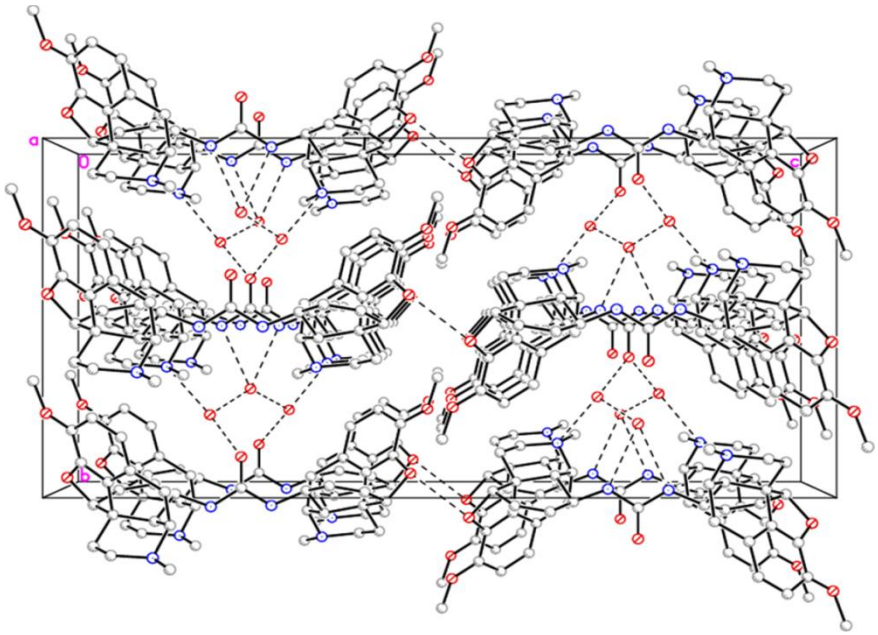

Fig. 2.28 Packing diagram of *N,N'*-disubstituted urea derivative (**6**) viewed along the a-axis. Hydrogen atoms omitted for clarity. Dashed lines indicate strong hydrogen-bonding (Packing diagram viewed perpendicular to the b axis).

2.4 Future work

The synthesis of a number of *N,N'*-disubstituted thiourea and urea derivatives has been achieved. Both *N,N'*-disubstituted thiourea and urea derivatives were synthesised in five steps from codeine and the synthetic routes are described within. Some methods for the synthesis of opioid derivatives have been improved to obtain better yields. However, the yields of *N,N'*-disubstituted thiourea and urea derivatives are relatively low, so the reaction conditions for the synthesis of thiourea and urea compounds need to be further optimized. Characterization of the *N,N'*-disubstituted thiourea and urea derivatives were successfully completed by melting point, NMR, IR, $[\alpha]_d$ and MS. Using X-ray analysis the structures of both the thiourea and the urea compound were confirmed.

The failure of synthesis of chiral phosphoric acid based opioid derivative revealed the C6-hydroxyl group in the codeine molecule could be easily substituted by a variety of reagents. Regarding the synthesis of VAPOL-like chiral phosphoric acids, modification of functional groups in the C-ring needs to be prioritized before coupling of opioid scaffolds. With gaining inspiration from the success associated with the 8,8'-diaryl VAPOL derivatives in the asymmetric catalysis, which was reported by Wulff *et al.*,[44] there are two proposed synthetic routes can be designed for the future synthesis of a proposed chiral phosphoric acid based opioid derivative. As the retrosynthetic analysis shown in Scheme 2.14, in the route 1, deoxycodeine could be synthesised from 6-*O*-tosylcodeine (**1**).[45] After the demethylation of deoxycodeine, for example using BBr_3,[45] dimerization of the two codeine-derived scaffolds (desomorphine derivative) at the 2 and 2' position, which can be achieved with $K_3[Fe(CN)_6]$[5]. This leads to synthesize another novel opioid derivative, a pseudomorphine derivative, which has a rigid structure and two hydroxyl groups at the 3 and 3' position, respectively. Therefore, an interesting target compound series (**I**) could be subsequently synthesised by the reaction of the pseudomorphine derivative with $POCl_3$. The other interesting synthetic chiral phosphoric acid based opioid derivative (**II**) in the route 2 can be achieved by coupling of desoxycodeine-A. Starting with β-bromocodide (**6**), which can also be synthesised from 6-*O*-tosylcodeine (**1**).[46] Using Zn in dry ethanol, cleavage of the tetrahydrofuran (E) ring in the β-bromocodide (**6**) gives the desoxycodeine-A with having a phenolic

reaction site.[4] The two desoxycodeine-A units may then be linked at the 4 and 4' position to form the target compound series (**II**) using $POCl_3$.

On the other hand, with regards to utilizing the thiourea and urea cores as hydrogen-bond donor catalysts,[47] bifunctional squaramide moieties have appeared as powerful hydrogen-bonding groups for Lewis acid catalysis.[48-51] Squaramides consist of a four-membered ring system and possess hydrogen-bond accepting and donating functionality *via* carbonyl and NH groups, respectively. Therefore, squaramide compounds have shown to be competent for many chemical reactions, including biomimetic transport,[50,52] molecular recognition,[53,54] ion sensing[55,56] and organocatalysis.[57,58] Hence, in order to extend the number of opioid derivatives and the study of their catalytic activities and selectivities in asymmetric organocatalysis, it is necessary to synthesise a squaramide-based dimeric opioid derivative alongside after the successfully synthesised thiourea- and urea-based opioid derivatives. With reference to the synthetic method of the dimerization of the cinchona alkaloid reported by Song *et al.*,[59] which was mentioned in Chapter 1, the squaramide-based dimeric opioid derivative catalyst (**III**) could be simply achieved in one-step by the reaction of 8-amioncodide (**4**) with dimethyl squarate at room temperature in the route 3.

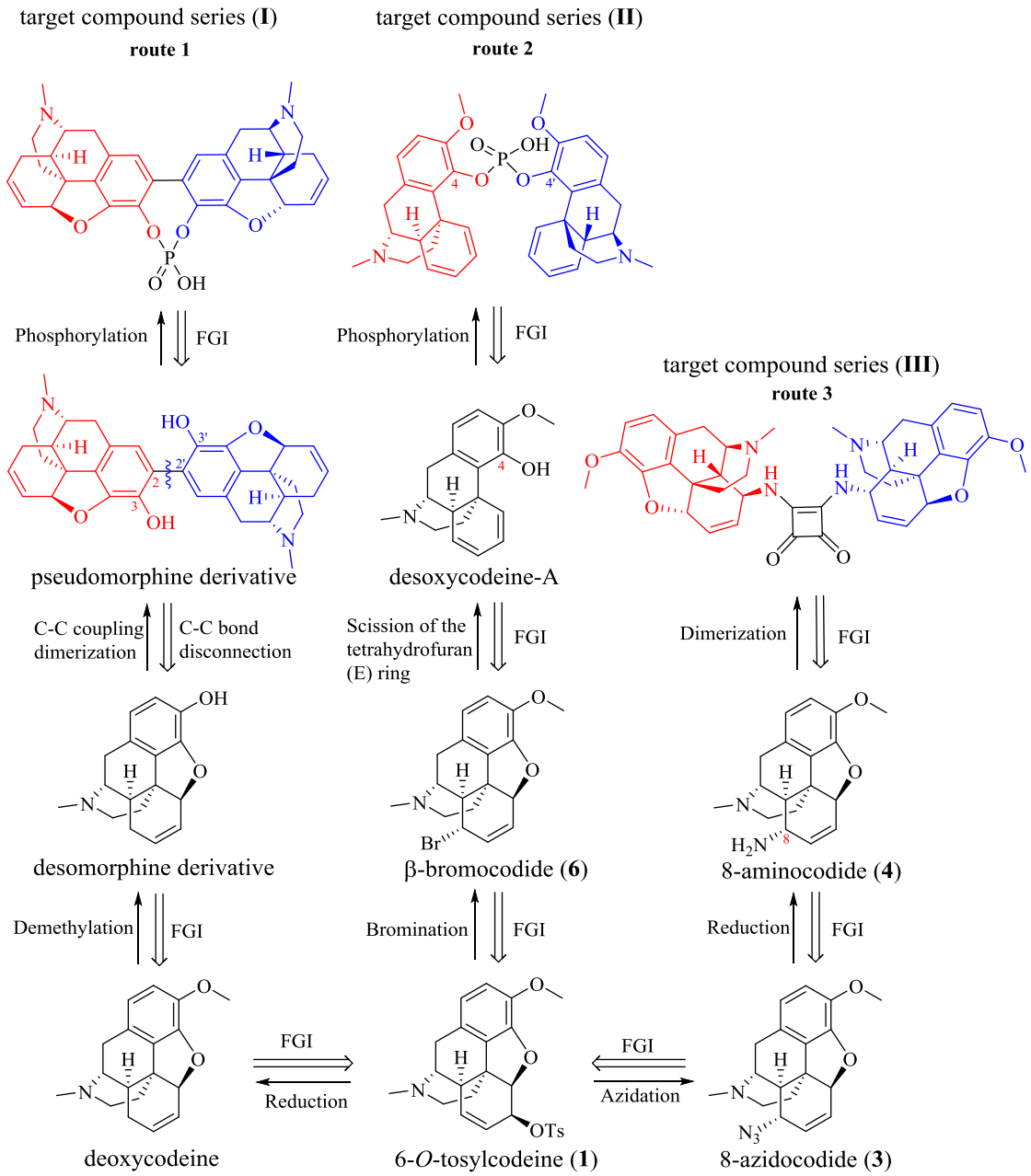

Scheme 2.14 Retrosynthetic analysis routes to design novel opioid derivatives **I**, **II** and **III** (FGI: Functional Group Interconversion).

2.5 References

(1) West, S.; Kannar, D. Phosphate Derivatives of Pharmaceutical Products. U.S. Patent Application. No.10/551,201., **2004**.

(2) Pasternak, G. W.; Pan, Y. X. Mu Opioids and Their Receptors: Evolution of a Concept. *Pharmacol. Rev.* **2013**, *65* (4), 1257–1317.

(3) Cunningham, C. W.; Deschamps, J. R.; Coop, A. A One-Step Synthesis of β-Bromocodide from Codeine. *J. Pharm. Sci. Pharmacol.* **2014**, *1* (1), 54–56.

(4) Linders, J. T. M.; Adriaansens, R. J. O.; Lie, T. S.; Maat, L. Scission of the Epoxy Ring in 4,5α-Epoxymorphinans: A Convenient Synthesis of β-Dihydrothebaine, 6-Demethoxy-β-Dihydrothebaine and Desoxycodeine-A (Chemistry of Opium Alkaloids, Part XXI). *Recl. Trav. Chim. Pays-Bas* **1986**, *105* (1), 27–29.

(5) Bentley, K. W.; Dyke, S. F. The Structure of Pseudo Morphine. *J. Chem. Soc.* **1959**, No. 512, 2574–2577.

(6) Smith, J.; Liras, J. L.; Schneider, S. E.; Anslyn, E. V. Solid and Solution Phase Organic Syntheses of Oligomeric Thioureas. *J. Org. Chem.* **1996**, *61* (25), 8811–8818.

(7) Storace, L.; Anzalone, L.; Confalone, P. N.; Davis, W. P.; Fortunak, J. M.; Giangiordano, M.; Haley, J. J.; Kamholz, K.; Li, H. Y.; Ma, P.; Nugent, W. A.; Parsons, R. L.; Sheeran, P. J.; Silverman, C. E.; Waltermire, R. E.; Wood, C. C. An Efficient Large-Scale Process for the Human Leukocyte Elastase Inhibitor, DMP 777. *Org. Process Res. Dev.* **2002**, *6* (1), 54–63.

(8) Patrick, G. L. Synthesis of Mesylates and Tosylates. In *Instant Notes in Organic Chemistry*; Owen, E., Ed.; Taylor & Francis, **2012**; p 217.

(9) Berényi, S.; Makleit, S.; Szilágyi, L. Conversions of Tosyl and Mesyl Derivatives of the Morphine Group, XXIII: Preparation of New

6-Substituted-6-Demethoxythebaine Derivatives. *Acta Chim. Hung.* **1984**, *117* (3), 307–312.

(10) Coulter, V. Various Elements. In *Advanced Organic Chemistry*; Global Media, **2009**; p 11.

(11) Long, S. Opioids as Enantioselective Organocatalysts, PhD Thesis, Dublin City University, Ireland, **2012**.

(12) Bognár, R.; Mile, T.; Makleit, S.; Berényi, S. Conversions of Tosyl and Mesyl Derivatives of the Morphine Group, XII. 14-Hydroxi Derivatives of Morphine, III. Isothiocyanato Derivatives. *Acta Chim. Hung.* **1973**, *75* (3), 297–301.

(13) Shi, F.; Deng, Y.; SiMa, T.; Peng, J.; Gu, Y.; Qiao, B. Alternatives to Phosgene and Carbon Monoxide: Synthesis of Symmetric Urea Derivatives with Carbon Dioxide in Ionic Liquids. *Angew. Chem., Int. Ed.* **2003**, *42* (28), 3257–3260.

(14) Eckert, H.; Forster, B. Triphosgene, a Crystalline Phosgene Substitute. *Angew. Chem., Int. Ed.* **1987**, *26* (9), 894–895.

(15) Majer, P.; Randad, R. S. A Safe and Efficient Method for Preparation of *N*,*N*'-Unsymmetrically Disubstituted Ureas Utilizing Triphosgene. *J. Org. Chem.* **1994**, *59* (7), 1937–1938.

(16) Zhang, Q.; You, Q.; Zhou, H.; Diao, Y. Safe and Efficient One-Pot Synthesis of Nitro-Containing Unsymmetrical Diaryl Ureas. *Chin. J. Pharm.* **2012**, *43* (4), 247–250.

(17) Ballini, R.; Fiorini, D.; Maggi, R.; Righi, P.; Sartori, G.; Sartorio, R. TBD-Catalysed Solventless Synthesis of Symmetrically *N*,*N*'-Substituted Ureas from Primary Amines and Diethyl Carbonate. *Green Chem.* **2003**, *5* (4), 396–398.

(18) Desai, A. A.; Huang, L.; Wulff, W. D.; Rowland, G. B.; Antilla, J. C.

Gram-Scale Preparation of VAPOL Hydrogenphosphate: A Structurally Distinct Chiral Brønsted Acid. *Synthesis* **2010**, No. 12, 2106–2109.

(19) Small, L. F.; Cohen, F. L. DESOXYCODEINE STUDIES. I. THE DESOXYCODEINES. *J. Am. Chem. Soc.* **1931**, *53* (6), 2214–2226.

(20) Erhard, T.; Ehrlich, G.; Metz, P. A Total Synthesis of (±)-Codeine by 1,3-Dipolar Cycloaddition. *Angew. Chem., Int. Ed.* **2011**, *50* (17), 3892–3894.

(21) Batterham, T. J.; Bell, K. H.; Weiss, U. The Nuclear Magnetic Resonance Spectra of the Codeine Isomers and Their Derivatives. *Aust. J. Chem.* **1965**, *18* (11), 1799–1806.

(22) Carroll, F. I.; Moreland, C. G.; Brine, G. A.; Kepler, J. A. Carbon-13 Nuclear Magnetic Resonance Spectra of Morphine Alkaloids. *J. Org. Chem.* **1976**, *41* (6), 996–1001.

(23) Váradi, A.; Gergely, A.; Béni, S.; Jankovics, P.; Noszál, B.; Hosztafi, S. Sulfate Esters of Morphine Derivatives: Synthesis and Characterization. *Eur. J. Pharm. Sci.* **2011**, *42* (1), 65–72.

(24) Jacobson, A. E.; Yeh, H. J.; Sargent, L. J. Nuclear Magnetic Resonance Spectra of Codeine and Isocodeine Derivatives. *Org. Magn. Reson.* **1972**, *4* (6), 875–883.

(25) Yeh, H. J. C.; Wilson, R. S.; Klee, W. A.; Jacobson, A. E. α- and β-Halomorphides: Stereochemistry, Analgesic Potency, Toxicity, and Interaction with Narcotic Receptors in Vitro. *J. Pharm. Sci.* **1976**, *65* (6), 902–904.

(26) Wenkert, E.; Gaii, M. J.; Hagaman, E. W.; Kwart, L. D. Long Range Substituent Effects Relfected in the ^{13}C NMR Spectra of Allyl Alcohols and Their Derivatives. *Org. Magn. Reson.* **1975**, *7*, 51–53.

(27) Akitt, J. W.; Mann, B. E. The Description of Spin System. In *NMR and*

Chemistry: An introduction to modern NMR spectroscopy; CRC Press, **2000**; p 65.

(28) Sternhell, S. Correlation of Interproton Spin–spin Coupling Constants with Structure. *Q. Rev. Chem. Soc.* **1969**, *23* (2), 236–270.

(29) Jirman, J.; Lyčka, A. ^{15}N, ^{13}C, and ^{1}H NMR Spectra of Acylated Ureas and Thioureas. *Collect. Czech. Chem. Commun.* **1987**, *52* (10), 2474–2481.

(30) Imrich, J.; Bušová, T.; Kristian, P.; Džara, J. Synthesis and the ^{13}C NMR Spectra of *N*,*N*'-Disubstituted Benzoylthioureas and Their Seleno and Oxo Analogues. *Chem. Pap.* **1994**, *48* (1), 42–46.

(31) Haushalter, K. A.; Lau, J.; Roberts, J. D. An NMR Investigation of the Effect of Hydrogen-Bonding on the Rates of Rotation about the CN Bonds in Urea and Thiourea. *J. Am. Chem. Soc.* **1996**, *118* (37), 8891–8896.

(32) Wiles, D. M.; Gingras, B. A.; Suprunchuk, T. The C=S Stretching Vibration in the Infrared Spectra of Some Thiosemicarbazones. *Can. J. Chem.* **1967**, *45* (5), 469–473.

(33) Zayed, M. A.; Hawash, M. F.; Fahmey, M. A. Structure Investigation of Codeine Drug Using Mass Spectrometry, Thermal Analyses and Semi-Emperical Molecular Orbital (MO) Calculations. *Spectrochim. Acta, Part A* **2006**, *64* (2), 363–371.

(34) Zhang, Z.; Yan, B.; Liu, K.; Bo, T.; Liao, Y.; Liu, H. Fragmentation Pathways of Heroin-Related Alkaloids Revealed by Ion Trap and Quadrupole Time-of-Flight Tandem Mass Spectrometry. *Rapid Commun. Mass Spectrom.* **2008**, *22* (18), 2851–2862.

(35) Raith, K.; Neubert, R.; Poeaknapo, C.; Boettcher, C.; Zenk, M. H.; Schmidt, J. Electrospray Tandem Mass Spectrometric Investigations of Morphinans. *J. Am. Soc. Mass Spectrom.* **2003**, *14* (11), 1262–1269.

(36) Poeaknapo, C.; Fisinger, U.; Zenk, M. H.; Schmidt, J. Evaluation of the Mass Spectrometric Fragmentation of Codeine and Morphine after ^{13}C-Isotope Biosynthetic Labeling. *Phytochemistry* **2004**, *65* (10), 1413–1420.

(37) Violette, A.; Averlant-Petit, M. C.; Semetey, V.; Hemmerlin, C.; Casimir, R.; Graft, R.; Marraud, M.; Briand, J. P.; Rognan, D.; Guichard, G. *N*,*N*'-linked Oligoureas as Foldamers: Chain Length Requirements for Helix Formation in Protic Solvent Investigated by Circular Dichroism, NMR Spectroscopy, and Molecular Dynamics. *J. Am. Chem. Soc.* **2005**, *127* (7), 2156–2164.

(38) Wiberg, K. B.; Wang, Y. A Comparison of Some Properties of C=O and C=S Bonds. *ARKIVOC* **2011**, No. 5, 45–56.

(39) Kunchur, N. R.; Truter, M. R. A Detailed Refinement of the Crystal and Molecular Structure of Thiourea. *J. Chem. Soc.* **1958**, 2551–2557.

(40) Mackay, M.; Hodgkin, D. C. A Crystallographic Examination of the Structure of Morphine. *J. Chem. Soc.* **1955**, 3261–3267.

(41) Canfield, D. V.; Barrick, J.; Giessen, B. C. Structure of Codeine. *Acta Crystallogr., Sect. C: Cryst. Struct. Commun.* **1987**, *43* (5), 977–979.

(42) Kartha, G.; Ahmed, F. R.; Barnes, W. H. Refinement of the Crystal Structure of Codeine Hydrobromide Dihydrate, and Establishment of the Absolute Configuration of the Codeine Molecule. *Acta Crystallogr.* **1962**, *15* (4), 326–333.

(43) Okuda, S.; Yamaguchi, S.; Kawazoe, Y.; Tsuda, K. Studies on Morphine Alkaloids. I. Nuclear Magnetic Resonance Spectral Studies on Morphine Alkaloids.(I). *Chem. Pharm. Bull.* **1964**, *12* (1), 104–112.

(44) Desai, A. A.; Wulff, W. D. New Derivatives of VAPOL and VANOL: Structurally Distinct Vaulted Chiral Ligands and Brønsted Acid Catalysts. *Synthesis* **2010**, No. 21, 3670–3680.

(45) Srimurugan, S.; Su, C. J.; Shu, H. C.; Murugan, K.; Chen, C. A Facile and Improved Synthesis of Desomorphine and Its Deuterium-Labeled Analogue. *Monatsh. Chem.* **2012**, *143* (1), 171–174.

(46) Goto, K.; Yamamoto, I. The Three Isomers of (+)-Codeine and Some Codeimethines from Them. *Proc. Jpn. Acad.* **1959**, *35* (6), 472–475.

(47) Connon, S. J. Organocatalysis Mediated by (Thio)urea Derivatives. *Chem. Eur. J.* **2006**, *12* (21), 5418–5427.

(48) Alemán, J.; Parra, A.; Jiang, H.; Jørgensen, K. A. Squaramides: Bridging from Molecular Recognition to Bifunctional Organocatalysis. *Chem. Eur. J.* **2011**, *17* (25), 6890–6899.

(49) Zhang, H.; Lin, S.; Jacobsen, E. N. Enantioselective Selenocyclization *via* Dynamic Kinetic Resolution of Seleniranium Ions by Hydrogen-Bond Donor Catalysts. *J. Am. Chem. Soc.* **2014**, *136* (47), 16485–16488.

(50) Roca-López, D.; Uria, U.; Reyes, E.; Carrillo, L.; Jørgensen, K. A.; Vicario, J. L.; Merino, P. Mechanistic Insights into the Mode of Action of Bifunctional Pyrrolidine-Squaramide-Derived Organocatalysts. *Chem. Eur. J.* **2016**, *22* (3), 884–889.

(51) Wang, Y.; Pan, J.; Jiang, R.; Wang, Y.; Zhou, Z. Stereocontrolled Construction of 3,4-Dihydrocoumarin Scaffolds with a Quaternary Amino Acid Moiety *via* Chiral Squaramide-Catalyzed Cascade Michael Addition/Lactonization Reaction. *Adv. Synth. Catal.* **2016**, *358* (2), 195–200.

(52) Jiang, H.; Paixão, M. W.; Monge, D.; Jørgensen, K. A. Acyl Phosphonates: Good Hydrogen-Bond Acceptors and Ester/Amide Equivalents in Asymmetric Organocatalysis. *J. Am. Chem. Soc.* **2010**, *132* (8), 2775–2783.

(53) Soberats, B.; Martínez, L.; Sanna, E.; Sampedro, A.; Rotger, C.; Costa, A. Janus-Like Squaramide-Based Hosts: Dual Mode of Binding and

Conformational Transitions Driven by Ion-Pair Recognition. *Chem. Eur. J.* **2012**, *18* (24), 7533–7542.

(54) Rostami, A.; Wei, C. J.; Guérin, G.; Taylor, M. S. Anion Detection by a Fluorescent Poly (Squaramide): Self-Assembly of Anion-Binding Sites by Polymer Aggregation. *Angew. Chem., Int. Ed.* **2011**, *50* (9), 2059–2062.

(55) Wu, X.; Busschaert, N.; Wells, N. J.; Jiang, Y. B.; Gale, P. A. Dynamic Covalent Transport of Amino Acids across Lipid Bilayers. *J. Am. Chem. Soc.* **2015**, *137* (4), 1476–1484.

(56) Gaeta, C.; Talotta, C.; Della Sala, P.; Margarucci, L.; Casapullo, A.; Neri, P. Anion-Induced Dimerization in *p*-Squaramidocalix[4]arene Derivatives. *J. Org. Chem.* **2014**, *79* (8), 3704–3708.

(57) Han, X.; Zhou, H. B.; Dong, C. Applications of Chiral Squaramides: From Asymmetric Organocatalysis to Biologically Active Compounds. *Chem. Rec.* **2016**, *16* (2), 897–906.

(58) Held, F. E.; Tsogoeva, S. B. Asymmetric Cycloaddition Reactions Catalyzed by Bifunctional Thiourea and Squaramide Organocatalysts: Recent Advances. *Catal. Sci. Technol.* **2016**, *6* (3), 645–667.

(59) Lee, J. W.; Ryu, T. H.; Oh, J. S.; Bae, H. Y.; Jang, H. B.; Song, C. E. Self-Association-Free Dimeric Cinchona Alkaloid Organocatalysts: Unprecedented Catalytic Activity, Enantioselectivity and Catalyst Recyclability in Dynamic Kinetic Resolution of Racemic Azlactones. *Chem. Commun.* **2009**, No. 46, 7224–7226.

Chapter 3

Catalytic Study of *N,N'*-disubstituted Thiourea Opioid Derivative in Michael Addition Reactions

3.1 Introduction

Naturally occurring cinchona alkaloids and their derivatives have been developed as organocatalysts for many catalytic asymmetric reactions, such as oxidations and carbon-carbon bond formation reactions. Due to the multiple functionalities in the cinchona backbone, a wide array of novel organocatalysts has been synthesised without extensive and time-consuming chiral resolution, which are often involved in other catalysts' syntheses. Therefore, there is no doubt that further development of cinchona-based organocatalysts for asymmetric reactions will continue to have a major impact on chemistry research. The opiates are a similar class of alkaloids. However, they have rarely been used despite their potential in organocatalytic reactions. The majority of this research is to evaluate the catalytic potential of a small number of opioid derivatives which have been derived from sustainable alkaloids such as codeine. Hypothetically, with five asymmetric center carbons and a heterocyclic ring structure, the increased steric bulk from the opiate scaffold may give increased enantioselectivity.

3.2 Catalysis of Michael addition reaction by Takemoto catalyst

Asymmetric organocatalysis has contributed as a powerful and mild methodology for accelerating reactions and synthesis of enantiomerically pure products in an efficient and environmentally friendly approach.[1] Particularly, thiourea and urea derivatives represent a large and very important group of organocatalysts and provide explicit double hydrogen-bonding interactions to coordinate and activate hydrogen-bond accepting substrates.[2] Furthermore, the bifunctional compounds which consist of both a thiourea/urea moiety and an amine group on a chiral scaffold have been applied as useful organocatalysts for numerous applications in organic synthesis.[1] On the other hand, among the numerous asymmetric C-C bond formation reactions, the conjugate Michael reaction plays an important role, because it is a highly versatile synthetic tool to join two chemical entities together during the reaction.[3] Examples mentioned in chapter 1 are the bifunctional thiourea catalysts based on cinchona for catalysis of the Michael addition reaction of nitroolefins. The first enantioselective Michael addition was reported by Takemoto's group using a bifunctional amine thiourea-organocatalyst (**26**) which they reported in 2003.[4] The bifunctional organocatalyst has a thiourea moiety and an amino group on a cyclohexane ring (chiral scaffold), which has a double

activation function: activating both the nitroolefin and nucleophile simultaneously, and controlling the approach of the nucleophile to the nitroolefin.[5] Furthermore, in order to investigate the effects of the amino group on the reactivity and selectivity of the reaction, two additional thiourea catalysts were synthesised: one (**49**) has no amino group on the cyclohexane ring and the other (**50**) is an achiral bifunctional organocatalyst. Evaluation of their catalytic abilities in the catalysis reaction compared to the Takemoto catalyst (**26**) was carried out.[5] Under the optimised conditions (room temperature in toluene) the Takemoto catalyst efficiently promoted the Michael reaction of diethyl malonate to *trans*-β-nitrostyrene to afford an 86% yield and excellent enantioselectivity (93% *ee*), whereas not only were moderate yields obtained from the other two catalysts (**49** and **50**), no enantioselectivity was observed (Scheme 3.1).[5]

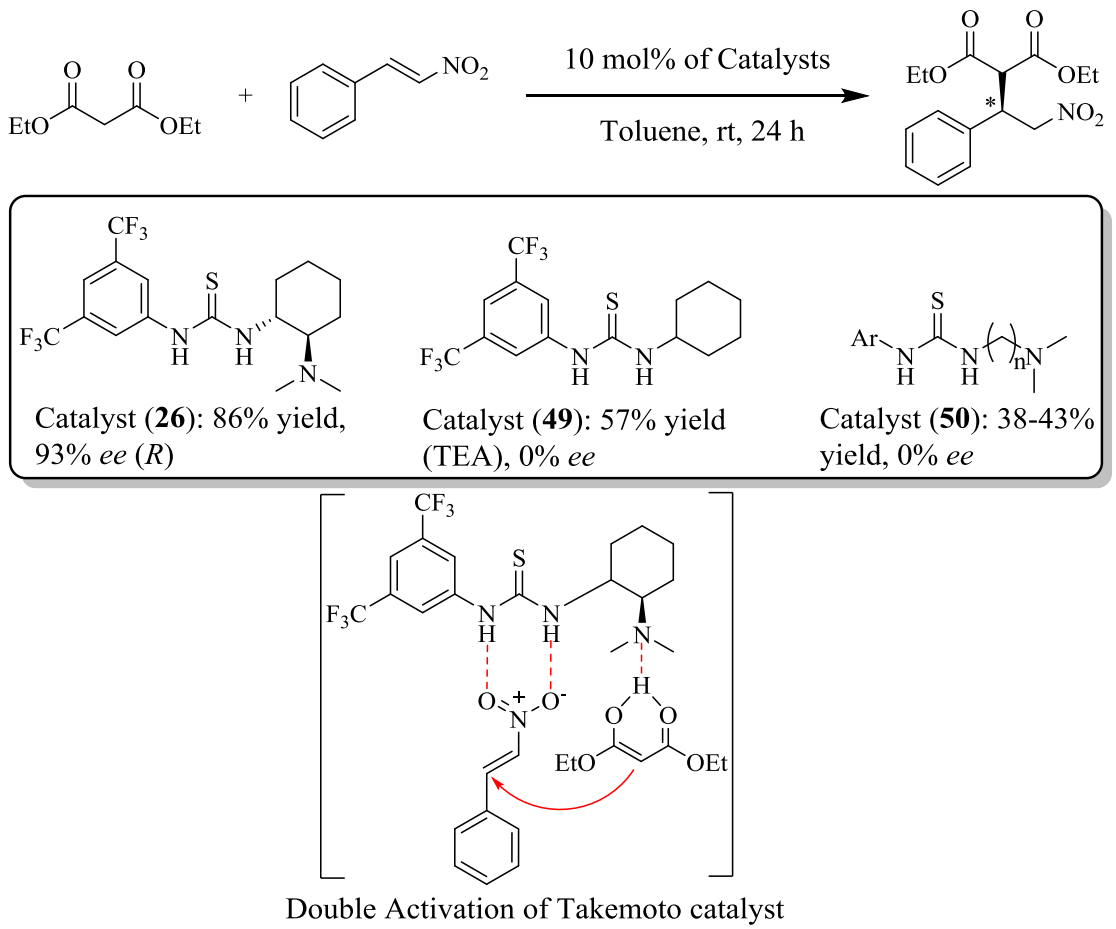

Scheme 3.1 Catalysis of Micheal addition reaction of diethyl malonate to *trans*-β-nitrostyrene by double activation Takemoto catalyst (**26**) and two other thiourea derived catalysts.[4,5]

Therefore, based on the results, a plausible reaction mechanism for chiral amine-thiourea catalysis was proposed to demonstrate how the bifunctional catalyst enhances the reaction rate and enantioselectivity more effectively than a monofunctional catalyst (Scheme 3.2).[5]

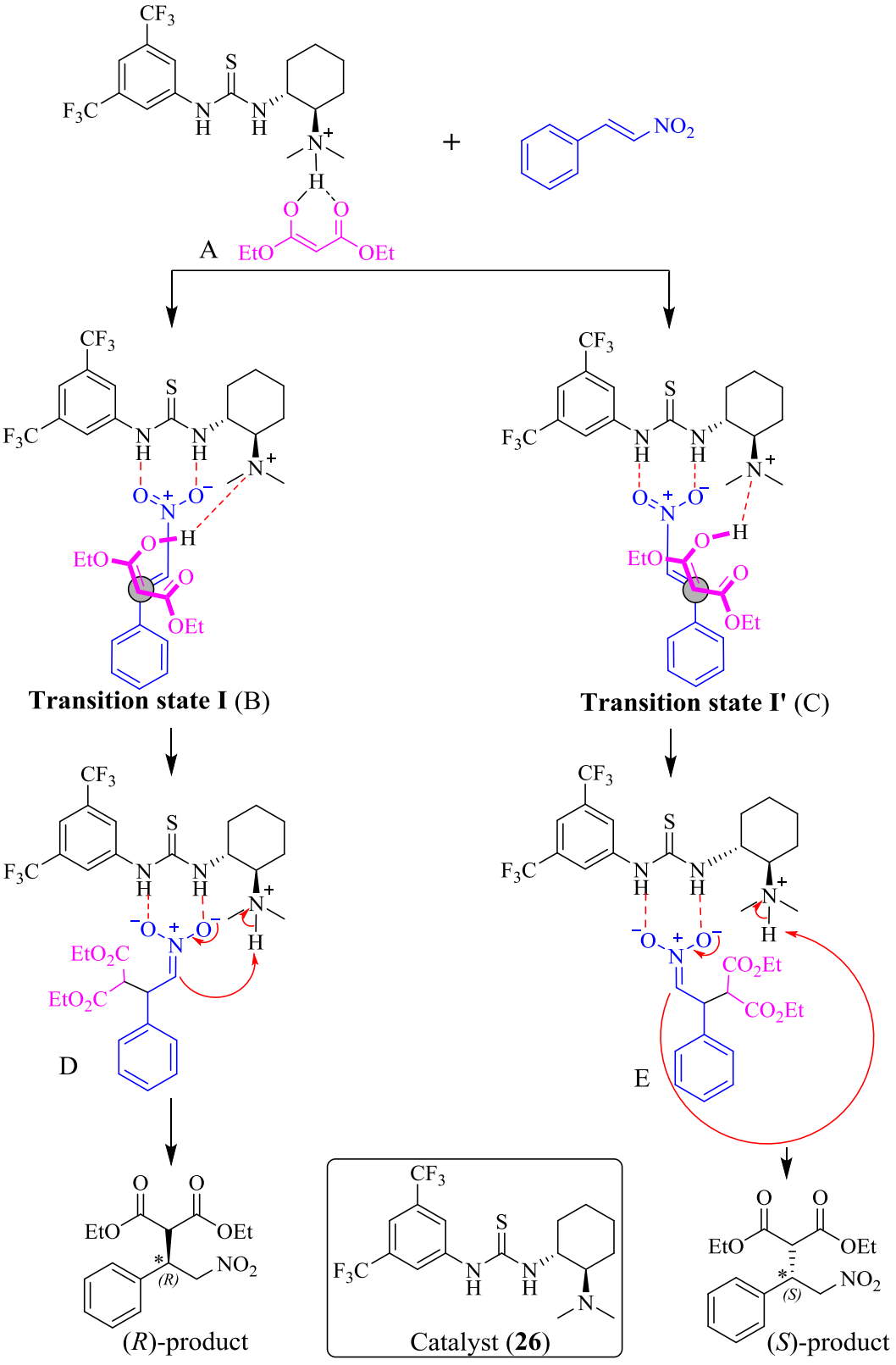

Scheme 3.2 Plausible reaction mechanism of Michael addition reaction of diethyl malonate to *trans*-β-nitrostyrene by Takemoto catalyst (**26**).[4]

According to the mechanism above, the amino group of the Takemoto catalyst (**26**) first deprotonates an acidic proton from the six-membered cyclic enol form of diethyl

malonate to generate the binary complex A. Meanwhile, *trans*-β-nitrostyrene is activated by the thiourea moiety on the Takemoto catalyst *via* hydrogen-bonding, to form a new ternary complex B or complex C. Based on the absolute configuration of the final product, Takemoto suggested that complex B should give nitronate complex D, bearing an *R* configuration *via* transition state **I**, rather than giving *S* enantiomer through transition state **I**'. This is because the chiral scaffold of the catalyst restricts the approach of diethyl malonate to *trans*-β-nitrostyrene. The final step in the reaction is the regeneration of the catalyst through deprotonation of the amino group by the nitronate moiety to give the product.[5]

The mechanism of this reaction was also investigated through density functional theory (DFT) computations by Pápai *et al.*.[6] They proposed an alternative mechanistic route using acetylacetone as a substrate. In their double activation mode (transition state **II** and **II**'), *trans*-β-nitrostyrene preferred to coordinate with quaternary ammonium through single hydrogen-bonding interactions, while the enolate forms hydrogen-bonding with thiourea moiety of the catalyst. As seen in Fig. 3.1, although this scenario was distinct from the Takemoto study, substrates in both transition state **I** and **II** are aligned in a staggered conformation along the forming C-C bonds, which can minimize steric intermolecular interactions, whereas the C-C bonds of the two substrates are nearly eclipsed to destabilize the complex E and F in transition state **I**' and **II**'. Therefore, the *R* enantiomer is proposed to be preferred over the *S* enantiomer in both mechanisms for the Michael addition reaction.[6]

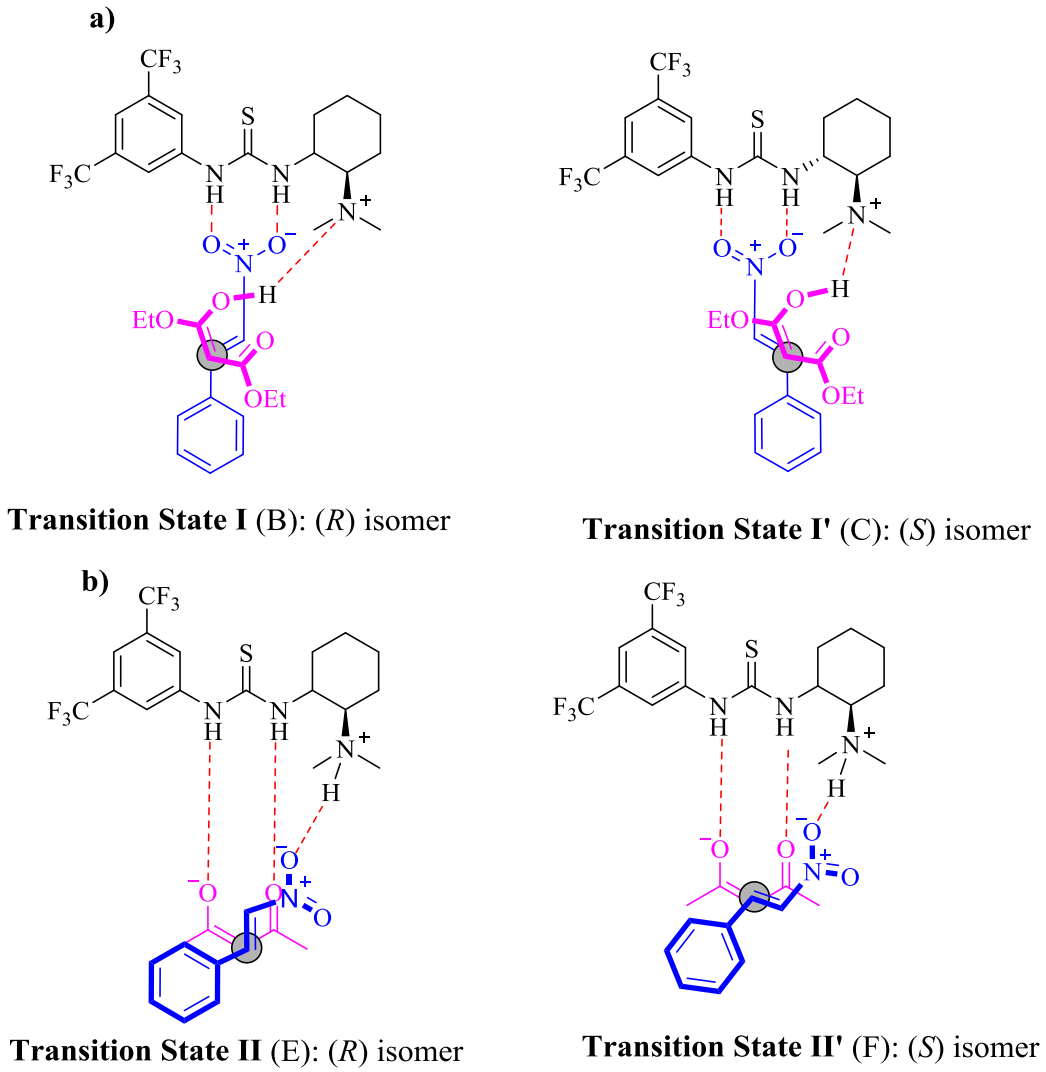

Fig. 3.1 Plausible transition states of Michael addition reaction: a) Transition state **I** and **I**' by Takemoto *et al.*[5] b) Transition state **II** and **II**' by Pápai *et al.*.[6]

In order to evaluate the catalytic ability of *N,N'*-disubstituted thiourea (**5**) for the Michael addition reaction, the bifunctional Takemoto catalyst (**26**) was used as a reference for the reaction. The Takemoto catalyst (**26**) and *N,N'*-disubstituted thiourea (**5**) both containing a thiourea moiety. They also have amino groups on the chiral scaffolds, with the only difference between them being that there is only one chiral scaffold in the Takemoto catalyst (**26**), whereas there are two symmetric chiral opiate scaffolds on the *N,N'*-disubstituted thiourea (**5**), which could confer an advantage in enhancing enantioselectivity (Fig. 3.2).

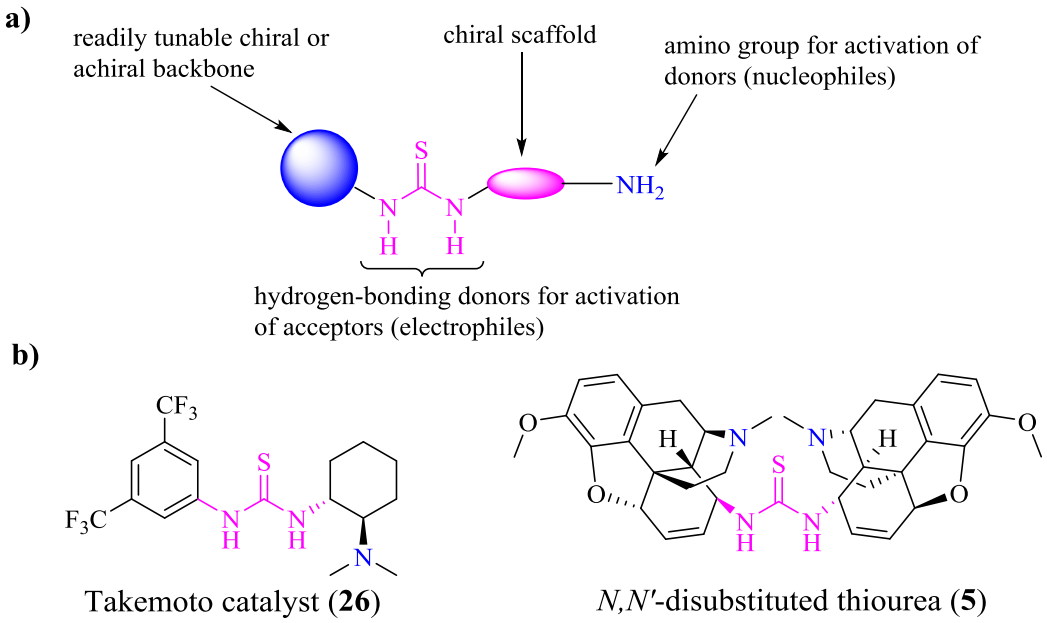

Fig. 3.2 a) Description of structure of bifunctional amine thiourea-organocatalyst.[1] b) Comparison of Takemoto catalyst (**26**) and *N,N'*-disubstituted thiourea (**5**) (common features are highlighted in colour).

3.3 Evaluation of *N,N'*-disubstituted thiourea in the Michael addition reaction

The procedure used for the study of the Michael addition reaction was described by Takemoto *et al.* (Scheme 3.3).[4,5] The products were formed using the Takemoto catalyst under literature conditions to optimize the HPLC conditions before catalyst screening, including the racemate which was formed by the use of KOtBu (5 mol%).[7] In order to ensure reproducible reactions and results in the laboratory, reference data was initially produced by repeating the catalysis reaction with the Takemoto catalyst (**26**) in toluene and the obtained isolated yield (90.8%) and enantioselectivity (91.6% *ee*) were in agreement with the data from the literature paper (86% yield, 93% *ee*).[4,5] Catalysis of the Michael addition reaction of diethyl malonate with *trans*-β-nitrostyrene by the *N,N'*-disubstituted thiourea catalyst (**5**) was subsequently investigated focusing on the effects of various parameters such as the type of solvent, reagent ratio and catalyst loading (Scheme 3.3).

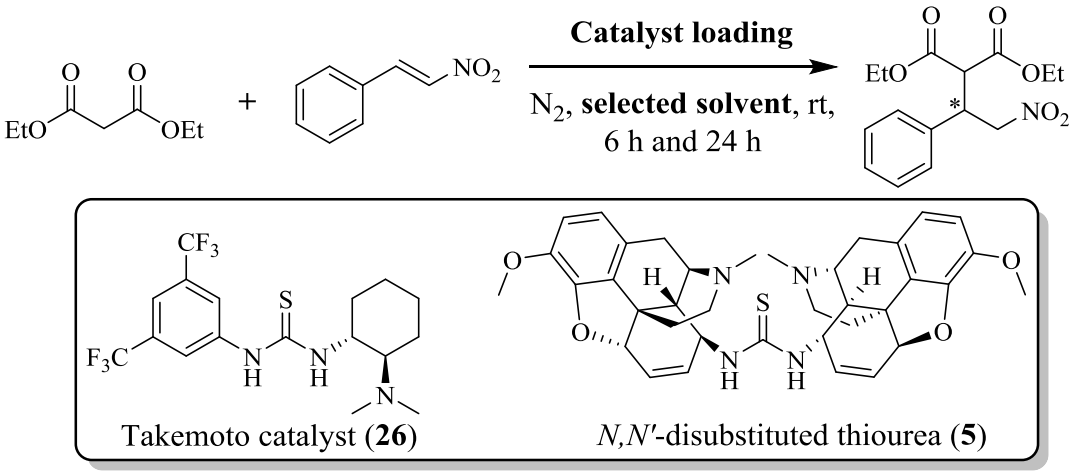

Scheme 3.3 Catalysis of Micheal addition reaction of diethyl malonate to *trans*-β-nitrostyrene by Takemoto catalyst (**26**) and *N,N'*-disubstituted thiourea catalyst (**5**) for the initial solvent screening.

3.3.1 Evaluation of the effects of selected solvents

The polarity of a solvent can affect the isolated yield and even enantioselectivity in the catalysis reaction. Therefore, investigation of the catalytic activity of the *N,N'*-disubstituted thiourea catalyst (**5**) in selected solvents was carried out as a primary test. The solvents selected to screen for the catalysis reaction ranged from non-polar to polar solvents. Generally, the monofunctional (thio)ureas exhibit low solubility in nonpolar solvents due to strong intermolecular hydrogen-bonding. However, as well as having a similar structure to the Takemoto catalyst (**26**), the *N,N'*-disubstituted thiourea catalyst derivative (**5**) catalyst has two tertiary amine groups from the piperidine rings (D-ring) on both sides of the opiate scaffold. This leads to the formation of another intermolecular hydrogen-bond between the amino group and the N-H groups of the thiourea moiety, leading to a potential increased solubility in nonpolar solvents. Indeed, the *N,N'*-disubstituted thiourea catalyst (**5**) was soluble in toluene. All the solvent screen studies were carried out with 10 mol% catalyst loading and a 2:1 reagent ratio (diethyl malonate:*trans*-β-nitrostyrene = 2:1). The reaction condition was controlled at room temperature and under an inert atmosphere. The conversion was monitored by NMR after 6 hours and 24 hours and enantioselectivity was determined by chiral HPLC after 24 hours.

From Table 3.1, all the reactions for the solvent study were almost complete after 24 hours. However, in nonpolar solvents such as hexane, *N,N'*-disubstituted thiourea

catalyst (**5**) efficiently promoted the reaction to afford the product within 6 hours even though it is insoluble in hexane; the reaction with toluene was also completed after 6 hours and afforded a high yield (86.4% yield in hexane; 89.8% yield in toluene). Both results from non-polar solvents confirmed that less polar solvents enhance the thiourea catalytic activity and generate a higher yield and faster reactions. A moderate yield was obtained from DCM as well as no enantioselectivity being observed. Polar solvents such as THF and MeCN, which could undergo hydrogen-bonding with the *N,N'*-disubstituted thiourea catalyst (**5**) or potential transition states, had a reduced reaction rate compared to the non-polar solvents. Thus, the conversions and yields of the polar reactions were relatively lower: 63.4% conversion (after 6 h) with a final isolated yield of 80.4% yield for THF and 77.6% conversion (after 6 h) and final isolated yield of 82% yield for MeCN. MeOH is an exception as it gave a 91.2% conversion after 6 hours.

Table 3.1 The initial solvent screening of *N,N'*-disubstituted thiourea catalyst (**5**) for the Michael reaction of diethyl malonate to *trans*-β-nitrostyrene.[a]

Exp. Set	Catalyst Loading (10 mol%)	Solvent (4 mL)	Time (h)	Conversion (%)[b]	Yield (%)[c]	*ee* (%)[d]
Ref.	Takemoto Catalyst (**26**)	Toluene	6, 24	6 h: 96 24 h: 100	90.8	91.6 (*R*)
1	*N,N*'-disubstituted thiourea (**5**)	Hexane	6, 24	6 h: 100 24 h: 100	86.4	3.3 (*S*)
2	*N,N*'-disubstituted thiourea (**5**)	Toluene	6, 24	6 h: 97 24 h: 100	89.8	9.6 (*S*)
3	*N,N*'-disubstituted thiourea (**5**)	DCM	6, 24	6 h: 88.5 24 h: 100	79.6	0
4	*N,N*'-disubstituted thiourea (**5**)	THF	6, 24	6 h: 63.4 24 h: 100	80.4	6.5 (*S*)
5	*N,N*'-disubstituted thiourea (**5**)	MeOH	6, 24	6 h: 91.2 24 h: 100	74.3	6.5 (*S*)
6	*N,N*'-disubstituted thiourea (**5**)	MeCN	6, 24	6 h: 77.6 24 h: 97.7	82	4.2 (*S*)

[a]: Reactions were carried out with diethyl malonate (0.4 mmol), *trans*-β-nitrostyrene (0.2 mmol) and the catalyst (0.02 mmol) under N_2 at room temperature, using selected dry solvents (0.4 mL).
[b]: By NMR.
[c]: Isolated yields after flash column chromatography: Ethyl Acetate:Hexane (1:12 to 1:5) after 24 h.
[d]: The % *ee* values were determined *via* chiral HPLC using a Phenomenex chiral column (Lux 5μ, cellulose-2, 250 x 4.60 mm).

Compared to the Takemoto catalyst, modest values of enantioselectivity were obtained from all selected solvents with the highest from toluene, which is close to 10% *ee*. Based on these results, toluene was used as the optimised solvent for the subsequent reactions. It is interesting that the configuration of the product obtained is the *S* isomer when using the *N,N'*-disubstituted thiourea catalyst (**5**), rather than the *R* isomer which is obtained when using the Takemoto catalyst. As seen from Fig. 3.3, the minor peak of the *S* isomer from the Takemoto catalyst run has a tail, which appears at a slightly longer retention time. It might be caused by the presence of impurities in the product or the column. If the tailing is caused by an impurity, it stands to reason that it is possible for the true *ee* value to be higher with respect to the *R* isomer if this is factored out. However, with the control providing similar enantioselectivity (91.6% *ee*) to the literature value (93% *ee*), a void that forms in the inlet of the column could be considered as a possible cause of this issue and may lead to peak tailing.[8] This issue was pervasive throughout all HPLC runs performed under the column conditions used. (Appendix B).

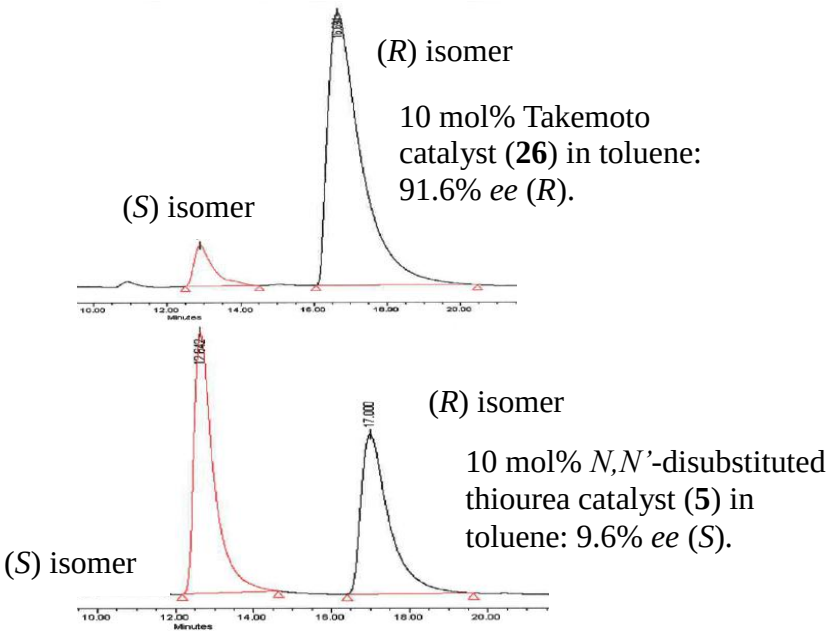

Fig. 3.3 Comparison of chromatogram of isomers from Takemoto catalyst (**26**) and *N,N'*-disubstituted thiourea catalyst (**5**).

3.3.2 Evaluation of the effects of reagent ratios

In order to measure the efficiency of the Michael addition reaction with the *N,N'*-disubstituted thiourea catalyst (**5**), the determination of yields and enantioselectivities based on the limiting reagent were also carried out as part of the study of the catalysis reaction. It is plausible that a base-containing catalyst would enhance the reaction rate by assisting in the deprotonation of the nucleophile. This would potentially offer some improvements over catalyst system which required a large excess of malonate.[9] Therefore, using the reagent ratio for the Takemoto catalyst (diethyl malonate:*trans*-β-nitrostyrene = 2:1) as a standard where diethyl malonate is used in excess, efficiency of the reactions with *N,N'*-disubstituted thiourea catalyst (**5**) was determined using lower quantities of diethyl malonate, with reagent ratios for the tests being 2:1, 1.5:1 and 1:1 (Table 3.2).

Table 3.2 Reagent ratios of *N,N'*-disubstituted thiourea catalyst (**5**) for the Michael reaction of diethyl malonate to *trans*-β-nitrostyrene.[a]

Exp. Set	Reagent Ratio (Mal : N-Styr/mmol)	Time (h)	Conversion (%)[b]	Yield (%)[c]	*ee* (%)[d]
1	0.4 mmol : 0.2 mmol	6, 24	6 h: 94.8 24 h: 100	89.8	9.6 (*S*)
2	0.3 mmol : 0.2 mmol	6, 24	6 h: 94.8 24 h: 100	85.3	7.3 (*S*)
3	0.2 mmol : 0.2 mmol	6, 24	6 h: 95.4 24 h: 100	86.8	5.3 (*S*)

[a]: Reactions were carried out with 10 mol% *N,N'*-disubstituted thiourea catalyst (**5**) (0.02 mmol) and toluene (0.4 mL) under N_2 at room temperature, using reagent ratios of diethyl malonate and *trans*-β-nitrostyrene: 0.4 mmol:0.2 mmol, 0.3 mmol:0.2 mmol and 0.2 mmol:0.2 mmol, respectively.
[b]: By NMR.
[c]: Isolated yields after flash column chromatography: Ethyl Acetate:Hexane (1:12 to 1:5) after 24 h.
[d]: The % *ee* values were determined *via* chiral HPLC using Phenomenex chiral column (Lux 5*μ*, cellulose-2, 250 x 4.60 mm).

With a different ratio of diethyl malonate and *trans*-β-nitrostyrene, all the reactions were *ca.* 95% completed after 6 hours with similar yields. According to the graph in Fig. 3.4, interestingly, the quantities of reagents used did not affect the conversion of the reaction very much, but slightly affected the enantioselectivity. It should be noted that lower enantioselectivity was obtained with decreasing quantities of diethyl malonate used. It is reasonable that deprotonation of the diethyl malonate occurs more

quickly at higher reaction concentration and thus results in more probabilities of formation of (*S*)-product by the direct conjugate addition of enolate to nitroolefin.[9] Therefore, the optimized ratio of diethyl malonate and *trans*-β-nitrostyrene is considered to be 0.4 mmol:0.2 mmol.

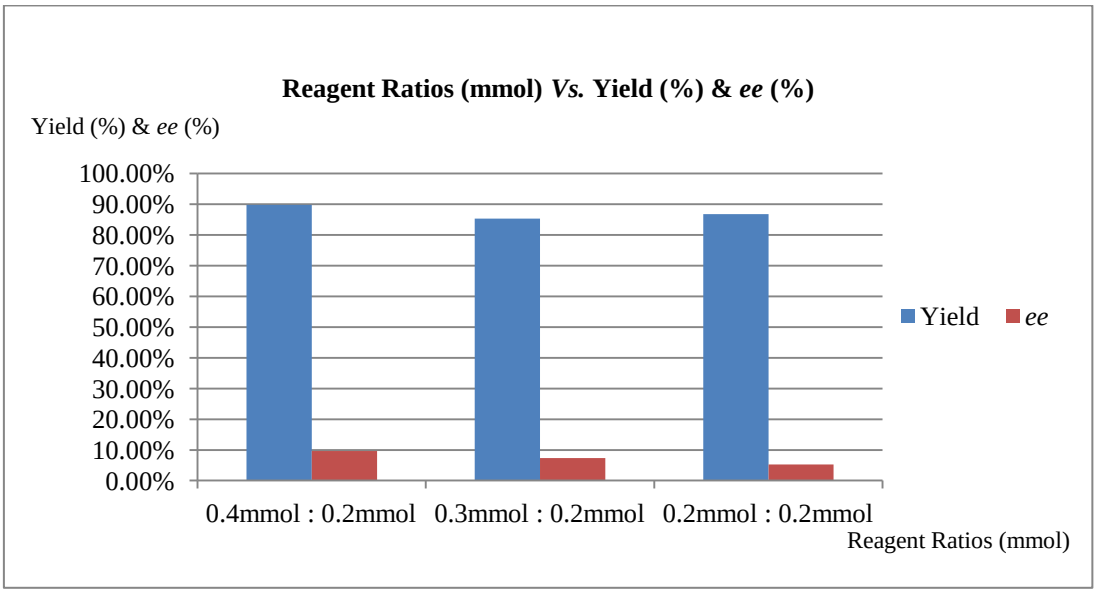

Fig. 3.4 Graph of effect on yield (%) and enantioselectivity (%) by reagent ratios.

3.3.3 Evaluation of the effects of catalyst loading

In a catalytic enantioselective reaction, the amount of catalyst needed is an important factor in determining the practicality of the methodology, especially when the catalyst requires many steps to be synthesised or is expensive. The investigation into optimum catalyst loading was conducted at four different catalyst loadings in the range of 10 mol% to 1 mol% (Table 3.3). The 10 mol% of catalyst loading provides 100% conversion of the reaction within 6 hours. However, with reducing quantities of catalyst used, the reaction rate decreased, especially with 1 mol% of catalyst loading which produced only 39.3% conversion after 6 hours, however, the reaction reached nearly full conversion after 24 hours. This result proves that hydrogen-bond formation is a factor controlling the reaction rate. Decreased catalyst loadings not only resulted in a slowing down of the reaction rate, but also had a large effect on the enantioselectivity of the reaction with decreasing in the probability of correlation between catalyst and substrate. Enantioselectivities at 10 mol% loading decreased from 9.6% *ee* to 4.6% *ee* at 5 mol% loading and to 2.6% *ee* at 2.5 mol% loading. Although the precise reason

for the effect of less catalyst loading on the enantioselectivity is not clear at this time, it can be hypothesized that with higher catalyst loading, there are more availabilities of stable pro-*S* enantiomer complex in the reaction solution and this result in the formation of desired product, even if only with low enantioselectivity. This also reveals thiourea catalyst's one of significant drawbacks: frequently necessitating high catalyst loading, due to having relatively weak activity.[10] Therefore, as seen in Table 3.3, those needs of long reaction time to achieve a satisfactory yield. Another reason may be a second competitive reaction pathway which leads to racemic product. At high catalyst loadings (10 mol%) the reaction attains 95% conversion within 6 hours, compared to only 39% conversion with 1 mol% catalyst. The racemic product formed would have a greater reduction in the *ee* of the product in the latter case due to the longer time to attain high conversion. As shown in graph (Fig. 3.5), it is clear that a direct relationship between enantioselectivity and catalyst loading was observed, rather than the inverse relationship.[11]

Table 3.3 Catalyst loading of *N,N'*-disubstituted thiourea catalyst (**5**) for the Michael reaction of diethyl malonate to *trans*-β-nitrostyrene.[a]

Exp Set	Catalyst Loading	Time (h)	Conversion (%)[b]	Yield (%)[c]	*ee* (%)[d]
1	10 mol% of *N,N*'-disubstituted thiourea (**5**)	6, 24	6 h: 94.8 24 h: 100	89.8	9.6 (*S*)
2	5 mol% of *N,N*'-disubstituted thiourea (**5**)	6, 24	6 h: 86.7 24 h: 100	86.3	4.6 (*S*)
3	2.5 mol% of *N,N*'-disubstituted thiourea (**5**)	6, 24	6 h: 47.1 24 h: 95.1	85.8	2.6 (*S*)
4	1 mol% of *N,N*'-disubstituted thiourea (**5**)	6, 24	6 h: 39.3 24 h: 94.3	85.2	2.3 (*S*)

[a]: Reactions were carried out with diethyl malonate (0.4 mmol), *trans*-β-nitrostyrene (0.2 mmol) and toluene (0.4 mL) under N_2 at room temperature with loading 10 mol%, 5 mol%, 2.5 mol% and 1 mol% of *N,N'*-disubstituted thiourea catalyst (**5**), respectively.
[b]: By NMR.
[c]: Isolated yields after flash column chromatography: Ethyl Acetate:Hexane (1:12 to 1:5) after 24 h.
[d]: The % *ee* values were determined *via* chiral HPLC using Phenomenex chiral column (Lux 5μ, cellulose-2, 250 x 4.60 mm).

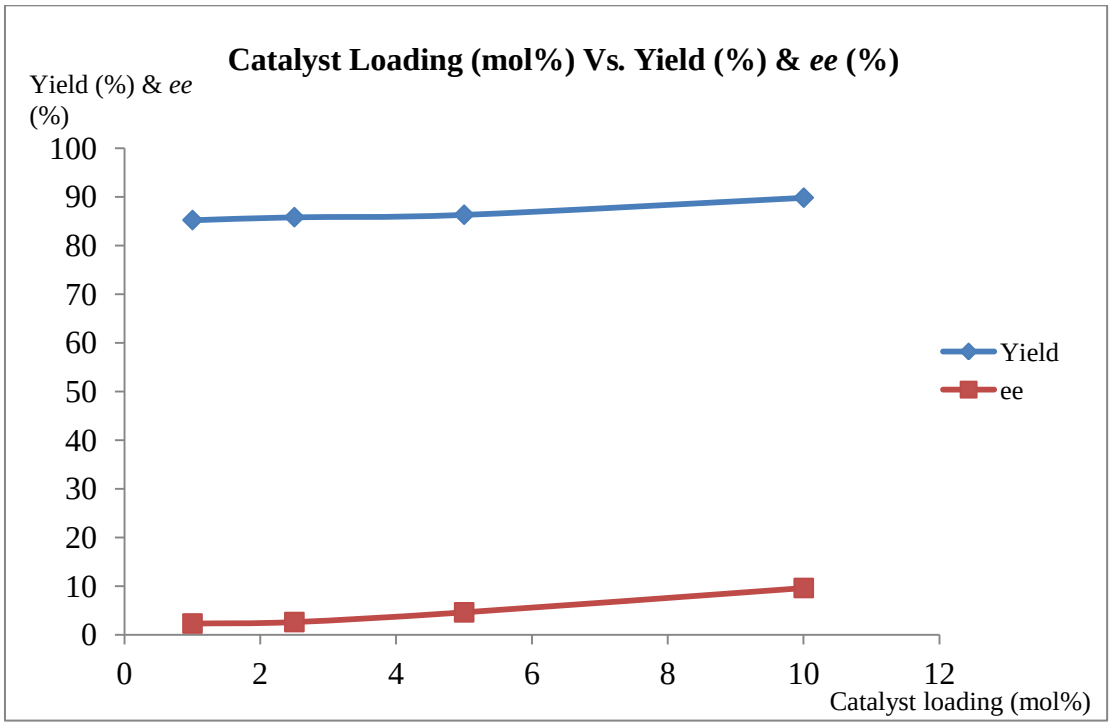

Fig. 3.5 Graph of effect on yield (%) and enantioselectivity (%) by catalyst loading.

3.4 Discussion

The *N,N'*-disubstituted thiourea catalyst (**5**) efficiently promoted the Michael addition reaction to give a full conversion with high yields after 24 hours, but gave low enantioselectivities. The crystal structure of the Takemoto catalyst (**26**) (Fig. 3.6) indicates that the amino group and N-H of the thiourea moiety orient to the same direction, which leads the nucleophiles to approach nitroolefins in an ideal way when the thiourea moiety and amino group interact with nitroolefins and nucleophiles respectively.[5,12] However, according to the crystal structure of the *N,N'*-disubstituted thiourea catalyst (**5**) in Fig. 3.7, the N-H of the thiourea moiety and the two tertiary amine groups orient in a different direction, with the thiourea H-N perpendicular to each of the tertiary amine groups. Thus, this might be preventing the nucleophile from approaching the nitroolefins. Moreover, the N-H of the thiourea moiety is too far removed from the two tertiary amine groups. In contrast, in the Takemoto catalyst, the N-H of the thiourea moiety is relatively close to the amino group of the cyclohexane rings (Fig. 3.6). Therefore, the distance between the amine groups and the thiourea N-H could be another factor that could influence the enantioselectivity of the catalyst.

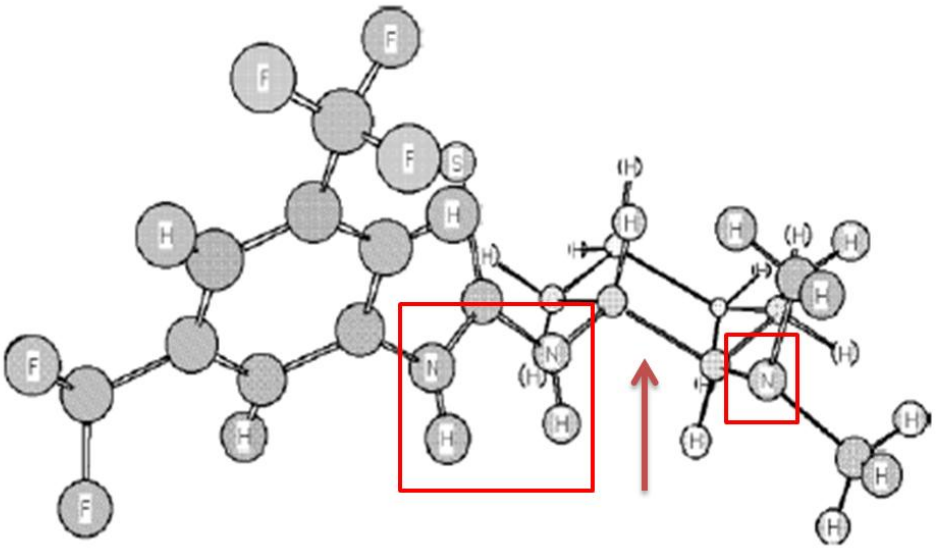

amino group and thiourea N-H orient toward the same direction.

Fig. 3.6 Crystal structure of Takemoto catalyst (**26**).[5,12]

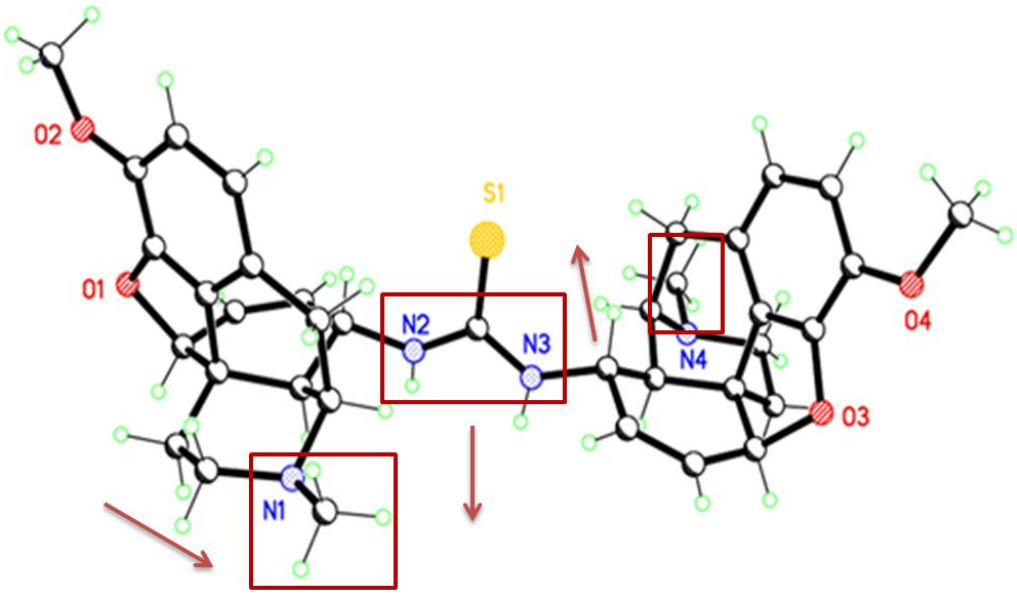

amino groups and thiourea N-H orient face different directions.

Fig. 3.7 Crystal structure of the *N*,*N*'-disubstituted thiourea catalyst (**5**).

3.5 Future work

Due to limitations regarding the chiral HPLC system used, the other synthesised *N,N'*-disubstituted urea (**6**) derivative was unable to be evaluated for its catalytic activity in the same reaction. In further work, it should be considered for primary testing. On the other hand, it appears that the *N,N'*-disubstituted thiourea catalyst (**5**) did not successfully catalyse the Michael addition reaction as a bifunctional catalyst as low enantioselectivity was observed possibly due to the orientation of the amino group on the natural state of opiate scaffold, although the conversion reached 100% after 24 hours. The same result was also obtained from a previously studied thiourea based opioid derivative (**51**).[13] This thiourea catalyst has one opiate scaffold and a 1,3-bis(trifluoromethyl)benzene group, which has a similar structure to the Takemoto catalyst. However, low enantioselectivity was also obtained with this compound in the Michael addition reaction (Fig. 3.8). According to the crystal structure (Fig. 3.9), the N-H of the thiourea moiety is far away from the tertiary amine group and both also orient in a different direction and perpendicular to each other which is exactly same as the *N,N'*-disubstituted thiourea (**5**).

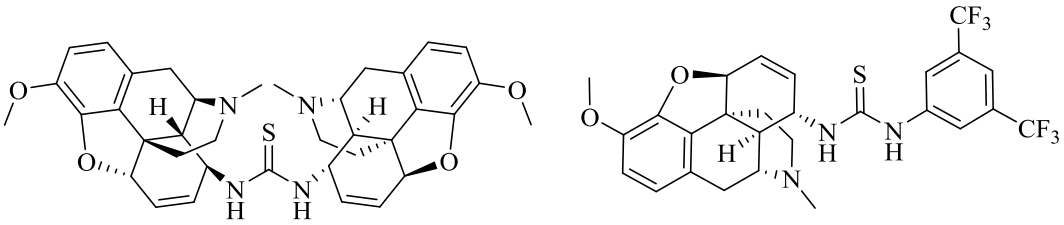

N,N'-disubstituted thiourea catalyst (**5**)
91.6% yield, 9.6% *ee* in Toluene

thiourea catalyst (**51**)
97% yield, 12% *ee* in DCM[10]

Fig. 3.8 Structure of *N,N'*-disubstituted thiourea catalyst (**5**) and thiourea catalyst (**51**)[13] and their yields and enantioselectivites in Michael addition reaction.

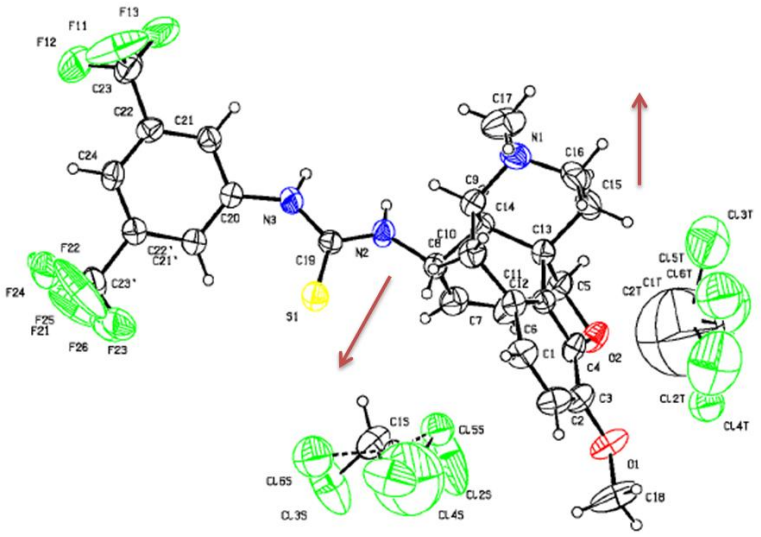

Fig. 3.9 Crystal structure of the thiourea catalyst (**51**).[13]

Therefore, it is certain that the tertiary amine groups from both thiourea derivatives do not perform as well as the Takemoto catalyst in the Michael addition reaction due to the orientation stereochemistry of the tertiary amine group. Therefore, in order to improve the selectivity of reaction, it may be required to modify the structures of both thiourea derivatives by substitution of an additional amino group or a hydroxyl group at the C7 or C6 position on the C-ring of the opiate scaffold after removal of the double bond. Thus, the long distance between the N-H of thiourea moiety and the amino group is shortened and both the N-H of the thiourea moiety and the amino group are orientated in the same direction.

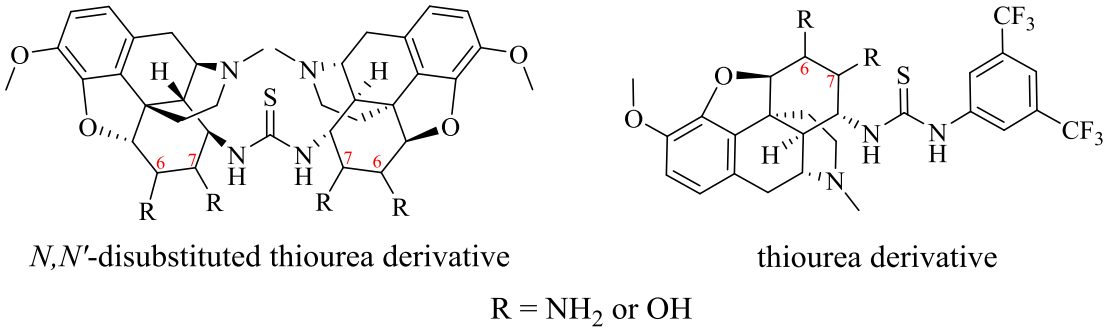

Fig. 3.10 Possible modification of thiourea opioid derivatives.

3.6 References

(1) Serdyuk, O. V; Heckel, C. M.; Tsogoeva, S. B. Bifunctional Primary Amine-Thioureas in Asymmetric Organocatalysis. *Org. Biomol. Chem.* **2013**, *11* (41), 7051–7071.

(2) Madarász, Á.; Dósa, Z.; Varga, S.; Soós, T.; Csámpai, A.; Pápai, I. Thiourea Derivatives as Brønsted Acid Organocatalysts. *ACS Catal.* **2016**, *6* (7), 4379–4387.

(3) Siau, W. Y.; Wang, J. Asymmetric Organocatalytic Reactions by Bifunctional Amine-Thioureas. *Catal. Sci. Technol.* **2011**, *1* (8), 1298–1310.

(4) Okino, T.; Hoashi, Y.; Takemoto, Y. Enantioselective Michael Reaction of Malonates to Nitroolefins Catalyzed by Bifunctional Organocatalysts. *J. Am. Chem. Soc.* **2003**, *125* (42), 12672–12673.

(5) Okino, T.; Hoashi, Y.; Furukawa, T.; Xu, X.; Takemoto, Y. Enantio-and Diastereoselective Michael Reaction of 1,3-Dicarbonyl Compounds to Nitroolefins Catalyzed by a Bifunctional Thiourea. *J. Am. Chem. Soc.* **2005**, *127* (1), 119–125.

(6) Hamza, A.; Schubert, G.; Soós, T.; Pápai, I. Theoretical Studies on the Bifunctionality of Chiral Thiourea-Based Organocatalysts: Competing Routes to C-C Bond Formation. *J. Am. Chem. Soc.* **2006**, *128* (40), 13151–13160.

(7) Gavin, D. P.; Stephens, J. C. Organocatalytic Enantioselective Michael Addition of β-Diketones to β-Nitrostyrene: The First Michael Addition of Dipivaloylmethane to an Activated Olefin. *ARKIVOC* **2011**, No. 9, 407–421.

(8) Snyder, L. R.; Dolan, J. W. *High-Performance Gradient Elution: The Practical Application of the Linear-Solvent-Strength Model*; John Wiley & Sons, **2007**.

(9) Pansare, S. V; Lingampally, R. Synthesis and Evaluation of Guanidinyl Pyrrolidines as Bifunctional Catalysts for Enantioselective Conjugate Additions

to Cyclic Enones. *Org. Biomol. Chem.* **2009**, *7* (2), 319–324.

(10) Rodriguez, A. A.; Yoo, H.; Ziller, J. W.; Shea, K. J. New Architectures in Hydrogen-Bond Catalysis. *Tetrahedron Lett.* **2009**, *50* (49), 6830–6833.

(11) Rabalakos, C.; Wulff, W. D. Enantioselective Organocatalytic Direct Michael Addition of Nitroalkanes to Nitroalkenes Promoted by a Unique Bifunctional DMAP-Thiourea. *J. Am. Chem. Soc.* **2008**, *130* (41), 13524–13525.

(12) Takemoto, Y. Recognition and Activation by Ureas and Thioureas: Stereoselective Reactions Using Ureas and Thioureas as Hydrogen-Bonding Donors. *Org. Biomol. Chem.* **2005**, *3* (24), 4299–4306.

(13) Long, S. Opioids as Enantioselective Organocatalysts, PhD Thesis, Dublin City University, Ireland, **2012**.

Chapter 4 Experimental

4.1 Chemicals and instruments

Chemicals:

Toluene-4-sulfonyl chloride, sodium azide, potassium thiocyanate, diethyl carbonate, diethyl malonate, *trans*-β-nitrostyrene, lithium aluminium hydride solution (1.0 M in THF), potassium *tert*-butoxide, 1,5,7-triazabicyclo[4.4.0]dec-5-ene (TBD) and 1-[3,5-bis(trifluoromethyl)phenyl]-3-[(1*R*,2*R*)-(−)-2(dimethylamino)cyclohexyl]-thiourea (Takemoto catalyst) were purchased from Sigma Aldrich. Merck silica gel (pore size 60 Å, 220-440 mesh, 35-75 μm) was used for flash chromatography. All solvents used were distilled and dried over molecular sieves (3 Å and 4 Å) before use.

NMR Analysis:

All NMR analysis was carried out on a Bruker 400 MHz spectrometer, operating at 400 MHz for ^{1}H NMR and 100 MHz for ^{13}C NMR or on a Bruker 600 MHz spectrometer, operating at 600 MHz for ^{1}H NMR and 150 MHz for ^{13}C NMR. All spectra were recorded in deuterated chloroform ($CDCl_3$) or DMSO-d_6. Chemical shifts are reported in parts per million (ppm) and coupling constants (J) are measured in Hertz (Hz).When stating multiplicity of peaks in NMR the following abbreviations are used: s: singlet; d: doublet; t: triplet; q: quartet; dd: doublet of doublets; dt: doublet of triplets; td: triplet of doublets; m: multiplet; br: broad.

FT-IR analysis:

All IR analysis was performed by a Perkin Elmer 100 FT-IR spectrometer with ATR. Weak (w), medium (m), strong (s), narrow (n), very strong (vs), broad (b) and sharp (sh) are used to describe the appearance and intensities absorption bands.

Melting point:

All melting points were determined using a Griffin melting point apparatus and values are expressed in degrees Celsius (ºC).

Chiral HPLC:

Percent enantiomeric excess was determined by Waters HPLC Automated System and a Phenomenex HPLC chiral column (Lux 5 μm, cellulose-2, 250 x 4.60 mm). Mobile phase: Hexane/Isopropanol=90/10; λ=254 nm; flow rate: 1.0 mL/min.

Optical Rotation:

All optical rotation measurements were carried out on a Perkin Elmer 343 Polarimeter in chloroform at 20 ºC.

4.2 Preparation of opioid derivatives

6-*O*-Tosylcodeine (1)

(4*R*,4a*R*,7a*R*,12b*S*)-9-Methoxy-3-methyl-2,3,4,4a,7,7a-hexahydro-1H-4,12-methanobenzofuro[3,2-e]isoquinlin-7-yl 4-methylbenzensulfonate (**1**)

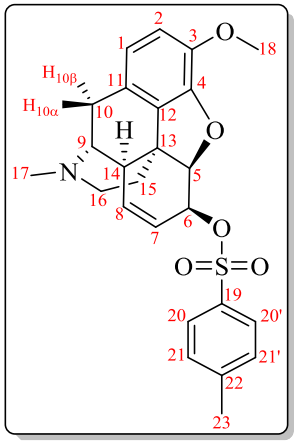

The procedure followed was according to the literature.[1,2] Codeine (6.00 g, 20.0 mmol) was dissolved in dry DCM (4 mL) and dry pyridine (5 mL) was added. Tosyl chloride (4.81 g, 25.2 mmol) in pyridine (5 mL) was added dropwise to the stirred codeine solution at 0 ºC. The reaction mixture was stirred for a further 2 h at this temperature and refrigerated for 24 h. It was then poured into a saturated aqueous $NaHCO_3$ solution (500 mL) and extracted with DCM (3 x 100 mL). The DCM solution was washed with deionized water (3 x 300 mL), dried with $MgSO_4$ and evaporated to dryness. The oily product was triturated with diethyl ether to give the title product (**1**) as red/pink crystals in 84% yield (7.61 g, 16.8 mmol).

Molecular formula: $C_{25}H_{27}NO_5S$

Molecular weight: 453.55 g/mol.

m.p.: 126 ºC, **Lit. m.p.**: 121 ─ 125 ºC.[2]

$[\alpha]^{20}_D$: −213.0 (1.0 c, $CHCl_3$), **Lit. $[\alpha]^{20}_D$**: −209.0 (0.99 c, dioxane).[2]

IRν_{max} (neat): 2945 (w), 1598 (m), 1498 (m, sh), 1440 (m), 1359 (s, sh), 1174 (s, sh), 973 (s, sh), 866 (vs, sh), 650 (vs, sh). IR spectrum is in agreement with the literature.[3]

^{1}H NMR (400 MHz, $CDCl_3$) δ ppm 7.82 (2H, d, *J* = 8.2 Hz, H20, H20'), 7.28 (2H, d, *J* = 8.2 Hz, H21, H21'), 6.56 (1H, d, *J* = 8.2 Hz, H2), 6.44 (1H, d, *J* = 8.2 Hz, H1), 5.50 (1H, br d, *J* = 9.9 Hz, H7), 5.30 (1H, dt, *J* = 10.0, 2.7 Hz, H8), 4.88 ─ 4.84 (1H, m, H6), 4.79 (1H, dd, *J* = 6.2, 1.2 Hz, H5), 3.76 (3H, s, H18), 3.27 (1H, dd, *J* = 3.1, 2.5 Hz, H9),

2.95 (1H, d, *J* = 18.5 Hz, H10β), 2.58 (1H, br t, *J* = 2.5 Hz, H14), 2.49 (1H, dd, *J* = 8.4, 4.2 Hz, H16a), 2.38 (3H, s, H17), 2.35 (3H, s, H23), 2.30 (1H, td, *J* = 8.5, 3.2 Hz, H16b), 2.20 (1H, dd, *J* =12.4, 6.5 Hz, H10α), 1.92 (1H, td, *J* = 7.7, 5.0 Hz, H15a), 1.77 (1H, m, H15b).

^{13}C NMR (100 MHz, $CDCl_3$) δ ppm 147.0 (C4), 144.9 (C22), 142.1 (C3), 133.7 (C19), 130.9 (C8), 130.4 (C12), 129.8 (C21, C21'), 128.1 (C20, C20'), 127.5 (C7), 126.9 (C11), 119.4 (C1), 114.6 (C2), 89.1 (C5), 74.4 (C6), 58.8 (C9), 57.0 (C18), 46.3 (C16), 43.3 (C13), 43.1 (C17), 40.9 (C14), 35.5 (C15), 21.7 (C23), 20.4 (C10). ^{1}H and ^{13}C NMR spectra are in agreement with the literature.[3]

8-Isothiocyanocodide (2)

(4*R*,4a*R*,5*S*,7a*S*,12b*S*)-5-Isothiocyanato-9-methoxy-3-methyl-2,3,4,4a,5,7a-hexahydro-1H-4,12-methanobenzofuro[3,2-e]isoquinoline (**2**)

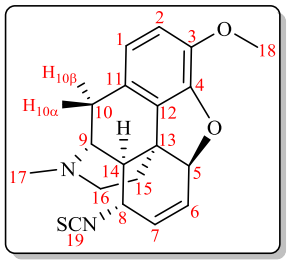

The procedure was followed as per a previously established method.[3] 6-*O*-tosylcodeine (**1**) (3.06 g, 6.75 mmol) and potassium thiocyanate (1.31 g, 13.5 mmol) were dissolved in dry acetone (50 mL). The reaction was refluxed at 56 ºC for 4 h. After cooling, the reaction mixture was filtered and the solvent was removed. The residue was purified by flash column chromatography (SiO_2, DCM: MeOH: NH_4OH = 98:1:1). The column purified material was triturated with hexane to give a white solid (**2**) in 61% yield (1.40 g, 4.11 mmol).

Molecular formula: $C_{19}H_{20}N_2O_2S$.

Molecular weight: 340.44 g/mol.

m.p.: 108 ─ 110 ºC, **Lit. m.p.**: 109 ─ 111 ºC.[3]

$[\alpha]^{20}_D$: +145.1 (1.0 c, $CHCl_3$), **Lit. $[\alpha]^{20}_D$**: +151.7 (0.5 c, $CHCl_3$).[3]

IRν_{max} (neat): 2925 (m, sh), 2911 (m), 2788 (w), 2163 (m), 2115 (m, br), 1606 (w), 1500 (s, sh), 1275 (s, sh), 1156 (s, sh), 1076 (s, sh), 1029 (s, sh), 887 (vs, sh). IR spectrum is in agreement with the literature.[3]

^{1}H NMR (400 MHz, $CDCl_3$) δ ppm 6.64 (1H, d, *J* = 8.2 Hz, H2), 6.58 (1H, d, *J* = 8.2

Hz, H1), 5.80 ─ 5.71 (2H, m, H7, H6), 4.93 ─ 4.88 (1H, m, H5), 3.77 (3H, s, H18), 3.72 (1H, d, *J* = 10.5 Hz, H8), 3.42 (1H, dd, *J* = 3.2, 2.7 Hz, H9), 3.04 (1H, d, *J* = 19.1 Hz, H10β), 2.51 ─ 2.44 (2H, m, H14, H16a), 2.42 ─ 2.34 (4H, m, H17, H10α), 2.20 (1H, td, *J* = 8.6, 3.6 Hz, H16b), 1.87 (1H, td, *J* = 7.4, 5.1 Hz, H15a), 1.75 (1H, dd, *J* = 7.2, 1.7 Hz, H15b).

^{13}C NMR (100 MHz, $CDCl_3$) δ ppm 144.4 (C4), 143.4 (C3), 135.0 (C19), 133.3 (C12), 131.5 (C6/C7), 128.2 (C11), 126.3 (C6/C7), 119.3 (C1), 113.6 (C2), 86.2 (C5), 56.3 (C18), 56.2 (C9), 53.1 (C8), 46.8 (C14/C16), 46.5 (C14/C16), 43.2 (C17), 40.9 (C13), 35.3 (C15), 19.7 (C10).^{1}H and ^{13}C NMR spectra are in agreement with the literature.[3]

8-Azidocodide (3)

(4*R*,4a*R*,5*S*,7a*S*,12b*S*)-5-Azido-9-methoxy-3-methyl-2,3,4,4a,5,7a-hexahydro-1H-4,12-methanobenzofuro[3,2-e]isoquinoline (**3**)

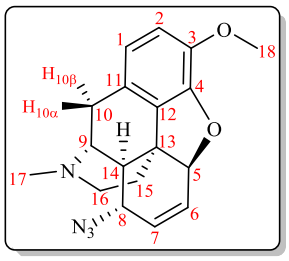

The procedure was followed according to the literature.[4] 6-*O*-tosylcodeine (**1**) (3.00 g, 6.61 mmol) and sodium azide (0.86 g, 13.2 mmol) were dissolved in DMF (10 mL). The reaction was refluxed at 90 ºC for 3 h. After cooling, the precipitate was formed by adding water (200 mL). The mixture was extracted with diethyl ether (3 x 100 mL). The ether phase was washed with brine (100 mL) and dried with $MgSO_4$. After removal of ether, recrystallization from acetone to give a pale yellow crystalline solid (**3**) in 64% yield (1.37 g, 4.22 mmol).

Molecular formula: $C_{18}H_{20}N_4O_2$

Molecular weight: 324.38 g/mol.

m.p.: 135 ─ 138 ºC, **Lit. m.p.**: 138 ─ 139 ºC.[3]

$[\alpha]^{20}_D$: −19.7 (1.0 c, $CHCl_3$), **Lit. $[\alpha]^{20}_D$**: −18.6 (1.1 c, $CHCl_3$).[3]

IRν_{max} (neat): 2927 (w, sh), 2802 (w, sh), 2098 (m, sh), 1601 (w), 1505 (s, sh), 1448 (s, sh), 1276 (vs, sh), 1156 (s, sh), 1015 (s, sh), 905 (vs, sh), 891 (s, sh), 784 (s, sh). IR spectrum is in agreement with the literature.[3]

^{1}H NMR (400 MHz, $CDCl_3$) δ ppm 6.64 (1H, d, *J* = 8.2 Hz, H2), 6.57 (1H, d, *J* = 8.2

Hz, H1), 5.87 ─ 5.74 (2H, m, H7, H6), 4.95 ─ 4.85 (1H, m, H5), 3.77 (3H, s, H18), 3.42 (1H, dd, *J* = 3.2, 2.7 Hz, H9), 3.21 (1H, d, *J* = 10.2 Hz, H8), 3.02 (1H, d, *J* = 18.8 Hz, H10β), 2.51 ─ 2.44 (1H, dd, *J* = 8.3, 3.8 Hz, H16a), 2.42 ─ 2.32 (4H, m, H17, H10α), 2.28 (1H, dd, *J* = 7.4, 2.8 Hz, H14), 2.18 (1H, td, *J* = 8.4, 3.7 Hz, H16b), 1.87 (1H, td, *J* = 7.4, 5.0 Hz, H15a), 1.74 (1H, m, H15b).

^{13}C NMR (100 MHz, $CDCl_3$) δ ppm 143.1 (C4), 142.3 (C3), 130.5 (C6/C7), 127.8 (C12), 126.2 (C6/C7), 125.8 (C11), 118.1 (C1), 112.3 (C2), 85.4 (C5), 55.5 (C18), 55.3 (C9), 55.1 (C8), 45.6 (C16), 44.4 (C14), 42.2 (C17), 39.8 (C13), 34.2 (C15), 18.8 (C10).

^{1}H and ^{13}C NMR spectra are in agreement with the literature.[3]

8-Aminocodide (4)

(4*R*,4a*S*,5*S*,7a*S*,12b*S*)-9-Methoxy-3-methyl-2,3,4,4a,5,7a-hexahydro-1H-4,12-methanobenzofuro[3,2-e]isoquinolin-5-amine (**4**)

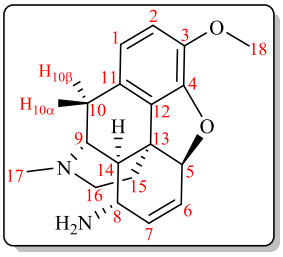

8-Azidocodide (**3**) (1.00 g, 3.08 mmol) was dissolved in dry THF (4 mL) and added dropwise to a $LiAlH_4$ solution in THF (12.3 mL, 1.0 M) under an N_2 atmosphere. The reaction was refluxed for 3 h. After cooling, the reaction was quenched by slow addition of aqueous THF (50 mL) and ice water (50 mL) over an ice bath, and then the resultant alumina solid was removed by filtration. After removal of THF, the reaction solution was extracted with chloroform (3 x 100 mL) and dried over $MgSO_4$. Solvent was removed and the residue was purified by flash column chromatography (SiO_2, DCM : MeOH : NH_4OH = 94:5:1) to give an oily compound (**4**) in 46% yield (0.42 g, 1.41 mmol).[3]

Molecular formula: $C_{18}H_{22}N_2O_2$

Molecular weight: 298.39 g/mol.

m.p.: 126 ─ 129 ºC, **Lit. m.p.**: 128 ─ 129 ºC.[5]

$[\alpha]^{20}_D$: −75.5 (1.0 c, $CHCl_3$), **Lit. $[\alpha]^{20}_D$**: −79.2 (0.5 c, EtOH).[5]

IRν_{max} (neat): 3353 (w, br), 2921 (m, br), 2837 (w), 2567 (w), 2073 (w, br), 1603 (w), 1506 (s), 1450 (s), 1440 (s), 1277 (vs, sh), 1189 (m), 1161 (m), 1140 (m), 1102 (m), 1089 (m), 1069 (vs, sh), 1019 (s), 905 (vs, sh), 855 (s, sh), 804 (s, sh). IR spectrum is in agreement with the literature.[3]

^{1}H NMR (400 MHz, $CDCl_3$) δ ppm 6.63 (1H, d, *J* = 8.2 Hz, H2), 6.55 (1H, d, *J* = 8.2 Hz, H1), 5.67 (1H, dd, *J* = 8.9, 1.5 Hz, H7), 5.60 (1H, dt, *J* = 10.1, 4.4 Hz, H6), 4.90 (1H, dd, *J* = 3.9, 1.9 Hz, H5), 3.78 (3H, s, H18), 3.51 (1H, dd, *J* = 3.2, 2.7 Hz, H9), 3.00 (1H, d, *J* = 18.2 Hz, H10β), 3.21 (1H, dd, *J* = 7.9, 1.9 Hz, H8), 2.43 (1H, dd, *J* = 10.1, 3.5 Hz, H16a), 2.42 ─ 2.33 (4H, m, H17, H10α), 2.22 (1H, td, *J* = 8.2, 3.8 Hz, H16b), 1.96 (1H, dd, *J* = 9.9, 2.9 Hz, H14), 1.84 (1H, td, *J* = 7.4, 4.9 Hz, H15a), 1.75 (1H, dd, *J* = 6.8, 2.0 Hz, H15b), 1.18 (2H, br s, NH_2).

^{13}C NMR (100 MHz, $CDCl_3$) δ ppm 144.3 (C4), 143.2 (C3), 139.5 (C7), 129.8 (C12), 127.3 (C11), 123.7 (C6), 118.8 (C1), 112.9 (C2), 87.5 (C5), 56.3 (C18), 56.2 (C9), 49.4 (C14), 46.9 (C16), 46.3 (C8), 43.2 (C17), 41.09 (C13), 35.6 (C15), 19.8 (C10).^{1}H and ^{13}C NMR spectra are in agreement with the literature.[3]

***N,N'*-disubstituted thiourea (5)**

1,3-Bis[(4*R*,4a*S*,5*S*,7a*S*,12b*S*)-9-methoxy-3-methyl-2,3,4,4a,5,7a-hexahydro-1H-4,12-methanobenzofuro[3,2-e]isoquinolin-5-yl]thiourea (**5**)

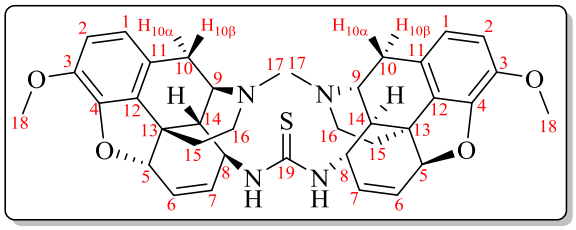

A mixture of 8-isothiocyanocodide (**2**) (0.39 g, 1.15 mmol) and 8-aminocodide (**4**) (0.34 g, 1.15 mmol) was stirred in dry THF (8 mL) and heated under reflux conditions for 24 h. After removal of the solvent, the residue was purified by column chromatography (SiO_2, DCM : MeOH : NH_4OH = 96:3:1) to give a white solid after drying (**5**) in 44% yield (0.32 g, 0.50 mmol).[3]

Molecular formula: $C_{37}H_{42}N_4O_4S$

Molecular weight: 638.83 g/mol.

m.p.: 226 ─ 230 ºC.

$[\alpha]^{20}_{D}$: −61.01 (1.0 c, $CHCl_3$).

MS (ESI) calculated for $[M+H]^+$, $C_{37}H_{42}N_4O_4S^+$ requires 639.2900, found 639.2977.

IRν_{max} (neat): 3351 (w, br), 2908 (m, br), 2837 (w), 1636 (w), 1606 (w), 1527 (s), 1502 (vs, sh), 1439 (m, br), 1247 (vs), 1155 (vs, sh), 1096 (s), 984 (w), 938 (w), 889 (vs), 855

(s), 791 (s), 702 (s).

^{1}H NMR (600 MHz, DMSO-d$_6$) δ ppm 7.50 (1H, br s, NH), 6.74 (1H, d, *J* = 8.2 Hz, H2), 6.63 (1H, d, *J* = 8.2 Hz, H1), 5.66 (2H, s, H7, H6), 4.98 (1H, d, *J* = 1.9 Hz, H5), 4.48 (1H, br s, H8), 3.74 (3H, s, H18), 3.10 (1H, dd, *J* = 3.2, 2.7 Hz, H9), 2.91 (1H, d, *J* = 18.5 Hz, H10β), 2.64 (1H, dd, *J* = 12.8, 5.4 Hz, H10α), 2.43 (1H, dd, *J* = 9.3, 4.3 Hz, H16a), 2.28 (3H, s, H17), 2.18 (1H, dd, *J* = 9.8, 2.5 Hz, H14), 2.09 (1H, td, *J* = 9.3, 2.9 Hz, H16b), 1.86 (1H, td, *J* =7.6, 4.8 Hz, H15a), 1.60 (1H, d, *J* = 11.2 Hz, H15b).
^{13}C NMR (150 MHz, DMSO-d$_6$) δ ppm 183.2 (C19), 143.9 (C4), 142.5 (C3), 135.3 (C6/C7), 129.1 (C12), 127.4 (C11), 124.8 (C6/C7), 118.8 (C1), 113.6 (C2), 85.9 (C5), 55.9 (C18), 55.5 (C9), 48.8 (C8), 46.2 (C16), 45.4 (C14), 42.8 (C17), 40.4 (C13), 34.8 (C15), 20.0 (C10).

***N,N'*-disubstituted urea (6)**

1,3-Bis[(4*R*,4a*S*,5*S*,7a*S*,12b*S*)-9-methoxy-3-methyl-2,3,4,4a,5,7a-hexahydro-1H-4,12-methanobenzofuro[3,2-e]isoquinolin-5-yl]urea (**6**)

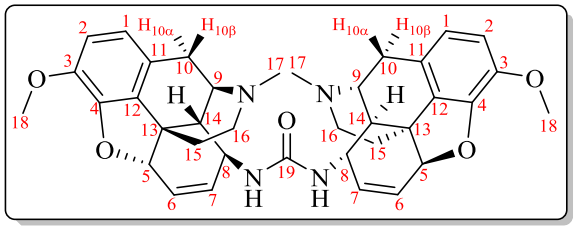

A solution of 8-aminocodide (**6**) (0.39 g, 1.30 mmol) and TEA (0.55 mL, 3.92 mmol) in dry DCM (2 mL) was added dropwise to a solution of triphosgene (0.14 g, 0.46 mmol) in dry DCM (0.5 mL) at 0 ºC under an N_2 atmosphere . After 1 h of stirring at 0 ºC, the addition of the second portion of 8-aminocodide (**6**) (0.39 g, 1.30 mmol) in DCM (2 mL) was added slowly into the flask and the mixture was further stirred at room temperature for 72 h. The reaction mixture was washed with a saturated aqueous $NaHCO_3$ solution (10 mL) and the organic layer was dried with $MgSO_4$ and concentrated. The crude product was purified by column chromatography (SiO_2, DCM: MeOH: NH_4OH = 96:3:1) to give a white solid (**8**) in 28% yield (0.23 g, 0.37 mmol).[6,7]

Molecular formula: $C_{37}H_{42}N_4O_5$
Molecular weight: 622.77 g/mol.
m.p.: 235 ─ 239.9 ºC.

[α]$^{20}_{D}$: −11.7 (1.0 c, $CHCl_3$).

MS (ESI) calculated for $[M+H]^+$, $C_{37}H_{42}N_4O_5^+$ requires 623.3200, found 623.3202.

IRν_{max} (neat): 3372 (w, br), 2923 (m, br), 2837 (w), 1700 (w, br), 1635 (m), 1605 (w), 1538 (s), 1501 (vs, sh), 1439 (vs, sh), 1275 (vs, sh), 1248 (s, sh), 1155 (s, sh), 1037 (vs, sh), 901 (vs ,sh), 857 (s), 790 (s), 751 (s), 732 (s).

^{1}H NMR (600 MHz, DMSO-d$_6$) δ ppm 6.72 (1H, d, *J* = 8.2 Hz, H2), 6.61 (1H, d, *J* = 8.2 Hz, H1), 6.03 (1H, d, *J* = 9.4 Hz, NH), 5.63 (2H, m, H7, H6), 4.96 (1H, d, *J* = 1.9Hz, H5), 3.73 (3H, s, H18), 3.62 (1H, dt, *J* = 9.6 Hz, H8), 3.09 (1H, dd, *J* = 3.2, 2.7 Hz, H9), 2.85 (1H, d, *J* = 18.5 Hz, H10β), 2.46 (1H, dd, *J* = 12.5, 6.1 Hz, H10α), 2.40 (1H, dd, *J* = 7.6, 4.2 Hz, H16a), 2.25 (3H, s, H17), 2.06 (2H, m, H14, H16b), 1.82 (1H, td, *J* = 7.5, 5.0 Hz, H15a), 1.57 (1H, d, *J* = 11.0 Hz, H15b).

^{13}C NMR (150 MHz, DMSO-d$_6$) δ ppm 158.4 (C19), 144.5 (C4), 143.0 (C3), 137.2 (C6/C7), 129.8 (C12), 128.2 (C11), 125.2 (C6/C7), 119.2 (C1), 114.2 (C2), 86.7 (C5), 56.5 (C18), 56.0 (C9), 46.9 (C14), 46.7 (C16), 44.8 (C8), 43.3 (C17), 41.0 (C13), 35.4 (C15), 19.9 (C10).

α-Chlorocodide (7)

(4*R*,4a*R*,7*R*,7a*R*,12b*S*)-7-Chloro-9-methoxy-3-methyl-2,3,4,4a,7,7a-hexahydro-1H-4,12-methanobenzofuro[3,2-e]isoquinoline (**7**)

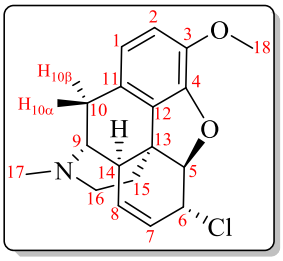

Method 1: $SOCl_2$ (2.74 mL, 37.8 mmol) was added to a solution of codeine (1.13 g, 3.77 mmol) in dry DCM (3 mL). The solution was stirred for 1 h at 0 ºC. The reaction solution was quenched with H_2O (10 mL) and then made alkaline (pH approx. 8) with a saturated aqueous $NaHCO_3$ solution. The aqueous mixture was extracted with diethyl ether (3 x 20 mL) and the organic extracts were washed with water (3 x 20 mL). The ether layer was reduced down and the resultant solid was collected and washed with a small amount of cold ethanol to remove trace impurities and dried, giving a white solid (**7**) in 86% yield (1.03 g, 3.24 mmol).[8,9]

Method 2: To a stirred solution of codeine (0.30 g, 1.00 mmol) and pyridine (3 mL) in Schlenk tube under an N_2 atmosphere (1 atm) at 0 ºC. $POCl_3$ (0.05 mL, 0.50 mmol) was

added dropwise. The solution stirred at room temperature for 6 h. H_2O (10 mL) was then added and the mixture was stirred at room temperature for 2 h. The reaction solution was then extracted with DCM (3 x 30 mL) and the organic layer was washed with deionised water (3 x 30mL). The organic layer was dried over $MgSO_4$ before being reduced down. The resultant oily product was triturated with diethyl ether to give a white solid in 88% yield (0.28 g, 0.88 mmol).

Molecular formula: $C_{18}H_{20}ClNO_2$
Molecular weight: 317.81 g/mol.
m.p.: 150 ─ 153 ºC, **Lit. m.p.**: 149 ─ 151 ºC.[10]
$[\alpha]^{20}_D$: −363.8 (1.0 c, $CHCl_3$), **Lit. $[\alpha]^{20}_D$**: −381.1 (0.78 c, $CHCl_3$).[11]

IRν_{max} (neat): 2935 (w), 2911 (w), 1636 (w), 1605 (m), 1503 (s), 1498 (m, sh), 1450 (m), 1331 (m, sh), 1275 (s, sh), 1153 (s, sh), 1057 (s, sh), 935 (s, h), 803 (vs, sh), 757 (vs, sh), 738 (vs, sh).

^{1}H NMR (400 MHz, $CDCl_3$) δ ppm 6.69 (1H, d, *J* = 8.2 Hz, H2), 6.59 (1H, d, *J* = 8.2 Hz, H1), 6.00 (1H, m, H7), 5.69 (1H, d, *J* = 9.8 Hz, H8), 5.05 (1H, dd, *J* = 6.2, 1.2 Hz, H5), 4.55 (1H, dt, *J* = 9.8, 2.6 Hz, H6), 3.85 (3H, s, H18), 3.39 (1H, dd, *J* = 3.2, 2.4 Hz, H9), 3.17 (1H, br t, *J* = 2.6 Hz, H14), 3.09 (1H, d, *J* = 18.6 Hz, H10β), 2.62 (1H, dd, *J* = 8.2, 4.1 Hz H16a), 2.45 (3H, s, H17), 2.40 (1H, td, *J* = 8.7, 3.5 Hz, H16b), 2.35 (1H, dd, *J* =12.4, 6.5 Hz, H10α), 2.19 (1H, td, *J* = 7.4, 5.0 Hz, H15a),1.88 (1H, m, H15b).
^{13}C NMR (100 MHz, $CDCl_3$) δ ppm 145.8 (C4), 141.9 (C3), 135.3 (C8), 130.1 (C12), 128.7 (C7), 127.4 (C11), 119.3 (C1), 112.9 (C2), 93.9 (C5), 58.7 (C9), 56.3 (C18), 53.9 (C6), 46.7 (C16), 44.5 (C13), 43.2 (C17), 40.0 (C14), 36.3 (C15), 20.3 (C10).
^{1}H and ^{13}C NMR spectra are in agreement with the literature.[9]

β-Bromocodide (8)

(4*R*,4a*R*,5*S*,7a*S*,12b*S*)-5-Bromo-9-methoxy-3-methyl-2,3,4,4a,5,7a-hexahydro-1H-4,12-methanobenzofuro[3,2-e]isoquinoline (**8**)

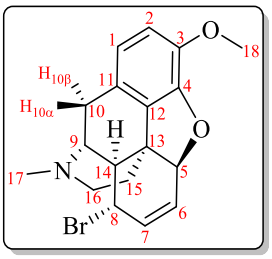

A mixture of 6-*O*-tosylcodeine (**1**) (2.27 g, 5.00 mmol) and lithium bromide (2.82 g, 32.5 mmol) was stirred in dry acetone (10 mL) at reflux for 3 h. Water (200 mL) was poured into the reaction solution and extracted with toluene (3 x 100 mL). After removal of toluene, the residue was recrystallized in ethanol and dried to give a white solid (**8**) in 80% yield (1.45 g, 4.00 mmol).[11]

Molecular formula: $C_{18}H_{20}BrNO_2$

Molecular weight: 362.27 g/mol.

m.p.: 158 ─ 160 ºC, **Lit. m.p.**: 156─159 ºC.[12]

[α]$^{20}_{D}$: +50.2 (1.0 c, $CHCl_3$), **Lit. [α]$^{20}_{D}$**: +47.6 (1.4 c, $CHCl_3$: EtOH = 9:1).[12]

IRν_{max} (neat): 2931 (w, br), 2795 (w, br), 1636 (w), 1605 (w), 1503 (s), 1450 (s), 1275 (vs, sh), 1153 (m), 1057 (s), 1029 (m), 935 (s, sh), 803 (vs, sh), 757 (vs, sh), 738 (s, sh), 687 (m).

^{1}H NMR (400 MHz, $CDCl_3$) δ ppm 6.73 (1H, d, *J* = 8.2 Hz, H2), 6.66 (1H, d, *J* = 8.2 Hz, H1), 6.00 (1H, dt, *J* = 8.04, 1.2 Hz, H7), 5.69 (1H, dt, *J* = 8.04, 2.8 Hz, H6), 5.05 (1H, m, H5), 4.14 (1H, dd, *J* = 8.04, 2.0 Hz, H8), 3.86 (3H, s, H18), 3.58 (1H, dd, *J* = 6.5, 2.5 Hz, H9), 3.09 (1H, d, *J* = 18.75 Hz, H10β), 2.73 (1H, dd, *J* = 7.1, 2.8 Hz, H14), 2.55 (1H, dd, *J* = 8.6, 3.8 Hz, H16a), 2.50 ─ 2.42 (4H, m, H17, H10α), 2.29 (1H, td, *J* = 8.6, 3.6 Hz, H16b), 1.95 (1H, td, *J* = 7.4, 5.0 Hz, H15a), 1.75 (1H, td, *J* = 7.4, 1.8 Hz, H15b).

^{13}C NMR (100 MHz, $CDCl_3$) δ ppm 144.0 (C4), 143.4 (C3), 135.4 (C7), 128.4 (C12), 126.8 (C11), 125.7 (C6), 119.2 (C1), 113.4 (C2), 86.4 (C5), 57.0 (C9), 56.3 (C18), 49.2 (C14), 47.1 (C8), 46.7 (C16), 43.2 (C17), 42.8 (C13), 35.3 (C15), 19.5 (C10).

^{1}H and ^{13}C NMR spectra are in agreement with the literature.[13]

4.3 Study of Michael addition reaction

General procedure

The procedure was followed according to the literature[14] and the enantiomeric excess was determined and compared to the literature value.[14]

Catalysis reaction using the Takemoto catalyst

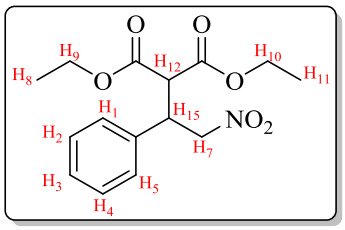

To a stirred solution of *trans*-β-nitrostyrene (29.8 mg, 0.20 mmol) and diethyl malonate (2.0 eq., 0.06 mL, 0.40 mmol) in dry toluene (0.40 mL) under an N_2 atmosphere, Takemoto (thiourea) catalyst (**42**) (0.1 eq., 8.3 mg, 0.02 mmol) was added. The reaction was monitored after 6 h and 24 h and conversion was calculated by NMR analysis. The residue was purified by flash chromatography (Ethyl acetate : Hexane = 1:12 to 1:5) to afford the conjugate addition product: (*R*)-diethyl 2-(2-nitro-1-phenylethyl) malonate (**9**) in 90.8 % yield (56.2 mg, 0.18 mmol). HPLC retention time of the two isomers of product (**9**): S_{minor}= 12.90 min, R_{major}=16.69 min, 91.6 % *ee*.[14]

Catalysis reaction using *N,N'*-disubstituted thiourea catalyst (5)

To a stirred solution of *trans*-β-nitrostyrene (29.8 mg, 0.20 mmol) and diethyl malonate (2.0 equiv., 0.06 mL, 0.40 mmol) in dry selected solvent (0.40 mL) under an N_2 atmosphere, *N,N'*-disubstituted thiourea catalyst (0.1eq., 12.8 mg, 0.02 mmol) was added. The reaction was monitored after 6 h and 24 h and conversion was calculated by NMR analysis. The residue was purified by flash chromatography (Ethyl acetate : Hexane = 1:12 to 1:5) to afford conjugate addition product: (*S*)-diethyl 2-(2-nitro-1-phenylethyl) malonate (**9**) in 74.3 % (45.9 mg, 0.15 mmol) ─ 89.8 % (55.6 mg, 0.18 mmol) and 0 % ─ 9.6 % *ee* (Table 3.1). HPLC retention times of peaks of two isomers are shown in Appendix B and listed in Table 3.4. The corresponding racemic product was synthesised using potassium tert-butoxide (KOtBu 5 mol%) in dry toluene (0.40 mL) according to a literature method.[15]

Table 4.1 Retention time of isomeric product: diethyl 2-(2-nitro-1-phenylethyl) malonate (**9**) in selected dry solvents.

selected dry solvent	Retention time of two isomers of conjugate addition product (9)
Hexane	S_{major}= 12.5 min, R_{minor}= 16.2 min
Toluene	S_{major}= 12.6 min, R_{minor}= 17.0 min
THF	S_{major}= 12.6 min, R_{minor}= 16.4 min
DCM	S_{major}= 12.6 min, R_{minor}= 17.1 min
MeOH	S_{major}= 12.7 min, R_{minor}= 16.6 min
MeCN	S_{major}= 13.1 min, R_{minor}= 17.9 min

Diethyl 2-(2-nitro-1-phenylethyl) malonate (9)

^{1}H NMR (400 MHz, $CDCl_3$) δ ppm 7.36 ─ 7.18 (5H, m, H1 ─ H5), 4.97 ─ 4.80 (2H, m, H7), 4.30 ─ 4.14 (3H, m, H15, H10), 4.00 (2H, q, *J* = 7.2 Hz, H9), 3.81 (1H, d, *J* = 9.4 Hz, H12), 1.26 (3H, t, *J* = 7.3 Hz, H8), 1.04 (3H, t, *J* = 7.3 Hz, H11).

^{13}C NMR (100 MHz, $CDCl_3$) δ ppm 167.5 (C13), 166.8 (C14), 136.2 (C6), 129.0 (C2/C4), 128.4 (C3), 128.0 (C1/C5), 62.2 (C7), 61.9 (C9/C10), 54.9 (C12), 42.9 (C15), 13.9 (C8), 13.7 (C11). ^{1}H and ^{13}C NMR spectra are in agreement with the literature.[14]

4.4 References

(1) Berényi, S.; Makleit, S.; Szilágyi, L. Conversions of Tosyl and Mesyl Derivatives of the Morphine Group, XXIII: Preparation of New 6-Substituted-6-Demethoxythebaine Derivatives. *Acta Chim. Hung.* **1984**, *117* (3), 307–312.

(2) Rapoport, H.; Bonner, R. M. Δ7- and Δ8-Desoxycodeine. *J. Am. Chem. Soc.* **1951**, *73* (6), 2872–2876.

(3) Long, S. Opioids as Enantioselective Organocatalysts, PhD Thesis, Dublin City University, Ireland, **2012**.

(4) Bognár, R.; Mile, T.; Makleit, S.; Berényi, S. Conversions of Tosyl and Mesyl Derivatives of the Morphine Group, XII. 14-Hydroxi Derivatives of Morphine, III. Isothiocyanato Derivatives. *Acta Chim. Hung.* **1973**, *75* (3), 297–301.

(5) Small, L.; Palmer, F. S. The Aminomorphides and Aminocodides. *J. Am. Chem. Soc.* **1939**, *61* (8), 2186–2190.

(6) Majer, P.; Randad, R. S. A Safe and Efficient Method for Preparation of *N*,*N*'-Unsymmetrically Disubstituted Ureas Utilizing Triphosgene. *J. Org. Chem.* **1994**, *59* (7), 1937–1938.

(7) Zhang, Q.; You, Q.; Zhou, H.; Diao, Y. Safe and Efficient One-Pot Synthesis of Nitro-Containing Unsymmetrical Diaryl Ureas. *Chin. J. Pharm.* **2012**, *43* (4), 247–250.

(8) Small, L. F.; Cohen, F. L. Desoxycodeine Studies. I. the Desoxycodeines. *J. Am. Chem. Soc.* **1931**, *53* (6), 2214–2226.

(9) Erhard, T.; Ehrlich, G.; Metz, P. A Total Synthesis of (±)-Codeine by 1,3-Dipolar Cycloaddition. *Angew. Chem., Int. Ed.* **2011**, *50* (17), 3892–3894.

(10) Stork, G.; Clarke, F. H. The S_N2' Reaction. III. Structure and S_N2' Reactions of

the Halocodides. *J. Am. Chem. Soc.* **1956**, *78* (18), 4619–4624.

(11) Goto, K.; Yamamoto, I. The Three Isomers of (+)-Codeine and Some Codeimethines from Them. *Proc. Jpn. Acad.* **1959**, *35* (6), 472–475.

(12) Beyerman, H. C.; Crabbendam, P. R.; Lie, T. S.; Maat, L. Convenient Conversions of Codeine into 6-Demethoxythebaine *via* Bond Rearrangement (Chemistry of Opium Alkaloids, Part XVIII). *Recl. Trav. Chim. Pays-Bas* **1984**, *103* (4), 112–114.

(13) Cunningham, C. W.; Deschamps, J. R.; Coop, A. A One-Step Synthesis of β-Bromocodide from Codeine. *J. Pharm. Sci. Pharmacol.* **2014**, *1* (1), 54–56.

(14) Okino, T.; Hoashi, Y.; Furukawa, T.; Xu, X.; Takemoto, Y. Enantio-and Diastereoselective Michael Reaction of 1,3-Dicarbonyl Compounds to Nitroolefins Catalyzed by a Bifunctional Thiourea. *J. Am. Chem. Soc.* **2005**, *127* (1), 119–125.

(15) Gavin, D. P.; Stephens, J. C. Organocatalytic Enantioselective Michael Addition of β-Diketones to β-Nitrostyrene: The First Michael Addition of Dipivaloylmethane to an Activated Olefin. *ARKIVOC* **2011**, No. 9, 407–421.

Appendices

Appendix A: NMR Spectra

6-*O*-Tosylcodeine (1)

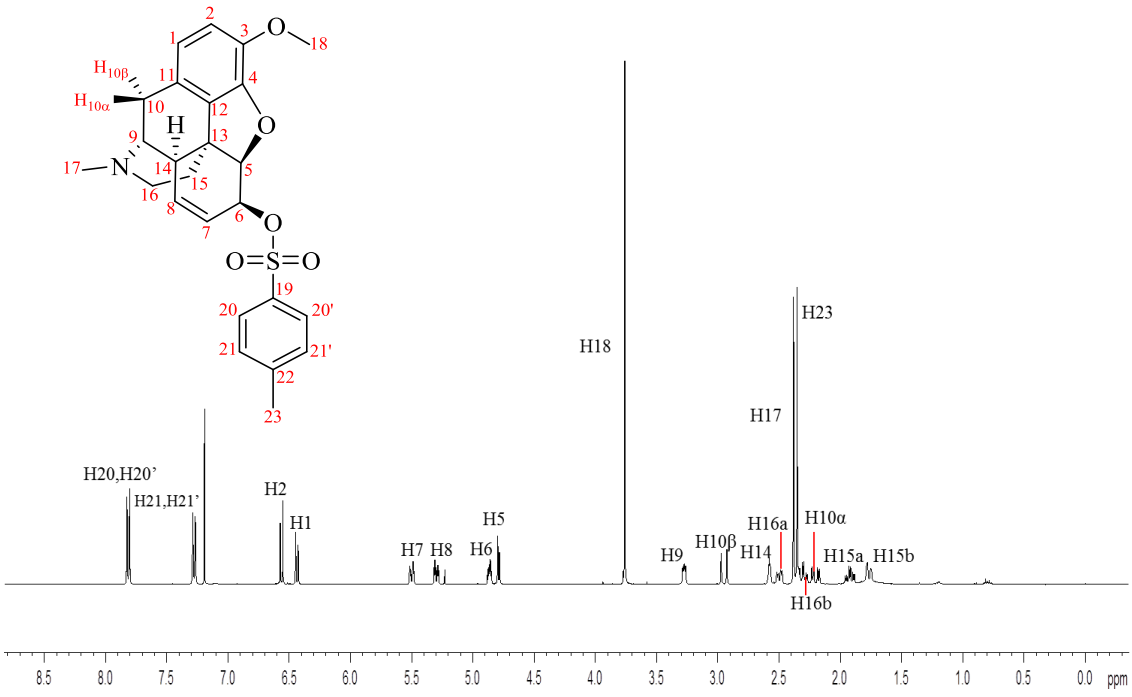

Fig. A1 ^{1}H NMR spectrum (400 MHz) of 6-*O*-tosylcodeine (**1**) in $CDCl_3$.

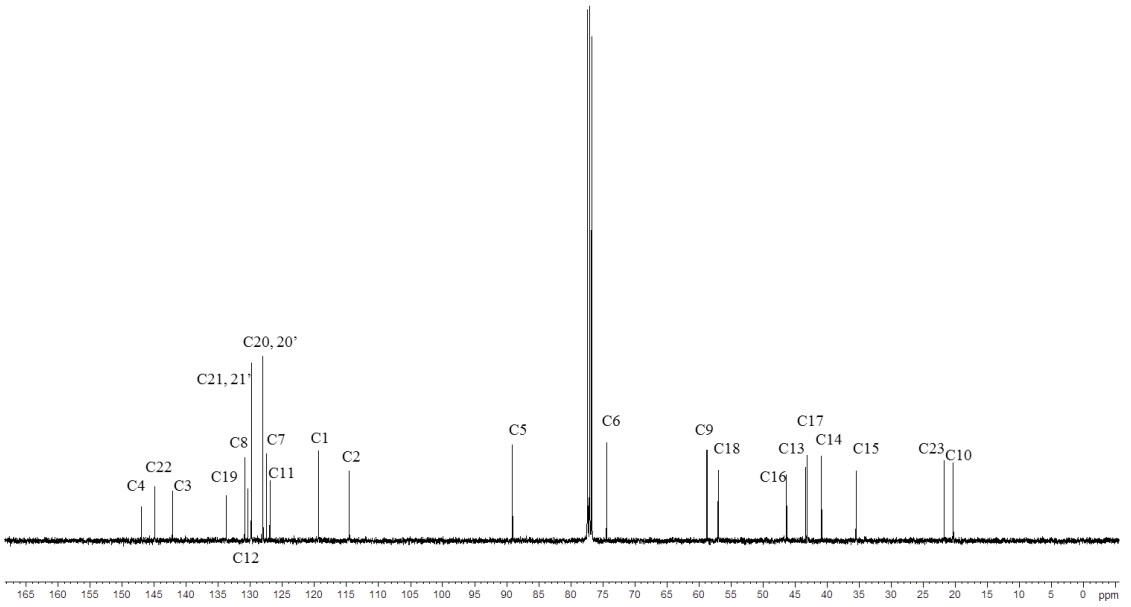

Fig. A2 ^{13}C NMR spectrum (100 MHz) of 6-*O*-tosylcodeine (**1**) in $CDCl_3$.

8-Isothiocyanocodide (2)

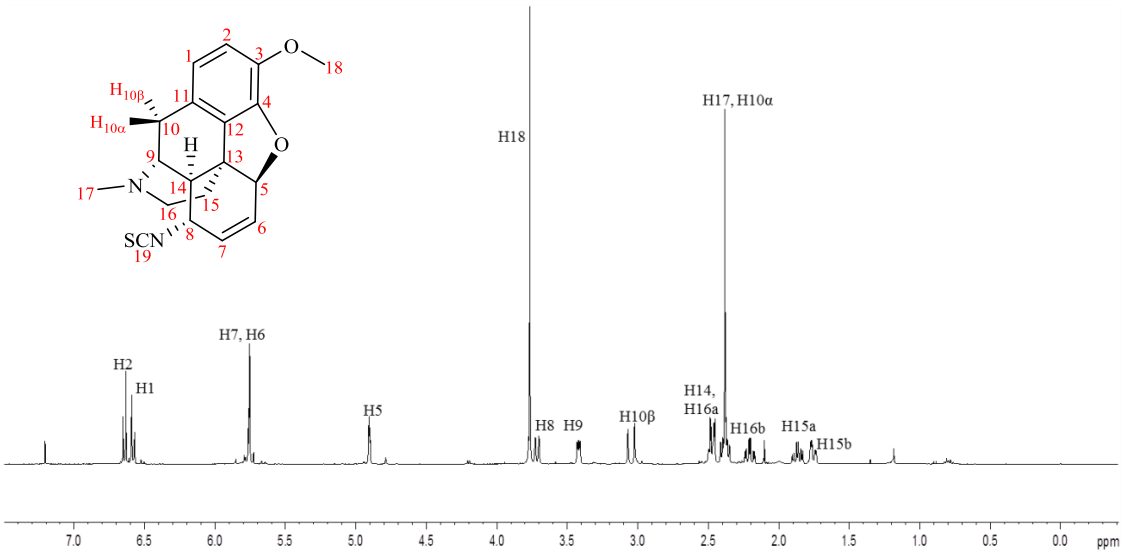

Fig. A3 ^{1}H NMR spectrum (400 MHz) of 8-isothiocyanocodide (**2**) in $CDCl_3$.

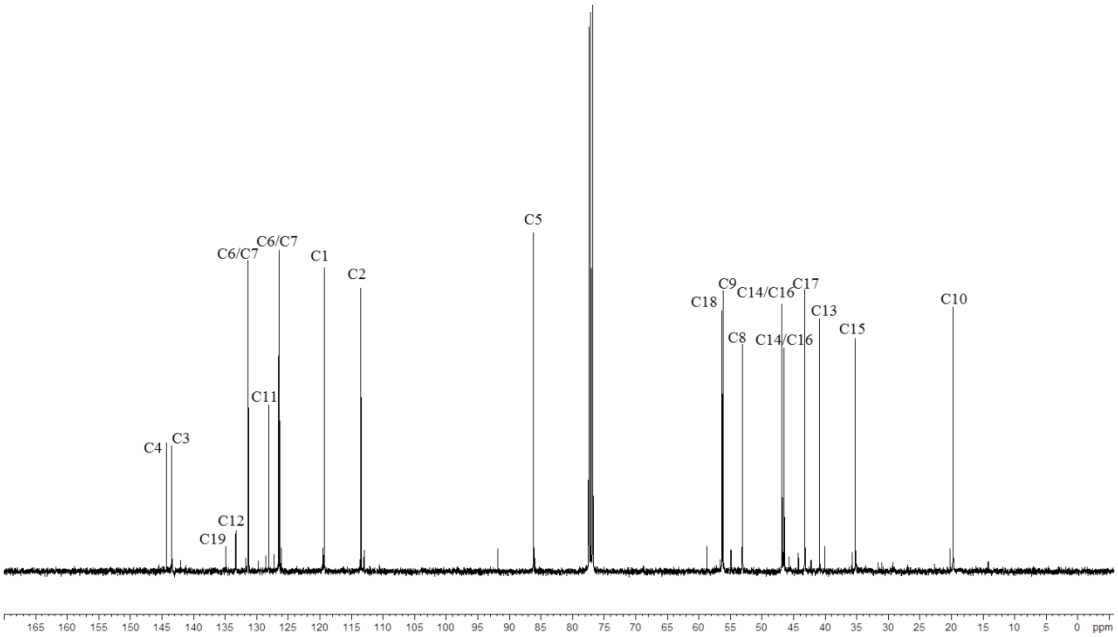

Fig. A4 ^{13}C NMR spectrum (100 MHz) of 8-isothiocyanocodide (**2**) in $CDCl_3$.

8-Azidocodide (3)

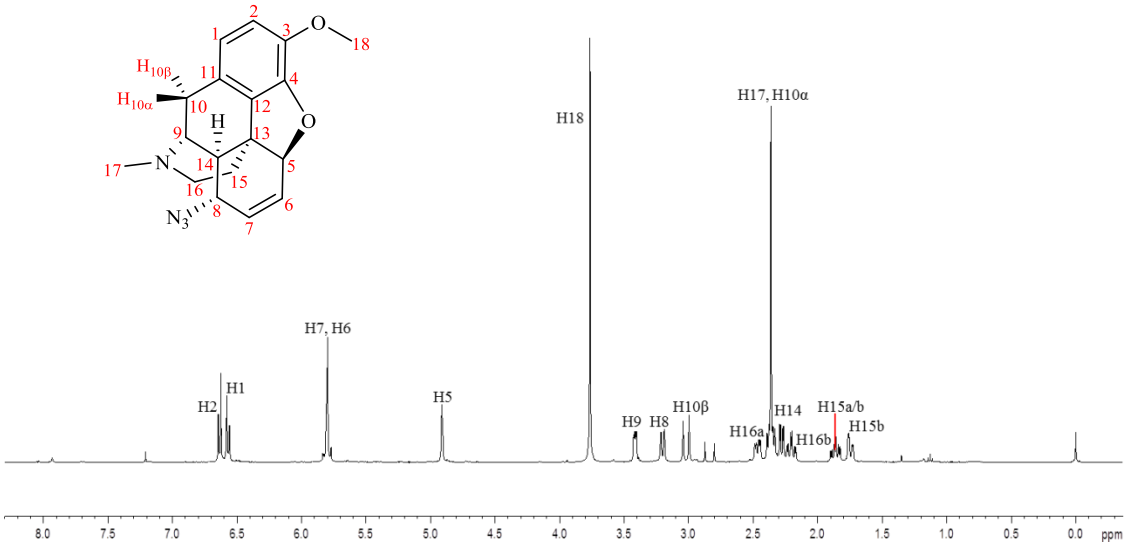

Fig. A5 ^{1}H NMR spectrum (400 MHz) of 8-azidocodide (**3**) in $CDCl_3$.

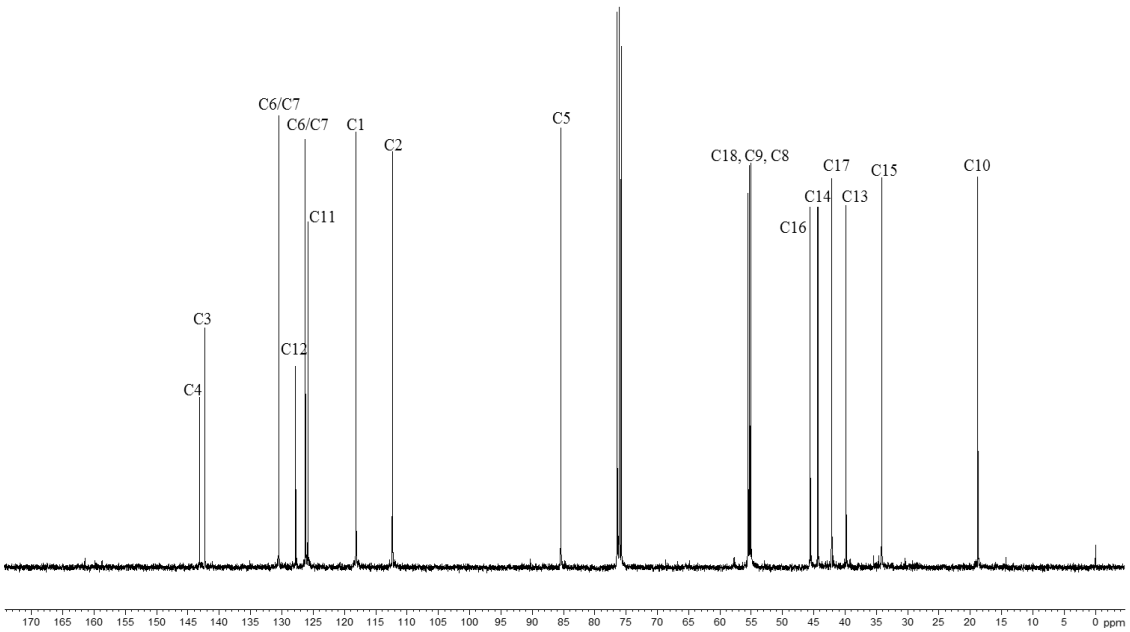

Fig. A6 ^{13}C NMR spectrum (100 MHz) of 8-azidocodide (**3**) in $CDCl_3$.

8-Aminocodide (4)

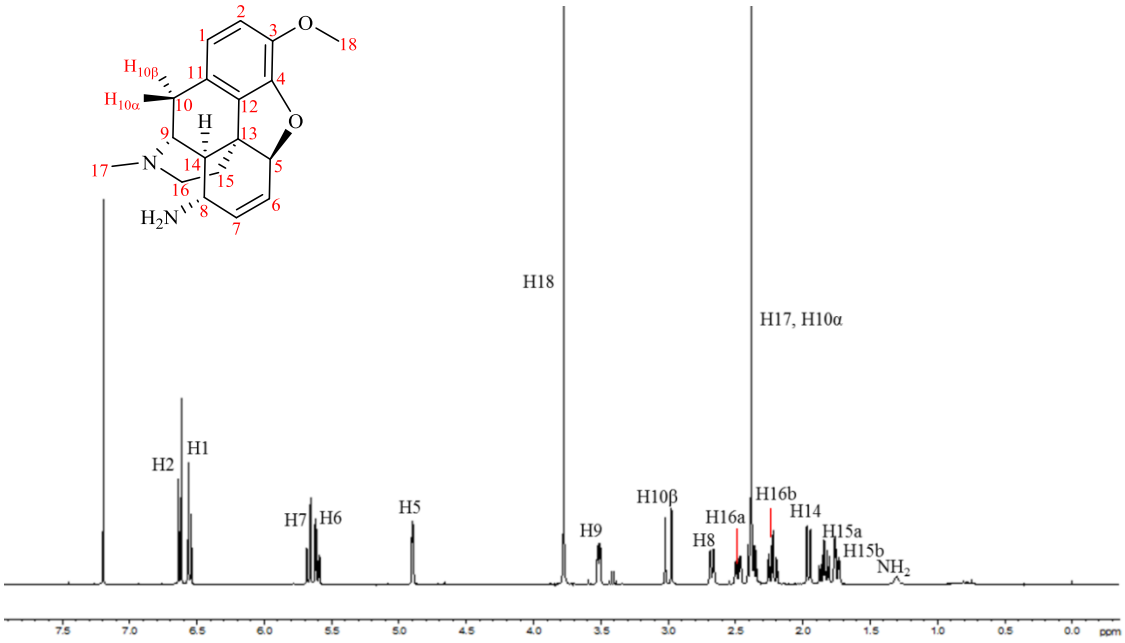

Fig. A7 ^{1}H NMR spectrum (400 MHz) of 8-aminocodide (**4**) in $CDCl_3$.

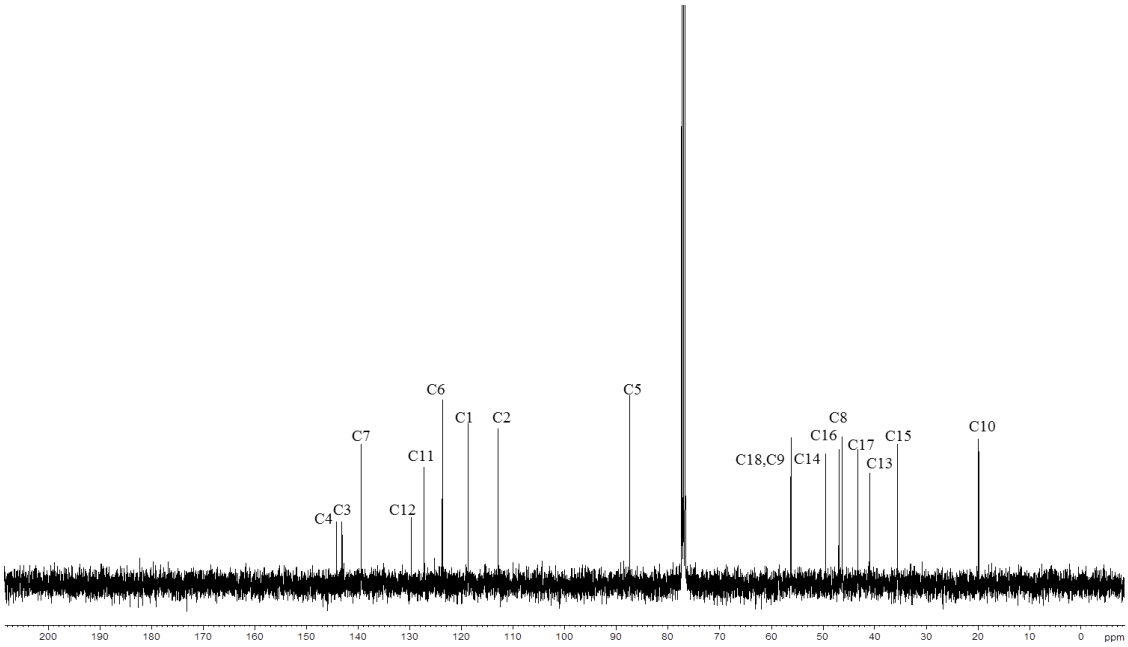

Fig. A8 ^{13}C NMR spectrum (100 MHz) of 8-aminocodide (**4**) in $CDCl_3$.

***N,N'*-disubstituted thiourea (5)**

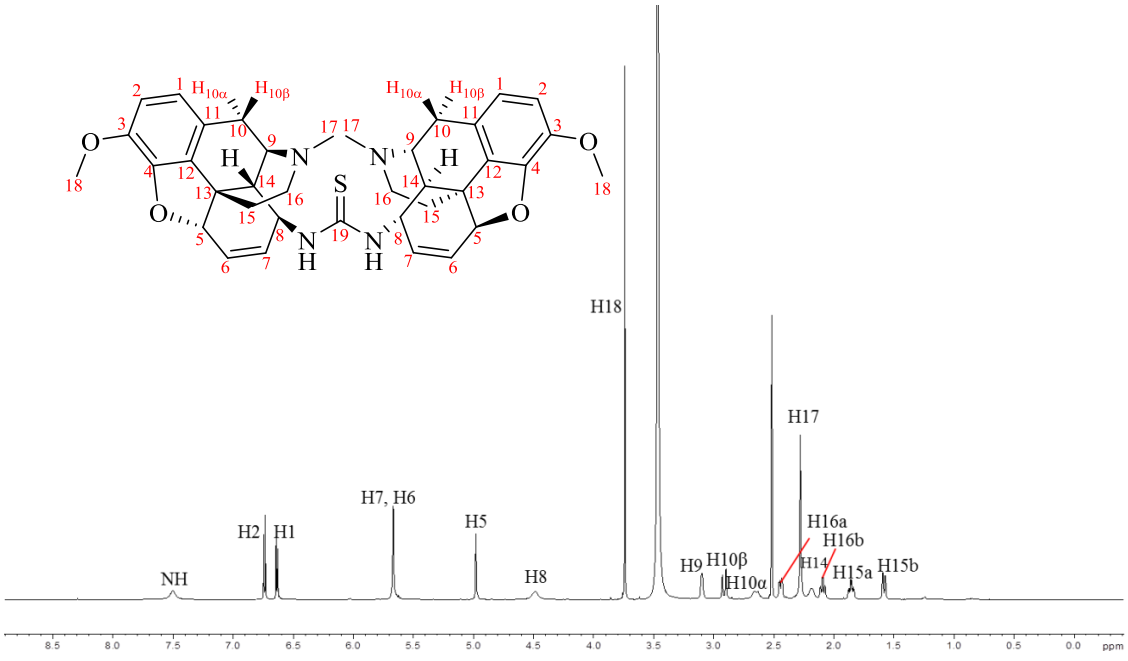

Fig. A9 ^{1}H NMR spectrum (600 MHz) of *N,N'*-disubstituted thiourea (**5**) in DMSO-d_6.

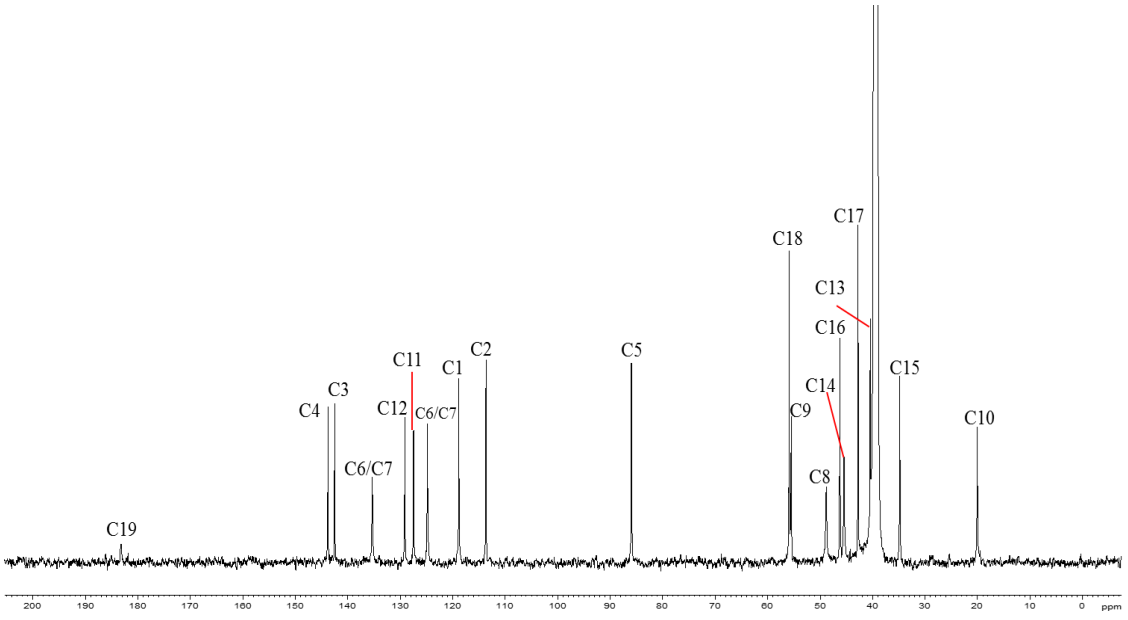

Fig. A10 ^{13}C NMR spectrum (150 MHz) of *N,N'*-disubstituted thiourea (**5**) in DMSO-d_6.

***N,N'*-disubstituted urea (6)**

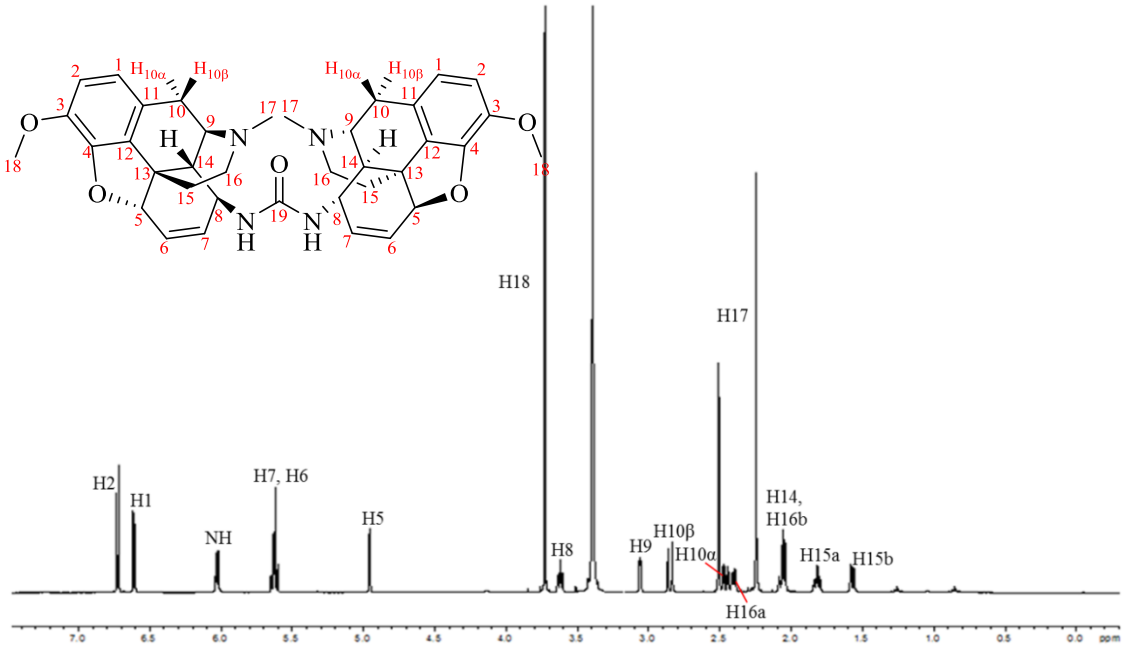

Fig. A11 ^{1}H NMR spectrum (600 MHz) of *N,N'*-disubstituted urea (**6**) in DMSO-d_6.

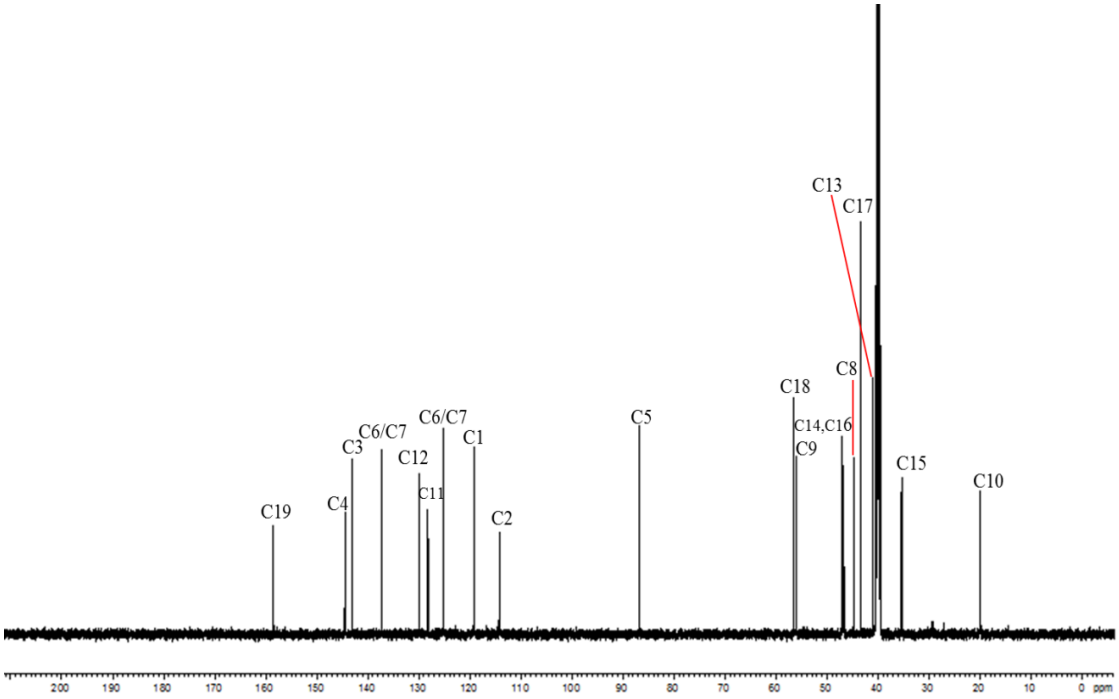

Fig. A12 ^{13}C NMR spectrum (150 MHz) of *N,N'*-disubstituted urea (**6**) in DMSO-d_6.

α-Chlorocodide (7)

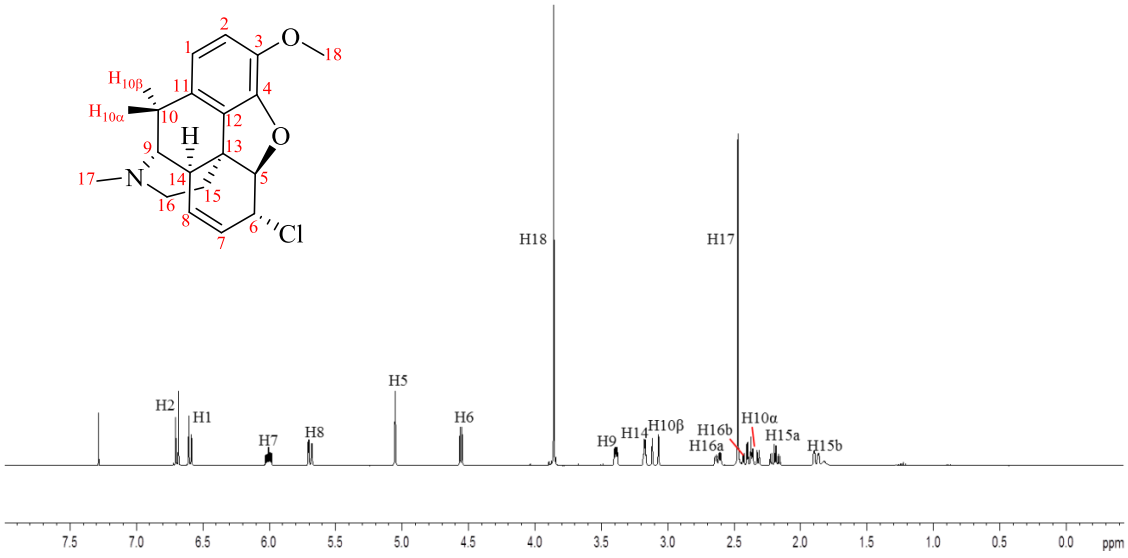

Fig. A13 ^{1}H NMR spectrum (400 MHz) of α-chlorocodide (**7**) in $CDCl_3$.

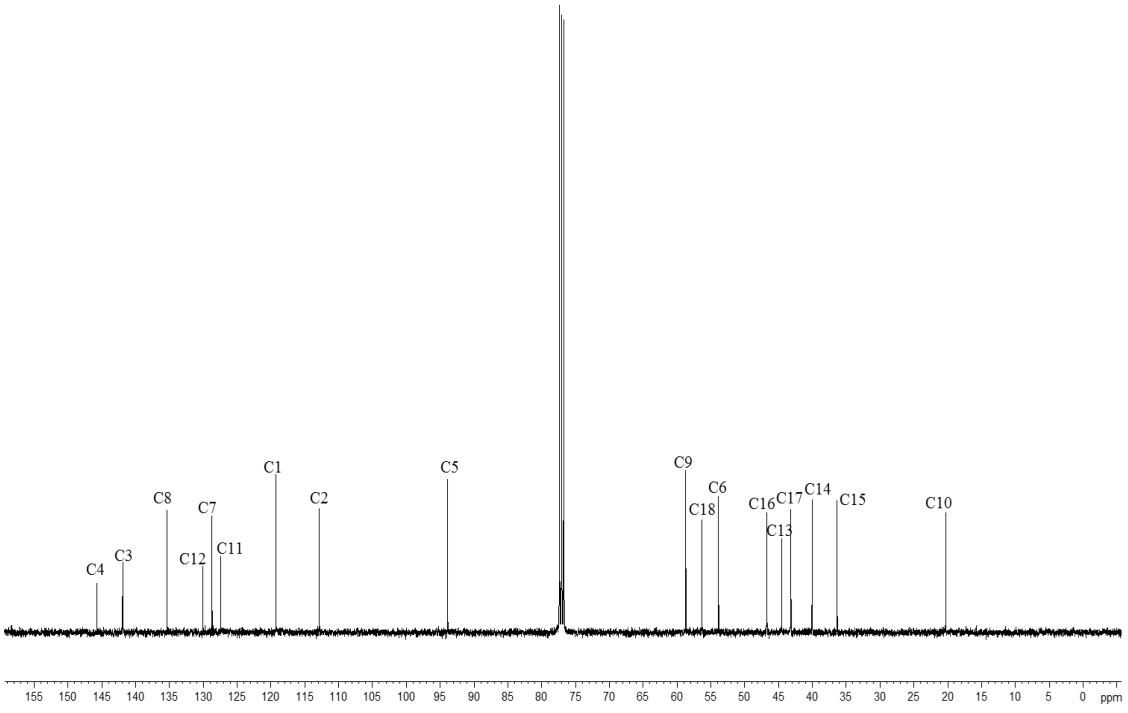

Fig. A14 ^{13}C NMR spectrum (100 MHz) of α-chlorocodide (**7**) in $CDCl_3$.

β-Bromocodide (8)

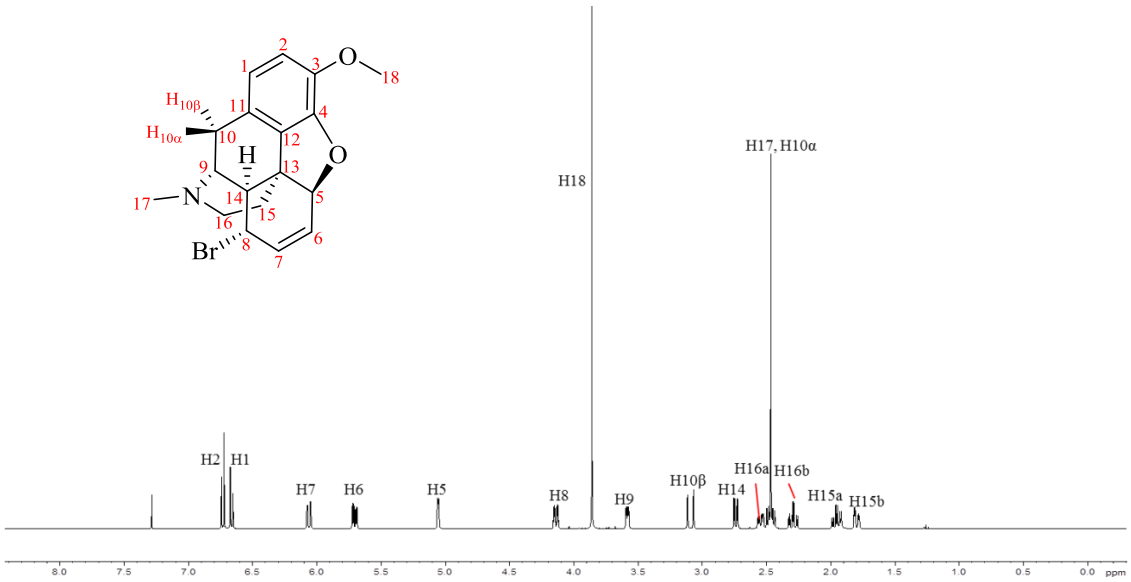

Fig. A15 ^{1}H NMR spectrum (400 MHz) of β-bromocodide (**8**) in $CDCl_3$.

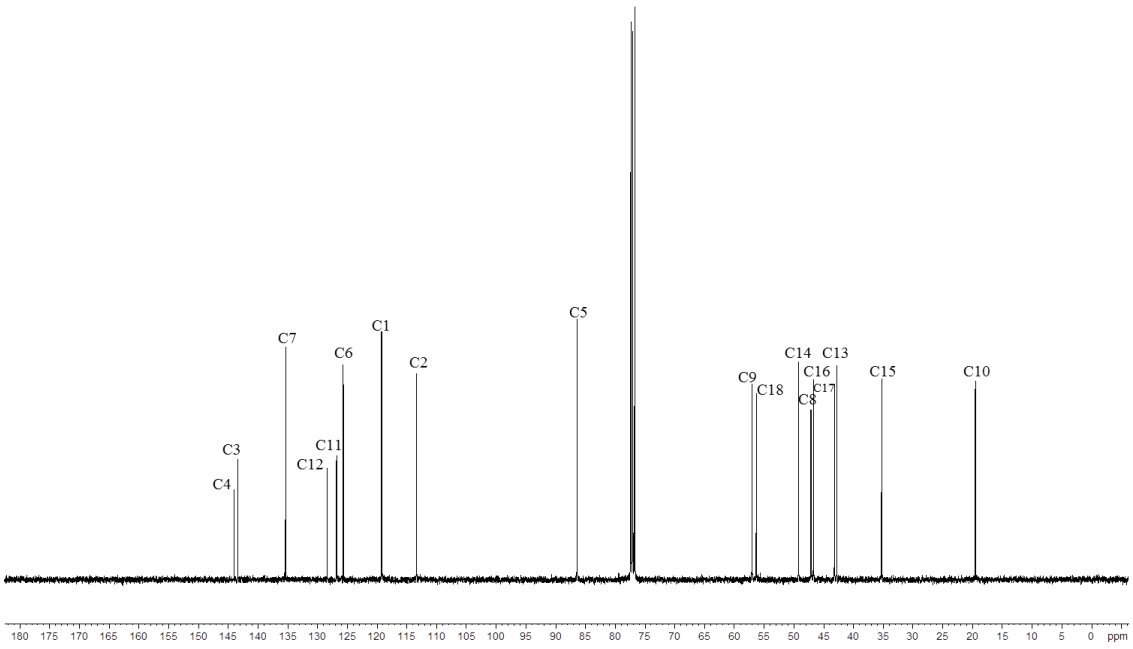

Fig. A16 ^{13}C NMR spectrum (100 MHz) of β-bromocodide (**8**) in $CDCl_3$.

Diethyl 2-(2-nitro-1-phenylethyl) malonate (9)

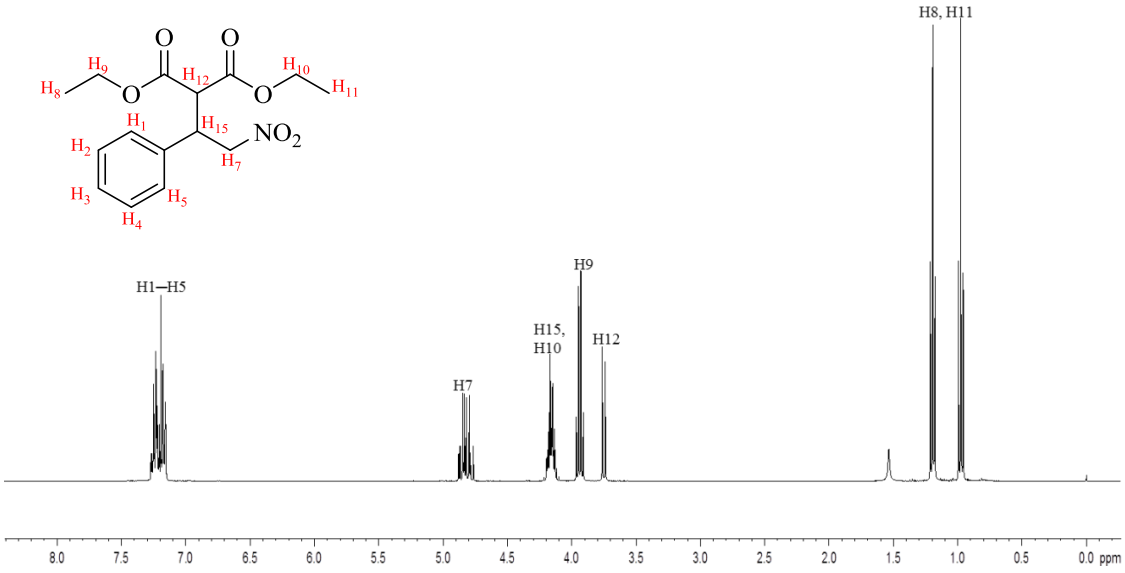

Fig. A17 ^{1}H NMR spectrum (400 MHz) of diethyl 2-(2-nitro-1-phenylethyl) malonate (**9**) in $CDCl_3$.

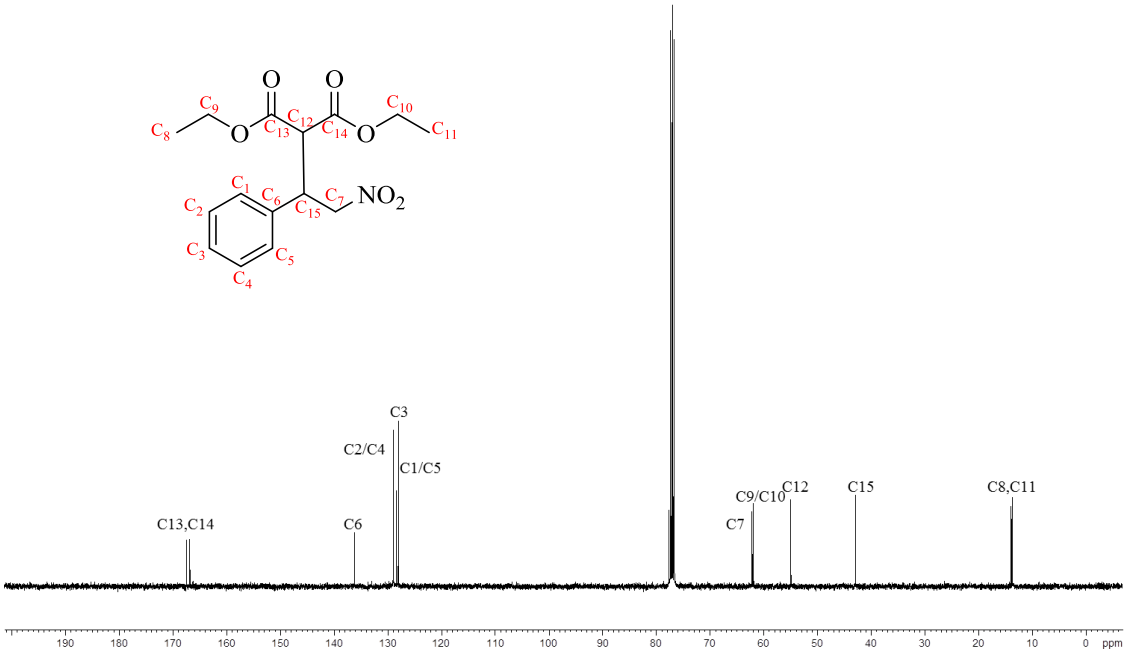

Fig. A18 ^{13}C NMR spectrum (100 MHz) of diethyl 2-(2-nitro-1-phenylethyl) malonate (**9**) in $CDCl_3$.

Appendix B: HPLC Chromatograms (Solvent Tests)

HPLC trace of isomeric compound: diethyl 2-(2-nitro-1-phenylethyl) malonate (9) in selected solvents

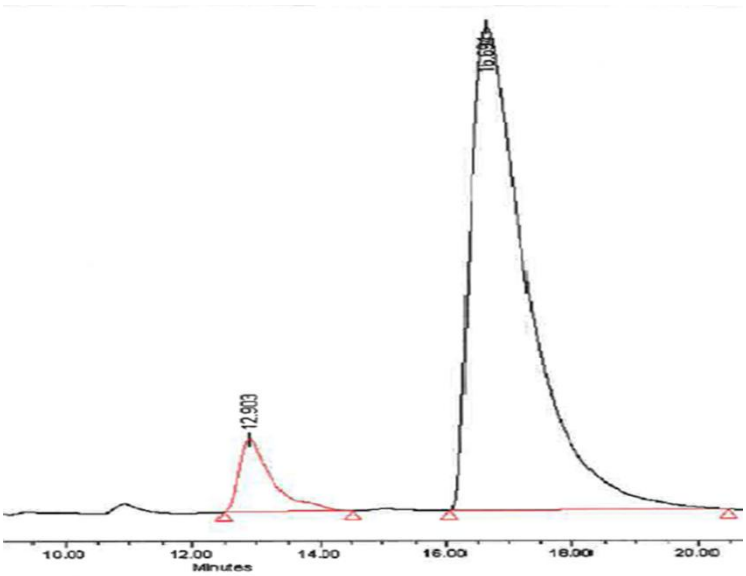

Fig. B1 Chromatogram of isomeric product (**9**) with 10 mol% Takemoto catalyst in toluene (diethyl malonate:*trans*-β-nitrostyrene = 0.4 mmol:0.2 mmol).

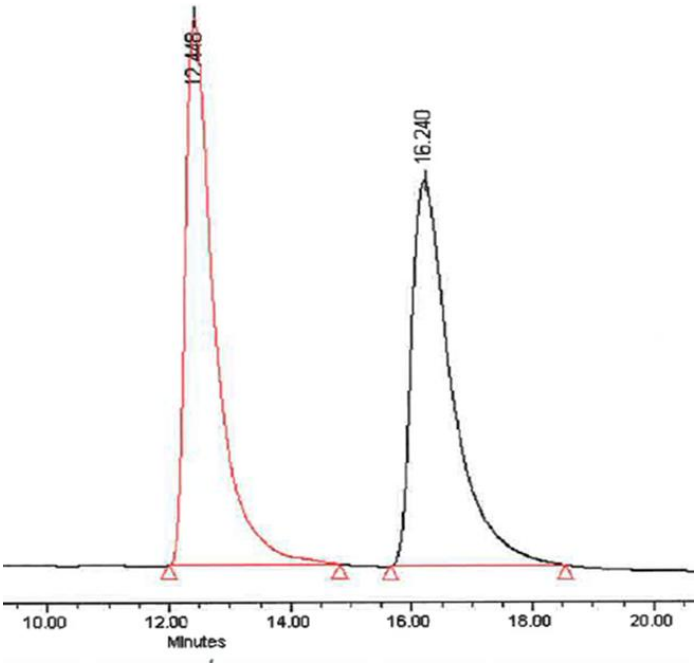

Fig. B2 Chromatogram of isomeric product (**9**) with 10 mol% *N,N'*-disubstituted thiourea catalyst (**5**) in hexane (diethyl malonate:*trans*-β-nitrostyrene = 0.4 mmol:0.2 mmol).

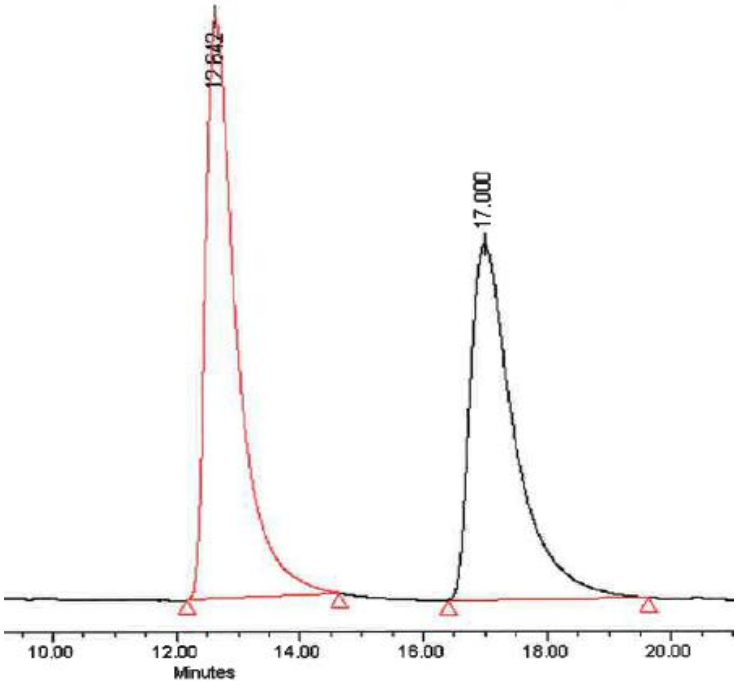

Fig. B3 Chromatogram of isomeric product (**9**) with 10 mol% *N,N'*-disubstituted thiourea catalyst (**5**) in toluene (diethyl malonate:*trans*-β-nitrostyrene = 0.4 mmol:0.2 mmol).

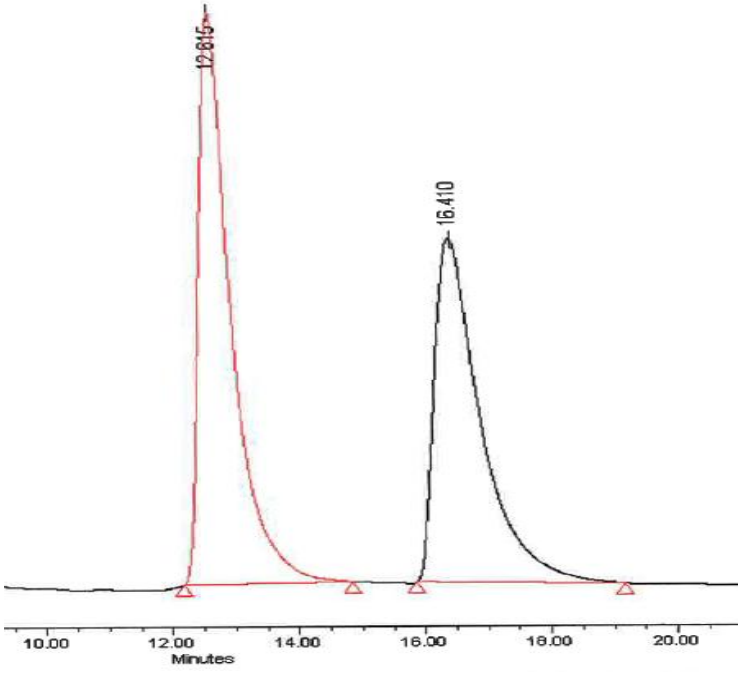

Fig. B4 Chromatogram of isomeric product (**9**) with 10 mol% *N,N'*-disubstituted thiourea catalyst (**5**) in THF (diethyl malonate:*trans*-β-nitrostyrene = 0.4 mmol:0.2 mmol).

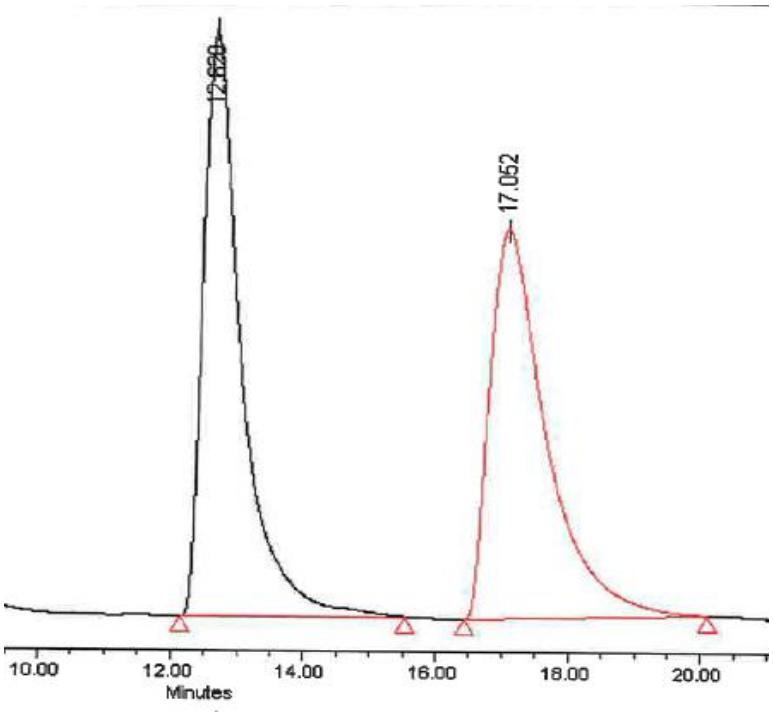

Fig. B5 Chromatogram of isomeric product (**9**) with 10 mol% *N,N'*-disubstituted thiourea catalyst (**5**) in DCM (diethyl malonate:*trans*-β-nitrostyrene = 0.4 mmol:0.2 mmol).

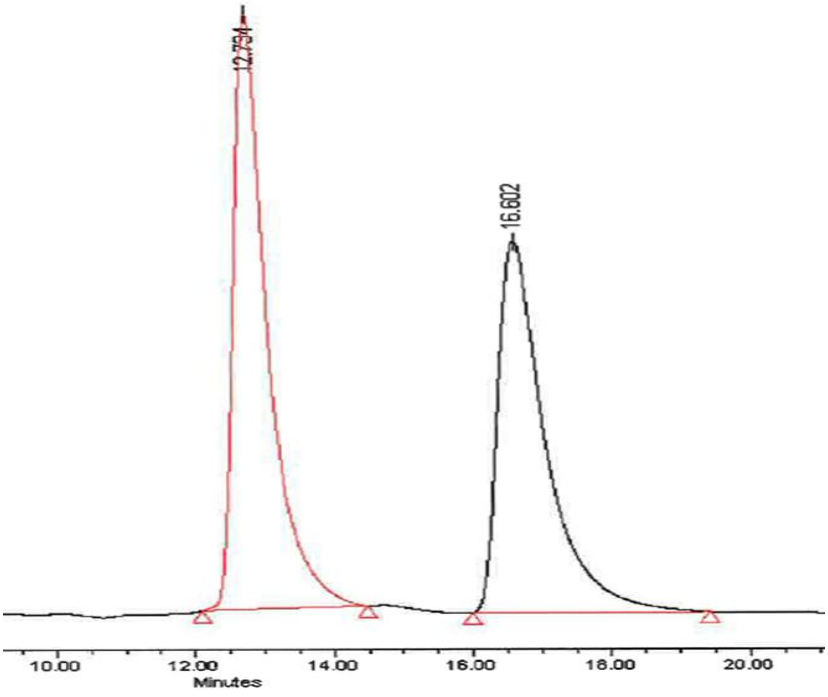

Fig. B6 Chromatogram of isomeric product (**9**) with 10 mol% *N,N'*-disubstituted thiourea catalyst (**5**) in MeOH (diethyl malonate:*trans*-β-nitrostyrene = 0.4 mmol:0.2 mmol).

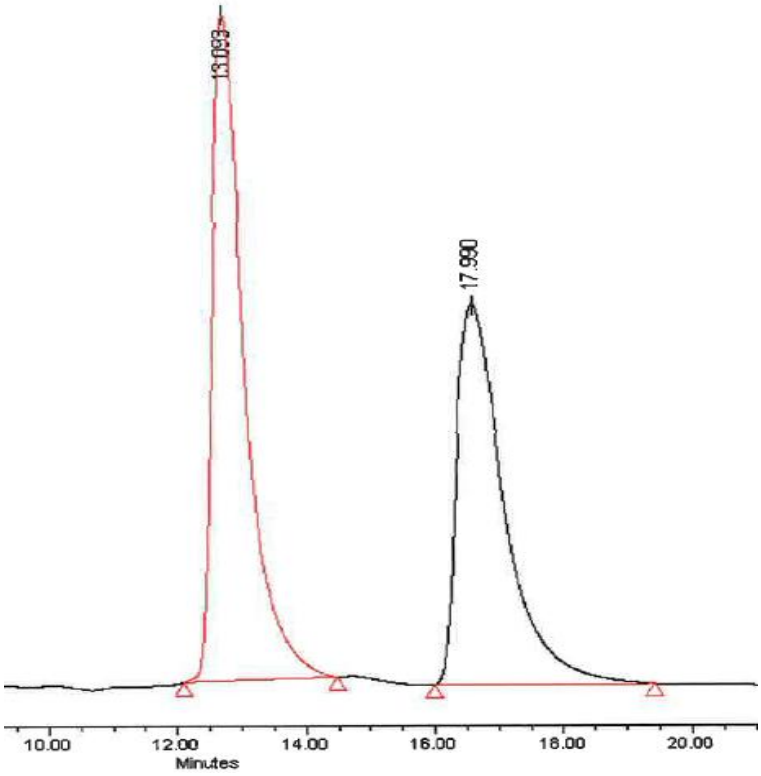

Fig. B7 Chromatogram of isomeric product (**9**) with 10 mol% *N,N'*-disubstituted thiourea catalyst (**5**) in MeCN (diethyl malonate:*trans*-β-nitrostyrene = 0.4 mmol:0.2 mmol).

Appendix C: Crystal data and structure refinement for *N,N'*-disubstituted thiourea and urea derivatives

Table C1 Crystal data and structure refinement for *N,N'*-disubstituted thiourea derivative (**5**).

Crystal data of *N,N'*-disubstituted thiourea derivative (**5**)	
Chemical formula	$C_{37}H_{42}N_4O_4S \cdot 9(H_2O)$
Formula weight M_r	800.95
Crystal system, space group	Orthorhombic, $P2_12_12_1$
Temperature (K)	150
Unit cell dimensions *a*, *b*, *c* (Å)	8.6271(3),15.0275 (6), 31.0543(11)
Volume (Å^3)	4026.0 (3)
Z (number of formula units per cell)	4
Radiation type	Mo *K*α
μ (mm^{-1})	0.15
Crystal size (mm)	0.27 × 0.15 × 0.10
Data collection	
Diffractometer	Apex II CCD area detector diffractometer
Absorption correction	Multi-scan *SADABS* v2008/1, Sheldrick, G.M., (2008)
T_{min}, T_{max}	0.641, 0.746
No. of measured, independent and observed [$I > 2(I)$] reflections	55033, 9967, 8369
R_{int}	0.052
$(\sin \theta/\lambda)_{max}$ (Å^{-1})	0.668
Refinement	
R[F^2 > 2σ(F^2)], wR(F^2), S	0.039, 0.095, 1.03
No. of reflections	9967
No. of parameters	554
No. of restraints	27
H-atom treatment	H atoms treated by a mixture of independent and constrained refinement
$\Delta\rangle_{max}$, $\Delta\rangle_{min}$ (e Å^{-3})	0.23, -0.20
Absolute structure	Flack x determined using 3284 quotients [(I+)-(I-)]/ [(I+) + (I-)] (Parsons, Flack and Wagner, Acta Cryst. B69 (2013) 249-259).
Absolute structure parameter	-0.02 (3)

Table C2 Crystal data and structure refinement for *N,N'*-disubstituted urea derivative (**6**).

Crystal data of *N,N'*-disubstituted urea derivative (**6**)	
Chemical formula	$C_{37}H_{42}N_4O_5 \cdot 3(H_2O)$
Formula weight *M*	676.79
Crystal system, space group	Orthorhombic, $C222_1$
Temperature (K)	100 (2)
Unit cell dimensions *a*, *b*, *c* (Å)	8.1075(3), 14.4775(6), 29.3808(12)
Volume ($Å^3$)	3448.6(2)
Z (number of formula units per cell)	4
Density (calculated)	1.304 Mg/m^3
Absorption coefficient	0.752 mm^{-1}
F(000)	1448
Crystal size	0.380 x 0.260 x 0.050 mm^3
Theta range for data collection	3.008 to 68.370°.
Index ranges	$-9 \leq h \leq 9$, $-16 \leq k \leq 17$, $-35 \leq l \leq 35$
Reflections collected	38660
No. of measured, independent and observed [$I > 2(I)$] reflections	3152 [R(int) = 0.0423]
Completeness to theta = 67.679°	100.0 %
Absorption correction	Semi-empirical from equivalents
Max. & Min. transmission	0.7531 and 0.6292
Refinement method	Full-matrix least-squares on F^2
Data / restraints / parameters	3152 / 0 / 241
Goodness-of-fit on F^2	1.050
Final R indices [$I > 2\sigma(I)$]	R1 = 0.0299, wR2 = 0.0819
R indices (all data)	R1 = 0.0304, wR2 = 0.0824
Largest diff. peak and hole	0.163 and -0.177 e. $Å^{-3}$
Absolute structure parameter	0.06 (5)